

# Geology of Uranium Deposits in the Dripping Spring Quartzite Gila County, Arizona

---

GEOLOGICAL SURVEY PROFESSIONAL PAPER 595

*Prepared on behalf of the  
U.S. Atomic Energy Commission*





# Geology of Uranium Deposits in the Dripping Spring Quartzite Gila County, Arizona

By HARRY C. GRANGER and ROBERT B. RAUP

---

GEOLOGICAL SURVEY PROFESSIONAL PAPER 595

*Prepared on behalf of the  
U.S. Atomic Energy Commission*



---

UNITED STATES GOVERNMENT PRINTING OFFICE, WASHINGTON : 1969

**UNITED STATES DEPARTMENT OF THE INTERIOR**

**STEWART L. UDALL, *Secretary***

**GEOLOGICAL SURVEY**

**William T. Pecora, *Director***

Library of Congress catalog-card No. GS 68-295

---

For sale by the Superintendent of Documents, U.S. Government Printing Office  
Washington, D.C. 20402 - Price \$2.25 (paper cover)

## CONTENTS

	Page		Page
<b>Abstract</b>	1	<b>Structure—Continued</b>	
<b>Introduction</b>	1	<b>Faults</b>	43
Location	2	Prediabase and syndiabase faults	43
Previous work	4	Postdiabase faults	45
Acknowledgments	4	<b>Joints</b>	48
<b>Geologic history of Gila County</b>	4	Types	48
<b>Dripping Spring Quartzite</b>	5	Tension joints	48
Barnes Conglomerate Member	7	Shear joints	50
Middle member	7	Joint systems	50
Upper member	7	Movement on joints	52
Red unit	7	History and age	56
Gray unit	7	<b>Radioactivity and uranium content of selected rocks</b>	56
Gray facies	7	Precambrian granite	60
Gray sandstone	8	Pioneer Formation	60
Black facies	8	Dripping Spring Quartzite	61
Buff unit	8	Unmetamorphosed rock	61
White unit	8	Metamorphosed rock	61
Sedimentary structures	9	Mescal Limestone	62
Ripple marks	9	Basalt	62
Shrinkage cracks	9	Diabase	62
Pseudochannels	9	<b>Uranium deposits</b>	63
Preconsolidation deformation features	9	Mining history	63
Fucoidlike markings	9	Production	63
Stylolites	9	Tenor of ore	64
<b>Diabase</b>	10	General character of deposits	64
Petrography	11	Vein deposits	64
Differentiation facies	15	Blanket deposits	70
Syenite facies	16	Irregular deposits	70
Aplite facies	18	<b>Distribution of deposits</b>	70
Black deuteritic veins	21	Stratigraphic position	70
Classification	22	Areal distribution	70
Significance	23	Relations to major structural features	71
Differentiation history	23	Relations to diabase and related rocks	71
<b>Age</b>	24	Age of the uranium deposits	76
Effects of metamorphism	25	Radioactivity of the uranium deposits	78
Dripping Spring Quartzite	25	<b>Mineralogy</b>	79
Normal hornfels	26	Primary uranium-bearing minerals	79
Petrography	26	Uraninite 1	80
Chemical composition	30	Uraninite 2	82
Coarse-grained hornfels	32	Uraninite 3	83
Petrography	32	Uraniferous chlorite	83
Chemical composition	34	Uraniferous carbon	84
Alteration of normal and coarse-grained	34	Coffinite	86
hornfels	34	<b>Primary sulfide minerals</b>	86
Mobilized hornfels	34	Molybdenite	86
Spotted rocks	38	Pyrrhotite	86
Pioneer Formation	39	Chalcopyrite	87
Mescal Limestone	40	Cubanite	88
Wallrock reactions	40	Sphalerite	88
<b>Structure</b>	42	Galena	88
Monoclines	42	Pyrite	89
Sierra Ancha monocline	42	Marcasite	90
Cherry Creek monocline	43	<b>Primary gangue and alteration minerals</b>	91
Canyon Creek monocline	43	Fluorite	91
Rock Canyon monocline	43	Calcite	91
Mule Hoof monocline	43	Ankerite	92

<b>Uranium deposits—Continued</b>		<b>Uranium deposits—Continued</b>	
<b>Mineralogy—Continued</b>		<b>Mineralogy—Continued</b>	
Primary gangue and alteration minerals—Con.		Secondary minerals—Continued	
Phlogopite-----	92	Kaolinite-----	96
Chlorite-----	92	Paragenetic sequence of primary minerals-----	96
Nontronite-----	93	Ore deposition-----	97
Unidentified clay-----	93	Emplacement controls-----	97
Quartz-----	93	Structural control-----	97
Secondary minerals-----	93	Mineralogy and chemical composition-----	98
Metatorbernite-----	93	Components of the ore-forming fluids-----	98
Bassettite-----	93	Factors that determined the mineralogy-----	99
Metanovacekite-----	94	Spatial relation to diabase-----	99
Saléeite-----	94	Type of host rock-----	99
Meta-autunite-----	94	Weathering-----	100
Sodium analog of zippeite-----	94	Temperature of deposition-----	100
Metazeunerite-----	94	Origin of the deposits-----	101
Uranophane and beta-uranophane-----	94	Behavior of uranium during the intrusion and differentiation of diabase-----	102
Hyalite-----	95	Transportation and localization of uranium-----	103
Limonite and goethite-----	95	Suggestions for prospecting-----	104
Chrysocolla-----	95	Stratigraphic considerations-----	104
Hemimorphite-----	95	Structural considerations-----	104
Malachite and azurite-----	95	Prospecting media-----	104
Barite-----	95	Prospecting for concealed deposits-----	104
Gypsum-----	95	Suggestions for development-----	104
Jarosite-----	96	Suggestions for mining procedure-----	105
Copiaipite-----	96	References cited-----	105
Chalcanthite-----	96	Index-----	107
Unidentified white sulfate minerals-----	96		

## ILLUSTRATIONS

[Plates are in pocket]

- PLATE**
1. Geologic map of the vicinity of the Little Joe and Workman deposits.
  2. Geologic map and sections of the Workman Creek area.
  3. Geologic maps and sections of Hope deposits.
  4. Geologic map and sections showing the results of drilling in and near adit 7, Red Bluff deposits.

<b>FIGURE</b>		<b>Page</b>
1. Index map of part of Gila County, Ariz., showing location of monoclines and uranium deposits-----	3	
2. Columnar section of the Dripping Spring Quartzite-----	6	
3. Geologic map of the vicinity of the Hope deposits-----	17	
4. Photomicrographs showing texture of aplites-----	19	
5. Photograph showing swarm of short black deuteritic veinlets in diabase dike-----	21	
6. Photomicrographs of black deuteritic veinlet and associated zircon grains-----	22	
7. Photographs of polished sections of hornfels showing textures-----	27	
8. Photomicrographs showing gradational sequence of normal hornfels to coarse-grained hornfels-----	29	
9. Photomicrograph showing partial replacement of normal hornfels by albite porphyroblasts-----	30	
10. Graph showing chemical changes during metamorphism of the gray unit of the Dripping Spring Quartzite-----	30	
11. Photograph of hornfels breccia cemented by mobilized hornfels-----	35	
12. Photomicrograph showing margin of a calcite-filled vug in mobilized hornfels-----	36	
13. Geologic map and sections of adit 1, Workman deposits-----	38	
14. Photomicrograph of one of many varieties of spotted rock from the gray facies in the gray unit of the upper member, Dripping Spring Quartzite-----	39	
15. Ternary diagram showing trends of mafic and alkalic components of rocks related to diabase and to siltstones of the gray unit, Dripping Spring Quartzite-----	41	
16. Geologic map and section of the Red Bluff area-----	44	
17. Geologic map and section of the Red Bluff deposits-----	46	

## CONTENTS

V

**FIGURES 18-21. Geologic maps:**

	Page
18. Vicinity of Lost Dog and Lucky Stop adits.....	49
19. Tomato Juice adits.....	50
20. Adits 1-5, Lucky Stop deposits.....	51
21. Big Buck adit.....	52
22. Contour diagram of poles of 762 joints in gray unit, Dripping Spring Quartzite, northern Gila County.....	53
23. Geologic map and section of the Lucky Boy deposit.....	54
24. Maps of adits, Shepp 2 deposits.....	55
25. Map of the Andy Gump adit.....	56
26. Maps of adits 1-3, First Chance deposits.....	57
27. Geologic map and sections of the Jon adit.....	58
28. Maps of adits 1-4, Lost Dog deposits.....	59
29. Map and sections of the Rainbow adit.....	59
30. Diagrammatic section showing typical uranium content of Dripping Spring Quartzite and several related rocks.....	59
31. Photograph of working face in the Hope 3 mine.....	64
<b>32-36. Graphs showing concentration of selected elements in the vein zone of:</b>	
32. Hope 3 mine.....	66
33. Adit 5 of the Lucky Stop deposits.....	67
34. Tomato Juice mine.....	68
35. Portal of the Rainbow adit.....	68
36. Second sublevel of the Lucky Boy mine.....	68
37. Composite geologic map and sections of the Suckerite mine.....	72
38. Maps and sections of the Lucky Boy mine.....	74
39. Map and sections of the Cataract adit.....	75
40. Map and sections of the Black Brush adit.....	75
41. Graph showing parent-daughter isotope relationships of uraninites from the Dripping Spring Quartzite.....	77
42. Graph showing age of uraninites by unit-cell-edge dimension.....	77
43. Graph showing relation between uranium content and radioactivity of weathered and unweathered samples from 18 deposits in the Dripping Spring Quartzite.....	78
44. Photomicrographs of uraninite.....	81
45. Photomicrograph of fractured grains of uraninite 1.....	82
46. Photomicrograph of intergrowth of uraninite and an unknown mineral.....	83
47. Scatter diagrams showing correlations between uranium and various elements in deposits in the Dripping Spring Quartzite.....	85
48. Map and section of the Horse Shoe adit.....	90
49. Photomicrograph showing well-developed concentric pattern in marcasite formed by the decomposition of pyrrhotite.....	91
50. Chart showing paragenetic sequence of mineral deposition in uranium deposits in the Dripping Spring Quartzite.....	97

---

**TABLES**

---

	Page
<b>TABLE 1. Chemical analyses of diabase and its differentiates.....</b>	<b>12</b>
2. Typical properties of diabase and related differentiates.....	14
3. Specific gravities of selected rocks.....	26
4. Radioactivity and uranium content of the Dripping Spring Quartzite, diabase, and associated rocks.....	60
5. Isotope ages of uraninite and galena from deposits in the Dripping Spring Quartzite.....	76
6. Minerals found in the uranium vein zones.....	80
7. Analyses of sphalerite, sample 115G56, Jon adit.....	101
8. X-ray data and unit-cell edge of sphalerite.....	101



# GEOLOGY OF URANIUM DEPOSITS IN THE DRIPPING SPRING QUARTZITE, GILA COUNTY ARIZONA

By HARRY C. GRANGER and ROBERT B. RAUP

## ABSTRACT

Uranium deposits in the Dripping Spring Quartzite of younger Precambrian age occur largely as disseminated veins in a carbon-and-potassium-rich siltstone facies near diabase intrusive bodies, also of Precambrian age. The deposits are confined mostly to the northern part of Gila County, Ariz., and have been extensively explored and developed, but production has been small.

The Dripping Spring is a formation in the Apache Group, which is a sequence of clastic sedimentary rocks, dolomitic limestone, and basalt flows. Uranium deposits in the Dripping Spring are found only in the upper member, which is composed largely of siltstone and very fine grained sandstone.

The Apache Group, and particularly the upper member of the Dripping Spring, is extensively intruded by sill-like sheets of diabase interconnected by dikes. Textures of the diabase range from intersertal at the chilled margins to ophitic in the central parts of the bodies. Differentiation has resulted in a variety of more salic facies represented by intermediate syenite and culminated by alkalic aplite and a very late stage femic facies called deuteritic veinlets. Simple differentiation by crystallization of the constituents that formed early is masked by pervasive deuteritic alteration that has affected all the igneous rocks.

Effects of regional metamorphism on these rocks are negligible, but the upper member of the Dripping Spring is locally metamorphosed adjacent to large diabase bodies. This contact metamorphism has progressively formed hornfels, a more completely crystallized rock called coarse-grained hornfels, and a facies which is probably transient called mobilized hornfels.

Metamorphism was accomplished without much change in the chemical composition of the potassium-rich siltstone except for the addition of sodium which is believed to be related to the alkalic aplite stage of diabase differentiation.

In the area that contains most of the uranium deposits, rocks are affected by several northward-trending monoclinal folds of prediabase age. Faults and joints aligned subparallel to the monoclines and in various other directions provided feeder channels for the diabase magma. The oldest joints seem to be of two types nearly superposed on each other and containing sets of high-angle joints that trend north-northeast and west-northwest. The earlier of the two types, tension joints, seems to have controlled the shapes and positions of the uranium deposits. The later type, shear joints, generally crosses the uranium deposits at a low angle, although locally shear joints may follow the trend of a uranium vein for a short distance.

Most of the uranium deposits occur in the gray unit of the upper member of the Dripping Spring, either above or below a thin quartzite stratum called the barren quartzite. The largest veins are several hundred feet long and a few feet wide and extend several tens of feet vertically. All the larger veins occur

near diabase, and many of these occur in hornfels. Structural relations indicate that ore minerals were deposited after the hornfels had formed, but the association of high-temperature minerals in the vein zones nearest diabase suggests that they were deposited prior to complete cooling of the diabase.

The vein minerals are largely disseminated in the wallrock adjacent to a poorly defined central joint or fracture zone. Locally, uraninite forms small lenticular fissure fillings, but these are sparse. Close to diabase the vein minerals consist principally of uraninite of two ages associated with pyrrhotite, pyrite, chalcopyrite, and galena and sparse molybdenite, cubanite, and iron-rich sphalerite. Farther from diabase the minerals are poorly crystallized uraninite, pyrite, chalcopyrite, galena, and sparse sphalerite. Fluorite, ankerite, calcite, and phlogopite are variously associated with the deposits. The most common alteration and gangue mineral is chlorite that locally may grade into a nontronite clay.

Isotope ages, determined for the uraninite, indicate an age of about 1,050 million years. Because of the apparent genetic association between diabase and the uranium deposits, the diabase is considered to have the same age as the uraninite.

Uranium-bearing solutions are believed to have originated within the cooling diabase and to have been fed to the vein zones at the time of formation of the late-stage femic deuteritic veinlets. Chemical analyses of the deuteritic veinlets and the presence in them, locally, of abundant zircon surrounded by pleochroic halos show that uranium was a constituent of the deuteritic fluids.

Experience has shown that airborne radiometric exploration guided by geologic considerations and followed by ground checking is the most efficient exploration procedure. Drilling has been of limited value because of the small targets presented by the deposits.

## INTRODUCTION

The discovery of several uranium deposits in the Dripping Spring Quartzite of southeast-central Arizona between 1950 and 1954 and the finding of widespread abnormally high background radioactivity in that formation led to increased mining activity in the area and indicated the likelihood of finding additional deposits in the Dripping Spring over a much broader area. Consequently, in mid-1954, the U.S. Geological Survey, on behalf of the Division of Raw Materials of the U.S. Atomic Energy Commission, began a study to determine the geologic setting of the deposits.

The timing of the study proved to be particularly advantageous, as the fieldwork was begun during a peri-

od of intense prospecting activity and continued during a period of development and mining. By late 1956 it had become evident that the deposits were difficult to mine at a profit, and the Atomic Energy Commission declared that the ore was not economically amenable to the then current milling methods.

By mid-1957 more than 100 uranium deposits were known in the Dripping Spring Quartzite, and of these about 50 had been explored by workings or drill holes. Only 16 deposits, however, had produced enough ore for shipment. Production has been small because of the difficulty of selective mining and the generally small size of the deposits. Only five mines have produced more than 2,000 tons of ore, and total production from the formation by May 1957 was less than 22,000 tons. Since 1957, there has been very little mining or exploration in the Dripping Spring.

During this study it became evident that a close spatial and temporal relation existed between the uranium deposits and the diabase bodies that intruded the host rocks. Initially, we believed that the uranium deposits resulted from redistribution and concentration of uranium that was syngenetic with the host rocks, perhaps under thermo-chemical conditions imposed by the diabase intrusives. Later, this hypothesis seemed to be untenable because of evidence that pointed to a direct genetic relation between the uranium deposits and the diabase (Neuerburg and Granger, 1960). Accordingly, throughout this report we have made an effort to demonstrate that the diabase magma was the progenitor of the uranium deposits, and we have placed considerable emphasis on the petrography and petrology of diabase and its associated differentiates and metamorphic phenomena.

Fieldwork for this study was conducted during July–December 1954, May–June and October–December, 1955, and June–September 1956. Field investigations were largely detailed examinations of the deposits and their relation to the surrounding rocks, but from October to December 1955, studies were confined to the stratigraphy of the Dripping Spring Quartzite (Granger and Raup, 1964).

This report summarizes and generalizes the results of the geologic studies of the ore deposits. Supplementary detailed descriptions of individual deposits are presented in an open-file report (Granger and Raup, 1969). The following list indicates which deposits are described in the open file. Copies of part, or all, of that report may be obtained at cost from the U.S. Geological Survey library, Federal Center, Denver, Colorado, 80225.

Deposit	Location in figure 1, this report	Open-file report	
		Includes description	Includes illustrations
Alta Vista.....	1	X	-----
Andy Gump.....	2	X	-----
Big Buck.....	3	X	-----
Big Six.....	4	X	-----
Black Brush.....	5	X	-----
Black Diamond.....	6	X	-----
Blevins Canyon.....	7	X	-----
Blue Rock.....	8	X	-----
Brushy Basin Trap.....	9	X	-----
Cataract.....	10	X	-----
Donna Lee.....	11	X	X
Easy.....	12	X	-----
Fairview.....	13	X	-----
First Chance.....	14	X	-----
Grand View.....	15	X	-----
Great Gain.....	16	X	-----
Grindstone.....	17	X	-----
Heigh Power.....	18	-----	-----
Hope.....	19	X	-----
Horse Shoe.....	20	X	-----
Iris.....	21	X	X
Jim.....	22	X	-----
Jon.....	23	X	-----
Little Joe.....	24	X	X
Lost Dog.....	25	X	-----
Lucky Boy.....	26	X	X
Lucky Stop.....	27	X	-----
Major Hoople.....	28	X	-----
May.....	29	X	-----
Navajo.....	30	X	-----
North Star.....	31	X	-----
Peacock.....	32	X	-----
Quartzite.....	33	X	-----
Rainbow.....	34	X	-----
Red Bluff.....	35	X	X
Red Cliffs.....	36	-----	-----
Rock Canyon.....	37	X	-----
Roxy.....	38	X	-----
Shepp No. 2.....	39	X	-----
Sky.....	40	X	-----
Snakebit.....	41	X	-----
Sorrel Horse.....	42	X	-----
Suckerite.....	43	X	-----
Sue.....	44	X	X
Tomato Juice.....	45	X	-----
Workman.....	46	X	X

#### LOCATION

The Dripping Spring Quartzite, a formation in the Apache Group of younger Precambrian age, is exposed sporadically in an area of more than 8,000 square miles in southeast-central Arizona. Known exposures are in Gila, Graham, Pima, Pinal, Cochise, Maricopa, and Navajo Counties. Because nearly all the known uranium deposits in the formation are in Gila County (fig. 1), this report deals largely with data gathered from that county.

## INTRODUCTION

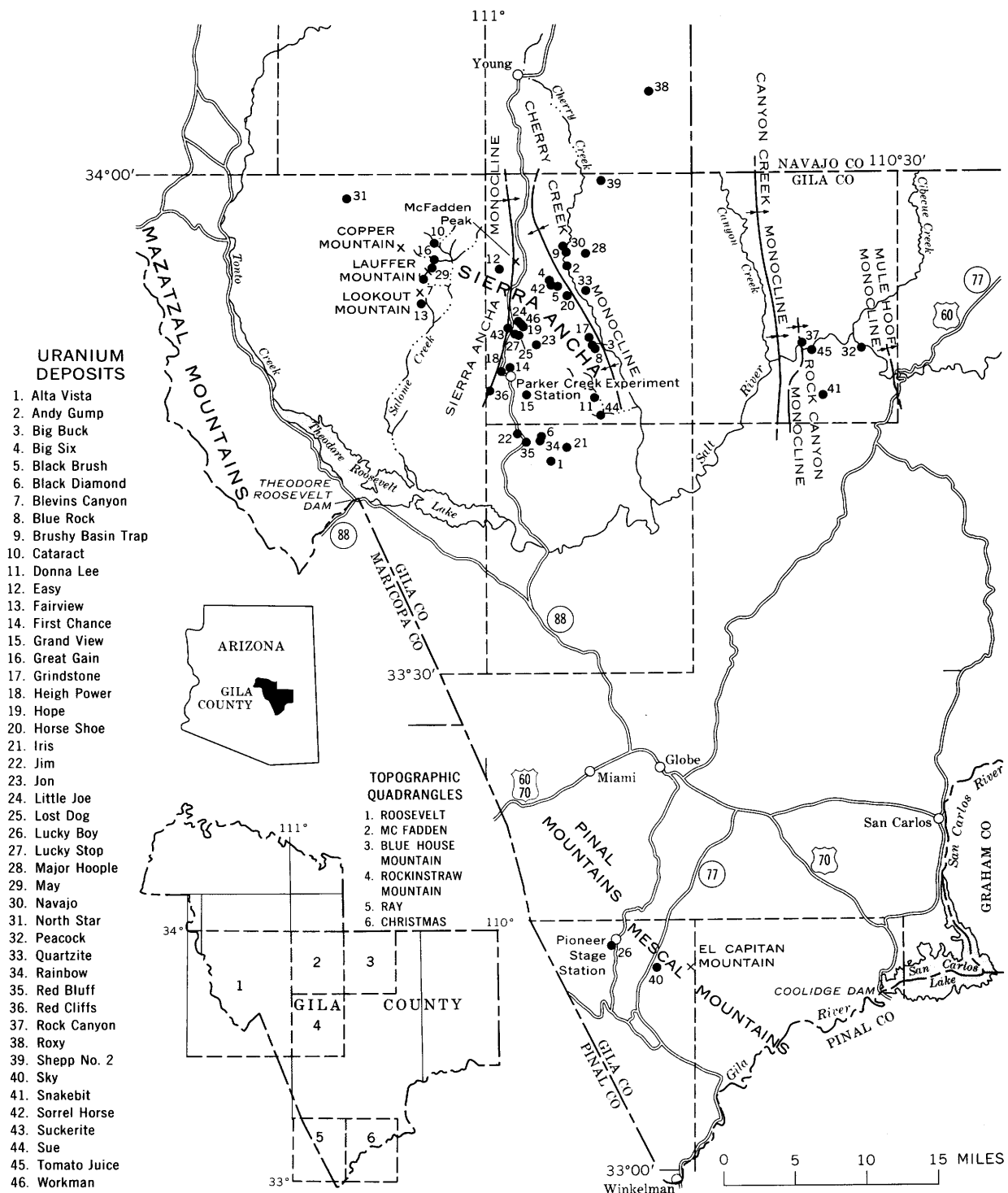


FIGURE 1.—Index map of part of Gila County, Ariz., showing location of monoclines and uranium deposits.

That part of Gila County which lies north of the Salt River and east of Tonto Creek and contains nearly all the uranium deposits has characteristics that closely resemble those of the Colorado Plateaus physiographic province. The rock strata rarely are steeply tilted by block faulting, and the physiography is that of a plateau intricately incised by deep rugged canyons. The Mogollon Rim, which forms much of the northern boundary of Gila County and is ordinarily considered to be the southern boundary of the Colorado Plateaus physiographic province, evidently has been moved northward by erosional migration.

The vegetation is sparse below elevations of about 5,000–6,000 feet. Cacti of many species are represented, as well as desert trees, mesquite, and palo verde. Juniper grows between about 3,000 and 5,000 feet. Where water is more readily available, cottonwood and other more hygrophytic plants are present. In general, the low country appears desolate.

Vegetation above 6,000 feet is more plentiful, and the highest country, as in the Sierra Ancha, is well wooded. Pine is the most plentiful tree, but sycamore and black walnut are also common where water is adequate. In high but unforested terrain, grass is abundant, particularly on the mesa tops.

Precipitation in Gila County ranges from very meager in the low country to moderately plentiful in the higher mountains. At lower elevations, where precipitation is generally less than 20 inches per year and evaporation is rapid, semiarid conditions prevail. In the Sierra Ancha, however, precipitation, which includes snow during the winter months, may be considerably more than 20 inches per year. Much of the precipitation occurs during two periods: rain and snow in the mountainous areas in January and February, and short but violent rainstorms in the entire area in July and August.

Gila County is very sparsely populated except for the immediate vicinity of Globe and Miami. The combined population of these towns and the intervening area was about 10,000 in 1960. Each of the other towns in the county has a population of 3,000 or less, and miles of nearly uninhabited country separate the communities. All the towns are supported mainly by mining and ranching.

Access to the principal towns is good, but, for the most part, roads in Gila County are sparse. All-weather Federal or State highways lead to within 50 miles of most of the uranium deposits, and a network of county and private roads reaches to within at least a mile of most of the deposits. Unimproved roads are commonly impassable during the rainy seasons owing to washouts and mud.

Several smelters in and near Gila County can process base-metal ores, but the nearest uranium ore-buying depot prior to mid-1955 was at Bluewater, N. Mex.,

nearly 400 miles by road from the ore source. In June 1955, a uranium ore-buying depot was constructed at Cutter, about 8 miles east of Globe; this depot purchased ore until it closed in June 1957.

#### PREVIOUS WORK

The first geological work on uranium deposits in the Dripping Spring Quartzite began in the summer of 1950 when R. J. Wright (1950), of the U.S. Atomic Energy Commission, conducted a brief preliminary examination of the Red Bluff deposit. E. P. Kaiser, U.S. Geological Survey, made a more detailed study of the deposit and adjacent area in October 1950 (Kaiser, 1951). In March 1953, W. E. Mead and R. L. Wells, U.S. Atomic Energy Commission, made a brief field check of the radioactivity of the Dripping Spring Quartzite in Gila and Pinal Counties (Mead and Wells, 1953). Later in 1953, R. L. Wells and A. J. Rambosek (1954) examined the newly discovered Stockman and Shepp claims in the northern part of the Sierra Ancha. R. G. Gastil (1953) mapped the east half of the Diamond Butte quadrangle and made a reconnaissance study of the Apache Group in Gila County. During 1954 and 1955, F. J. Williams (1957) studied the structural controls and related features of the uranium deposits in the Dripping Spring for the U.S. Atomic Energy Commission. In February 1955 the Raw Materials Office of the U.S. Atomic Energy Commission established an office in Globe for the purpose of studying the deposits and aiding the uranium miners. During the Spring of 1955, B. J. Sharp (1956) mapped an area along Cherry Creek and studied the Black Brush uranium deposit.

#### ACKNOWLEDGMENTS

We wish to express our appreciation to the many geologists and mining men who aided in the present study. In particular we thank G. J. Neuerburg, J. C. Antweiler, A. F. Shride, C. T. Wrucke, F. B. Moore, and R. A. Christman, all of the U.S. Geological Survey, who made helpful contributions at various stages of the study. R. J. Schwartz and others at the Globe office of the U.S. Atomic Energy Commission provided us with much unpublished information concerning the uranium deposits.

#### GEOLOGIC HISTORY OF GILA COUNTY

The oldest rocks exposed in Gila County are older Precambrian detrital sedimentary, pyroclastic, and volcanic rocks that have been metamorphosed to gneiss and schist near large bodies of intrusive rock. These rocks are called Pinal Schist in the southern part of the county and Yavapai Schist (Group or Series) in the northern part of the county.

The Mazatzal Revolution brought an end to older Precambrian sedimentation and faulted and uplifted the

existing rocks. Granitic rocks were intruded in batholithic proportions during the period of pronounced orogeny; mafic rocks were intruded in much smaller amounts. Lead-uranium age determinations on zircon from granitic rocks elsewhere in Arizona that are believed to be comparable in age to the granite in Gila County indicate an age of more than 1,200 m.y., (million years) and perhaps as much as 1,660 m.y. (Granger and Raup, 1964).

A long period of erosion reduced the massive ranges produced by the Mazatzal Revolution to a more subdued terrain; however, some highlands capped by older Precambrian sedimentary rocks remained, particularly in the northern part of the county. On this surface were deposited younger Precambrian sedimentary rocks of the Apache Group, which comprises the Pioneer Formation, Dripping Spring Quartzite, Mescal Limestone, and basalt flows at and near the top of the Mescal. The Scanlan Conglomerate Member, the basal conglomerate of the Pioneer Formation, is made up entirely of indurated detrital material ranging from silt and feldspathic sand to pyroclastic fragments. The Barnes Conglomerate Member, the basal conglomerate of the Dripping Spring, was deposited disconformably on an erosion surface cut in the Pioneer Formation; this disconformity suggests that an epeirogeny occurred that produced a pronounced change of conditions in the basin of deposition or in the source area without attendant deformation of the floor of the basin. In general, the Dripping Spring becomes finer grained and more evenly and thinly stratified upward; these features suggest a gradual return to stable conditions.

Poorly sorted sandstones and siltstones at the base of the Mescal Limestone were then deposited disconformably on the Dripping Spring. The Mescal, composed principally of argillaceous and siliceous limestone and dolomite capped by feldspar-rich siltstone, marks the end of the sedimentary cycle of the Apache Group; the depositional history was climaxed by an outpouring of basaltic lavas that disconformably overlie the sedimentary rocks and may have once covered the entire region. A possible forerunner of the culminating lava flows is a thin basaltic layer locally present at the base of the upper member of the Mescal.

Another period of erosion occurred. Then a sequence of unfossiliferous clastic rocks, largely sandstone and quartzite—the Precambrian Troy Quartzite—was deposited.

The Troy Quartzite and the Apache Group were intruded by great sheets and interconnecting dikes of diabase in late Precambrian time. At the time of intrusion the Troy was probably covered with many feet of rocks that have since been removed.

Overlying the Troy with a remarkably parallel contact are the basal Paleozoic strata. These strata locally contain Middle and Late Cambrian fossils which suggest that the strata may be correlatives of the Bolsa Quartzite and Abrigo Limestone to the south. These strata, in many places in Gila County, are lithologically similar to the Precambrian Troy, but they were deposited after a considerable hiatus. This hiatus, however, was not marked by strong structural disturbance, as the erosion surface separating the Paleozoic from earlier rocks is obscure.

The Paleozoic strata overlying the Cambrian rocks range in age from Late Devonian to Permian; no record of Ordovician or Silurian rocks has been found. The post-Cambrian rocks are dominantly marine limestone.

The only Mesozoic rocks preserved in Gila County are sparse exposures of Cretaceous clastic and volcanic rocks in the extreme southern part of the county. Culminating the Mesozoic Era was a period of structural disturbances and granitic igneous activity related to the Laramide orogeny. Neither the structural nor the igneous activity had a significant effect on the uranium deposits in the Dripping Spring; the activity apparently was largely restricted to the area south of the Sierra Ancha. Another intrusion of diabase may have occurred at this time; diabase dikes that cut Pennsylvanian limestone in the south-central part of the county have been reported by Ransome (1917, 1919), Darton (1925, p. 254), and Peterson, Gilbert, and Quick (1951).

Tertiary and Quaternary strata are largely locally consolidated gravel and sand that were deposited during and after a period of block faulting. Volcanic activity continued intermittently throughout most of Tertiary time. The most common extrusive rocks of Tertiary age are of dacitic, andesitic, and basaltic composition. The most abundant sedimentary rocks are consolidated gravels that fill the intermontane basins and form a thin veneer on pediments; the gravels are called Gila Conglomerate on the basis of similarities to the Gila Conglomerate described and named by Gilbert (1875, p. 540-541).

#### DRIPPING SPRING QUARTZITE

The Dripping Spring Quartzite was studied in detail to determine the relations between it and its contained uranium deposits. A more complete compilation and interpretation of the stratigraphic data are included in a separate report on the stratigraphy of the Dripping Spring (Granger and Raup, 1964).

The Dripping Spring Quartzite is a sequence of strata composed largely of feldspar-rich silty and arenaceous clastic rocks ranging in thickness in Gila

County from about 325 feet to 700 feet. The formation overlies the Pioneer Formation with only local evidence of pre-Dripping Spring erosion. Overlying the Dripping Spring Quartzite with erosional unconformity is the Mescal Limestone.

The Dripping Spring is divided into three members (fig. 2). The basal Barnes Conglomerate Member is

composed largely of well-rounded quartzose pebbles and cobbles set in a medium- to coarse-grained feldspathic sandstone matrix. The middle member is composed primarily of arkosic and feldspathic sandstone and orthoquartzite. The upper member—the host for the uranium deposits—comprises principally arkosic and feldspathic siltstone to fine-grained sandstone.

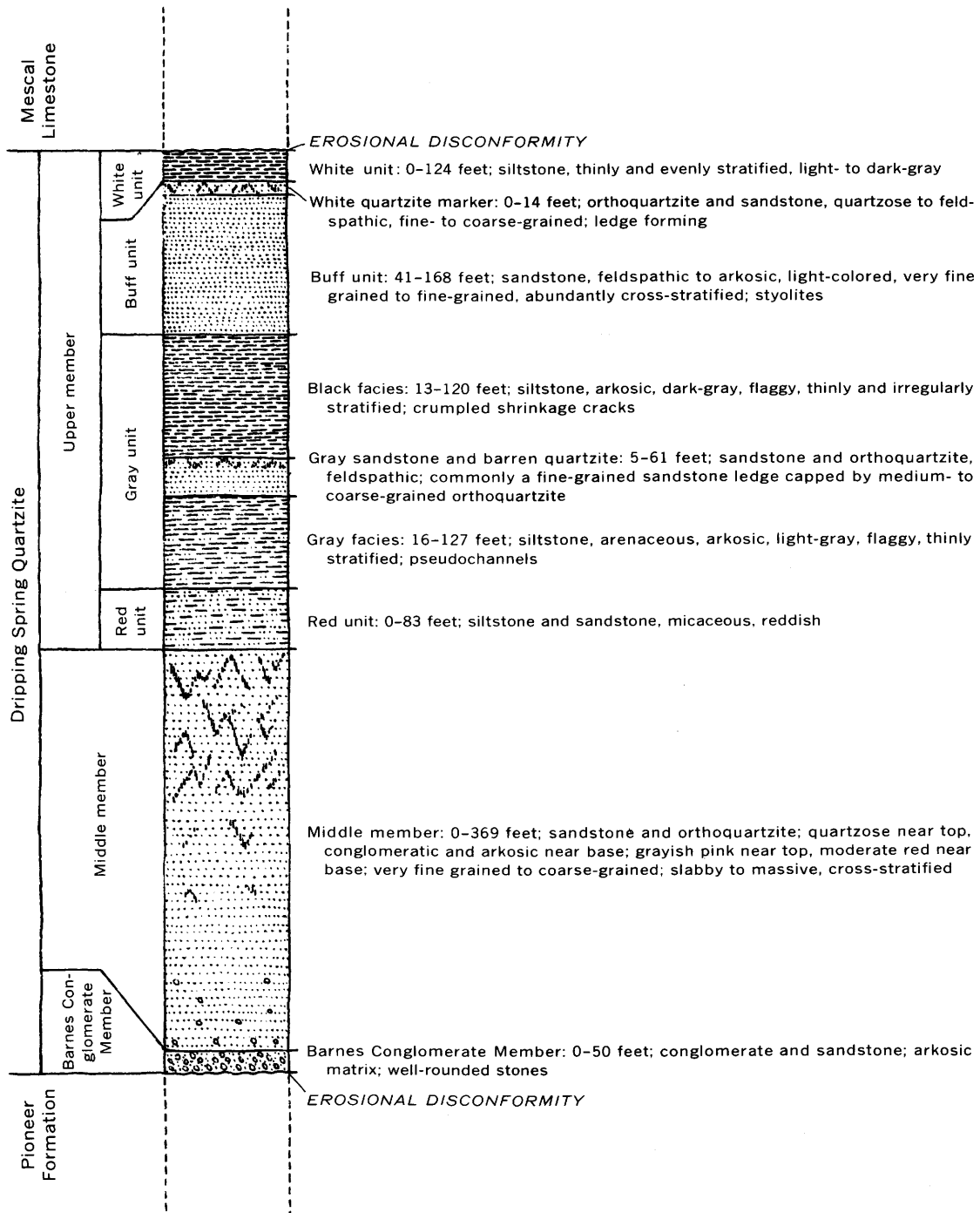


FIGURE 2.—Columnar section of the Dripping Spring Quartzite (Granger and Raup, 1964, fig. 4).

**BARNES CONGLOMERATE MEMBER**

The Barnes Conglomerate Member is a basal conglomerate characteristically made up of quartzose stones (Granger and Raup, 1964) set in an arkosic matrix; it crops out as a grayish-red cliff. In general the conglomerate is from 5 to 20 feet thick; but thicknesses of as much as 55 feet outside Gila County are reported (Ransome, 1919, p. 41), and locally it is missing.

The contact between the conglomeratic Barnes and the underlying shaly Pioneer Formation is readily distinguishable by the abrupt change in lithology. The strata at the contact appear to be generally conformable, but evidence of local angular unconformity and scouring of the contact suggest that the Pioneer was eroded prior to deposition of the Barnes. Paleochannels as much as 2 feet deep that are filled with the Barnes are common in the top of the Pioneer.

The matrix of the Barnes Conglomerate Member is an arkosic to feldspathic sandstone that ranges in grain size from fine to very coarse and averages smaller than medium. The feldspar content ranges from about 15 to nearly 60 percent; iron stain in the feldspar contributes greatly to the general reddish hue of the rock. In general, the matrix is well indurated; joints commonly cut stones as well as the matrix.

The top of the Barnes is generally obvious; the coarse conglomerate commonly stops at a stratigraphic plane above which the arkosic sandstone is only locally pebbly. In some exposures, however, the Barnes grades upward into the sandstone, and the top of the Barnes is arbitrarily drawn where the matrix constitutes more than 50 percent of the rock.

**MIDDLE MEMBER**

The middle member of the Dripping Spring Quartzite in Gila County is typically made up of medium-grained feldspathic crossbedded strata that crop out as bold reddish-brown cliffs, but its character ranges widely. Commonly the member grades upward from a fine-grained and very fine grained moderately well sorted pale-red arkose with argillaceous cement to a medium- and coarse-grained well-sorted moderate-orange-pink orthoquartzite with siliceous cement. In most sections (fig. 2) the middle member ranges from 140 to 369 feet thick, but is locally missing.

Ripple marks, occurring as irregularly spaced cusp-shaped depressions about 4–12 inches across, are sparsely present near the top of the middle member. Shrinkage cracks are even less common than ripple marks and occur in the silty strata that cap graded sets and cosets near the top of the unit. Pockmarked beds are common, particularly near the top of the member. The pockmarks are shallow iron-stained indentations about 1 inch

in diameter and appearing on the weathered surfaces of orthoquartzitic strata. The indentations apparently represent more easily weathered concretionary zones that were cemented by iron minerals rather than by quartz. The middle member is nearly everywhere conformably overlain by the upper member.

**UPPER MEMBER**

The upper member (fig. 2) is a thinly stratified sequence of silty to fine-grained clastic rocks that, in Gila County, ranges in thickness from 180 feet to about 420 feet.

The member is divided into four parts. We have named these, from bottom to top, the red unit, the gray unit, the buff unit, and the white unit. The gray unit, which is the host rock for most of the uranium deposits, is subdivided into the gray facies at the bottom, a gray sandstone capped by a barren quartzite in the middle, and the black facies at the top. Commonly capping the buff unit is a thin light-colored feldspathic sandstone or quartzite. The white unit is very thin or absent at many localities, but it is as much as 124 feet thick in the Workman Creek area.

The contact between the middle and upper members of the Dripping Spring Quartzite can be confidently located in most places on the basis of lithologic changes; changes in topographic expression commonly further aid in determining the contact. Rocks at the base of the upper member are silty to very fine grained, whereas the topmost strata of the middle member are fine to medium grained. The diagnostic compositional feature of the upper member is the abundance of detrital mica in the basal strata. The contact commonly is marked topographically by a change from cliffs in the middle member to ledgy cliffs and slopes at the bottom of the upper member.

**RED UNIT**

The red unit comprises micaceous siltstone and silty very fine grained arkosic sandstone strata that generally are dusky red in weathered exposures. The unit, locally absent, is characterized by its red color and by its content of abundant detrital mica. Thickness of the red unit is 0–83 feet but is generally less than 60 feet.

**GRAY UNIT****GRAY FACIES**

The gray facies of the gray unit is a sequence of thinly stratified feldspar-rich siltstone intercalated locally with very fine grained sandstone; color of the facies is predominantly medium and light gray. Diagnostic characteristics of the facies are the gray color, thin and irregular stratification, slope and ledgy-slope outcrop, and presence of pseudochannels (p. 9). Where pseudo-

channels are not present, the gray facies is commonly difficult to distinguish from the black facies. Thickness of the gray facies averages about 60 feet in Gila County but ranges from 16 to 127 feet in measured sections.

Where the red unit is not present and the gray facies of the gray unit directly overlies the middle member, the detrital mica content of the gray facies is considerably higher than where the red unit is present.

Several uranium deposits occur in gray-facies rocks.

#### GRAY SANDSTONE

The gray sandstone strata commonly present between the gray and black facies of the gray unit are composed of very fine grained to medium-grained feldspathic sandstone and orthoquartzite. The contact between gray-facies rocks and gray sandstone is not everywhere well defined, and locally very little gray sandstone is present. In general the grain size of the sandstone increases upward, as does the percentage of quartz. Toward the top of the sandstone sequence lenticular orthoquartzite strata are common. Thickness of the gray sandstone most commonly ranges from 15 to 35 feet in Gila County.

The most diagnostic features of the gray sandstone are preconsolidated deformation structures, locally present near the base, and topographic expression in relation to the dark siltstone above and below. The sandstone forms cliffs and ledgy cliffs that in most places contrast with the ledges and ledgy slopes formed by the siltstone.

A thin medium-grained and locally coarse-grained quartzite bed, the barren quartzite, caps the gray sandstone. The bed rarely exceed 2 feet in thickness. Both above and below this quartzite, locally, other lenticular quartzite strata may make identification of the barren quartzite somewhat difficult.

Diagnostic characteristics of the barren quartzite are its medium to coarse grain size, apparent lack of lenticularity, light color relative to that of the overlying siltstone, and position at the top of a cliff and below a ledgy slope.

Uranium deposits in immediately overlying or underlying rocks commonly terminate against or are interrupted by the barren quartzite. The quartzite bed rarely contains significant concentrations of uranium minerals.

#### BLACK FACIES

The black facies of the gray unit is mainly a dark-gray thinly and irregularly stratified feldspar-rich siltstone that generally forms ledgy slopes and cliffs. Not uncommonly the outcrop characteristic is smooth rounded ledges; the rounding is due to exfoliationlike

weathering. Thickness of the black facies in Gila County ranges from 13 to 120 feet. Most measured sections range in thickness from 60 to 105 feet, however, and the average is about 77 feet.

The potassium content of black-facies rocks is extremely high (Granger and Raup, 1964) and averages about 10 percent. Study of the rock by X-ray diffraction spectrometer methods indicated that potassium feldspar generally is the major constituent.

Diagnostic features of the rock are the dark-gray color caused by finely divided carbon and pyrite, presence of crumpled mudcracks, thin and irregular stratification, and stratigraphic position below light-colored cliffs.

The black facies is the principal host rock for uranium deposits in the Dripping Spring Quartzite. Most of the deposits are near the base of the black facies, just above the barren quartzite.

#### BUFF UNIT

The buff unit is dominantly a sequence of pale feldspathic to arkosic sandstone intercalated with orthoquartzite. Much of the unit is very fine to fine grained, but the intercalated layers are very fine to medium grained. Commonly capping the buff unit is a feldspathic orthoquartzite bed that corresponds to Kaiser's (1951) "upper white marker." This bed, however, is not sufficiently widespread to be a reliable regional marker bed; locally, two or more such beds occur near the top of the unit. All of these beds are considered to be part of the bluff unit.

Thickness of the buff unit in Gila County averages about 85 feet, but ranges from 41 to 168 feet. Diagnostic features of the bluff are the light color, abundantly cross-stratified sandstone sets and cosets, presence of preconsolidation deformation features in some strata near the base of the unit, and general topographic expression as a cliff above the slope-forming siltstone strata.

#### WHITE UNIT

The white unit is composed of thinly stratified arkosic to feldspathic siltstone. In general the unit is very pale orange to pale yellowish brown, although some exposures of the unit are dark gray near the base.

Thickness of the white unit varies widely in Gila County; in several measured sections it is absent, apparently because of pre-Mescal erosion. Thicknesses are mostly less than 20 feet, but as much as 124 feet of the unit is preserved in the Workman Creek area.

Diagnostic characteristics of the unit are the color, even stratification, and stratigraphic position above the contrasting orthoquartzites in the buff unit and below the Mescal Limestone.

## SEDIMENTARY STRUCTURES

## RIPPLE MARKS

Ripple marks are common in the upper member, particularly in the red unit and the gray facies of the gray unit; a few were noted in the buff unit, but they are uncommon in the black facies of the gray unit and in the white unit. Current and oscillation-wave ripple marks consisting of subparallel ridges and furrows with a wavelength of from 1 to 3 inches are most abundant. Some ripple marks consist of irregularly spaced and shaped cusplike depressions about 4-12 inches across.

## SHRINKAGE CRACKS

Shrinkage cracks, generally filled with very fine grained sandstone, occur in argillaceous and arenaceous siltstone strata throughout the upper member, with the exception of the white unit, where they were not noted. The cracks commonly form a polygonal pattern on stratification planes, but subparallel and randomly oriented patterns are not uncommon.

Where compaction of the enclosing argillaceous rocks has been pronounced, the less compactible fillings have been contorted or crumpled. Crumpled shrinkage cracks commonly are found in the uranium deposits in the black facies.

## PSEUDOCHANNELS

Pseudochannels occur in the lower part of the gray unit and are most abundant near the top of the gray facies. The pseudochannels are alined parallel or subparallel to many of the uranium deposits; this alinement suggests a possible relation between pseudochannels and trends of tension joints that in turn control the uranium deposits.

Pseudochannels (Granger and Raup, 1964) are filled by indurated sandstone cores that are roughly U-shaped in cross section and cigar-shaped in plan and that are embedded in downward and truncated finer grained material. They range in size from several inches in length and an inch in depth to more than 20 feet in length and as much as 3 feet in depth; widths commonly are slightly greater than depths.

The long axes of the pseudochannels are remarkably parallel within local exposures throughout the entire stratigraphic interval that contains pseudochannels. In the northern part of Gila County, the general trend is north-northeast, whereas to the southeast it is more north, and to the southwest it is northeast to east-north-east.

The pseudochannel cores commonly are composed of thin laminae of very fine grained sand or silt that is somewhat cleaner than the enclosing rock. The laminae in the cores are not contorted and commonly are flat

lying; they rarely dip more than 10° relative to the enclosing strata.

The enclosing rock is predominantly very thinly stratified argillaceous siltstone that is feldspar rich and generally dark colored owing to its content of finely divided carbon and pyrite. Many of the laminae have been thinned and truncated against the sides of the cores as well as downwarped around the bottom of the cores.

The origin of the pseudochannels is uncertain. Vaguely similar sedimentary features can be caused by concretions, algae, or preconsolidation deformation, but the dissimilarities between pseudochannels and these sedimentary features are numerous. It is also difficult to regard the pseudochannels strictly as channels because of their striking parallelism through a considerable vertical interval, and because the locally truncated enclosing laminae seem to be greatly compacted rather than scoured.

## PRECONSOLIDATION DEFORMATION FEATURES

A prevalent type of preconsolidation deformation in the upper member resulted in contorted sandstone strata. Local overloading and slumping during deposition probably caused the deformation. The deformed beds generally total less than 4 feet in thickness; some are as thin as 18 inches. The deformed strata, which are truncated at the top, are underlain and overlain by undeformed rock. Most of the contorted sandstone beds are near the base of the gray sandstone of the gray unit and of the buff unit. Deformed strata are present but less common in the red unit and in the gray facies of the gray unit.

## FUCOIDLIKE MARKINGS

Randomly oriented impressions occur on the bedding planes of arenaceous siltstone and very fine grained sandstone strata mostly in the lower part of the upper member. These impressions, called fucoidlike markings, typically from a profusion of shallow elongate impressions (Granger and Raup, 1964, fig. 16) that are commonly about 0.5 inch long, 0.2 inch across, and 0.5 inch deep. They narrow and become shallower toward the ends. Some have an angular outline; others have a somewhat vermicular and more nondescript form.

## STYLOLITES

Stylolites are abundant in the very fine grained sandstone and siltstone of the gray and buff units. They are more easily seen in the buff unit because of their greater amplitude and the lighter color of the rock that encloses them. In the buff unit, stylolites with amplitudes of as much as 2 cm are not uncommon, whereas stylolites in the gray unit generally have amplitudes of 2 mm or

less. In the gray unit as many as 30 stylolites have been counted in a stratigraphic interval of 1 inch.

In fresh rock all the observed stylolites are partly filled with pyrite; in the gray unit carbon is also an abundant constituent. In oxidized rock, however, the stylolites are filled with an iron-stained clay mineral or a chloritelike mineral.

The stylolites are commonly parallel or subparallel to the stratification, but locally a few cut the stratification at high angles.

#### DIABASE

Tremendous quantities of diabase have intruded rocks in the Apache Group throughout most of its outcrop area. Large locally discordant sheets interconnected by dikes are particularly common in the Pioneer Formation, the upper member of the Dripping Spring Quartzite, and the lower member of the Mescal Limestone. In some places the diabase has intruded the Troy Quartzite in a similar manner. Feeder dikes in many places are common in the underlying older Precambrian rocks.

Most of the diabase occurs as massive sheets. Although the sheets are sill-like in general, locally they commonly have discordant contacts; rarely are the sheets truly concordant for more than a few hundred yards. Smaller bodies of diabase form interconnecting dikes between the sheets. In some places, particularly near Superior (Short and others, 1943), large blocks of the Apache Group and Troy Quartzite reportedly have foundered in the diabase sheets. In general, however, these blocks have retained their alignment with the attitudes of surrounding rocks. Despite many irregularities in the sheets and dikes, intrusive forms such as stocks, laccoliths, and chonoliths have not been recognized.

The sheets of diabase range in thickness from a few tens of feet to nearly 1,000 feet. Thin sills and sheets are generally small apophyses from larger bodies. The total thickness of diabase in most sections of the Apache Group is considerably more than 10 percent of that of the sedimentary rocks. In a few sections the thickness may equal or exceed that of the sedimentary rocks (Short and others, 1943). More rarely, diabase is missing.

Interconnecting dikes are rarely more than 200 feet wide; most of them are considerably narrower. Dikes are much less abundant and have far less continuity than the sheets. Their total volume is probably less than 1 percent of that of the sheets.

Distribution and extent of the diabase are controlled by prediabase structures, as is well shown by the Sierra Ancha diabase sheet. This large body of diabase, nearly a thousand feet thick, lies in an area roughly bounded by the Globe-Young road on the west, by Cherry Creek

on the east, and by McFadden Peak on the north. The sheet extends south as far as the southern limits of the Sierra Ancha. At its north end, the diabase sheet abuts a westward-trending prediabase fault. Near its west edge, near the Globe-Young road, the sheet abruptly changes stratigraphic position at a fault near the axis of a large north-trending monocline. The sheet continues west of the monocline but at a lower stratigraphic position, and it probably thins considerably. At its east edge, the sheet apparently terminates or thins abruptly and shifts stratigraphic position near the axis of the Cherry Creek monocline. At its south end, the diabase sheet is exposed by erosion, and its original extent farther south is not known.

At its northwest end, near McFadden Peak, the Sierra Ancha diabase sheet intruded the lower member of the Mescal; near the Parker Creek Experiment Station it intruded the middle member of the Dripping Spring, yet not more than 1 mile away it also intruded the upper member of the Dripping Spring and contains a large xenolith of the Mescal. On the northeast, near Cherry Creek, it intruded the upper member of the Dripping Spring, but generally it intruded progressively higher horizons toward the south. Little is known about the southeastern part of the sheet.

The Sierra Ancha diabase sheet is thicker than most of the other diabase bodies, but its intrusive characteristics are typical. Dikes are generally common at the margins of sheets, and they provided the avenues by which sheets were fed and by which they changed stratigraphic position.

The duration of diabase intrusion may have been lengthy, but no other geologic events were recorded during this interval that provide a measurement of time. Some of the large sheets in the Salt River Canyon near U.S. Highway 60 apparently represent multiple intrusions. There, and near Pioneer Stage Station, we noted discordant diabase bodies with chilled borders that cut earlier diabase sheets. There is no evidence, however, that these intrusions are of significantly different geologic ages; in fact, the similarity in composition of the two diabase bodies near Pioneer Stage Station (Neuerburg and Granger, 1960) suggests that they were derived from the same magma.

The diabase probably intruded the enclosing rocks passively; there is no evidence of rapid forcible injection, such as shattering of the enclosing rocks or intrusive breccia. The diabase apparently slowly welled up through steeply dipping tension structures, such as faults and faulted monoclines, and thence moved outward as huge sheets into thinly stratified weakly cemented rocks. Intrusion rather than extrusion of the sheets might have been exclusively the result of the

capacity of more competent overlying rocks to contain the plutonic pressures, but it might also be related, in part, to the buoyancy of the overlying rocks in the denser diabase magma. Plutonic pressures sufficient to cause the diabase to well up into gravity faults probably were also adequate to cause inflation of the intruded rocks.

Diabase exposures are weathered variably from place to place. In general the diabase is more readily weathered and eroded than are the enclosing rocks. Spheroidal weathering, initiated along joints, is common and ultimately results in a dark-olive friable granular, saprolitic aggregate that encloses a few scattered more resistant, rounded blocks of diabase. In many places, however, as in Salt River Canyon near U.S. Highway 60, parts of some diabase sheets are particularly resistant to erosion and stand as bluffs and cliffs. The surface expression can vary from place to place in the same diabase body for no obvious reason. A diabase sheet locally cropping out as a cliff can grade laterally into a rubble-covered slope. The more salic differentiation facies commonly are more resistant than normal diabase.

The surfaces of resistant diabase exposures, especially spheroidally weathered blocks, commonly have a knobby appearance caused by the resistance of large poikilitic augite crystals. These crystals locally separate as nodules in the saprolite upon strong weathering. Weathered diabase surfaces are not everywhere knobby, however, and the smoother surfaced rocks probably represent subophitic and intersertal textural varieties.

#### PETROGRAPHY

Where fresh, the diabase is typically a tough medium-to dark-gray holocrystalline rock, largely of medium to coarse grain size. Plagioclase, pyroxene, magnetite, and, in some places, olivine are visible in hand specimens. Varieties (tables 1 and 2) range from a dense aphanitic chilled border facies to diabase pegmatite.

For the purposes of this report, the term "diabase" is used to describe mafic intrusive rocks of approximate basaltic composition and having ophitic, subophitic, and intersertal textures. Closely related albite-rich rocks are discussed as differentiation products of the normal diabase.

Fourteen thin sections of diabase from the Sierra Ancha region were studied by C. T. Wrucke for this report. Several additional sections were examined by us and by G. J. Neuerburg. Most of the thin-section specimens were collected from the upper third of the sheets, but enough were collected in the lower two-thirds to provide some information concerning the variation from top to bottom.

The diabase of the Sierra Ancha region is largely a medium-grained ophitic rock, invariably partly altered

but composed principally of calcic plagioclase and augite. Variations in grain size, texture, and mineralogy occur in each sheet, however. Close to the margins of the sheets the ophitic texture grades into subophitic, and the subophitic texture in turn grades into intergranular at the chilled borders. The subophitic diabase has mineralogy similar to that of the ophitic type, but it is finer grained and is restricted to zones near the edges of the sheets. The grain size of the plagioclase generally ranges from 0.002 mm at the chilled selvages to 1.5 mm in the interior of the sheets and locally coarsens to 6.0 mm where the diabase grades into salic differentiates or diabase pegmatite. Rock other than the medium-grained ophitic type, however, constitutes only a minor part of the intrusive material.

In the normal ophitic diabase, olivine is the most common varietal mineral; biotite and hornblende are present in varietal amounts locally but are only accessory constituents in most thin sections. Other common minerals are apatite, zircon, sphene, ilmenitic magnetite, stilpnomelane(?), and chlorite. Pigeonite and hypersthene are present in a few sections but are not abundant.

Plagioclase makes up approximately half the volume of the ophitic diabase. The laths almost invariably have albite twinning; some have carlsbad twinning as well. Great variations in length of laths and in ratio of length to width can be found in most thin sections, but the length of the average lath is 1-4 mm and is three to seven times the width.

Fresh plagioclase in the central part of the laths in 10 thin sections was found to be  $An_{55-71}$ ; in seven of these sections the range was  $An_{62-67}$ . Most laths are zoned, and the outer zone commonly is as sodic as  $An_{40-45}$ , the soda content increasing progressively outward from the core. A few, however, are as sodic as  $An_{29}$ , and apparently the more sodic rims are more abundant in the subophitic textural varieties. In many crystals, zoning is noticeable only near the margin. The anorthite content was determined by the Michel-Levy method and by the method of determining extinction angles in sections normal to a bisectrix. Several determinations made by these methods were checked by use of refractive index oils, which gave compatible results.

Sericite and prehnite are common alteration products of the plagioclase. Both tend to be concentrated along the core of the laths, but this relation is not clearcut in most examples. Both minerals may or may not occur in the same slide. The prehnite forms aggregates of irregular slightly elongate crystals which have clouded margins; only in rare examples does it exhibit the characteristic bow-tie structure.

TABLE 1.—*Chemical analyses of diabase and*

[Table adapted from Neuer-

Sample No. Laboratory No.	Mafic differentiates										
	Chilled selvages					Diabase facies					
	<sup>1</sup> 55N64F C621	<sup>1</sup> 55N65A-1 C622	<sup>1</sup> 74G55 C626	<sup>2</sup> 746	<sup>2</sup> 7806	<sup>1</sup> 57N10A E1940	<sup>3</sup> 130G54 145746	<sup>1</sup> 77G55 C627	<sup>1</sup> 55N65D C623	<sup>1</sup> 55N64A C620	<sup>1</sup> S846A
SiO <sub>2</sub>	42.92	43.33	43.71	47.54	47.76	52.35	43.8	43.91	43.98	45.12	
Al <sub>2</sub> O <sub>3</sub>	14.82	15.61	15.12	11.11	18.62	18.75	15.1	15.56	15.87	13.62	
FeO	3.63	4.10	2.10	6.38	.71	6.61	3.4	2.26	3.38	1.80	
MgO	12.83	11.36	12.07	11.17	10.21	2.33	10.6	12.42	11.61	13.07	
CaO	5.79	5.57	6.14	6.59	4.81	1.83	5.7	6.70	5.42	4.05	
Na <sub>2</sub> O	6.57	7.96	6.75	7.70	6.37	.59	7.6	8.06	7.76	8.16	
K <sub>2</sub> O	2.46	2.94	1.99	2.96	3.52	.25	2.8	2.93	2.94	3.56	3.00
H <sub>2</sub> O	3.06	1.71	4.42	1.21	2.08	12.65	2.2	1.77	2.02	1.77	.33
H <sub>2</sub> O+	.11	.25	.07	.06	.14	.09	2.7	{ .04	.13	.15	
TiO <sub>2</sub>	1.97	1.96	2.05	2.50	2.00	1.49		1.79	2.22	2.08	
CO <sub>2</sub>	4.15	3.61	3.76	2.85	3.00	2.15	3.4	3.40	3.33	4.26	
P <sub>2</sub> O <sub>5</sub>	.04	.01	.01	0.00			<.05	.02	.03	.40	
F	.99	1.17	1.13	.37	.39	.41	1.1	1.04	1.10	1.60	
S	.11	.11	.13					.09	.11	.14	
MnO	.15	.19	.11				.12	.17	.14	.11	
BaO	.23	.21	.36	.26	.30	.13	.21	.20	.20	.22	
Total	<sup>6</sup> 99.87	<sup>6</sup> 99.99	<sup>6</sup> 99.86	100.70	99.91	99.73	99	<sup>6</sup> 100.26	<sup>6</sup> 100.15	<sup>6</sup> 100.04	

<sup>1</sup> Standard rock analysis by F. H. Neuerburg.<sup>2</sup> Standard rock analysis by H. B. Wiik (Williams, 1957).<sup>3</sup> Rapid rock analysis by P. L. D. Elmore, K. E. White, and S. D. Botts.<sup>4</sup> Standard rock analysis by D. F. Powers.<sup>5</sup> A calculated correction was made for FeO present as pyrite based on percent S.

It was assumed that all sulfur is present as pyrite.

<sup>6</sup> Less O for S.

## DESCRIPTION OF SAMPLES

- 55N64F. First half inch of chilled zone of diabase sheet intruded into the upper member of the Dripping Spring Quartzite about 1½ miles southeast of Pioneer Stage Station.  
 55N65A-1. First half inch of chilled zone of diabase dike that cuts the diabase sheet represented by samples 55N64A and F.  
 74G55. Lower chilled zone of the Sierra Ancha diabase sheet in contact with silty basal part of the Mescal Limestone in Warm Creek canyon north of the Red Bluff deposits.  
 746. Lower chilled zone of the Sierra Ancha diabase sheet in contact with upper member of the Dripping Spring Quartzite about 1½ miles south of the Parker Creek Experiment Station. Altitude, 4,500 ft.  
 7806. Upper chilled zone of the Sierra Ancha diabase sheet in contact with hornfels in the upper member of the Dripping Spring Quartzite exposed just below the ore body in Hope adit 1.  
 57N10A. Upper chilled zone of diabase sheet in contact with Pioneer Formation about 1 mile southwest of Theodore Roosevelt Dam.  
 130G54. Diabase from dike in Warm Creek canyon near portal of adit 7, Red Bluff deposits.  
 77G55. Diabase in Sierra Ancha diabase sheet about 30 ft above 74G55.  
 55N65D. Diabase from the same dike as sample 55N65A-1, about 5 ft in from the chilled zone.  
 55N64A. Diabase about 100 ft in from the chilled zone of the same diabase sheet as sample 55N64F.  
 742. Diabase from the lower half of the Sierra Ancha diabase sheet about 75 ft above sample 746. Altitude, 4,575 ft.

Augite constitutes close to half the volume of some specimens, but in most it accounts for no more than about 40 percent. It mostly occurs as nearly equidimensional crystals 5–20 mm in diameter, but some of the crystals are as much as 4 cm in diameter. It includes both plagioclase and olivine ophitically. Its optical properties are not precisely known, but the 2V is near 55° in every section studied, and  $Z \wedge c$  ranges from –43° to –47°. Much of the augite is pleochroic— $X+Y$ =pale pinkish brown,  $Z$ =colorless—but some of it is colorless and nonpleochroic. Most crystals have an irregular mottled extinction. Twinned individuals with (100) as the twin plane are present but are not abundant. Zoning is evident in a few specimens.

Augite commonly is altered to hornblende or to mixtures of hornblende, green biotite, and chlorite. Brown biotite also has formed from augite but is not so abundant as hornblende of the same origin. Green stilpnomelane (?) may be a principal alteration product of augite in the vicinity of Salt River canyon west of U.S. Highway 60 and at Chrysotile, but more work is needed to confirm this opinion. The stilpnomelane (?) was identified principally on the basis of its similarity to biotite and its distinct but poor micaceous cleavage.

Hypersthene, the only orthopyroxene present, was found in eight of the sections studied. It occurs as anhedral crystals averaging 0.25 mm in diameter, and it has the characteristic pleochroic colors of pale pink and pale green. Much of the hypersthene occurs as irregular embayed crystals at the edge of olivine crystals. Both hypersthene and olivine are badly altered in most sections, so it is difficult to determine the original size of the hypersthene grains or whether they partly or completely surrounded the olivine. In one section, seven small separate hypersthene grains showing optical continuity are present around the edge of three closely spaced olivine crystals in an area 2 mm in diameter. This relation suggests that the original hypersthene at least partly enveloped the olivine crystals and that its crystals may have been considerably larger than the average size of the grains now present. Hypersthene crystals associated with olivine, and some that are not, exhibit schiller structure: extremely fine closely spaced striae—probably exsolved augite lamellae—parallel to the  $c$  axis. Hypersthene that occurs along basal partings in augite is clear and does not have striations. None of the hypersthene shows ophitic relations with plagioclase. The distribution of hypersthene is not well known,

its differentiates, in percent, Gila County, Ariz.

burg and Granger (1960)]

Mafic differentiates—Continued				Salic differentiates								Aplite facies		
Diabase facies—Continued				Syenite facies				In diabase				In hornfels		
<sup>2</sup> 742	<sup>3</sup> 89G55 145754	<sup>2</sup> 738	<sup>2</sup> 722	<sup>3</sup> 105G54 145741	<sup>3</sup> 106G54 145742	<sup>4</sup> 56G54/A D1689	<sup>3</sup> 96G54 145740	<sup>1</sup> 56G54/B C624	<sup>1</sup> 74G54 C625	<sup>4</sup> 95G54 D1690	<sup>3</sup> 51G55 145751	<sup>3</sup> 53G55 145752	<sup>3</sup> 56G55 145753	
45.94	46.4	47.11	47.24	46.6	46.9	47.90	52.6	54.43	55.39	58.81	65.3	68.7	77.0	
17.50	18.5	20.28	15.95	13.2	13.0	12.71	14.2	14.89	14.75	14.71	15.3	14.5	11.3	
3.41	1.1	1.14	2.48	3.2	1.8	3.73	3.8	1.16	1.42	3.29	1.4	1.3	.74	
9.46	8.6	7.33	9.25	8.4	12.2	9.02	10.2	6.91	<sup>5</sup> 9.36	5.85	2.2	1.2	.21	
6.62	11.0	9.17	8.03	5.8	4.9	4.83	1.4	2.75	2.01	1.46	1.0	.30	.56	
8.60	8.8	9.67	9.92	11.8	9.0	9.97	5.2	6.98	3.45	2.87	3.2	.60	.55	
2.79	2.5	3.09	2.81	3.0	3.0	3.11	4.5	5.00	4.57	5.09	6.5	.74	.54	
.87	.47	.29	.81	.60	1.5	2.00	3.3	2.38	4.06	3.73	3.3	11.4	8.4	
.02 }	1.1 {	.03	.06 }	2.1	2.3 {	.25 }	1.6 {	.13	.24	.40 }	.57	.74	.80	
2.30	1.0	.69	2.14	3.3	4.3	3.90	2.0	2.58	1.33	1.27 }	.73	.41	.42	
0.00	<.05	0.00	0.00	.08	<.05	0.00	.07	.10	.12	0.00	.41	<.05	<.05	
.44	.16	.12	.26	.40	.50	.48	.70	.90	.54	.47	.16	.08	.04	
.23	<.04	.14	.09	.23	.14	.20	.13	.11	.17	.09	<.04	.84	<.04	
				.38	.27	.33	.36	.19	.29	.14	.06	.02	.02	
100.25	100	100.47	100.33	99	100	99.77	100	<sup>6</sup> 100.01	<sup>6</sup> 99.77	99.54	100	100	101	

- 89G55. Diabase from Sierra Ancha diabase sheet exposed in cut along Globe-Young road about 3½ miles south of Workman Creek.  
 738. Diabase above sample 742. Altitude, 4,700 ft.  
 722. Diabase above sample 738. Altitude, 5,120 ft.  
 105G54. Coarse-grained syenite from layer about 30 ft below the upper contact of the Sierra Ancha diabase sheet near the Hope deposits.  
 106G54. Medium-grained syenite about 3 ft below the upper contact of the Sierra Ancha diabase sheet and above sample 105G54. This is part of a body that occupies the position normally occupied by a chilled zone.  
 56G54/A. Medium-grained syenite from a layer about 15 ft thick in diabase along the Workman Creek road between the Hope deposits and the Jon adit.  
 96G54. Coarse-grained syenite from a layer just above the large xenolith of basal part of the Mescal Limestone that contains the Suckerite deposit in the Workman Creek area.  
 56G54/B. Coarse-grained syenite facies from same locality as that of 56G54/A.  
 74G54. Medium-grained syenite that occupies the normal position of the chilled zone at the top of the Sierra Ancha diabase sheet in the bed of Workman Creek near the Jon adit.  
 95G54. Medium-grained syenite that occupies the normal position of the chilled zone at the top of a diabase body exposed about 1 mile southwest of the Red Bluff deposits. Siltstone in the overlying upper member of the Mescal Limestone is converted to hornfels.  
 51G55. Aplite dike, 4–6 in. wide, in the Sierra Ancha diabase sheet near the Hope deposits. The attitude of the dike is nearly vertical, and it penetrates the upper contact of the diabase about 50 ft above the sample locality.  
 53G55. Same aplite dike as sample 51G55, but taken where the dike intrudes hornfels in the Dripping Spring Quartzite about 15 ft above the diabase sheet.  
 56G55. Aplite from a north-trending dike, 6 in. wide, in hornfels in the Dripping Spring Quartzite near the Jon adit.

but these studies suggest that it is not confined to the chilled phases and the lower third of the sills, as Walker (1940, p. 1072) reported for the Upper Triassic Palisade Diabase in New Jersey.

Pigeonite was found in only three thin sections. It is colorless, and in habit it is similar to augite, as it occurs in equidimensional crystals which ophitically include plagioclase. The pigeonite crystals, however, are smaller than the augite crystals in the same sections; they are 1–2 mm in diameter whereas the augite crystals are as much as 10 mm across. Identification was based on the small (+)2V, estimated to be 5°–20°. Birefringence and refractive indices seem to be close to those of augite, but definitive data were not obtained from thin sections, principally because the mineral resembles augite so closely that a distinction can be made only if interference figures are obtainable.

Olivine is a common constituent of the diabase but was present in varietal amounts in only a few of the thin sections studied. Investigations of outcrops have shown that olivine is abundant in some sills, especially in their lower half; so it is probably more common as a varietal mineral than petrographic work has indicated. Most of the olivine occurs as rounded crystals, 1.0–1.5 mm in

diameter; in some thin sections a few subhedral crystals are present. Most subhedral outlines are relict, the original olivine having been partly or completely replaced by alteration products. Well-formed crystals are more abundant near the chilled zones than in the ophitic rock. A few of the crystals are twinned. No zoned olivine has been found.

Refractive indices of four olivine crystals were determined by use of index oils. Remarkably close results were obtained, as  $\beta$  was found to be 1.730–1.735, which indicates a composition of  $\text{Fa}_{37-40}$  according to the diagram of Deer and Wager (1939, p. 21). Further work on the olivine in diabase of Gila County might reveal a greater range in fayalite content than is given here.

Olivine is surprisingly fresh in many sections, even in those that contain partly altered plagioclase and augite, though some of the olivine is altered in the freshest specimens. A green to brownish-green fibrous mineral tentatively identified as bowlingite is the most abundant alteration product; chlorite is common, whereas talc and iddingsite are present in very small amounts and are not found in most specimens. Minute granules of magnetite in a sogenetic web pattern are present where

TABLE 2.—*Typical properties of diabase and related differentiates*  
 [Primary and alteration minerals listed in order of decreasing abundance]

	Diabase				Related differentiates		
	Chilled selvages	Border phase	Interior phase	Pegmatites	Syenite facies	Aplitic facies (in diabase)	Black deuteritic veins
Texture	Intergranular	Intergranular to subophitic.	Subophitic to ophitic.	Ophitic	Hypidiomorphic granular.	Xenomorphic granular.	Xenomorphic granular to fibrous.
Grain size.	Very fine	Fine	Medium	Coarse to very coarse.	Medium to very coarse.	Fine	Very fine.
Color	Melanocratic	Melanocratic	Melanocratic	Melanocratic	Mesocratic to leucocratic.	Leucocratic	Melanocratic.
Primary minerals.	Calcic plagioclase, augite, hyperssthene, olivine, iron, iron ores (?).	Calcic plagioclase, augite, olivine, hypersthene, pigeonite, apatite, sphene, ilmenomagnetite, zircon.	Calcic plagioclase, olivine, augite, hypersthene, pigeonite(?), apatite, sphene, ilmenomagnetite, zircon.	Calcic plagioclase, augite, hornblende (?), ilmenite, apatite.	Alkalic plagioclase, augite, hornblende, orthoclase, apatite, sphene, ilmenomagnetite, zircon.	Albite, microcline, quartz, augite, apatite, sphene, ilmenite, zircon.	Hornblende, biotite, chlorite, zircon.
Alteration and deuteritic minerals.	Biotite, iron ores, clays, unidentifiable fine aggregate.	Biotite, hornblende, chlorite, sericite, prehnite, magnetite, bowlingite, serpentinite, tremolite, stilpnomelane.	Biotite, hornblende, chlorite, sericite, prehnite, magnetite, bowlingite, serpentinite, tremolite, stilpnomelane.	Biotite, sericite, leucoxene, pyrite.	Hornblende, biotite, sericite, pyrite, pyrrhotite, galena, chalcopyrite.	Hornblende, epidote, chlorite, biotite, pyrrhotite, galena, chalcopyrite.	Deuteritic minerals constitute the primary mineralogy.

the mineral is badly altered. In a few thin sections the original olivine has been completely replaced, but its former presence is attested to by the size and shape of the altered patches and in most sections by the presence of magnetite and bowlingite(?)

Amphibole is widely distributed, but in most specimens it occurs as a minor constituent of the ophitic diabase. Green hornblende is the most plentiful type, but tremolite and a blue-green amphibole occur in a few thin sections.

Green hornblende occurs principally as an alteration product of augite, but some of it may have crystallized among the early formed pyroxene grains. It occurs in elongate anhedral crystals and in columnar slightly plumose aggregates. Most of the hornblende has the pleochroic scheme  $X$ =very pale brown (nearly colorless),  $Y$ =brownish green,  $Z$ =green. The axial angle is large and negative. In a few sections a blue-green amphibole that has pleochroic colors similar to those of green hornblende is present, except that  $Z$ =blue green. It is probably a variety of hornblende, for the  $2V$  is large and negative, as in the green hornblende. A few specimens, particularly in some altered diabase, have the scheme  $X$ =brownish green,  $Y$ =green,  $Z$ =deep blue green. These crystals are negative also but have a smaller  $2V$ , estimated to be no greater than  $30^\circ$ , which is much smaller than that of the green hornblende.

These properties are similar to those of some varieties of the soda amphibole arfvedsonite, but the trace of the axial plane is parallel to the cleavage rather than normal to it, as in the soda amphibole. The crystals in which  $Z$ =deep blue green are therefore believed to be a variety of hornblende.

Tremolite, occurring in aggregates of fine needles as an alteration product of pyroxenes, was the only other amphibole identified.

Brown biotite, like hornblende, is a varietal mineral in some of the diabase, but in much of the rock it is only an accessory constituent. It is a varietal mineral only in the chilled borders, but it is a relatively abundant accessory mineral where diabase grades into albite-rich differentiates and commonly occurs partly or completely surrounding crystals of ilmenitic magnetite. In chilled borders in the Workman Creek area brown biotite poikiloblastically encloses other rock-forming minerals. Flakes of red biotite are present in a few specimens that also contain the brown variety.

Apatite and ilmenitic magnetite are the most common of the other minerals that occur as accessory constituents of the diabase; both are present in nearly every thin section. The term "ilmenitic magnetite" is used because under reflected light in thin section the opaque ore mineral appears to be striated and to have two components, and the abundance of leucoxene as an alteration product

indicates the presence of titanium. Ilmenitic magnetite occurs in subhedral form and as skeletal crystals.

Many minerals occur in small amounts. Sphene is a common accessory mineral but is not found in some specimens. Zircon, though a minor accessory constituent occurring as anhedral crystals generally less than 0.05 mm in diameter, is conspicuous because of the pleochroic halos, commonly in biotite or chlorite, that surround it. Small rounded quartz grains were seen in a few specimens, some of which contain olivine. Serpentine and chlorite minerals occur only in minor amounts as alteration products of mafic minerals, but field observations indicate that serpentine may also be abundant in some areas.

The chilled border rock has an intergranular texture consisting of a felted mass of slender plagioclase laths, mostly from 0.25 to 0.70 mm in length, and a very fine grained mixture, principally of augite, biotite, and iron ore, between these laths. The plagioclase is sodic labradorite. Olivine is present in some specimens as a constituent of this mixture and as phenocrysts as much as 0.15 mm in diameter. Hypersthene is present at the upper chilled border of the diabase in the Workman Creek area. Much of the iron ore is in slender rods about half as long as the plagioclase laths. A conspicuous feature of all but one specimen of the chilled-border rock studied is the abundance of biotite derived from augite; some of the biotite in the coarsest intergranular rocks also occurs molded between other crystals. The presence of abundant biotite as an alteration mineral indicates that unaltered chilled-border rock may be uncommon.

Most of the diabase has been deuterically altered. Alteration was commonly found to be negligible in the central parts of thick sheets and was indicated largely by sparse biotite around magnetite grains. Rocks within 150 feet of the top and 100 feet of the bottom of sheets are generally intensely altered, regardless of sheet thickness. Effects of alteration increase gradually toward the margins of the diabase bodies, although highly altered layers isolated within the central part of thick sheets interrupt this progression. In the outer part of diabase bodies, pyroxene is increasingly altered to fibrous green hornblende, chlorite, epidote, and serpentine; olivine is altered to magnetite and to minerals that resemble bowlineite and talc. Plagioclase is moderately to strongly sericitized and albitized. Near contacts, mafic minerals are almost entirely altered to hornblende, chlorite, biotite, and magnetite; plagioclase is sericitized or replaced by potassium feldspar. Within a few feet of contacts, especially upper contacts, biotite is abundant.

Some of the chilled-selvage diabase samples (table 1) have exceptionally high contents of potassium and iron

and low contents of silicon, magnesium, calcium, and sodium relative to most olivine diabases and basalts. Neuerburg and Granger (1960, p. 771-773) have shown that this apparently anomalous chemical composition of the more highly altered parts of the diabase bodies need not necessarily predicate an unusual magma composition or assimilation of the enclosing rocks. Although the extremely high potassium content of sample 57N10A (table 1) is almost certainly the result of reactions with the wallrock, the high potassium content of much of the marginal diabase apparently is partly the result of deuterian alteration rather than the formation of a granophytic residuum, which is more common in many diabase bodies elsewhere in the world. The uncommonly low content of silicon and the high contents of potassium and iron correlate with abundant alteration minerals, such as biotite, sericite, magnetite, and chlorite, that have a low silicon content, high potassium content, and (or) high iron content. Neuerburg and Granger (1960, p. 773) pointed out that the average composition of the homogeneous equivalent of the entire diabase system (the approximate composition(?) of the original magma) is similar to that of the "average olivine gabbro" given by Nockolds (1954, table 7, No. 3).

A specimen of rare diabase pegmatite collected in the Salt River canyon near U.S. Highway 60 and examined by Neuerburg proved to be mineralogically similar to normal diabase. The original composition of the pegmatite was estimated to be augite (about 80 percent), labradorite (13 percent), ilmenite (2 percent), and minor but common apatite. About 5-10 percent of alteration and secondary minerals consist of leucoxene, pyrite, sericite, clay, blue-green amphibole, and red-brown biotite.

The texture is very coarsely ophitic, and inch-sized augite grains poikilitically enclose plagioclase crystals which average about 2 mm wide by 10 mm long. The augite appears to partly replace the plagioclase; this replacement results in an unusual texture, similar to that of myrmekite.

#### DIFFERENTIATION FACIES

Leucocratic salic facies and thin black hornblende-bearing veins are common diabase differentiates in many places, particularly in the upper third of thick sheets. The general trend of differentiation (table 1) seems to have been toward alkali enrichment, which resulted in albite-rich rocks. At the close of the differentiation history in some places, however, apparently a significant volume of residual fluid enriched in iron, calcium, and magnesium but low in silica content escaped, in part, from the diabase bodies.

Salic differentiates of the diabase may be divided into two types, both of which are alkalic. The older of these is a heterogeneous group of albite-hornblende and albite-augite rocks called the syenite facies. The other type, which may have been derived from the syenite facies, is a more uniform group of aplitic rocks called the aplite facies.

#### SYENITE FACIES

The syenite facies is made up of a type of albite-rich rocks which might more properly be called albite diabase, albite pegmatite, granophyre, and albite syenite. They are grouped here because they seem to be closely related genetically, and any given albite-rich body may contain several textural and mineralogic types.

The syenite facies generally occurs as sill-like bodies (fig. 3) within the upper third of diabase sheets, but it also occurs locally in the lower parts. Most are subparallel to the borders of the enclosing sheet. Dikes of the syenite facies locally extend a few tens of feet into the enclosing sedimentary rocks. In many places in the Workman Creek area, a sheet of rock of the syenite facies occupies the position of the upper chilled border of the Sierra Ancha diabase sheet.

Invariably the syenite facies has characteristics of an intrusive rock. In many places, particularly where short dikes cut the Mescal Limestone, the relations are undoubtedly intrusive. Many of the sill-like bodies, however, are gradational into the enclosing diabase and probably represent deutereric metasomatism of the original diabase. Evidence for deutereric metasomatism is strong in an area where a chilled border of a large diabase body is absent and its position is occupied by a layer of the syenite facies.

The syenite facies is almost invariably more resistant to weathering and erosion than is the enclosing normal diabase; hence, it commonly stands in relief. It may stand out on diabase outcrops as randomly oriented or subparallel ribs ranging from an inch wide to cliffs 20-30 feet high and hundreds of feet long.

Surfaces of syenite facies outcrops are generally smooth and rounded, possibly owing to spheroidal weathering governed by joints. The rock is lighter colored than the associated diabase, partly because of the lighter color of the plagioclase and partly because of the larger size of the leucocratic mineral grains.

Megascopically, the syenite facies ranges from medium-grained ophitic rock slightly more leucocratic than the enclosing diabase to very coarse grained pegmatitic rock that has textures ranging from intersertal and subophitic to xenomorphic granular and, rarely, porphyritic. The most common variety is a medium-to coarse-grained hypidiomorphic granular rock that

contains hornblende, magnetite, and somewhat-lath-shaped white, pink, or light-greenish-gray plagioclase. Either hornblende or augite, or both is visible in all the rocks. Magnetite is generally visible, and apatite, biotite, and pyrite are common. In some places in the Workman Creek area, particularly at the top of the diabase sheets just below hornfels, pyrrhotite, galena, and chalcopyrite are present but may represent epigenetic mineralization.

Microscopically, the textures of the syenite facies are seen to range from ophitic to granular, and they include subophitic, intersertal, and micrographic varieties. Two or more of these textures commonly are present in a single thin section or hand specimen.

Albite generally is the characteristic mineral of the syenite facies. Other essential minerals are either augite or hornblende, or both. Accessory minerals consist generally of biotite, apatite, titaniferous magnetite, and pyrite. Very small amounts of zircon and sphene may be present. The albite is invariably altered.

Albite in the syenite facies is ordinarily no more calcic than  $An_6$ . Although it generally occurs as anhedral laths which are at least three times as long as wide, equidimensional and irregularly shaped grains are not uncommon. Some of the albite is rimmed with later microperthite that also occurs as discrete grains.

In some specimens the cores of the plagioclases are more strongly altered than the rims. In many specimens the alteration products are saussuritic, perhaps, indicating that the cores were more calcic than the less altered rims. In other sections there is little if any evidence of either calcic cores or a more calcic original plagioclase.

Augite, present in most specimens, is slightly or almost entirely uralitized. The augite is commonly colorless but may be slightly brown or pink. It is subhedral to anhedral and in ophitic varieties forms the largest grains present. The augite is biaxial (+) and has an optic axial angle of about  $55^\circ$  and an extinction  $Z \wedge c$  that apparently ranges from about  $40^\circ$  to  $47^\circ$ .

The chemical compositions of samples of the syenite facies are shown in table 1. The facies is distinguished chemically from the normal diabase principally by greater contents of silica, soda, and potassia and by less total iron, alumina, magnesia, and lime. Microperthite, biotite, and sericite contain most of the potassium.

The change in the soda and lime contents of the rock as compared with those of normal diabase may not seem adequate to develop albite to the exclusion of more calcic plagioclase. Presumably, this is because much of the calcium is utilized in the saussuritic alteration minerals, such as prehnite, and perhaps in part by uralitization. Very likely some of the varieties of the syenite

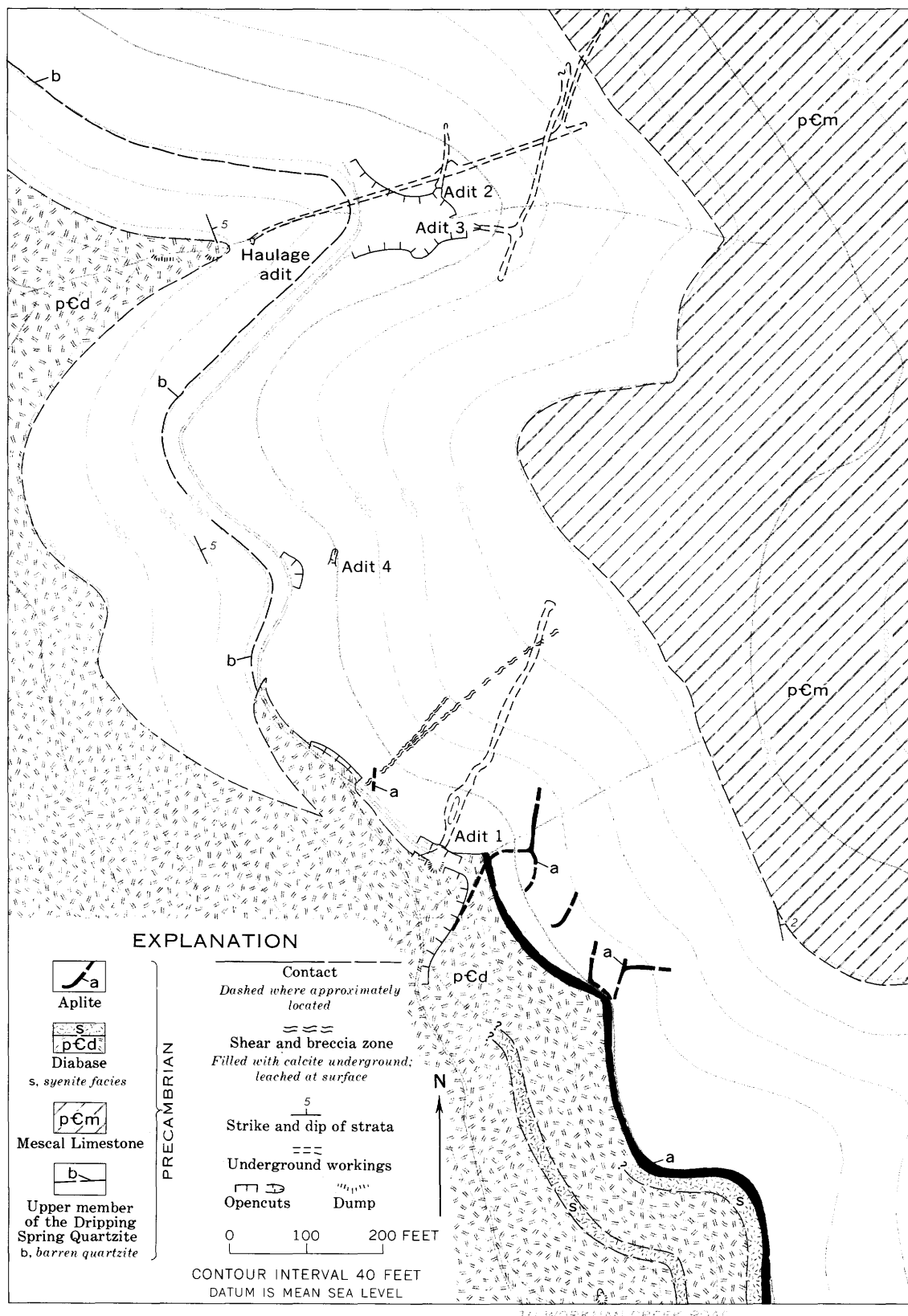


FIGURE 3.—Geology in the vicinity of the Hope deposits.

facies are a result of soda metasomatism by late-stage magmatic solutions. Slight additions of soda and silica and alteration of the plagioclase and pyroxene, might well result in a rock corresponding to the syenite facies by the tying up of the calcium in alteration minerals and by the releasing of most of the sodium for formation of albite. We believe that this reaction took place at the margins of most bodies of the syenite facies but that the central parts of these bodies were probably injected as a hydrous, reactive, intermediate-stage magma. Shrinkage related to cooling of the diabase presumably created the openings along which the fluid was injected.

#### APLITE FACIES

Aplite dikes are very sparse to locally common in the diabase, particularly in the upper third of large sheets. More rarely, the dikes are in the basal few tens of feet of the overlying sedimentary rocks in places such as the Workman Creek area.

A characteristic feature of the aplite facies is an abrupt change of composition (table 1), mineralogy, and texture where a dike crosses the contact between diabase and rock of the Dripping Spring Quartzite. Within the diabase the aplite is made up of a leucocratic rock in which alkali feldspar, particularly albite, is the major constituent. These rocks are mostly light gray or pink and fine grained and have a nearly saccharoidal texture. Aplite intruded into the Dripping Spring, however, contains more quartz than aplite intruded into the diabase; some of the quartz locally forms intergrowths with the feldspar; albite is a minor constituent, and potassium feldspar is abundant. Even aplite dikes that are composed dominantly of albite in the diabase (fig. 4A, B) abruptly change to a potassium feldspar-rich rock where they intrude the Dripping Spring.

Most aplite dikes are less than 2 feet wide; nearly all are less than 6 inches wide where restricted to the diabase, and some are nearly microscopic.

The areal distribution of aplite dikes is not well known. Nowhere are they very abundant in the diabase. Most aplite dikes we saw are in the Sierra Ancha diabase sheet, although they have been reported elsewhere in diabase by Bishop (1935) and A. F. Shride (oral commun., 1955). More than half the aplite dikes that we saw are in the Workman Creek area. Several of these had intruded a few tens of feet into the hornfels of the overlying Dripping Spring Quartzite.

Narrow stringers or veins of aplite less than a quarter of an inch wide are present in the diabase in many places. These commonly branch and are inconsistent in strike and dip. Wider dikes of aplite in the diabase, however, rarely branch except for a few narrow short

apophyses; and they seem to have relatively consistent strike, dip, and thickness. Aplite dikes that intrude the Dripping Spring, in contrast, commonly branch or form en echelon patterns. Most dikes, particularly those in the Dripping Spring (fig. 3; pl. 1), seem to have a general northward trend.

In the Workman Creek area and at the Sorrel Horse and Big Six deposits on the west side of Cherry Creek, the aplite forms sill-like bodies, particularly between diabase and the Dripping Spring. These bodies are recognized over outcrop distances of hundreds of feet. Aplite is intermittently traceable southeastward from the Hope adit 1 (fig. 3) to Workman Creek. The aplite sills are generally less than 10 feet thick, and they characteristically enclose many small hornfels xenoliths. The xenoliths are so abundant in some places, particularly at the Sorrel Horse and Big Six properties, that the rock might more properly be called an aplite-cemented hornfels breccia. In most places the breccia fragments and xenoliths are disoriented, or at least have been moved enough to make displacement unquestionable. With the exception of a few small feeder dikes, the contact between the aplite sills and diabase appears to be sharp and unbroken.

In the diabase, the aplites apparently formed by crystallization of a magmatic fluid, although gradational contacts of approximately 0.1 inch indicate at least a small amount of replacement at the margins of the dikes. Little evidence is found to support any hypothesis that the aplite dikes may be rheomorphic or replacement dikes similar to those described by Goodspeed and Fuller (1944) and Goodspeed (1948).

Where the aplite intruded the Dripping Spring it also seems to have been emplaced largely in open spaces rather than exclusively by rheomorphic or replacement action. Undoubtedly, however, the aplite-forming fluids were highly reactive and by some means derived potassium and silica from the wallrocks while sodium was being expelled.

The petrography of the aplite dikes enclosed by diabase is relatively simple. The texture invariably is xenomorphic granular (fig. 4A), and the grain size averages about 1 mm. Although most of the aplites are nearly equigranular, one specimen from a roadcut near the Sierra Ancha Experiment Station contained ragged-edged elongate microcline grains as much as 4.5 mm long and 0.5 mm across.

Albite forms the textural framework of most of the aplite and makes up about 70–90 percent of the rock, but in some specimens the feldspar is almost exclusively microcline. The microcline aplites may be more common in the central parts of the diabase bodies, but the albite aplites are more common near the borders. This suggests

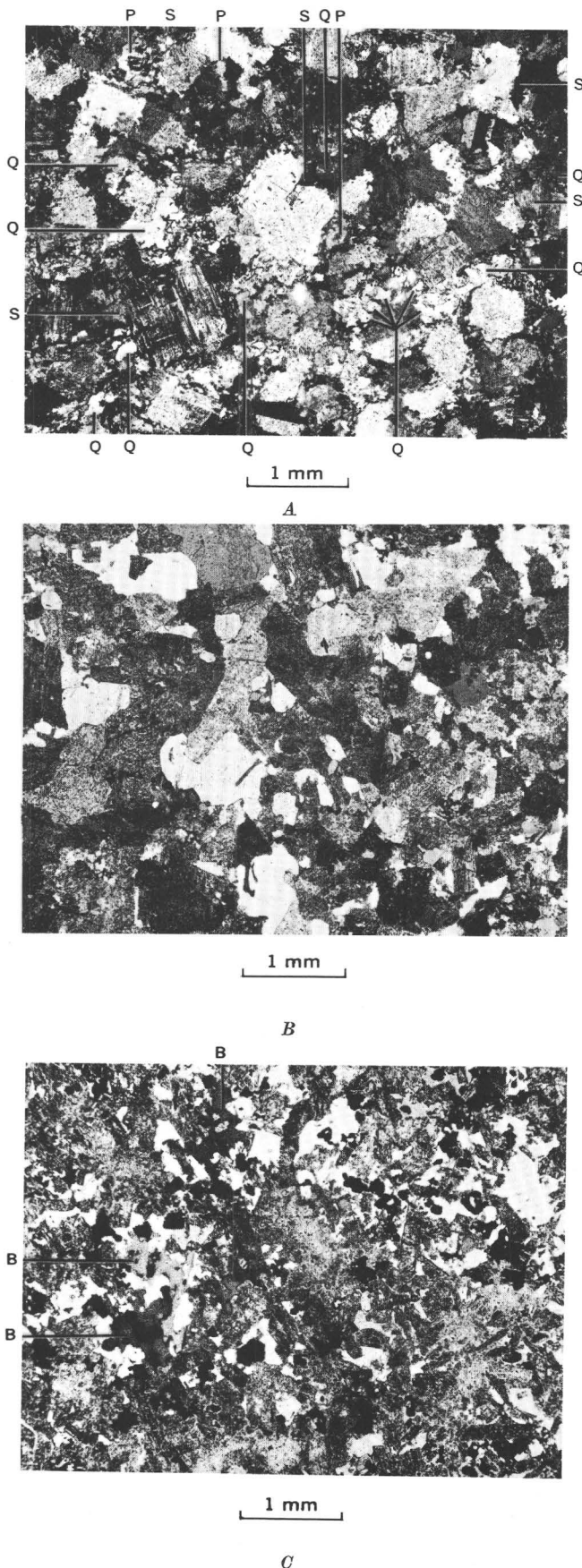


FIGURE 4.—Texture of aplites. *A*, Dike that cuts diabase. Sample 51G55, collected in bed of Workman Creek about 75 feet below top of diabase sheet. Albite makes up most of the field. Some of the larger quartz (Q), pyroxene (P), and sphene (S) grains are marked. The rest are small and scattered. X-ray studies indicate the presence of two feldspar phases. The dominant phase is a nearly pure albite. The subordinate phase is a triclinic potassium feldspar with  $Or > 90$  (the 201 peak is broad). Chemical analysis of the feldspar fraction gave  $Na_2O = 8.21$  percent,  $K_2O = 3.86$  percent. The feldspar is twinned on the albite, pericline, and carlsbad laws and is probably an X-ray perthite. Partly crossed nicols.  $\times 18.3$ . *B*, Dike that cuts hornfels. Sample 53G55, collected about 10–15 feet above diabase in dike illustrated in *A*. Between this sample and the sample illustrated in *A* the albite is rimmed and partly replaced by potassium feldspar. Replacement in *B* is nearly complete, and the dusty light-gray to nearly black grains are all triclinic (X-ray determination) potassium feldspar. The clear gray to white grains are quartz. Minute pyroxene grains scattered along the feldspar grain boundaries are too small to distinguish in the photomicrograph. The feldspar in this sample contains 14.6 percent  $K_2O$  and 0.77 percent  $Na_2O$ . Partly crossed nicols.  $\times 18.3$ . *C*, From sill-like body that interfingers with hornfels just above diabase. Sample 61G55, collected at the portal of the Jon adit. One of a large variety of textures manifested by aplite where it penetrates hornfels. Most of the groundmass is potassium feldspar (dusty gray). Quartz is clear light gray to white. Black grains are pyrrhotite. *B*, largest ragged biotite flakes.

a series that ranges from albite aplite to microcline aplite.

Quartz, where present, occurs as small grains interstitial to the feldspar. It ordinarily makes up considerably less than 15 percent of the rock.

Original femic minerals in the rock invariably are altered, probably deuterically, but a little pale-green augite remains locally. The most common alteration product is fibrous pleochroic green hornblende, but epidote, chlorite, and clays are also present. Together these compose as much as 25 percent of the rock but generally much less.

Apatite and interstitial anhedral sphene are accessory minerals in most specimens.

Where the aplite is intrusive into the Dripping Spring, both texture and mineralogy change abruptly. The texture (fig. 4*B*, *C*) is much less uniform and ranges from aplitic to micropegmatitic. Although hand specimens ordinarily appear aplitic, thin sections disclose a variety of symplectitic textures. In some specimens the feldspar forms a xenomorphic symplectitic framework in which the quartz evidently made room for itself interstitially by replacement of the feldspar along grain boundaries. In contrast are other textural varieties in which the feldspar forms a nearly panidiomorphic framework and the quartz merely fills the interstices.

Grain size in the aplite enclosed by the Dripping Spring also varies more widely than in the aplites enclosed by diabase. The average grain size, however, is about 1 mm, similar to that of aplites enclosed by diabase.

Potassium feldspar and quartz are the most abundant constituents of aplites in the Dripping Spring and ordinarily constitute 90 percent or more of the rock. The feldspar, as determined by X-ray, is largely microcline, although a monoclinic phase was present in some samples taken very near diabase. In these samples some of the feldspar grains have a small  $2V$ , indicating that sanidine formed locally near diabase. The feldspar, although generally anhedral, is locally euhedral against quartz, and it crystallized earlier than the quartz. Most of the other minerals that compose the rock occupy the interstices and partly replace the potassium feldspar.

Quartz varies greatly in abundance in the aplite that is intrusive into the Dripping Spring; in some places it makes up as much as 50 percent, in others as little as 10 percent. Generally, it either fills the interstices between hypidiomorphic feldspars or forms abundant rounded grains that are disseminated throughout and partly replace the feldspar framework. Locally, it forms a well-developed micrographic intergrowth with the feldspar.

Varietal minerals are pyroxene, albite, and biotite. Albite formed both earlier and later than potassium feldspar. Where the aplite passes from diabase into Dripping Spring Quartzite, relict albite is commonly rimmed and is partly replaced by potassium feldspar. Farther from the diabase, sparse albite of a later stage replaced the potassium feldspar at grain boundaries and interstices. Some small grains of albite enclosed by potassium feldspar may represent exsolution.

Pyroxene is present in most places, but biotite generally occurs where pyroxene is absent; both were not seen in the same specimen. The pyroxene occurs as clear rounded grains and stubby prisms that rarely exceed 0.2 mm in diameter and average about 0.05 mm—much smaller than the feldspar grains. The pyroxene grains commonly form aggregates clustered both within feldspar crystals and along feldspar-grain boundaries. These aggregates appear to have a synneusis texture in some specimens. The pyroxene ranges from colorless to light green and was determined by its optical properties to be augite, possibly diopsidic.

Brown biotite was noted only in a few pyroxene-free aplites. Aggregates and synneusis textures, however, were absent from these aplites, and crystal relations indicate that biotite formed later in paragenetic sequence than the potassium feldspar.

Sphene, ilmenite, apatite, and zircon are accessory minerals. Pleochroic brown sphene was present in

nearly every specimen and generally forms small anhedral grains along feldspar-grain boundaries. Euhedral grains are extremely sparse. The sphene evidently developed largely by replacement of feldspar, but a few completely enclosed grains in the plane of the thin section suggest that some could have formed before, or simultaneously with, the feldspar. Ilmenite forms skeletal grains partly altered to leucoxene and commonly bordered by sphene. Ilmenite is sparse, however, and its paragenetic position is not well defined, although it apparently is earlier than albite. Apatite is sparse except in specimens taken near diabase, where the mineral occurs as needles that penetrate most of the other minerals. Zircon is very sparse, but where present it is generally enclosed in either biotite or sphene.

Pyrrhotite may also be an accessory mineral, although it probably is a secondary mineral along with pyrite and other sulfides. Each of these sulfides appears to be late and to occupy interstices and minute vugs in the feldspar mesh. They are probably later than quartz but seem to be closely associated with it.

Alteration minerals such as chlorite and nontronitic clay are present in most samples. Chlorite is most common as a replacement of biotite and pyroxene, but it occurs in albite in some places. Pleochroic green nontronitic clay generally was introduced epigenetically, and it seems to be associated with the sulfide minerals. It occurs as aggregates and veinlets that cut or replace most of the other nonopaque minerals.

A paragenetic sequence of minerals and their content in the aplites, determined from the examination of several specimens from the Workman Creek area, are shown below:

[Dashed lines indicate indefinite position in sequence]

Mineral	Percent	Sequence of formation	
		Time	→
Original albite-----	0-90	—	
Augite-----	0-20	—	—
Potassium feldspar-----	0-80	—	
Biotite-----	0-5	—	
Ilmenite-----	0-3	—	—
Zircon-----	0-Tr	—	—
Sphene-----	1-10	—	—
Albite-----	0-5	—	—
Quartz-----	10-50	—	—
Pyrrhotite-----	0-4	—	—
Chlorite-----	<2	—	—
Pyrite-----	<1	—	—
Nontronite-----	<5	—	—
Leucoxene-----	<2	—	—

Rock analyses of the aplites are shown in table 1. As the silica and alkali oxide contents increase from diabase through syenite in the development of aplites, the total iron oxide, magnesia, lime, phosphate, and titania contents seem to decrease concurrently. As the

dikes leave the diabase and enter the Dripping Spring Quartzite, the total alkali oxide content does not change much, but the ratio of soda to potassa changes abruptly.

#### BLACK DEUTERIC VEINS

The term "deuteric vein" is used to refer to a type of narrow vein or dikelike body that cuts the diabase. Such bodies are made up of locally abundant black stringers less than a quarter of an inch wide. These veins or stringers are composed of late-magmatic-stage rock-forming minerals that fill joints, particularly in the upper parts of diabase sheets. One narrow pink stringer was observed in the Workman Creek area, and it consisted of nearly pure "bow tie"-textured prehnite that cut one of the syenitic rocks.

Black deuteric veins are largely made up of a dark-greenish-black amphibole fracture filling, generally less than 2 mm thick and ordinarily bounded by a dark zone less than 1 cm wide.

The abundance of deuteric veins varies considerably from place to place. The greatest concentration was found in the diabase dike along Warm Creek canyon (fig. 16); figure 5 shows a swarm of particularly abundant short subparallel veins in that area. Elsewhere in the dike, many of the deuteric veins are traceable for several tens of feet but the veins are not so abundant. Most of the deuteric veins in the Warm Creek canyon dike strike northward, subparallel to the walls of the dike, but transverse veins are common.

In the Workman Creek area, black deuteric veins are common but not so abundant as at Red Bluff. Ordinarily they are spaced several tens of feet apart, and

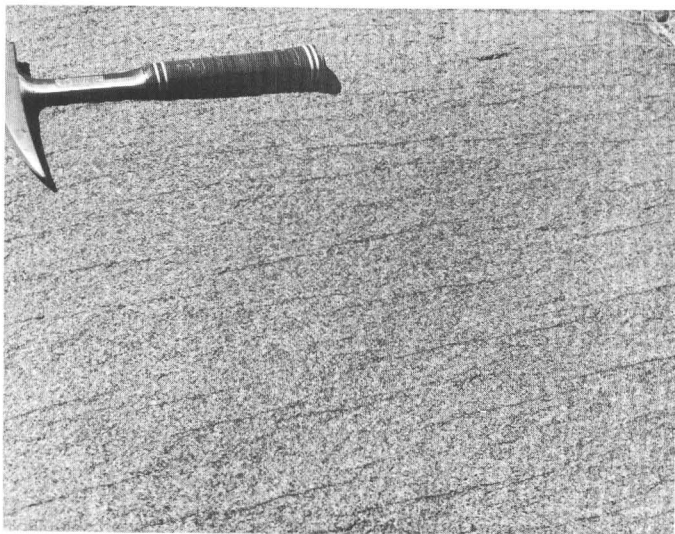


FIGURE 5—Swarm of short black deuteric veinlets in diabase dike. The veinlets are oriented subparallel to the walls of a diabase dike that cuts the Dripping Spring Quartzite in Warm Creek canyon on the Red Bluff claims.

parallelism is much less obvious than in Warm Creek canyon. Although they strike in all directions, those that have north-northeast and west-northwest strikes appear to be more prevalent.

The deuteric veins were also noted in the lower Cherry Creek area and in the Salt River canyon near U.S. Highway 60. In most places they are not readily seen unless the diabase is very well exposed and its surface only slightly weathered. For this reason black deuteric veins may have gone unrecognized in many areas.

In addition to the ordinary black deuteric veins, veins in which the central core is nearly black and the border zone is lighter have been reported by Neuerburg and Granger (1960). Some of these are deuteric veins in which mafic minerals have been abstracted from the adjacent diabase, leaving a selvage depleted in mafic constituents, but others seem to be narrow aplite stringers in which the original joint reopened, permitting the dark core to be deposited. Perhaps the ultimate development of this latter type of vein is the one noted in an aplite dike 2–6 inches wide in the Workman Creek area, where the central part of the dike contains a later green fibrous hornblende vein filling that pinches and swells from a hairline to 0.7 inch in width.

The black deuteric veins are simple in composition and consist of, in addition to fibrous amphibole, lesser amounts of chlorite, biotite, and zircon. The amphibole makes up 70–95 percent of the vein filling and forms the textural framework. It is also abundant in the border zone, where it largely replaces pyroxene in the diabase. The texture of the vein filling is ordinarily fibrous and felted, but in some veins the amphibole locally has isolated cores consisting of single crystalline grains bordered by subradiating curved fibers (fig. 6A). The amphibole is hornblende that has optical properties that are somewhat variable from vein to vein. Ordinarily the hornblende is pleochroic green:  $X$ =pale greenish brown to pale yellow brown;  $Y$ =pale brownish green;  $Z$ =green. The extinction  $Z \wedge c$  ranges from about  $14^\circ$  to  $22^\circ$ . Indices are approximately 1.66, but they were not precisely determined; birefringence is generally low second order in thin sections of normal thickness. Qualitative tests made with a spectrometer indicate that the hornblende contains appreciable sodium; no quantitative analyses were made.

Associated with the hornblende, and commonly appearing to have formed in part by replacement of the hornblende, are grains of brown biotite. Chlorite, which generally shows anomalous blue interference colors, has somewhat the same relations to the hornblende as does the biotite. Some grains of hornblende contain ragged

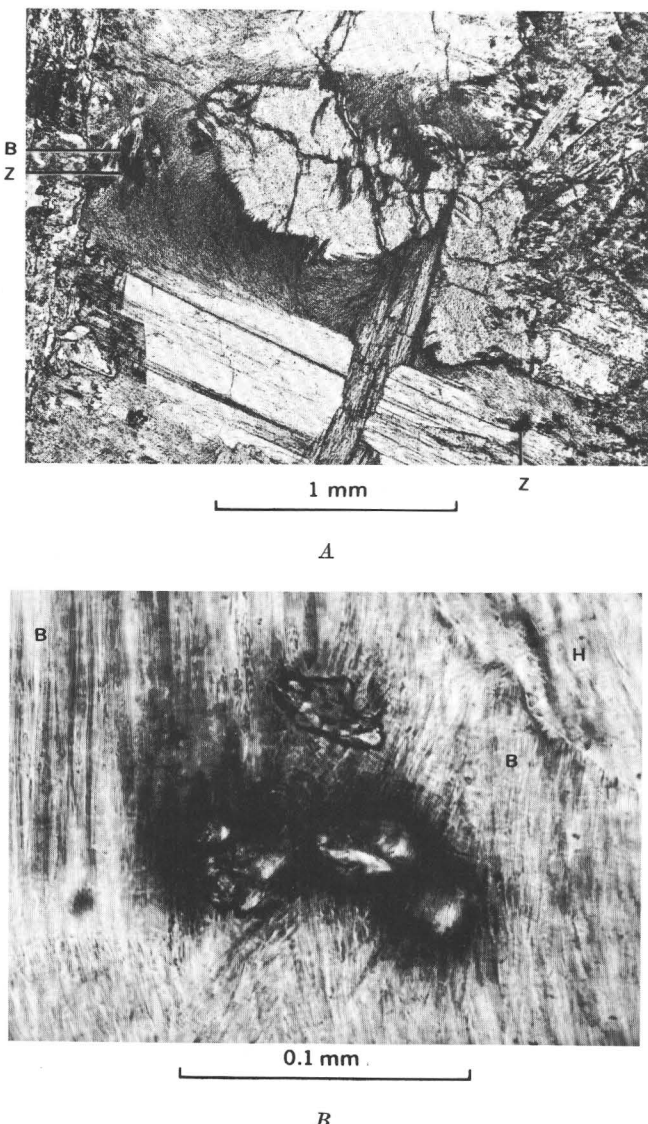


**FIGURE 6.**—Black deuteritic veinlet and associated zircon grains. *A*, Veinlet. Sample 83G56, collected from the Sierra Ancha diabase sheet in Workman Creek valley. The veinlet extends from top to bottom. Deuterically altered diabase can be seen on both sides of the photograph. Except for minor biotite (*B*) and zircon (*Z*), the veinlet is filled with hornblende. Note the plumose hornblende filling the interstices around hornblende crystals. Plane-polarized light. *B*, Zircon grains surrounded by pleochroic halos in deuteritic veinlet. Zircon cluster on left side of field of *A* under greater magnification. The radioactivity of zircon grains has produced radiation damage in both biotite (*B*) and hornblende (*H*) in *A*. Plane-polarized light.

patches of biotite and chlorite in which cleavages are aligned and boundaries are gradational. This relation also is evident in the felted fibrous amphibole, and it suggests that much of the chlorite and biotite formed from the hornblende.

Stubby prismatic zircon crystals (fig. 6*B*) about

0.02–0.07 mm long are present in most specimens. They are generally enclosed by either amphibole or biotite and are surrounded by dark pleochroic halos. The halos range in width from 0.015 to 0.025 mm, and they are almost certainly caused by uranium decay. Halos of this width probably are too narrow to indicate that the radioactivity is caused by the presence of thorium.

The average abundance of zircon in the deuteritic vein filling is far greater than that in the normal diabase. Although some parts of veins, and perhaps some individual veins, contain no zircon, it is not unusual for thin sections of a vein to contain about one zircon crystal per 2 square millimeters. This abundance of zircon is probably several hundred times its abundance in normal diabase. The border zone of the black deuteritic veins, in which pyroxene of the diabase appears to have been altered to a hornblende similar to the vein hornblende, also contains abnormal amounts of zircon, which is, however, more sparsely disseminated than in the vein filling.

To measure the alpha radioactivity of the zircon, stripping film was applied to a thin section of a black vein from the Workman Creek area. The film was developed after a 24-day exposure. Although all the zircon crystals were surrounded by pleochroic halos, few of them emitted more than two alpha tracks in the 24-day period. Strangely, however, 25 tracks were recorded on the film above one zircon grain about 0.03 by 0.05 mm that was embedded in hornblende of the border zone about 7 mm from the vein. The hornblende, zircon, and pleochroic halos appeared to be identical with those within the vein filling. No explanation is apparent for the anomalous radioactivity of this zircon grain.

#### CLASSIFICATION

Black deuteritic veins might ordinarily be classified as lamprophyres. In some characteristics, however, the veins differ from many so-called lamprophyres: they are not porphyritic, nor do they contain alkali feldspar or fractured crystal grains. The presence of hornblende in the border zone, apparently identical with the hornblende in the vein filling, suggests the effects of pervasive fluids on formation of minerals. The abundance of almost exclusively hydrous minerals such as hornblende, biotite, and chlorite suggests a water-charged transporting fluid.

The evidence suggests to us that the black deuteritic veins were formed by very late stage hydrothermal (deuteritic) solutions derived by the differentiation of the diabasic magma. The veins may be, in a sense, diaschistic; however, the aplites, their leucophytic counterpart, are earlier in every observed relation, and no clearcut diaschistic relation exists.

## SIGNIFICANCE

Neuerburg and Granger (1960) believed that the original diabase magma somehow lost uranium during its cooling history. The aplites and syenites are richer in uranium than are other facies of the diabase, but no evidence can be found that they served to transport uranium from the cooling diabase bodies. The amount of uranium now contained in them is not great enough to account for the loss of uranium from the original magma (Neuerburg and Granger, 1960). If the aplite-forming fluids did carry more uranium than is now present in the aplites, such content cannot now be proved.

A tentative hypothesis to explain the loss of uranium from the diabase magma is that the uranium was expelled through the channelways now filled by deuterian veinlets. Mafic igneous rocks are generally notably poor in uranium, yet here is an ultramafic material containing evidence, in the form of pleochroic halos, that uranium was at least locally abundant. The normal course of crystallization of an igneous rock should result in the expulsion of any uranium in excess of that which cannot be contained in the lattice of the rock-forming minerals. In this rock, zircon was formed and could contain at least a part of the uranium, but we believe that more uranium was in the mafic fluids than could be accommodated by the zircon formed. We postulate, therefore, that the water not utilized in formation of the hydrous vein minerals was expelled from the system and carried uranium with it. Such elements as silver, copper, lead, yttrium, and ytterbium could also have been expelled if they were concentrated in excess of amounts that could be accommodated by the crystal lattices of rock-forming minerals. The validity of this explanation will be further tested in the parts that follow. (See also Neuerburg and Granger, 1960.)

## DIFFERENTIATION HISTORY

The differentiation history of the large diabase bodies in the Apache Group is interpreted from extensive field and laboratory data. These data indicate that the differentiation sequence comprises a pyrogenic phase and a deuterian phase (Neuerburg and Granger, 1960), which, in part, overlap. During the pyrogenic phase, rock minerals were in approximate chemical equilibrium with the remaining magmatic fluids, but during the deuterian phase such equilibrium was not maintained. The deuterian phase is represented by deuterian veinlets and deuterically altered rocks of the diabase system. Syenite and aplite facies all have an overprint of deuterian alteration.

During intrusion of the diabase magma, a thin layer of quickly cooled rock, possibly glass, formed against

the enclosing sedimentary rock. This layer effectively sealed the remaining magma, at least temporarily, into a closed system. Early cooling was fairly rapid and produced, from the chilled border inward, a few inches to a few feet of fine-grained diabase; gradually the rate of cooling slowed as the temperature differential was distributed across a thicker and thicker layer of rock. As the cooling continued, olivine crystallized within the magmatic fluid and by gravity differentiation tended to concentrate below the central part of the diabase sheets. The gravitational concentration of the olivine, however, was less pronounced than in many diabases of other areas, and no dunite or peridotite layers were formed. There was, however, within the rock, some obscure layering of the facies that were slightly more plagioclase rich, coarser grained (pegmatitic), or olivine or pyroxene rich. Some of these facies were destined to be conspicuous later because of their greater susceptibility to deuterian alteration. When the diabase body had become somewhat rigid owing to the crystallization of calcic plagioclase and pyroxenes, a residual fluid in the interstices of the rock-forming minerals remained largely in the hotter, central part of the body. This fluid was alkalic and contained iron and magnesium and a considerably greater concentration of minor elements than did the original magma.

Thermal contraction in the outer parts of the diabase bodies forced the residual liquids into dilatant layers, principally parallel to the margins, where they initially formed the syenites. The variety of syenitic rocks resulted from the diversity of conditions at this time. Limiting factors were the pressure and temperature differences between the dilatant zone and the zones from which the residual fluids were drawn, as well as the stage of development of the fluid at the time of dilatancy. Although the syenites were largely a result of direct crystallization, the residual fluids were out of equilibrium with the new environment, and some reactions with the wallrock were inevitable.

Thermal contraction continued and, perhaps augmented by regional structural adjustments, formed fractures into which drained the residual fluids that had not already been drawn into the syenite layers as well as the fluids which had not been utilized in syenite formation. Dikes of syenite and aplite formed from these fluids. Locally, dikes extended into the enclosing rocks outside the diabase bodies. In each such occurrence, solidification of the dike once more sealed the entire diabase body into a closed system. Fluids not drawn into these intrusive units continually reacted with the earlier formed diabase and syenite. New minerals in equilibrium with the remaining fluids were formed at the expense of the earlier minerals, and

these generally were poorer in silica and richer in potassa than were the original minerals. Destruction of earlier minerals such as olivine and pyroxene, and perhaps calcic plagioclase resulted in release of iron, magnesia, and lime. Minor elements in the residual fluids were, in some places, taken up by the newly formed alteration minerals, but for the most part they probably were retained in the fluid phase. During this period the residual fluids were continually undergoing a change that resulted in corresponding changes in the alkali ratio (potassium : sodium) of the aplite dikes. These fluids probably became progressively more sodic as more and more potassium was bound up in the deuterio alteration minerals. The fluids from which the aplites formed also became more silicic, but the silica probably did not much exceed that held by alkali feldspar.

At the end stage of diabase cooling an abstraction of the mafic constituents from the residual fluid somehow occurred, perhaps by the direct crystallization of the alkalic constituents as aplite dikes. As thermal contraction continued, numerous joints formed and the rock fabric loosened to finally and permanently open the diabase system. The residual solutions drained from the diabase along these small fractures, depositing along them only those minerals, such as amphiboles, chlorite, and biotite, that were stable in the diabase system at the prevailing temperatures. Each diabase body was drained fairly uniformly over its entire surface.

These phases of the differentiation sequence were not necessarily progressive chronological steps throughout each diabase body. Local differences in cooling rates related to the volume-surface ratio or any extraneous event, such as local early or late fracturing, would upset the normal pattern so that different stages in the sequence might be reached at the same time in different parts of the same diabase body. Hence, conflicting age relationships between aplite dikes and deuterio veinlets, for example, can be expected.

#### AGE

The age of the diabase has been a subject of controversy for many years. Unfortunately for the attempt to clarify the age, diabase of vastly different ages reportedly (Ransome, 1919) intruded the Apache Group in the same areas.

In this report, diabase refers only to the diabase that forms large sills and related bodies in the Troy Quartzite, Apache Group, and older rocks. This diabase is known to have intruded only the Troy and older rocks; in some places Cambrian and Devonian sedimentary rocks were deposited on the eroded surface of the diabase sheets. Diabase bodies that intruded the Paleozoic

and Mesozoic rocks are generally of small size and reportedly are almost invariably dikes rather than large sills.

Very likely the intrusion of the great sheets that constitute the diabase persisted for several tens of thousands of years, but it is herein considered as one intrusive episode. (See p. 10.)

The ages proposed by others for the diabase have ranged from Precambrian through Tertiary. This diversity in proposed ages is probably a result of (1) inaccurate dating of the Troy Quartzite; (2) confusion in the distinction between the diabase discussed in this report and later diabase bodies; and (3) inaccurate dating and interpretation of structures and topographic expression presumed to be related to diabase intrusion. Ransome (1903, p. 38) and Short, Galbraith, Harshman, Kuhn, and Wilson (1943) classified the diabase as post-Middle Cambrian in the belief that all the rocks that had been included under the term "Troy Quartzite" were Middle Cambrian or younger, although Short agreed that the diabase is pre-Late Devonian. Ransome (1919, p. 56) apparently assumed that all the diabase was of one age, and, as narrow diabase dikes intruded Paleozoic limestones in the area he studied, he concluded that all the diabase was post-Pennsylvanian. Peterson, Gilbert, and Quick (1951, p. 34, 35) presented evidence that the large diabase bodies in the Castle Dome area are post-Pennsylvanian in age. Certainly the reported relations indicate the existence of post-Naco (Pennsylvanian) diabase, but they do not prove that all the diabase was limited to one period of intrusion. If the large bodies of diabase in the Castle Dome and Globe areas of central southeastern Arizona are, indeed, post-Pennsylvanian, this is very unusual; elsewhere in southeastern Arizona the large bodies of diabase can be readily proved to be of at least pre-Devonian age (Darton, 1925, p. 34, 257; Short and Ettlinger, 1926; Carpenter, 1947; Cooper, 1950; Huddle and Dobrovolny, 1952).

Sharp (1956) suggested that the large diabase sheets are Tertiary (?) in age. He noted that parts of an erosion surface in the Sierra Ancha were uplifted where underlain by a thick diabase sill. Because the erosion surface was interpreted to have been formed in Tertiary time, Sharp concluded that the intrusion of the diabase occurred in Tertiary (?) time. We believe that this erosion surface is controlled by certain resistant stratigraphic layers in the Troy Quartzite and that the planation of overlying rocks down to this stratigraphic position was different from any process of peneplanation that would be necessary to support the views of Sharp.

The evidence is conclusive that many of the large diabase sheets are overlain, in depositional contact, by rocks

originally referred to as Troy Quartzite (Darton, 1925, p. 34; Carpenter, 1947) and as Martin Limestone (Cooper, 1950; Huddle and Dobrovolny, 1952). There is now little doubt, however, that the rocks similar to Troy deposited on erosion surfaces cut in the diabase can be correlated with the Bolsa Quartzite or Abrigo Formation of Cambrian age (Krieger, 1961).

Other approaches to determining the age of the diabase are based on radioactive-isotope methods. One of these approaches is based on the assumption that uraninite was deposited in fractures in hornfels and mobilized hornfels(?) that were formed by heat and emanations from the diabase. Isotopic-age determinations of this uraninite should, therefore, give at least a minimum age for the diabase. If our hypothesis that the uranium was derived by differentiation at a late magmatic stage of the diabase is correct, then the diabase and uraninite are of approximately the same age. The best approximation of the age of the uranium deposits based on the isotopic analyses of uraninite and galena (see p. 76) is that all are older than 1,000 m.y. Hence, we are convinced that the large diabase sheets related to the uranium deposits, and probably most of the other large diabase sheets known to have intruded the Apache Group, are Precambrian in age. Substantiation of our conclusions comes from L. T. Silver (1960), who determined the minimum lead-lead age of zircon in a leucocratic differentiate of the Sierra Ancha diabase sheet in Reynolds Creek to be 1,075 m.y. In addition, Paul Damon, of Arizona University, reportedly (A. F. Shride, oral commun., 1963) obtained comparable ages by the potassium-argon method from biotite in similar rocks from the same locality.

#### EFFECTS OF METAMORPHISM

Cooling and solidification of huge masses of diabase magma that were intruded into the Apache Group necessitated the transfer of an immense quantity of heat into the surrounding rocks. Conditions were then ideal for metamorphism of any wallrock minerals that are unstable at high temperatures. Very little study has been devoted to metamorphic effects of the diabase other than that of serpentization which culminated in the development of chrysotile asbestos in the Mescal Limestone. Even this process is little known but has been receiving much attention in recent years (A. F. Shride, oral commun., 1958).

Metamorphic effects of the diabase were not very widespread or intense. Possibly this is because of the "dry" nature of the magma. Fluid matter expelled from the magma during most of its cooling history may have been scant or it may have been expelled only locally.

#### DRIPPING SPRING QUARTZITE

Metamorphism of the Dripping Spring Quartzite is most prevalent in the Sierra Ancha, where hornfels has been formed in the upper member at several places adjacent to the diabase. Elsewhere, metamorphism is negligible. Near Superior, Ariz., Galbraith (1935) noted that "In the Dripping Spring quartzite, the metamorphism is confined to a baking and darkening of the rocks for a few feet at the most on either side of the intrusive \* \* \*." Harshman (1940) stated that only a few miles away "\* \* \* a narrow zone of baked reddish-black quartzite is the only effect produced on the Dripping Spring quartzite by the intrusion of the diabase. This zone is rarely over 12 to 18 inches wide and in some places is missing." In the Ray-Miami areas Ransome (1919) noted that quartzite of the Dripping Spring is "exceptionally hard and well indurated" near large diabase bodies. To our knowledge, there is nothing in the literature earlier than 1919 that describes the metamorphosing effect of diabase on the upper member.

Contact metamorphism of the upper member of the Dripping Spring adjacent to diabase has resulted in a rock assemblage with apparently unique characteristics. The gray unit of the upper member has few presently known counterparts, and, therefore, metamorphism of this abnormal rock has resulted in rocks peculiar to south-central Arizona.

The contact action of diabase against the gray unit was not consistent from place to place. Metamorphic effects are barely detectable at many contacts, but locally the rocks are strongly affected for tens of feet. There is some evidence that the diabase bodies contain a greater quantity of differentiated alkalic facies near the more highly metamorphosed rocks. At Workman Creek, the best example of this type of contact action, widespread sheets of soda-rich syenite are found near and at the top of the diabase sill. In addition, aplite dikes are more abundant in the Dripping Spring above the contact in this area than in any other known area. Probably water and other volatiles that must have accompanied the concentration of diabase differentiates were instrumental in effecting metamorphism of the Dripping Spring.

The products of metamorphism of the upper member of the Dripping Spring are varied but may be classified primarily as hornfels and spotted rocks. Hornfels and related rocks are invariably formed near the diabase contact. Spotted rocks may also be present near diabase but are just as common more than 100 feet from diabase. Presumably the spotted rocks represent a lower degree of metamorphism than do the hornfels and related rocks.

Hornfels in the Dripping Spring is known almost exclusively from the Sierra Ancha region. Much of it is near the large diabase sheet in the southern Sierra Ancha.

Normal hornfels is most common and is characterized by total recrystallization but almost no attendant increase in grain size. Locally there is a coarser grained, possibly recrystallized, facies of the hornfels herein called coarse-grained hornfels. In some places the coarse-grained hornfels forms separate laminae in a mass of normal hornfels giving rise to a distinctly layered rock called lit-par-lit hornfels.

Hornfels and related rock are host rock for some of the richer uranium deposits in the Workman Creek and central Cherry Creek areas, and, therefore, a thorough understanding of the genesis and properties of hornfels is necessary.

#### NORMAL HORNFELS

Normal hornfels is considered in this report to be a fine-grained dense tough rock formed by the complete recrystallization of very fine grained sandstone and siltstone that are adjacent to diabase intrusives. Much of the Apache Group has been partly recrystallized and cemented by authigenic overgrowths without appreciable change in original mineral content. Most hornfels, however, is characterized by the presence of sphene, pyroxene, and, locally, biotite, none of which exists in the original rock. Pyrrhotite is the common sulfide in the hornfels in contrast to pyrite in the unaltered siltstone. These differences may be suspected in the field, but only with the aid of a microscope can much of the hornfels be positively distinguished from normal siltstone. Limited data indicate that the specific gravity (table 3) of hornfels is greater than that of the rock from which it formed.

Primarily, hornfels in the Apache Group results from the thermal metamorphism of susceptible sedimentary rocks without appreciable increase in grain size. Original planes of stratification are preserved (fig. 7A) and are indicated by slight differences in texture, grain size, and mineralogy. The rock most susceptible to metamorphism is the highly potassic gray unit of the upper member of the Dripping Spring. Hornfels in the black facies generally retains the dark-gray color of that facies, but in the gray facies it is commonly medium gray to very light gray.

In the Workman Creek area and on the Grand View claims, hornfels formed extensively in the black facies. At the Black Brush, Sorrel Horse, and Citation deposits it is mostly in the gray facies. The stratigraphic position of the hornfels in both places is largely due to the intrusive horizon of the diabase. Hornfels has also been noted in the gray unit just above diabase on hill 5132

#### SPRING QUARTZITE, GILA COUNTY, ARIZONA

TABLE 3.—*Specific gravities of selected rocks*

[Measurements by D. Todd and F. B. Moore]

Rock	Number of samples	Specific gravity	
		Range	Average
Chilled diabase.....	8	2.62–2.98	2.79
Normal diabase.....	13	2.89–3.04	3.0
Syenite.....	5	2.93–3.14	3.03
Aplite (cutting diabase).....	7	2.53–2.65	2.57
Aplite (cutting hornfels).....	8	2.46–2.64	2.55
Lower member, Dripping Spring Quartzite.....	5	2.50–2.60	2.54
Black facies, Dripping Spring Quartzite.....	6	2.24–2.53	2.39
Normal hornfels (black facies).....	3	2.67–2.78	2.71
Coarse-grained hornfels (black facies).....	3	2.53–2.80	2.65
Mobilized hornfels (?).....	8	2.51–2.59	2.56

(Rockin straw Mtn. quadrangle) about 1.3 miles north of the Red Bluff deposit. It may be present locally but was not positively identified at the Red Bluff, Lucky Boy, Suckerite, May 1, Fairview, and other deposits that are near diabase.

Silty facies of the Mescal locally take on a hornfels-like appearance adjacent to diabase. The dolomitic siltstone at the base of the Mescal is recrystallized below the diabase in the bottom of Warm Creek canyon a few hundred yards north of the Red Bluff deposits. On the crest of a low hill about a mile southwest of Red Bluff, the silty strata of the upper member of the Mescal have been altered to a hornfelslike rock.

Hornfels seems to be most common near large structural features, such as the Sierra Ancha and the Cherry Creek monoclines, and near large bodies of differentiated diabase. The diabase sheet in the southern Sierra Ancha, near which most of the hornfels is found, is nearly 1,000 feet thick. This sheet also contains an abundance of alkaline differentiates near and at its upper contact in the Workman Creek area. Sodic aplite is common as dikes intrusive into the hornfels in the Workman Creek area and as extremely irregular dikes and breccia cement just above the diabase in the Citation and Sorrel Horse area. A sill-like body of coarse-grained syenitic diabase separates the metamorphosed upper member of the Mescal from the normal diabase south of the Red Bluff mine.

If abnormal quantities of differentiates from the diabase were accompanied by large quantities of water in escaping into the surrounding rocks at the time of aplite intrusion, heat and fluids would be transferred from the diabase to loci in the surrounding rocks, so that these loci would be abnormally reactive relative to most of the country rock. This might explain in part why hornfels is formed in one place in contrast to almost complete lack of metamorphism under seemingly similar geologic conditions elsewhere.

#### Petrography

The hornfels ranges in color from very light to very dark gray. The lighter colors are more characteristic

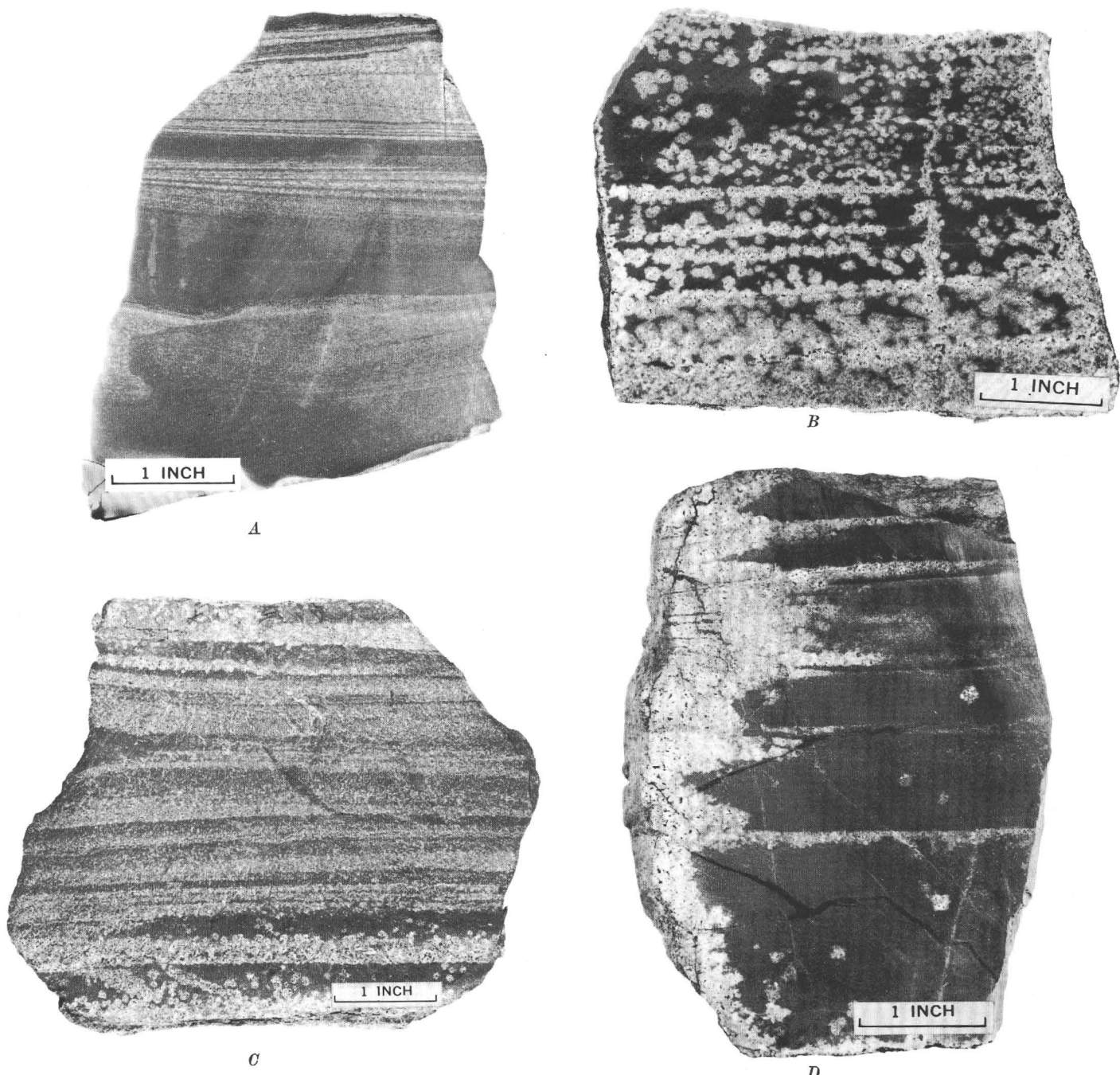


FIGURE 7.—Polished sections of hornfels showing textures. *A*, Relict stratification preserved in normal hornfels. Sample 28G55, collected in Little Joe adit 2. The light and dark laminae reflect the carbon and sulfide mineral content of the original siltstone. The apparent uniformity of grain size in normal hornfels in the various strata is in contrast to the marked difference of grain size in the other types of hornfels (*B*, *C*, *D*). *B*, Spotted hornfels. Sample 43G55, collected on the Little Joe claims. The formation of coarse-grained light-colored spots in normal hornfels seems to be controlled both by stratification and by fractures. At the bottom of the specimen the spots have coalesced to form typical coarse-grained hornfels. *C*, Lit-par-lit and spotted hornfels. Sample 61G54, collected on the Little Joe claims. The formation of the lighter colored coarse-grained hornfels was guided by, and served to preserve, the stratification. At least some of the coarse-grained hornfels seems to have formed by the coalescence of coarse-grained spots. *D*, Coarse-grained hornfels developed adjacent to a fracture. Sample collected on the Little Joe claims a few feet above diabase. Note the formation of isolated spots and lit-par-lit hornfels at the expense of normal hornfels.

of the gray facies and the darker of the black facies of the upper member of the Dripping Spring. A pink or red tint is not uncommon near ore deposits but provides no criterion for proximity to ore.

In hand specimen the grains are barely visible, but a definite crystalline appearance is caused by minute specks of light reflected from cleavage faces of feldspar. The grain size ordinarily corresponds to that of very fine grained sandstone and is little larger than the grain size of the original siltstone or very fine grained sandstone from which the hornfels was formed. The hornfels is a dense brittle rock with an irregular, almost conchoidal, fracture. Relict stratification (fig. 7A) and sedimentary structures are only a little less conspicuous than in the original rock.

Under the microscope in plane-polarized light a thin section of hornfels looks little different from the equivalent unmetamorphosed siltstone except in those varieties that contain abundant biotite and sphene. Grain boundaries of the feldspars are nearly invisible. Only minerals that have higher indices, that are opaque or are colored, stand out. Cloudiness is characteristic of most sections and is probably caused by the presence of alteration products. The potassium feldspars form an equigranular granoblastic mosaic throughout which sphene, biotite, pyroxene, quartz, albite, and opaque minerals are dispersed, particularly at grain boundaries and interstices. The texture (fig. 8A) is distinct only under crossed nicols.

Average grain size rarely exceeds 0.2 mm. Where it is larger, the rock grades into coarse-grained hornfels.

Potassium feldspars make up more than 75 percent of the rock. They are invariably clouded by a dust of clay(?) - mineral grains and in many places by evenly disseminated but extremely minute opaque grains of pyrrhotite(?). Because of the clouded nature and small grain size of the potassium feldspars, optical properties are difficult to determine. Crystals are untwinned, although in a few sections from the Workman Creek area an extremely faint suggestion of patchwork twinning was noted. This twinning is much fainter than any in microcline or anorthoclase that we have seen previously. The most diagnostic optical property easily determined on these feldspars is the optic angle (actually 2E, as the studies of these hornfelses were done on a flat stage). In most grains the angle is 70° or more. However, several slides show many of the grains to have a 2E as small as 20°. X-ray diffraction studies of the feldspars show that most of the material has monoclinic symmetry. Most samples contain a little potassium feldspar that has triclinic symmetry; plagioclase is very sparse or absent. The position of the (201) peak on the X-ray patterns

indicates that the potassium feldspar is nearly pure—about Or<sub>95</sub>. These data suggest that the dominant feldspar in the hornfels is orthoclase and that microcline is a minor constituent. Sanidine is seemingly present only locally.

Locally small patches of quartz and other minerals not much larger than the average grain size are bordered by euhedral feldspar faces. Apparently these patches represent minute vugs filled with quartz and other minerals. Where feldspar crystals abut each other they are anhedral; only where they face quartz patches are they euhedral.

Quartz generally does not exceed 10 percent in the hornfels. Adjacent to aplite dikes it may be significantly more abundant. It is clear and contains few inclusions. It is limited by euhedral grain boundaries and by open spaces in the feldspar matrix, indicating that it is later than the feldspar. It is most closely associated with albite, sulfide minerals, and perhaps sphene, although in a few places the quartz borders euhedral sphenes that face into vugs.

Sphene is a diagnostic mineral of the hornfels. Its presence is a strong indication that the rock is hornfels even if the texture is so clouded that other evidence of metamorphism is masked. The sphene is nearly everywhere anhedral except where it projects into quartz-filled areas. It is ordinarily pleochroic, from pale yellow to reddish brown. The optic angle is about 30°. Individual grains are much smaller than most feldspar grains and are found to occur interstitially among the feldspar grains and to project into quartz-filled vugs; they apparently are replacements of the feldspar in part. Not uncommonly the sphene is adjacent to sulfide minerals, and both bear similar relations to the feldspar.

Biotite is present in only about half the samples collected, but in these it constitutes as much as 4 percent of the rock. In general, the darker gray hornfels contains more biotite than the lighter colored varieties. In form the biotite is very irregular, tending to be elongate in the cleavage direction but ragged in outline. The biotite apparently replaced feldspar along grain boundaries and locally spread out in such a way as to give its individual grains an ameboid appearance where they partly enclose several grains of feldspar. Rarely a biotite grain is poikilitic around feldspar grains, but biotite commonly encloses several sulfide mineral grains. There is a suggestion of an association between the biotite and sulfide minerals owing to their similar position in the biotite and the feldspar framework. The biotite is pleochroic from very pale yellow through golden yellow to red brown. It generally has conspicuous bird's-eye structure.

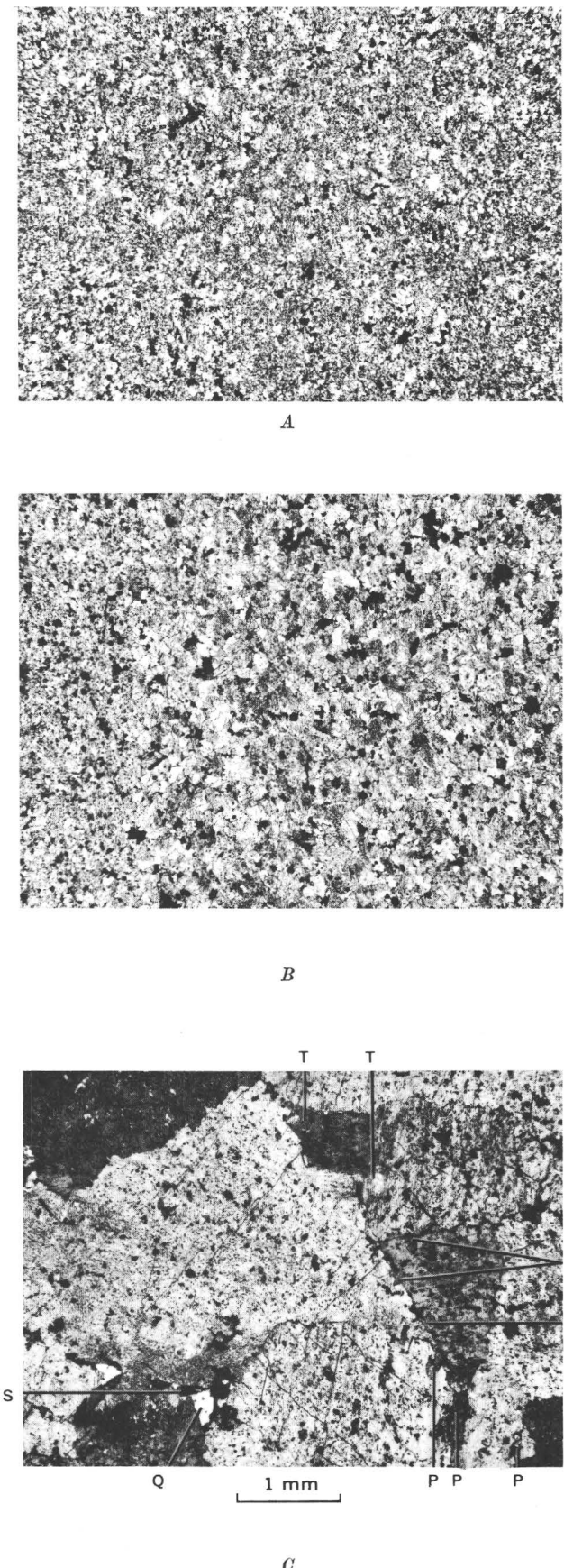


FIGURE 8.—Gradational sequence of normal hornfels to coarse-grained hornfels. Samples were collected about halfway between the Hope 1 and John adits. Sample 109G54 (A) was collected about 20 feet above diabase; sample 108G54 (B), about 8 feet above diabase; and sample 107G54 (C), about 3 feet above diabase. Partly crossed nicols. A, Normal hornfels. Optical and X-ray studies of the feldspars indicate that orthoclase is dominant with lesser amounts of microcline. The mineral assemblage is similar to that of B but is too fine grained to distinguish in this photograph. B, Stratification is from top to bottom in the photomicrograph. Normal hornfels is present to the left, and an intermediate size of coarse-grained hornfels is present to the right and in the center. The section was cut from lit-par-lit hornfels. Optical and X-ray studies indicate that both orthoclase and microcline are present. Potassium feldspar is cloudy and quartz is clear. The very black grains are largely pyrrhotite, commonly bordered by a flake of brown biotite. Spheine and pyroxene are common but too fine grained and scattered to be distinguished in the photomicrograph. C, Coarse-grained hornfels. The large grains are potassium feldspar; Q, quartz; T, spheine; P, pyroxene; S, sulfide minerals. The potassium feldspar has a patchy extinction, but nearly all of it has a small to intermediate optic angle. X-ray studies disclose a dominant monoclinic phase and subordinate triclinic phase. Sanidine seems to be dominant; lesser amounts of microcline are present but cannot be distinguished optically.

Pyroxene is not present in all specimens, but where present it constitutes as much as 5 percent of the rock. It occurs as single grains less than half the average grain size of the rock or as aggregates of rounded grains. In general, pyroxene appears to be concentrated in interstices and intergrain boundaries of the feldspar, but some of it appears to have mutual boundaries with feldspar and, thus, to be nearly contemporaneous with it.

The pyroxene is either colorless or light yellow. Maximum interference colors are low third order. The optic angle is large (+) and the extinction angle  $Z \wedge c = 40^\circ - 45^\circ$ . These properties suggest that the mineral is augite. Presumably the yellow color, the slightly high interference colors in some grains, and the various extinction angles are the result of an abnormal titanium content.

Sulfide minerals generally are disseminated throughout the rock. In some specimens a dust of minute opaque shiny grains, probably pyrrhotite, fills the feldspar crystals. Most of the grains identifiable as sulfide are concentrated along feldspar grain boundaries and in interstices and tiny vugs. The grain size of the sulfide is generally less than the average grain size of the feldspar. In hornfels that contains biotite, the larger sulfide grains are commonly associated with biotite. The most prevalent sulfide is pyrrhotite; it is the only one identifiable in some of the rocks. Chalcopyrite and py-

rite are common near uranium deposits but probably are later in sequence than the pyrrhotite.

Quartz is a common associate of sulfide grains. The sulfide minerals between feldspar grains apparently were deposited contemporaneously with or shortly after the quartz. The dustlike inclusions of sulfide minerals in the feldspar may represent original disseminated sulfides in the rock prior to metamorphism. Their grain size and distribution are similar to the grain size and distribution of pyrite in siltstone.

Albite is present in minor amounts but locally forms small grains and aggregates in the interstices among potassium feldspar grains. Its occurrence is similar to that of quartz, but it is less prevalent, nowhere constituting more than 1 percent of the rock except at the Lucky Stop claims, where some of the hornfels is strongly sodic (fig. 9). In general, albite is clear in contrast to the clouded potassium feldspar.

#### Chemical composition

Hornfels was formed from the original siltstone and sandstone with little change in composition. Locally, as at the Lucky Stop claims, soda metasomatism affected the rocks, but this probably was an effect of hydrother-

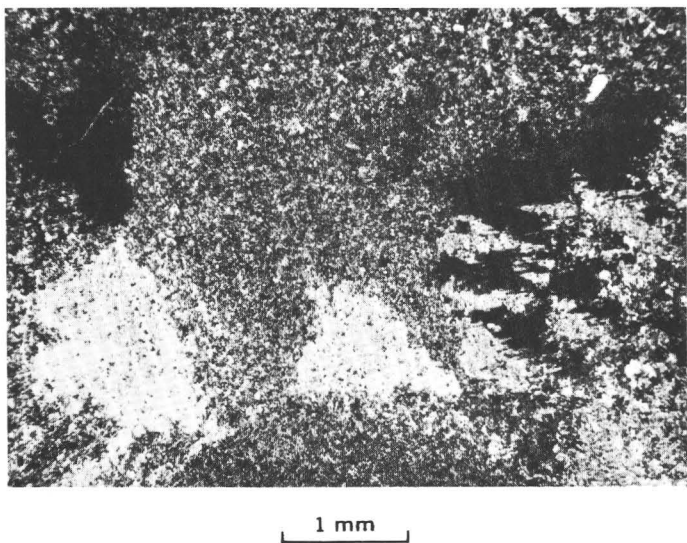


FIGURE 9.—Partial replacement of normal hornfels by albite porphyroblasts. Sample 134G54 from the Lucky Stop adit 1. The large ragged albite grains have completely replaced the finer grained potassium feldspar groundmass. The dustlike inclusions in the albite and throughout the hornfels consist of leucoxene, pyroxene, sphene, and sulfide minerals that were largely unaffected by the introduction of albite. Elsewhere in the slide some of the albite porphyroblasts look much like microcline because of polysynthetic albite and pericline twinning. Crossed nicols.

mal activity related to aplite dike intrusion rather than to thermal metamorphism.

Figure 10 shows a series of semiquantitative spectrographic analyses and chemical analyses of unmetamorphosed siltstone, hornfels, and related rocks. There is a remarkable uniformity between the metamorphosed and unmetamorphosed rocks, even though there are some minor differences between them. The most diagnostic change seems to be an increase of  $\text{Na}_2\text{O}$  from about 0.15–0.20 percent in the siltstones to several times this amount in the hornfels. This increase is probably a result of soda metasomatism related to the intrusion of soda aplite dikes into the hornfels. Several samples not reported here that were collected near the Lucky Stop adit 1 (fig. 9) were abnormally sodic indicating a much higher degree of soda metasomatism in that area than noted elsewhere. Erratic variations of such constituents as  $\text{MgO}$ ,  $\text{CaO}$ ,  $\text{TiO}_2$ , and total iron oxides probably reflect original sedimentary variations in the siltstone.

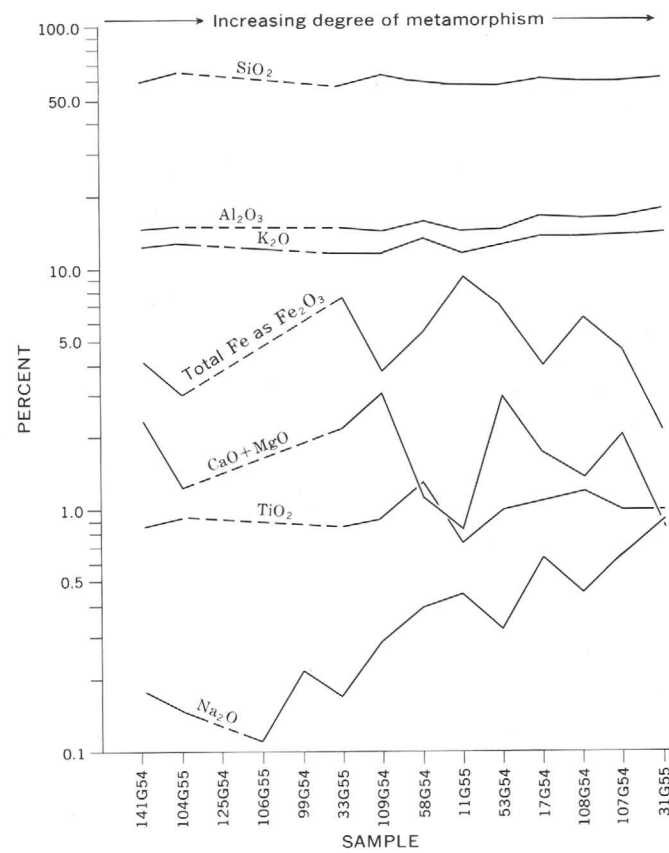


FIGURE 10.—Chemical changes during metamorphism of the gray unit of the Dripping Spring Quartzite. See table on facing page.

## DIABASE

## ANALYTICAL DATA AND NOTES FOR FIGURE 10

## Chemical analyses:

Samples 99G54 and 106G55, K<sub>2</sub>O and Na<sub>2</sub>O, rapid method analyses by Wayne Mountjoy and I. C. Frost. U, fluorometric analysis by D. L. Schafer and H. E. Bivens. Se, rapid method analysis by G. T. Burrow. All other analyses rapid method by P. L. D. Elmore, K. E. White, and S. D. Botts.

## Semiquantitative spectrographic analyses:

Tr., trace; O, looked for but not detected; M, major constituent, greater than 10 percent. Figures reported to the nearest number in the series 7, 3, 1.5, 0.7, 0.3, 0.15. Si, Al, Fe, Mg, Ca, Na, K, Ti, and Mn determinations by N. M. Conklin, R. G. Havens, and P. J. Dunton; all others by P. L. D. Elmore, K. E. White, and S. D. Botts.

Sample	Chemical analyses (percent)													
	141G54	104G55	125G54	106G55	99G54	33G55	109G54	58G54	11G55	53G54	17G54	108G54	107G54	31G55
SiO <sub>2</sub>	59.4	65.8	-	-	-	57.9	63.6	59.4	56.9	57.0	60.6	59.2	59.6	61.5
Al <sub>2</sub> O <sub>3</sub>	14.7	15.1	-	-	-	14.8	14.1	15.8	14.4	14.9	16.3	16.1	16.4	17.7
Fe <sub>2</sub> O <sub>3</sub>	3.7	1.7	-	-	-	.5	1.6	2.6	3.0	2.4	1.6	1.0	.4	1.6
FeO	.35	1.2	-	-	-	6.8	2.0	2.4	5.8	4.1	2.2	4.9	3.8	.54
MgO	1.0	.58	-	-	-	1.8	1.3	.53	.31	1.6	.31	.64	.46	.04
CaO	1.8	.63	-	-	-	.40	1.8	.60	.53	1.4	1.4	.72	1.6	.82
Na <sub>2</sub> O	.18	.15	-	0.11	0.22	.17	.38	.50	.55	.34	.64	.45	.67	.92
K <sub>2</sub> O	12.4	12.8	-	12.2	10.5	11.7	11.8	13.3	11.6	12.7	13.6	13.6	13.8	14.1
H <sub>2</sub> O	.77	.75	-	-	-	2.0	.37	.59	.72	1.9	.70	.46	.64	.72
TiO <sub>2</sub>	.86	.94	-	-	-	.86	.92	1.3	.72	1.0	1.1	1.2	1.0	1.0
P <sub>2</sub> O <sub>5</sub>	.11	.10	-	-	-	.08	.05	.08	.10	.16	.14	.11	.09	.12
MnO	.02	.02	-	-	-	.05	.04	.04	.03	.12	.02	.06	.03	.00
CO <sub>2</sub>	2.5	.32	-	-	-	.51	<.05	<.05	.56	.35	.06	.34	.11	<.05
Total	98	100	-	-	-	98	98	97	95	98	99	99	99	99
Total sulfur as S	2.7	0.60	-	-	-	2.7	1.7	2.7	3.7	2.1	1.7	2.7	1.8	1.1
U	.029	.002	0.001	0.002	0.002	-	.001	-	-	-	.001	-	.001	-
Se	.0001	-	<.00005	-	-	-	<.00005	-	-	-	.0005	<.00005	-	-

Sample	Spectrographic analyses (percent)							Sample	Spectrographic analyses (percent)						
	141G54	125G54	106G55	99G54	109G54	108G54	107G54		141G54	125G54	106G55	99G54	109G54	108G54	107G54
Ag	Tr.	0	Tr.	Tr.	0	0	0	Nb	0	Tr.	Tr.	Tr.	Tr.	Tr.	Tr.
As	0	0.03	0	0	0	0	0	Ni	0.007	0.003	0.003	0.007	0.003	0.003	0.003
Ba	0.07	.03	0.03	0.03	0.07	0.03	0.03	Pb	.007	.0015	.0015	.007	.003	.007	.003
Be	.00015	0	0	0	0	0	Tr.	Sc	.0015	.003	.003	.003	.0015	.0015	.0015
Ce	Tr.	.015	0	0	0	.015	.015	Sn	.003	.0007	0	0	Tr.	.0007	.0003
Co	.007	.0007	.0015	.003	.0007	.0015	.0007	Sr	.003	.007	.007	.003	.015	.015	.015
Cr	.015	.015	.007	.007	.007	.015	.015	V	.015	.015	.015	.015	.015	.015	.015
Cu	.03	.015	.007	.007	.007	.015	.007	Y	.015	.003	.007	.003	.003	.003	.003
Ga	.0015	.003	.0015	.003	.0015	.0015	.003	Yb	.0007	.0003	.0007	.0007	.0003	.0003	.0003
La	.007	.003	0	0	.003	.003	.007	Zr	.015	.015	.03	.03	.015	.015	.015
Mo	.007	.0007	.0015	.0015	.0003	.0007	.0003								
Sample	125G54	106G55	99G54	Sample	125G54	106G55	99G54	Sample	125G54	106G55	99G54	Sample	125G54	106G55	99G54
Si	M	M	M	Mg	3	1.5	3	Na	0.3	-	-	Ti	0.3	0.7	0.7
Al	M	M	M	Ca	.3	.3	.7	K	7	-	-	Mn	.015	.03	.03
Fe	7	3	7												

## SAMPLE DESCRIPTIONS

## Siltstone:

- 141G54. From waste dump of Shepp mine. X-ray diffractometer patterns showed that the potassium feldspar is monoclinic. Optical studies disclosed grains which had large 2V only. The nearest known diabase is at a distance of nearly ½ mile, but prior to erosion it may have been present as a sill in the overlying Mescal Limestone.
- 104G55. From about 55 ft above the barren quartzite, upper member, Dripping Spring Quartzite, near the Snakebit adit. Nearest diabase is a sheet that intrudes the middle member, Dripping Spring Quartzite, at least 250 ft stratigraphically below sample locality.
- 125G54. Similar to sample 104G55, but collected about 200 ft N. and at a slightly lower stratigraphic position.
- 106G55. Randomly selected fragments from diamond-drill core, Rainbow property. Several hundred feet from the nearest diabase. X-ray diffractometer patterns showed that the potassium feldspar is monoclinic.
- 99G54. Fragment from diamond-drill core on the Regal asbestos mine property about 0.3 mile S.E. of the Tomato Juice deposit. The nearest diabase body is several hundred feet away and is in discordant contact with the Dripping Spring Quartzite.
- 33G55. From just above the barren quartzite in the ore zone, Black Brush deposit. Uraniferous. The nearest diabase is the Sierra Ancha diabase sheet about 80 ft below the deposit.

## Hornfels:

- 109G54. From about 20 ft above the Sierra Ancha diabase sheet near the east boundary of sec. 30, T. 6 N., R. 14 E., on the north side of Workman

Creek. This is part of a suite that also includes samples 107G54 and 108G54. Dark-gray dense rock which X-ray diffractometer patterns showed to contain largely monoclinic potassium feldspar. Optical studies showed that all the potassium feldspar grains had a large 2V.

58G54. From a few feet above diabase several hundred feet southeast of locality of sample 109G54. Similar in appearance to sample 109G54.

11G55. From ore pile at Hope adit 1. Dense fine-grained light-brownish-gray specimen.

Mixed (lit-par-lit) hornfels and coarsely-grained hornfels:

53G54. At portal of Workman adit 1. Alternating layers of pinkish-gray hornfels and coarse-grained hornfels.

17G54. From outcrop near locality of sample 53G54. Similar lit-par-lit rock except that coarse-grained phase is a little coarser than that of sample 53G54.

Coarse-grained hornfels:

108G54. From about 8 ft above the Sierra Ancha diabase sheet in Workman valley. Part of the same suite that includes samples 109G54 and 107G54.

107G54. From about 3 ft above the Sierra Ancha diabase sheet in the Workman Creek valley. Medium to dark gray. Part of the same suite that includes samples 108G54 and 109G54. Potassium feldspars have patchy extinction, and most patches have a small 2V. X-ray diffractometer patterns show that most of the potassium feldspar is monoclinic but that minor amounts are triclinic.

31G55. From the ore pile of Little Joe adit 2. Light brownish gray.

Because of the appreciable organic carbon and sulfide contents of the samples, the  $\text{Fe}_2\text{O}_3$  and  $\text{FeO}$  analyses may have little meaning other than to represent the total iron content. Such strong reducing agents as organic carbon and sulfide sulfur cause difficulties in analysis for ferrous iron.

#### COARSE-GRAINED HORNFELS

A hornfelslike rock coarser grained than normal hornfels (fig. 7C, D) is called coarse-grained hornfels in this report. Although the term is contradictory, it serves to relate the fine- and coarse-grained varieties of these thermally metamorphosed rocks and is, therefore, preferable to introducing a new term.

The coarse-grained type of hornfels is generally present wherever hornfels occurs and is especially well developed from original siltstone strata in the upper member of the Mescal Limestone near the crest of a hill about a mile southwest of the Red Bluff deposit. A related similar hornfels material has been formed in the diabase (A.F. Shride, oral commun., 1956).

Stratification is preserved in the coarse-grained hornfels and is indicated by slight differences in texture, grain size, and mineralogy. Weathering of well-exposed outcrops intensifies the bedded appearance. Except for biotite developed mimetically on relict stratification planes, no apparent preferred orientation of the constituent minerals is present.

Various facies of the coarse-grained hornfels are present in the Workman Creek area. One of these is a spotted variety found on the Little Joe claims; it consists of small irregularly shaped bodies of coarser grained material (fig. 7B) from 1 to 5 mm across scattered throughout the normal hornfels. Some of the spots are coarse-grained hornfels that grades outward at its margins to hornfels; these spots contain euhedral or subhedral feldspar that juts into tiny quartz-sulfide-filled vugs at the centers. Locally these little blebs are coalesced along bedding planes or along short transverse fractures (fig. 7B). In some places they completely, or nearly completely, replace certain discrete layers in the hornfels to form a lit-par-lit hornfels (fig. 7C), or they replace the entire rock to form a nearly homogeneous coarse-grained hornfels. Variously shaped bodies of coarse-grained material in hornfels and partly replaced hornfels laminae are common in the Workman Creek area and their presence suggests that the formation of hornfels may have been necessary prior to a further recrystallization to the coarse-grained variety. However, much of the coarse-grained and lit-par-lit hornfelses probably did not go through a spotted stage but progressed directly (fig. 7D) from hornfels, or even siltstone, to their present forms.

The mineralogy and texture (fig. 8B, C) of coarse-grained hornfels are similar to the mineralogy and texture of the normal hornfels. Some evidence supports the augmentation of the basically thermal metamorphism of the hornfels by hydrothermal action. Biotite more commonly is concentrated parallel to bedding, and pyroxene is not as common as in normal hornfels. These characteristics suggest that hydrous solutions passed along bedding planes. Anhydrous minerals such as pyroxene likely do not form in the presence of abundant water, whereas biotite forms readily. Quartz-filled vugs are larger and more common in the coarse-grained hornfels than in the normal hornfels, and these vugs indicate the presence of abundant silica-rich solutions that persisted after the feldspar framework had crystallized.

Generally the coarse-grained hornfels is lighter colored than the corresponding normal hornfels. In the lighter colored hornfels, sulfides, largely pyrrhotite, are reconstituted as larger grains along feldspar grain boundaries and in vugs. The feldspar grains have fewer opaque inclusions than elsewhere. Presumably, the dark color in some coarse-grained hornfels is caused, in part, by dust of minute sulfide grains. In some samples, 107-G-54 (fig. 8C) for example, the coarse-grained hornfels is nearly as dark as the corresponding normal hornfels, and there is very little difference in the overall dispersion of the sulfides in the two.

#### Petrography

Coarse-grained hornfels is generally light to medium gray but not uncommonly is a grayish orange pink and light brown. The color is largely that of the potassium feldspars, but may in part reflect the abundance and degree of oxidation of included sulfides. Red tints are common near uranium-ore deposits but not so much so as to provide a criterion for proximity of ore. Medium-gray hornfels is also common near ore.

In hand specimen the rock is distinctly crystalline. The grain size ranges from that of normal hornfels to about 5 mm; rarely there are grains as long as 10 mm. In general, the rock looks like an igneous syenite except for common relict stratification. The arrangement of grains is visibly decussate, and locally in the coarsest grained varieties on the Little Joe claims, a radial texture is noticeable.

Under the microscope, with crossed nicols, the rock appears little different from normal hornfels except for its grain size (fig. 8). The texture is granoblastic, and potassium feldspar makes up the framework of the rock. Nearly all potassium feldspar crystals are anhedral, but where they border small quartz-filled vugs they may have some euhedral faces. Dispersed in and

among the potassium feldspar are albite, sphene, quartz, pyroxene, biotite, and pyrrhotite in various proportions.

Potassium feldspar makes up more than 75 percent of the rocks, except in certain strongly albitized specimens from the Lucky Stop claims. Most specimens of coarse-grained hornfels from the Dripping Spring contain feldspar that is clouded by extremely fine inclusions. Feldspar in coarse-grained hornfels from one locality in the upper Mescal, however, is nearly clear.

In thin section, some of the potassium feldspar grains have patchy extinction. The patches, which appear to represent at least two intergrown phases, range in diameter from submicroscopic to 0.05 mm and have very irregular shape. Interference figures in adjacent patches apparently have considerable diversity in optic angle.

Optic angles, measured on a universal stage, show a wide range, both for apparently homogeneous grains and for grains that display patchy extinction. The 2V's seem to form three groups: 20°–30°, 50°–60°, and 70°–80°. Perhaps the second group is a composite of the other two. Areas within thin sections commonly contain grains dominantly within one group.

X-ray diffraction patterns of the potassium feldspar indicates that samples that seem to contain largely monoclinic feldspar generally contain many grains with small 2V. Large 2V's, group 3, are most common in samples that contain largely triclinic feldspars.

These data suggest that the coarse-grained hornfels contains sanidine, microcline, and, perhaps, othoclase in proportions that vary from place to place. Sanidine seems to be more prevalent near the diabase than away from it.

In specimens from Lucky Stop adit 1, albite hornfels is partly developed at the expense of normal potassic hornfels. Albite grains as large as 4.5 mm by 2 mm and having extremely irregular shape and vague border seem to have formed as large ragged porphyroblasts by incorporating and replacing the finer potassium feldspar of the hornfels (fig. 9). This albite has been twinned on the albite and pericline laws and, in a few grains, on the baveno law. In a specimen from the upper member of the Mescal Limestone, untwinned albite has partly replaced a few of the potassium feldspar grains along the cleavages.

Quartz is more abundant in most coarse-grained hornfels than in normal hornfels, but in both it displays the same textural relations along grain boundaries where it has replaced feldspar and in vugs where it abuts euhedral feldspar. Even in the largest of these vugs (3–4 mm), the quartz commonly is monocrystalline and is optically continuous throughout. In some specimens no quartz is present; this is true of the specimen from the upper member of the Mescal.

Sphene ordinarily makes up nearly 1 percent of the coarse-grained hornfels. It is nearly everywhere anhedral, but where it projects into quartz-filled vugs it may be either subhedral or euhedral. It is distributed throughout most of the coarse-grained hornfels derived from the Dripping Spring but is either missing or extremely rare in that derived from the upper part of the Mescal. Although much of the sphene is localized along grain boundaries and appears to partly replace feldspar, some grains are completely surrounded by feldspar as shown in the plane of the thin sections. These may represent sphene crystals originally present in hornfels and then enclosed by the recrystallizing feldspar, but this relation would complicate the paragenetic sequence. Although generally free of inclusions, some sphene crystals enclose small opaque grains, probably pyrrhotite.

The average grain size of sphene is probably less than 0.2 mm, but locally its size is about 0.5 mm. Pleochroism ranging from reddish brown to light yellow is common; some grains are nearly colorless or are light yellow and almost nonpleochroic. The optic angle is estimated to be about 45°.

Biotite is an erratic constituent of coarse-grained hornfels. It was not noted in half the specimens examined. In the other half it makes up less than 5 percent of the rock, generally from about 1 to 2 percent. The biotite is strongly pleochroic, ranging from light yellow brown to deep red brown. Bird's-eye structure is conspicuous. In size and shape the grains are extremely irregular; they range from almost submicroscopic to nearly 1 millimeter across in thin sections we have examined, but poikiloblastic grains as much as 1 cm across have been noted by us in some hand specimens. These poikiloblastic grains are generally mimetically formed along relict bedding planes. In coarse-grained hornfels formed in the Dripping Spring, the biotite grains have extremely irregular, almost ameboid shape. The grains commonly are formed along grain boundaries replacing and partly enclosing feldspar. They rarely form books but generally are nearly equidimensional in the plane of cleavage. Most grains are nearly free of inclusions, but some contain small opaque grains, probably pyrrhotite. A few have formed sufficiently to surround grains of potassium feldspar and, thus, have a poikiloblastic appearance. Biotite is abundant in the coarse-grained hornfels in the upper member of the Mescal. Here it forms books 0.1 by 0.02 mm to 0.7 by 0.1 mm as seen in cross section. The books cross feldspar grains without regard for boundaries and are also included poikilitically by feldspar. In the specimen examined, many of the biotite grains are fresh but others are altered to ilmenite(?) and leucoxene and ultimately to

a saussuritic-appearing aggregate that contains abundant chlorite. This altered biotite has a strong pleochroism that ranges from light yellow brown to nearly black.

Albite is not abundant in most hornfels and generally forms small grains along potassium feldspar boundaries and adjacent to quartz. It forms large poikiloblastic porphyroblasts that in certain specimens from the Lucky Stop adit 1 have replaced the potassium feldspar groundmass by encroachment. This phenomenon is almost certainly genetically related to the sodic late-stage magmatic history of the differentiated diabase. Albite is also present as minute inclusions in potassium feldspar of some specimens; in these specimens it assumes elongate forms in a somewhat regular pattern diagonal to the (010) planes of both the feldspar and plagioclase. This albite may represent a sodic facies exsolved from the predominantly potassic feldspar grains. If so, the solid solution and exsolution history of these grains is very complex. Three phases are then present in some individual grains: (1) the predominant potassium feldspar of the groundmass with large  $2V$ ; (2) smaller amounts of patchily distributed potassium feldspar with a small optic angle; and (3) exsolved albite.

Pyroxene is absent from most specimens, and where present it makes up less than 5 percent of the rock, commonly less than 1 percent. The grains are ordinarily much smaller than the feldspar grains and have rounded stubby prismatic shapes. They occur singly or as aggregates along grain boundaries and interstices between feldspar grains. Rarely, the pyroxene grains are perched on and slightly replace feldspar grains that project into quartz-filled cavities; here the pyroxene apparently formed on the surface of the feldspar and was later enclosed by the quartz filling. The pyroxene is colorless to very pale green. The grains are biaxial (+) and of moderately large optic angle. Maximum interference colors are second-order green as seen in thin sections of standard thickness. Birefringence ranges slightly from specimen to specimen. The extinction angle  $Z \wedge c$  ranges from about  $40^\circ$  to  $47^\circ$ ; rarely a grain that is properly oriented appears to extinguish near  $30^\circ$ . Presumably most of the pyroxene is augite, but the smaller extinction angles suggest that some of the grains are diopsidic. The pyroxene seems to be closely related temporally to sphene and albite. It is probably later in sequence than is potassium feldspar, although some pyroxene grains are included in feldspar and are earlier than quartz.

Pyrrhotite is abundant in most coarse-grained hornfels. It is particularly abundant near uranium deposits but decreases away from them, which suggests a genetic relation between some of the pyrrhotite and the urani-

um deposits. Pyrrhotite appears to replace the potassium feldspar, to be associated with albite and pyroxene, to be locally included by sphene and biotite, and to be nearly contemporaneous with quartz. In the darker facies the pyrrhotite occurs as a fine dust disseminated throughout the rock without regard for rock texture. In the lighter colored facies, the pyrrhotite occurs largely as grains of irregular shape that are distributed along feldspar grain boundaries and interstices.

#### *Chemical composition*

The chemical composition of coarse-grained hornfels is almost identical with that of normal hornfels except for a higher sodium content. Chemical compositions of several samples are compared with those of normal hornfels in figure 10.

#### ALTERATION OF NORMAL AND COARSE-GRAINED HORNFELS

Except by weathering, hornfels is ordinarily little altered. Weathering readily oxidizes the sulfide minerals and converts most other minerals to various types of clay, or to leucoxene in the titanium-rich minerals. The interlocking texture of the rock makes it relatively resistant to weathering processes at more than a few inches from the surface or from fractures.

Normally, the hornfels is little affected by what is probably hydrothermal action, except very near uranium-bearing veins. The pyroxenes, which are more strongly affected than other minerals, are not uncommonly converted, in part, to chlorite or to a green nontronitic clay near uranium deposits. Generally, however, the nontronite is less discriminatory than the chlorite as to which mineral it replaces.

#### MOBILIZED HORNFELS

Several ore deposits in the Workman Creek area are parallel to and largely within a zone of breccia that is cemented by a pale-pink aplitic rock almost identical with a facies of the aplite differentiate of the diabase. Possibly the pale-pink rock is the differentiated aplite, but it has certain characteristics that prompt us to attribute its origin to metamorphism. This rock is herein termed "mobilized hornfels" on the assumption that it was a transient facies derived from fusion or solution of hornfels under conditions of lowered pressure and increased volatiles.

An incipient phase of mobilized hornfels has been noted in several specimens of lit-par-lit hornfels from the Workman Creek area. Some short, somewhat blunt apophyses from the coarse-grained hornfels layers extend transversely into the normal hornfels layers. A few laminae of hornfels apparently have been slightly brecciated and cemented by the coarser material. It is evident that the cementing rock locally has moved as a fluid.

Mobilized hornfels is best developed in the Hope adit 1 and the Workman adit 1. It is present but obscure in the Little Joe adit 2. It may be present locally elsewhere in the Workman Creek area, in the central part of the Cherry Creek area near the Big Six deposit, and near the Grand View deposit, but all the aplitelike rock recognized in the hornfels in these areas may be true aplite.

In the Hope adit 1, mobilized hornfels forms the cement in a zone of brecciated normal and coarse-grained hornfels (fig. 11). The breccia zone is coincident with the uranium-bearing vein zone. Locally, certain relict strata are brecciated for a few feet laterally and are also cemented by mobilized hornfels. Short apophyses of mobilized hornfels extend as sills or dikes into the adjacent hornfels. The margins of the zone occupied by mobilized hornfels are, therefore, very irregular.

In the Workman adit 1, mobilized hornfels tend to form a series of interconnected dikelets in a zone coincident with the ore body. Locally, it forms cement for typical breccia, but in most places the shattering and movement apparently were not adequate to form breccia. The mobilized hornfels is traceable from the portal to a stoped area, a distance of about 85 feet; neither the economically minable part of the ore body nor the mobilized hornfels extends beyond this stope, although the uranium-bearing vein is traceable by its radioactivity to a greater distance.

In the Little Joe adit 2, no breccia zone is traceable. Some specimens taken from the uranium-bearing vein zone, however, are obscurely brecciated. All the coarse-grained hornfels host rock has approximately the same composition, grain size, and texture, but locally the relict stratification abruptly terminates. In parts of some specimens the relict stratification is oriented differently than elsewhere. The remarkable similarity between rock that has obscure stratification and the mobilized hornfels makes brecciation difficult to recognize within the mine. Presumably the ore in the adit follows a brecciated zone, but the zone cannot be defined. No evidence of brecciation was noted in the normal hornfels in adit 3, which is directly above adit 2, even though the uranium-bearing vein is continuous between them.

Sill-like bodies of aplite commonly contain many hornfels xenoliths and grade into aplite-cemented hornfels breccias, so that any distinction based on abundance of xenoliths apparently is not dependable. Aplite dikes, however, rarely include an abundance of xenoliths, whereas the mobilized hornfels bodies in the Hope 1 and Workman 1 adits range from hornfels breccias cemented by mobilized hornfels dikelets that traverse a shattered zone in hornfels.



FIGURE 11.—Hornfels breccia cemented by mobilized hornfels. Sample 16G55 from the central vein zone of the Hope adit 1.

Mobilized hornfels generally is pink in hand specimen; most commonly it ranges from grayish orange pink to pale red. This coloration may be either very similar to or in sharp contrast with the typically gray wallrocks; in general, coarse-grained hornfels in the wallrock is nearly the same color as mobilized hornfels, but normal hornfels is considerably darker than mobilized hornfels.

Sulfide minerals commonly are abundant as macroscopically visible blebs in mobilized hornfels. Pyrrhotite is most common, but chalcopyrite is locally prevalent.

Mobilized hornfels resembles aplite mineralogically, but the two may have slight textural differences. The unquestionable aplites have a variety of textures, perhaps the most common of which is characterized by disseminated round quartz grains that partly replace the feldspar framework. Quartz, however, only slightly replaces the feldspars in mobilized hornfels and tends to occupy interstices in the hypidiomorphic feldspar mesh. Round quartz grains were not seen in rock believed to be mobilized hornfels.

Grain size is more uniform in unquestionable aplites, rarely departing much from an average of 1 mm. Feldspar grains as large as 4 by 10 mm, however, are present in mobilized hornfels in the Hope adit 1.

A possible distinction between mobilized hornfels and aplite is the local presence of calcite-filled vugs in the mobilized hornfels. These vugs range from a few millimeters to 12 cm in length and are generally somewhat oblate. Some vugs seem to have been formed on a well-healed fracture. Most calcite-filled vugs were seen in the Hope adit 1. They were also noted in questionable mobilized hornfels in the Lucky Stop adit 2. Not uncommonly, hornfels forms one wall of the vug and mobilized hornfels the other. In contrast with quartz-filled vugs in aplite that are lined with potassium feldspar grains, many of the calcite-filled vugs are lined with albite. The albite grains are subhedral and as much as four to five times as large as the normal grains in the mobilized hornfels. They have partly replaced the potassium feldspar and micropegmatite of the adjacent rock and are in turn partly replaced by the calcite.

An unusual vug in the Hope adit 1 is filled with quartz on one side and with calcite on the other (fig. 12). All the feldspar bordering the calcite filling is albite. Away from the vug, the mobilized hornfels (lower central part of photomicrograph) is largely a mixture of micrographic feldspar, quartz grains, and minor albite. The fractures that cut the calcite are filled with nearly opaque greenish-brown nontronite.

Certain features outside the area of this photomicrograph are so unusual as to warrant further description. For example, just below the field shown is a calcite-filled fracture that connects with the vug filling and extends into the mobilized hornfels. Wherever the fracture cuts a quartz grain within about 0.5 inch of the vug, the filling is quartz; farther away the fracture is dominantly quartz filled.

Although this part of the vug (fig. 12) is filled with calcite, the other half is filled with quartz. A few well-

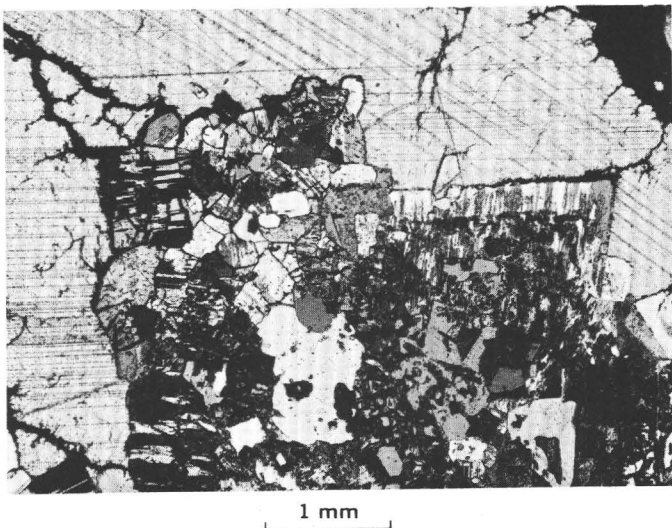


FIGURE 12.—Margin of a calcite-filled vug in mobilized hornfels. Sample 12G55 collected in the central vein zone in Hope adit 1. Partly crossed nicols.

developed quartz crystals locally project into the calcite-filled part of the vug indicating that the calcite is later than the quartz. Along part of the interface between calcite and quartz is an irregularly shaped sulfide-mineral aggregate that is pyrrhotite where it is in contact with the quartz but is largely pyrite where it touches the calcite. Nontronite forms veins in the sulfide minerals and tends to follow the grain boundaries between pyrite and pyrrhotite and between pyrite and calcite. The feldspar that lines the quartz-filled part of the vug is microperthite in contrast to albite in the calcite-filled part.

A residual mesh of either amphibole "whiskers" or green flaky nontronite partly fills some of the vugs after the calcite is dissolved by a weak acid. The fibers of amphibole are as much as 5 mm long but are less than 10 microns across, making positive identification impossible by optical means. Both the amphibole and the nontronite were identified by X-ray powder pattern. Indices of the nontronite are between 1.52 and 1.55. Commonly disseminated in the nontronite are minute (<0.3 mm) hexagonal flakes of pyrrhotite; slightly tarnished, they are similar in appearance to biotite flakes. Larger stubby hexagonal prisms and irregularly shaped masses of pyrrhotite as much as 5 mm across project into the vugs; they partly enclose the subhedral albite. Green pyroxene, which is probably diopsidic or diopsidic augite, also forms subhedral crystals that project into the vugs.

Some of the vugs contain very little nontronite, amphibole, or pyroxene. One of these from the Hope adit 1 contains several small hexagonal flakes and rosettes of

molybdenite less than 5 mm across that are perched on the surfaces of feldspar grains that project into the cavity. The molybdenite also occurs as anhedral flakes and aggregates associated with quartz in the interstices between feldspar grains within a few millimeters of the edge of the vug. No relations between the molybdenite and other sulfide minerals were noted.

A vug from the Lucky Stop adit 2 in an olive-green mobilized hornfels has somewhat different characteristics than do the vugs in the Hope mine. Potassium feldspar rather than albite projects into the cavity. A porous granular mesh consisting of minute green diopside and euhedral sphene crystals as much as 0.3 mm across seems to be partly included by the potassium feldspar. Some grains of sphene appear to be perched on feldspar. Pyrrhotite, marmatite, and chalcopyrite are later than the rock-forming minerals but are intimately intergrown with them. The pyrrhotite forms plates and irregular masses. Marmatite locally fills voids among the pyrrhotite crystals and presumably, on the basis of high iron content, it formed at elevated temperatures which persisted through the late stages of diabase cooling. Chalcopyrite veinlets cut both the marmatite and pyrrhotite.

Very narrow veinlets of calcite in some thin sections are seen to extend outward from the vugs into the surrounding rock. These calcite veinlets cut all the rock-forming minerals, but where they cut quartz the vein filling abruptly changes to quartz. The paths of the veins through the quartz are marked by strings of minute inclusions but otherwise are obscure, as the fillings are optically oriented with the surrounding quartz.

The paragenetic sequence of minerals in the vugs is interpreted as follows:

Mineral	Time →
Potassium feldspar	
Pyroxene	?
Sphene	?
Quartz	
Albite	
Amphibole	
Molybdenite	?
Pyrrhotite	
Nontronite	?
Marmatite	
Chalcopyrite	
Calcite	

Whether such a phase as mobilized hornfels exists or whether all rocks that we are designating as such are related to aplite is not known. It is certain that soda aplites from the diabase abruptly change composition where they penetrate the hornfels. This change indicates the strong reactivity of hornfels at the time of

aplite intrusion and suggests that any fluid penetrating the hornfels at this time resulted in the formation of a rock similar in composition to the hornfels.

Every unquestioned aplite is readily distinguishable from the enclosing hornfels. Some of the possible mobilized hornfels, however, would be nearly indistinguishable from coarse-grained hornfels except that the mobilized hornfels has no relict stratification and its crosscutting relationships with hornfels are easily recognizable.

Our interpretation of the genesis of the mobilized hornfels is as follows: At the time the hornfels was being formed by heat and fluid emanations from the cooling diabase magma, minor adjustments were made to stresses created by contractions in both the diabase and hornfels. (Contraction in the hornfels is suggested by a slight increase of specific gravity over that of the original siltstone (table 3).) The adjustments were minor slippages along relict bedding planes and fissures opened parallel to preexisting structures in the rocks. All fissures and other sites of movement resulted in zones of lowered pressures (Mead, 1925) into which were drawn any nearby mobile fluids. We assume that parts of the hornfels were saturated with a water-rich fluid phase, and that this solution was drawn into the dilute areas and therein deposited a part of its load of rock-forming mineral constituents. The composition of the solutions probably was governed by the composition of the hornfels and, hence, the resulting intrusive rock or vein had a composition approximating hornfels. Late-forming igneous minerals such as quartz and feldspar were more abundant than early-forming constituents, as in mobilized hornfels, for example.

In addition to the presence of calcite-filled vugs and the marked mineralogic similarity between coarse-grained and mobilized hornfels, other features may serve to distinguish mobilized hornfels from aplite.

Breccia fragments of wallrock and irregular walls are characteristic of mobilized hornfels (fig. 11), whereas in aplite dikes fragments of wallrock are only sporadic, and the walls are sharp and regular. Breccia fragments, however, are abundant in sill-like bodies of aplite that lie just above the normal diabase.

The trend of breccia zones cemented by mobilized hornfels (not mapped) in the Hope adit 1 and Workman adit 1 is north-northeast and is coincident with the trend of the zone of highest radioactivity (pl. 3; fig. 13). Although many aplite dikes also trend northeast, several dikes have other trends and several branch (pl. 1) irregularly.

Several uranium deposits are parallel and coincident with breccia zones that are cemented by mobilized

hornfels, but no abnormal radioactivity is known to be associated with unquestioned aplite dikes.

If the mobilized hornfels and aplite are of different origins, as we proposed, the mobilized hornfels most likely preceded most of the aplite. The albite that lines calcite-filled vugs was probably derived from the same source as aplite. Hence, pervasive solutions related to aplite must have, to some extent, followed some of the same channels as those occupied by the mobilized hornfels.

#### SPOTTED ROCKS

Spotted rocks are common in the upper member of the Dripping Spring but are generally inconspicuous unless the rocks are examined in detail. They have been noted in all parts of the member but seemingly are most common near the base of the buff unit. Several varieties have been distinguished. One of these represents an incipient development of coarse-grained hornfels (fig. 7B) near diabase; this type is described on page 32. The other varieties may also occur within a few feet of diabase; all are within at least a few hundred feet of it. The spotted rocks, therefore, may be partly a product of mild regional metamorphism, but more probably they represent the earliest stage of thermal metamorphism resulting from the intrusion of diabase.

Spotted rocks, perhaps, are similar in origin to spotted slate that occurs at the outermost zones of many metamorphic aureoles. Harker (1952, p. 15) has the following explanation for spotted slates: "The first step in the metamorphism was local solution beginning at many isolated points within the rock. This should have been followed by recrystallization, setting free the solvent to attack new portions of the rock mass."

In the example described by Harker, "the duration of high temperature conditions did not suffice for the complementary process of recrystallization. The dissolved spots passed therefore into a glassy \* \* \* state." Turner and Verhoogen (1951, p. 422) presumed this "glass" to be a chemically precipitated gel. Harker (1952, p. 48) also noted that graphite has a strong tendency to gather in clots during low-grade metamorphism, and that cordierite, andalusite, sericite, chlorite, and iron ores may also develop as discrete rounded spots. Turner and Verhoogen (1951, p. 421-422) described outermost zones of low-grade contact metamorphism in which muscovite, chlorite, quartz, feldspars, biotite, and cordierite had developed.

Nearly every description of spotted slate is concerned with metamorphosed aluminous pelitic sediments. Many sediments had already been converted to slate by regional metamorphism prior to igneous intrusion. Consequently this spotted slate is not directly comparable

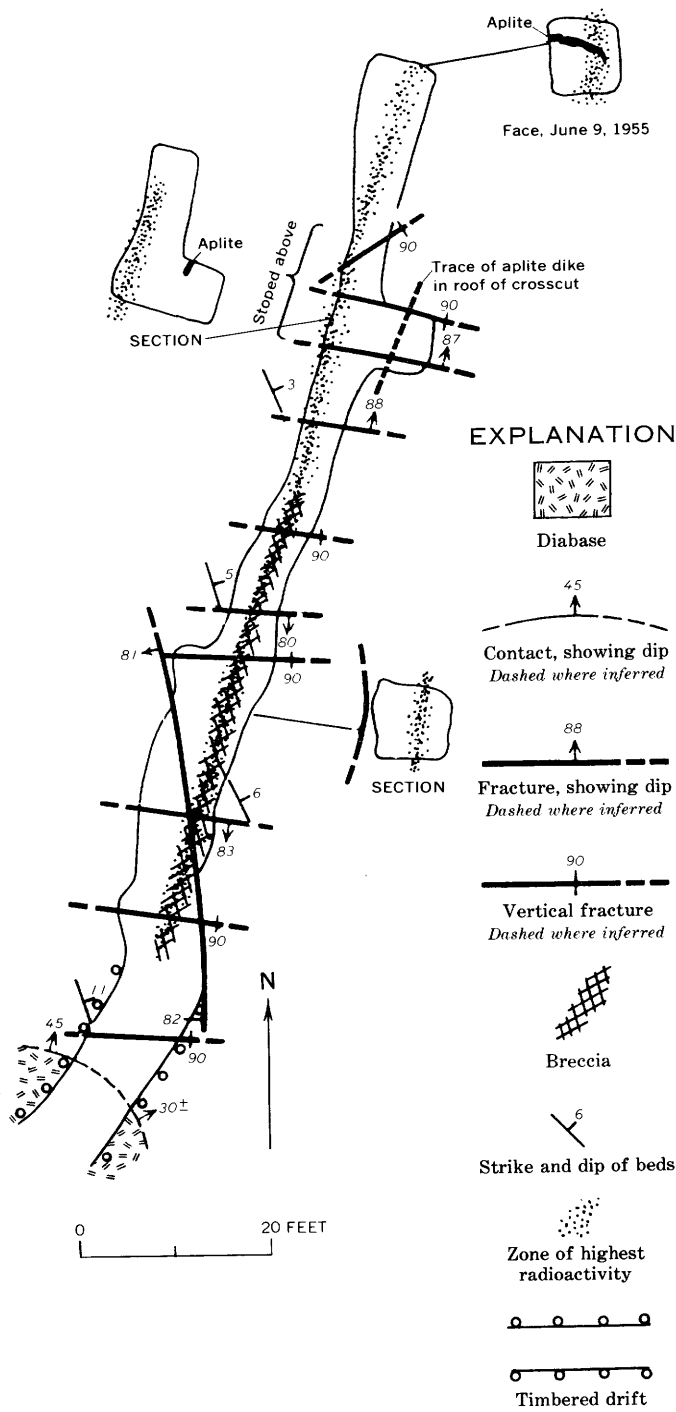


FIGURE 13.—Geologic map and sections of adit 1, Workman deposits (Granger and Raup, 1959, fig. 66).

to the spotted rock in the Dripping Spring even though it is the most similar counterpart.

The spots in the Dripping Spring range in diameter from 0.2 to 7 mm, but most are 0.5—1.5 mm. In hand specimen they are generally closely spaced and may appear as either light spots on a dark background or,

more commonly, dark spots on a lighter background. They invariably occur in siltstone or hornfels; none were seen in sandstone.

The texture (fig. 14) of the spots is commonly distinct from that of the surrounding rock. The constituent minerals of the spots are arranged in a decussate aggregate that has a somewhat larger grain size than that of the surrounding groundmass.

The spots can be divided mostly into three groups on the basis of the most abundant minerals in them; these are: (1) nontronite, (2) sericite-muscovite, and (3) orthoclase.

There is no constant stratigraphic position for spots of an individual mineralogy, but spots developed in the gray facies away from hornfels are mostly of the nontronite type.

The nontronite-type spots are generally a decussate aggregate of green pleochroic clay containing interspersed feldspar and quartz grains. The clay has positive elongation, second-order interference colors, and moderate relief. It is generally flaky and pleochroic in yellow greens and greenish browns. Possibly the brown colors are a result of oxidation of the contained iron caused by weathering. The clay mineral is very similar in appearance to some varieties of chlorite, but the abnormally high birefringence suggests that it is a nontronitic variety of clay.

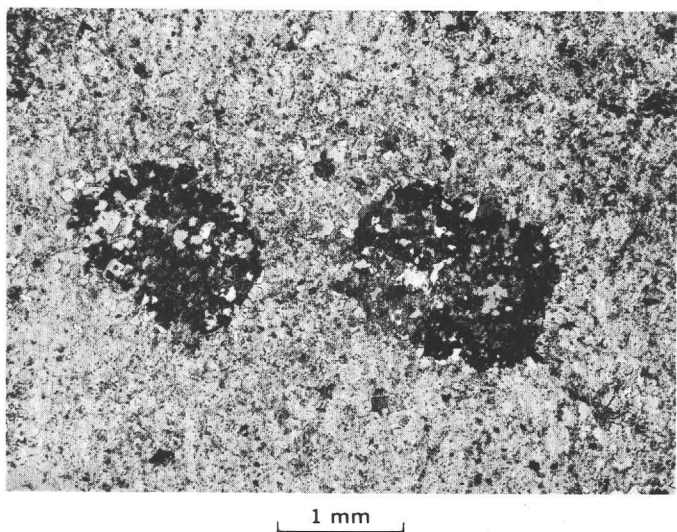


FIGURE 14.—Spotted rock from the gray facies in the gray unit of the upper member, Dripping Spring Quartzite. Sample 129G56 from the Big Six adit 1. This is one of many varieties of spotted rock. Here, the spots consist largely of quartz (clear white and gray), chlorite (largely penninite), and phlogopite (gray to black). The groundmass is nearly normal siltstone consisting of quartz and potassium feldspar, scattered mica flakes, and various detrital minerals with high relief. Mica in the groundmass is considerably more abundant than usual and is probably metamorphic in origin. Partly crossed nicols.

The muscovite-type spots are ordinarily composed of scattered quartz and potassium feldspar grains in a decussate aggregate of very fine grained pale-green muscovite (sericite). The muscovite grains may be a little larger than those in the surrounding groundmass, but few are more than 0.04 mm in diameter. The centers of a few spots consist of larger ragged poikiloblastic muscovite books as much as 0.4 mm in length. In this mica the optic angle is about 20°–30°, which is slightly smaller than is common in normal muscovite.

Spots developed in hornfels on the Big Six property are composed of an aggregate of muscovite and a pale-green pleochroic chlorite or chloritelike mineral. Scattered grains of zircons and allanite are contained in the aggregate, and some of the zircons are bordered by pleochroic halos. The locality of these spots is very near aplite-cemented hornfels breccia and other evidence of strong metamorphism. Spots developed in siltstone nearby (fig. 14) contain chlorite and phlogopite.

The feldspar-type spots are composed of an equigranular aggregate of potassium feldspar and sparse quartz of a grain size slightly larger than that of the surrounding groundmass. In both the muscovite and feldspar types the spots are much less cloudy than the surrounding groundmass. Many of the feldspars in the groundmass contain an allophanelike alteration mineral that is missing from the recrystallized minerals within the spots.

Although it is known that spots in hornfels represent an incipient development of coarse-grained hornfels, the relation of the remaining spotted rocks to hornfels is not known. Almost certainly, however, the spotted rocks result from a lower grade of metamorphism, occurring because of lower heat or because of lack of pore solutions, that would allow a quicker attainment of equilibrium conditions.

#### PIONEER FORMATION

Although we did not study contacts between diabase and the Pioneer Formation, other geologists seem to be in general agreement that the effect of diabase intrusion on the Pioneer is inconspicuous. For the most part the Pioneer is merely baked, hardened, and finely recrystallized near the contact (Gastil, 1953, p. 124; Ransome, 1919, p. 55). In some places the shales are bleached (Wardwell, 1941). Cook (1938) noted that the Pioneer is altered for as much as 2 feet from the diabase and the altered zone contained small pink concretions consisting of serpentine, feldspar, magnetite, and hematite. Carpenter (1947) noted the formation of scattered epidote in the Pioneer close to diabase contacts.

**MESCAL LIMESTONE**

The rock most reactive to diabase intrusion was the Mescal Limestone. A variety of mineral assemblages has resulted from metamorphism; the type of assemblage depends largely on the original composition of the Mescal at the site of intrusion. The most economically important of these is the serpentine-asbestos assemblage.

Serpentine and chrysotile asbestos deposits in the Mescal Limestone have been described by Bateman (1923), Allen and Butler (1921), Sampson (1924), Butler (1929), Wilson (1928), and Shride (1952). The deposits occur only in the algal and lower carbonate members of the Mescal, presumably in cherty or siliceous parts of the rock.

Shride (1952) stated:

Chrysotile occurs as cross-fiber veins that approximately parallel the bedding of the [Mescal] limestone. The host for the veins is serpentine which differentially replaced certain limestone beds.

Small-scale bedding-plane faults and thrust faults, probably the result of adjustment in the limestone when the diabase was intruded, constituted the most significant factor in determining the extent of the asbestos deposits.

Wilson (1928, p. 33) believed that:

asbestos was deposited from mobile solutions which used \* \* \* fissures as pathways of entry to such strata as were amenable to development of serpentine and asbestos \* \* \*. Probably a final emanation from the diabase magma brought about \* \* \* the development of the serpentine and asbestos. Sufficient magnesium and silicon for these minerals may have been derived wholly from the olivine of the diabase, or part of the magnesium may have been supplied by the Mescal dolomitic limestone.

Shride (oral commun., 1958) believed that the host rocks, which are serpentine-bearing limestones, were siliceous dolomite prior to diabase intrusion. The silicon and magnesium in serpentine and chrysotile, therefore, may have been supplied in large part by the Mescal.

All the economically minable chrysotile asbestos deposits in the Mescal are in the north half of Gila County, although serpentine and small quantities of asbestos are not uncommon farther south. It may be significant that most of the uranium deposits occur in the same general area although there is apparently no close spatial relation between individual uranium and asbestos deposits.

In many places tremolite and actinolite have been formed in the lower member of the Mescal near diabase. Galbraith (1935) noted the formation of "large quantities of tremolite" near Superior, and Harshman (1940) observed that the limestone had been "altered to a mass of fine-grained tremolite containing some chlorite and serpentine." Actinolite has been noted in several places in the Mescal in northern Gila County

and, in our experience, is most common near the base of the Mescal in argillaceous limestone strata.

Garnet, diopside, and other silicate minerals also have been recognized in some metamorphic facies of the Mescal near diabase (Galbraith, 1935; A. F. Shride, oral commun., 1957).

Magnetite in a matrix composed of serpentine, dense quartz, and pyrite, and rarely asbestos, occurs in the basal part of the Mescal on the Suckerite claims (Granger and Raup, 1968). Magnetite in contact metamorphic deposits in the Mescal is not uncommon elsewhere (A. F. Shride, oral commun., 1957).

An occurrence of coarse-grained hornfels formed by metamorphism of the upper member of the Mescal is noted on page 32-33.

Spotted rocks similar to the spotted rocks in the Dripping Spring also occur in the reddish upper member of the Mescal. The spots are very distinct, usually dark green or gray, and consist largely of an aggregate of a chloritic mineral and very fine black opaque minerals.

**WALLROCK REACTIONS**

Williams (1957) believed that the diabase magma engulfed and assimilated rocks of the upper member of the Dripping Spring to produce "hybrid rocks" that have certain characteristics of both parent rocks. Although local interchange of certain elements between the sedimentary rocks and all facies of the diabase occurred during the cooling history, the interchange probably was not so prevalent as he implies nor do all the examples that he presents seem to be valid.

Figure 15 is a ternary diagram that relates mafic and alkalic constituents of various rocks. The field occupied by diabase and its differentiates is sharply distinguishable from the fields occupied by siltstone and hornfels. These fields are distinctive whether the data plotted are the same as in our diagram, or are elements or atomic percent. They are also distinguishable if calcium oxide is added to the iron and magnesium oxides. Two samples classified by Williams (1957) as hybrid rocks seem to fall well within the trend of differentiation from diabase to albite aplite. As plotted on the diagram, they do not differ appreciably from samples of other rocks that he classified as a diabase pegmatite and a segregate of diabase, which are probably intermediate differentiates.

The rocks labeled *a* through *d* in figure 15 and all the aplites that cut the Dripping Spring show various degrees of reaction with the adjacent rocks. The chilled-border samples (*a*), one collected in the Mescal Mountains and the other near Red Bluff, seem to have acquired a little potassium from the adjacent rocks. The chilled-border sample (*b*), collected near Theodore

Roosevelt Dam, is from a diabase sill in the Pioneer Formation. The felted intergranular texture of this sample seems to be identical with the texture of chilled borders elsewhere, but presumably the plagioclase needles are metasomatically replaced by a highly potassic feldspar. Samples c and d, collected north of Workman Creek are of sodium-rich coarse-grained hornfels stratigraphically just above diabase and probably represent addition of sodium during late stage differentiation of the diabase. Inasmuch as c and d were collected

from a drill core where structural relations are difficult to determine, these samples may represent one of the intrusive materials that we have termed aplite or mobilized hornfels. Sample e was collected from the branching aplite dike just east of Workman adit 1 (pl. 1). It falls among the hornfelses on the diagram and may be a mobilized hornfels dike, but it could be an aplite that has reacted with the Dripping Spring and approaches the composition of the aplite dikes (solid symbols near the  $K_2O$  corner of the diagram)

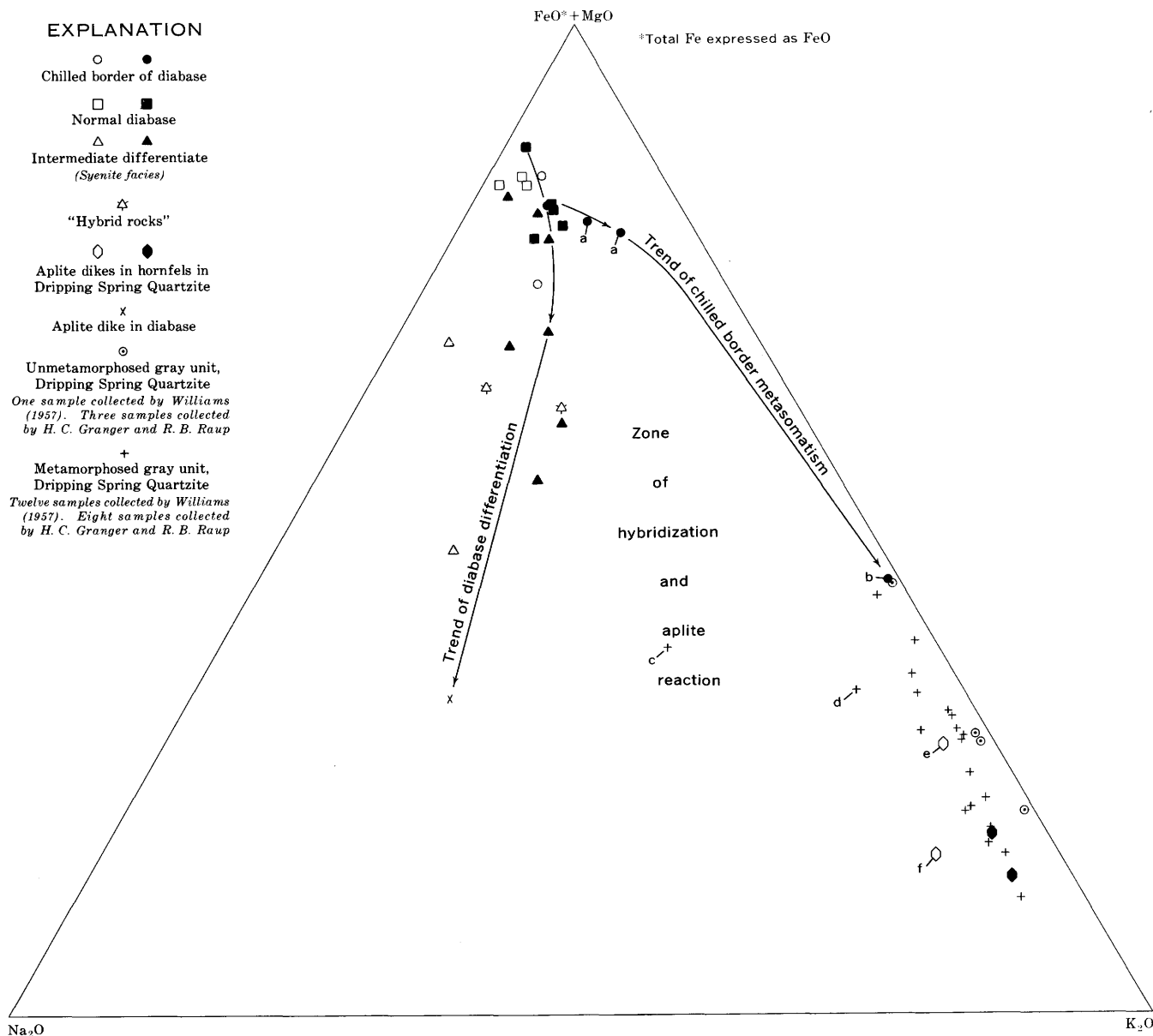


FIGURE 15.—Trends of mafic and alkalic components of rocks related to diabase and to siltstones of the gray unit, Dripping Spring Quartzite. Solid symbols represent samples collected by H. C. Granger and R. B. Raup, or by G. J. Neuerburg. Open symbols represent samples collected by F. J. Williams (1957). a and b, chilled borders that have reacted with adjacent rocks; c, sample 855, recrystallized rock just above diabase (Williams, 1957); d, sample 873, recrystallized rock just above diabase (Williams, 1957); e, sample 761, dike cutting Dripping Spring Quartzite (Williams, 1957); f, sample 88, probable "rheomorphic" dike (Williams, 1957).

that have reacted strongly with the enclosing Dripping Spring hornfels. Sample f is from a dike that cuts diabase on the Hope Claim but that is very close to the contact between the diabase and the Dripping Spring. In our experience the borders of albite grains within such aplite are progressively replaced by potassium feldspars where the dike crosses the contact into the Dripping Spring.

All the hornfels is richer in soda than is the siltstone. In some places the potassium feldspar grains of normal hornfels have been partly replaced by large ragged poikiloblastic albite grains, as shown in figure 9. This change undoubtedly denotes abstraction of sodium from the nearby diabase. Three of the four siltstone samples listed by Williams (1957) are plotted in figure 15 as hornfels; because they contained sphene they were reported to have been partly recrystallized, and they contained somewhat more soda than is normal for siltstone.

Blocks of Dripping Spring that have been engulfed by the diabase, such as the large xenolith along lower Workman Creek (pl. 2), show no more evidence of reaction or assimilation than do the rocks adjacent to the margins of the sills. Xenoliths such as this one retain nearly all their sedimentary features and are distinct both texturally and mineralogically from syenitic rocks that occur in the diabase.

Our conclusion is that in most places reaction or element exchange between diabase and the enclosing rocks has been minor. Where aplites passed from the diabase into the sedimentary rocks they ordinarily reacted extensively, and gave up much of their sodium, which was metasomatically replaced by potassium. Rocks formed by this metasomatism are generally distinct from rocks formed by differentiation within the diabase. A. F. Shride (oral commun., 1962) suggested that rocks containing free quartz were probably derived in large part from the sedimentary rocks, whereas quartz-free rocks were likely to be differentiates of the diabase. This hypothesis accords well with our conclusions. The syenites and albite aplites are ordinarily quartz free, but the aplites intrusive into the Dripping Spring contain abundant quartz. All phases of hornfels through mobilized hornfels also contain quartz.

#### STRUCTURE

Three principal types of structural features are known in the Dripping Spring Quartzite in the general areas of uranium deposits: monoclines, faults, and joints. The general trend of these features is north in northern Gila County and northwest in southern Gila County. The north trends generally reflect Precambrian structural features; the northwest trends reflect, in part, Mesozoic and later structural features.

#### MONOCINES

At least five monoclines affect the Apache Group (fig. 1). The monoclines, all of which are in north-central Gila County, trend north and, with one exception, are downwarped on the east side.

The monoclines from west to east are the Sierra Ancha, Cherry Creek, Canyon Creek, Rock Canyon, and Mule Hoof monoclines. The three western structures are the largest and can be traced for 20 miles or more, but they are intruded by diabase and breached by erosion so that only their flanks are exposed. The two eastern monoclines are smaller, but their entire flexures are exposed locally.

The monoclines clearly were formed before or during diabase intrusion, as is indicated by their great influence on the emplacement of the diabase masses. Locally shattered diabase in the flexure zones is the result of later structural stresses.

The axes of the three larger monoclines apparently were broken by longitudinal faults, as is indicated by the abrupt changes in thickness and stratigraphic position of diabase sills at the monoclines. Such faults may be the continuation of high-angle faults in the basement rocks. Initial movement along these faults resulted in monoclinal folding, but continued stresses later ruptured the strata.

#### SIERRA ANCHA MONOCLINE

The Sierra Ancha monocline trends north from about 2½ miles southwest of the Parker Creek Experiment Station to at least 5 miles north of the McFadden Peak quadrangle, a total of more than 14 miles. The Globe-Young road traverses the monocline near its axis throughout this distance. The east side of the monocline is downwarped, and although differential inflation by diabase has obscured the original displacement, normal displacement of nearly 500 feet persists in the Workman Creek area even after diabase inflation (pl. 2).

The monocline is breached south of McFadden Peak, and diabase is exposed along the axis. North of this peak the monocline may or may not be broken by an axial fault; only Apache Group sedimentary rocks are exposed along the axis.

The diabase exposed south of McFadden Peak is part of a thick sheet whose stratigraphic position abruptly changes at the monocline; this abrupt change in stratigraphic position indicates that the axis was faulted prior to diabase intrusion. In the Workman Creek area diabase west of the monocline intruded the Pioneer Formation and lower part of the Dripping Spring, and east of the monocline it intruded the upper member of the Dripping Spring. The diabase sheet east of the monocline is arbitrarily called the Sierra Ancha diabase sheet.

**CHERRY CREEK MONOCLINE**

The Cherry Creek monocline (fig. 1) can be traced for more than 20 miles along the west side of Cherry Creek canyon, principally in the McFadden Peak quadrangle. The southern part of the monocline trends about N.  $22^{\circ}$  W., but near the north border of the quadrangle it trends almost north.

This monocline is downwarped on the west, whereas the other monoclines are downwarped on the east. The amount of original displacement, although probably large, cannot be determined owing to faults and diabase inflation that have disrupted the monocline and, in effect, generally reversed the original movement. Erosion has also breached the monocline.

The monocline is an abrupt flexure as indicated by sharply warped, locally overturned strata, and a complex feature as indicated by adjacent drag folds and local branch folds. Subparallel normal faults, particularly on the east side of the monocline, further complicate the structural zone.

Longitudinal faults in the monocline are indicated by the local but pronounced effect of the monocline on the emplacement of diabase. The Sierra Ancha diabase sheet terminates or abruptly thins at the monocline, and only thin sheets and dikes of diabase are present in rocks exposed just east of the monocline along most of its strike length.

**CANYON CREEK MONOCLINE**

The Canyon Creek monocline (fig. 1) trends slightly west of north along the east side of Canyon Creek. The flexure begins a few miles south of the Salt River and is probably at least 25 miles long. Canyon Creek has deeply breached the flexure. The east side is downwarped at least several hundred feet. The effect of the flexure on intruded diabase is not known; the only extensive body of diabase known to be exposed is near the contact between Mescal Limestone and Troy Quartzite high on the canyon wall east of the creek. Subparallel normal faults are common on the west side of the monocline.

**ROCK CANYON MONOCLINE**

The Rock Canyon monocline (fig. 1) is well exposed on both sides of the Salt River near the mouth of Rock Canyon. Here the monocline appears as an unbroken flexure that trends about N.  $12^{\circ}$  W. and is downwarped on the east side. Displacement is at least 200 feet within a horizontal distance of a few hundred yards; the sharpness of the fold is indicated by nearly vertical strata exposed in Rock Canyon. The monocline is traceable for several miles south and about  $1\frac{1}{2}$  miles north of the Salt River, but it no doubt extends farther in both directions, particularly north.

The monocline, where exposed along the Salt River, has been intruded by a diabase sill, more than 200 feet thick, in the middle member of the Dripping Spring. The sill appears to be concordant even where the flexure is the sharpest. Small diabase dikes commonly cut rocks above the sill near the zone of flexure.

**MULE HOOF MONOCLINE**

The Mule Hoof monocline (fig. 1) is exposed along the Salt River about half a mile downstream from the U.S. Highway 60 bridge. The flexure was traced for only a short distance on either side of the river; its trend seems to be slightly west of north. Where exposed on the north side of the river, the strata are downwarped about 100–200 feet on the east side. The fold is less abrupt than in the other monoclines described.

The Mule Hoof monocline was intruded by a relatively thin concordant diabase sill in the upper member of the Dripping Spring. The chilled upper margin of the sill is not jointed or shattered, as would be expected if the fold had formed after solidification of the sill.

**FAULTS**

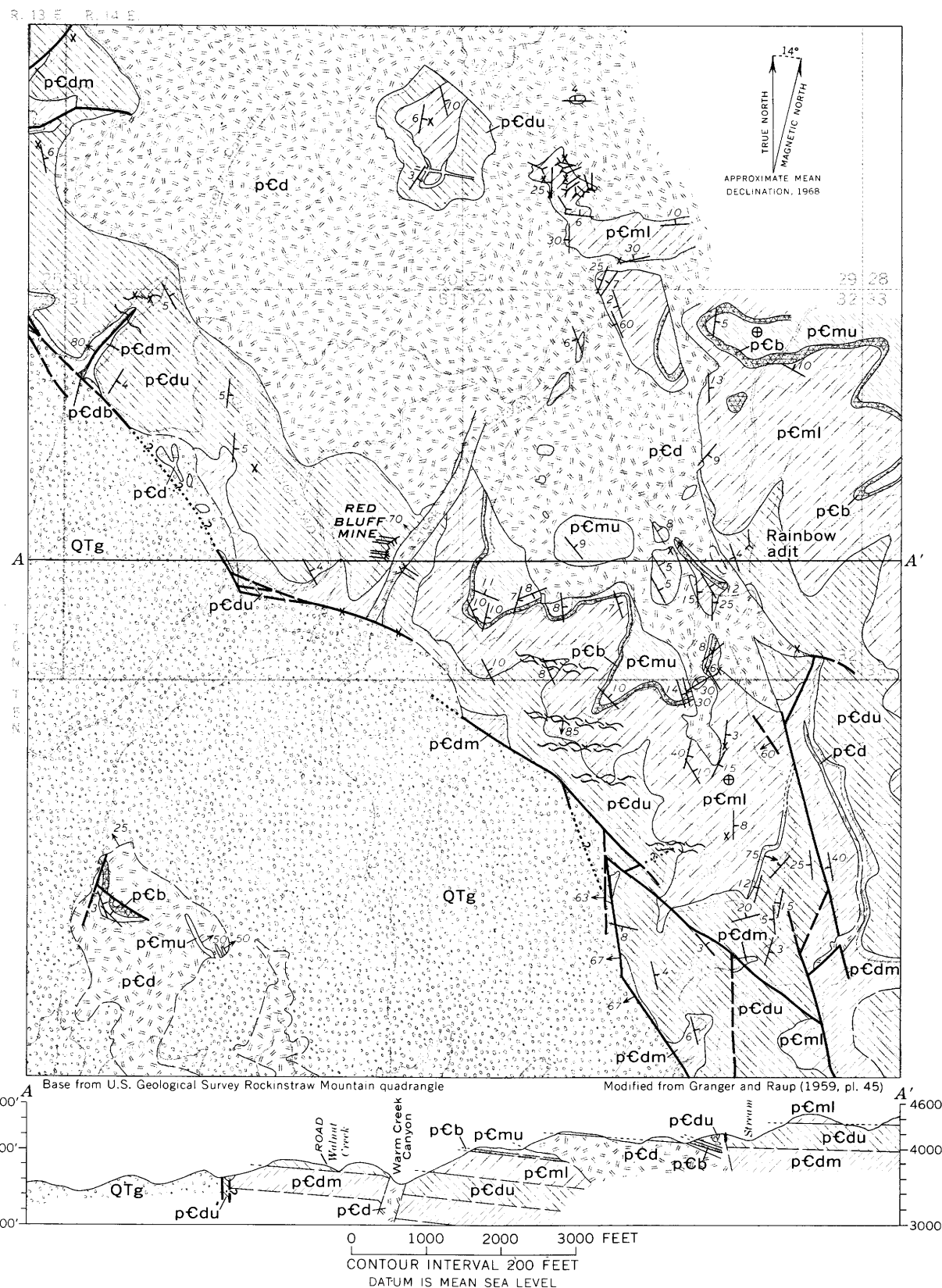
Faults that have affected the Dripping Spring Quartzite in the general areas of uranium deposits in Gila County fall into two broad categories: faults that formed before or contemporaneously with the intrusion of diabase, and faults that formed after the intrusion and cooling of diabase. The prediabase and syndiabase faults are dominant in the Sierra Ancha and Salt River Canyon parts of Gila County; postdiabase faults are more numerous and of greater magnitude south of the Salt River valley.

**PREDIABASE AND SYNDIABASE FAULTS**

Prediabase and syndiabase faults influenced the intrusion of diabase and are best observed in the Sierra Ancha region. They are partly obscured elsewhere in Gila County by later structural features.

Prediabase and syndiabase faults in the Sierra Ancha region are largely high-angle normal faults that trend predominantly northward as do the monoclines; eastward-trending and randomly oriented faults are less common. Diabase has intruded many of the faults, particularly those in and near the monoclines.

The northward-trending faults are principally those along which the monoclines ruptured and those parallel or subparallel to the monoclines in the monocline structure zones. Examples of faults in the monoclines are the faults along which the diabase changed its horizon of intrusion at the Sierra Ancha monocline and the faults along which the diabase abruptly thins or terminates at the Cherry Creek monocline.



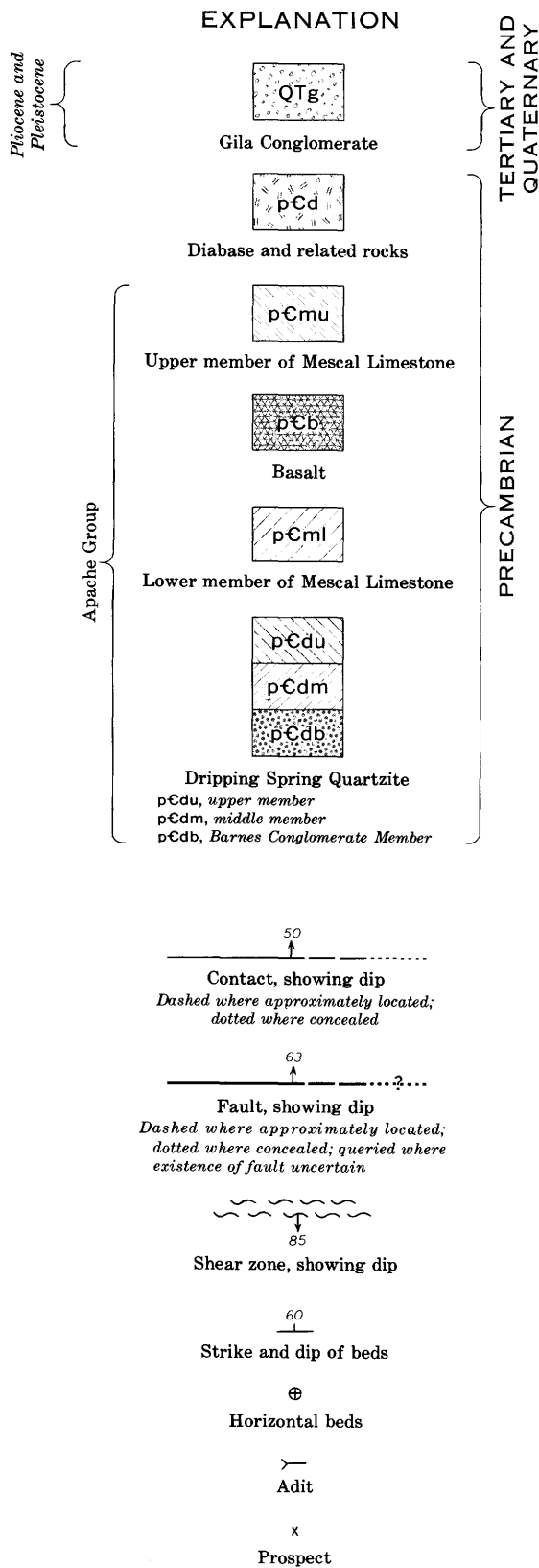


FIGURE 16.—Geologic map and section of the Red Bluff area.

Examples of faults parallel or subparallel to the monoclines are the fault in Deep Creek adjacent to the Sue and Donna Lee deposits, the easternmost fault shown on the cross section accompanying the map of the Red Bluff area (fig. 16), and the diabase-intruded fault in Warm Creek Canyon at the Red Bluff deposit (figs. 16, 17).

Eastward-trending faults or fault zones that cross the monoclines and that formed before or contemporaneously with diabase intrusion are expressed by the control they exercised on the emplacement of diabase. A good example of such a cross fault is just south of McFadden Peak and just north of the Big Six deposit. This fault is the north boundary of the Sierra Ancha diabase sheet.

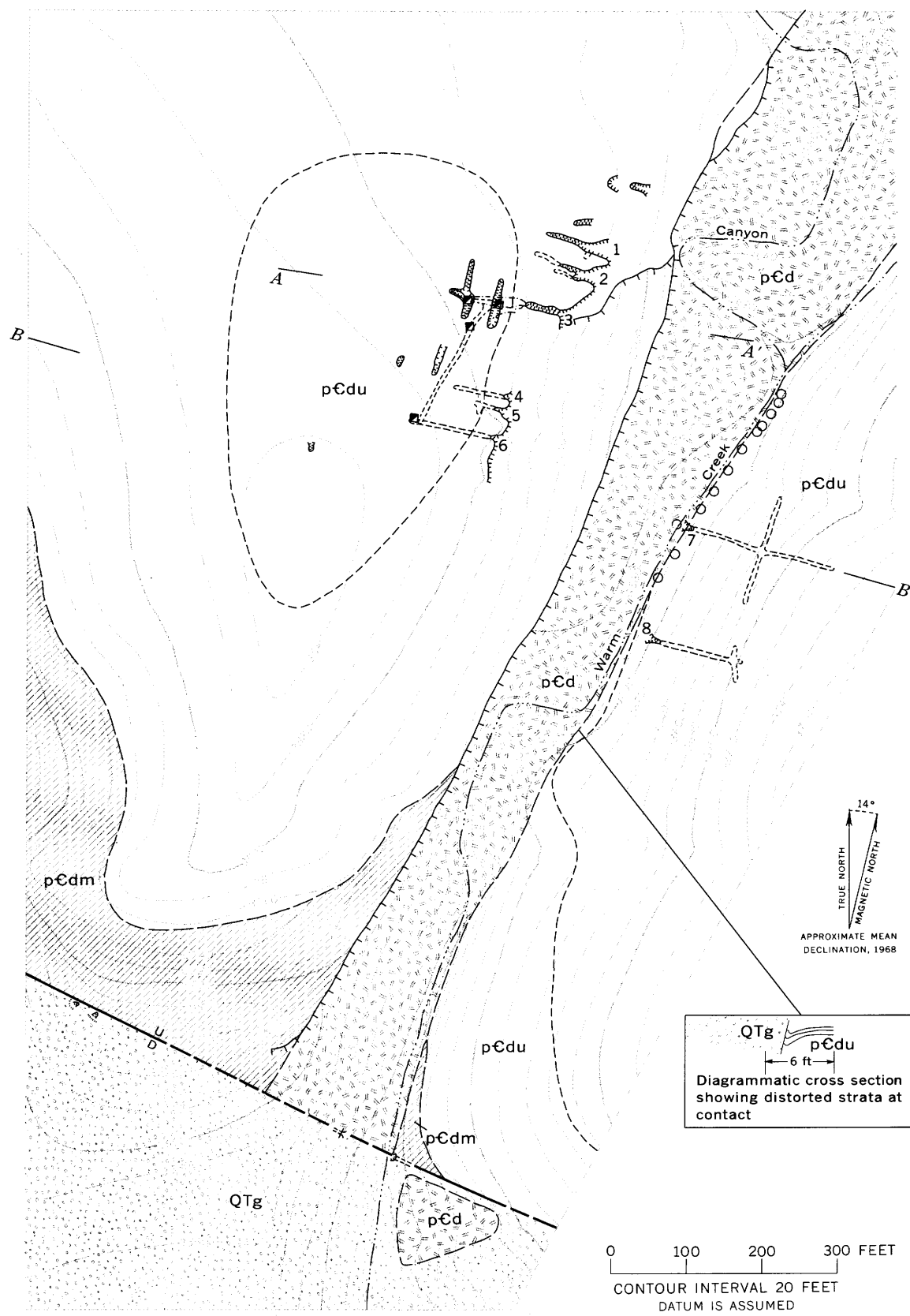
Randomly oriented prediabase or syndiabase faults commonly controlled emplacement of diabase sheets or were intruded by diabase dikes. Faults of this type have been noted in the Blevins Canyon area, in the Wilson Creek area, and just south of the Andy Gump deposit. The greatest displacement has been along faults in the monoclines, faults adjacent and generally parallel to the monocline structure zones, and cross faults. Most of the randomly oriented, less continuous faults have displaced the rocks to a lesser extent.

Original displacement along prediabase and syndiabase faults is principally normal, but reverse movement—probably due to later inflation by diabase—is common. Such renewed movement is indicated at the south ends of the Sierra Ancha and Cherry Creek monoclines, where the fault movement associated with diabase intrusion is reverse to that of the monoclines.

#### POSTDIABASE FAULTS

Postdiabase faults in Gila County are divisible into three broad age groups: Late Cretaceous(?) to early Tertiary, middle and late Tertiary, and Quaternary. Those of the first group are related to the Laramide revolution; those of the second group, to the formation of Basin and Range physiography; those of the third group, to a period of readjustment after the intense activity in the late Tertiary.

Postdiabase faults are abundant in the southern part of Gila County, but north of the Salt River they are relatively sparse. The faults are generally high-angle normal faults commonly of less than 1,000-foot displacement. Some are reverse faults (Ransome, 1919), and a few are classified as thrusts. Parallelism of faults is evident only locally, although the mountain ranges in the southern part of the county have a general northwest alignment, which is presumed to reflect the trends of large-scale block faults now mostly concealed by Cenozoic alluvium.



Base adapted from  
Kaiser (1951)

Modified from Granger and Raup (1959, pl. 46)  
Adit 8 mapped in June, 1955. Other workings  
mapped in November, 1954

0 100 200 300 FEET  
CONTOUR INTERVAL 20 FEET  
DATUM IS ASSUMED

## EXPLANATION

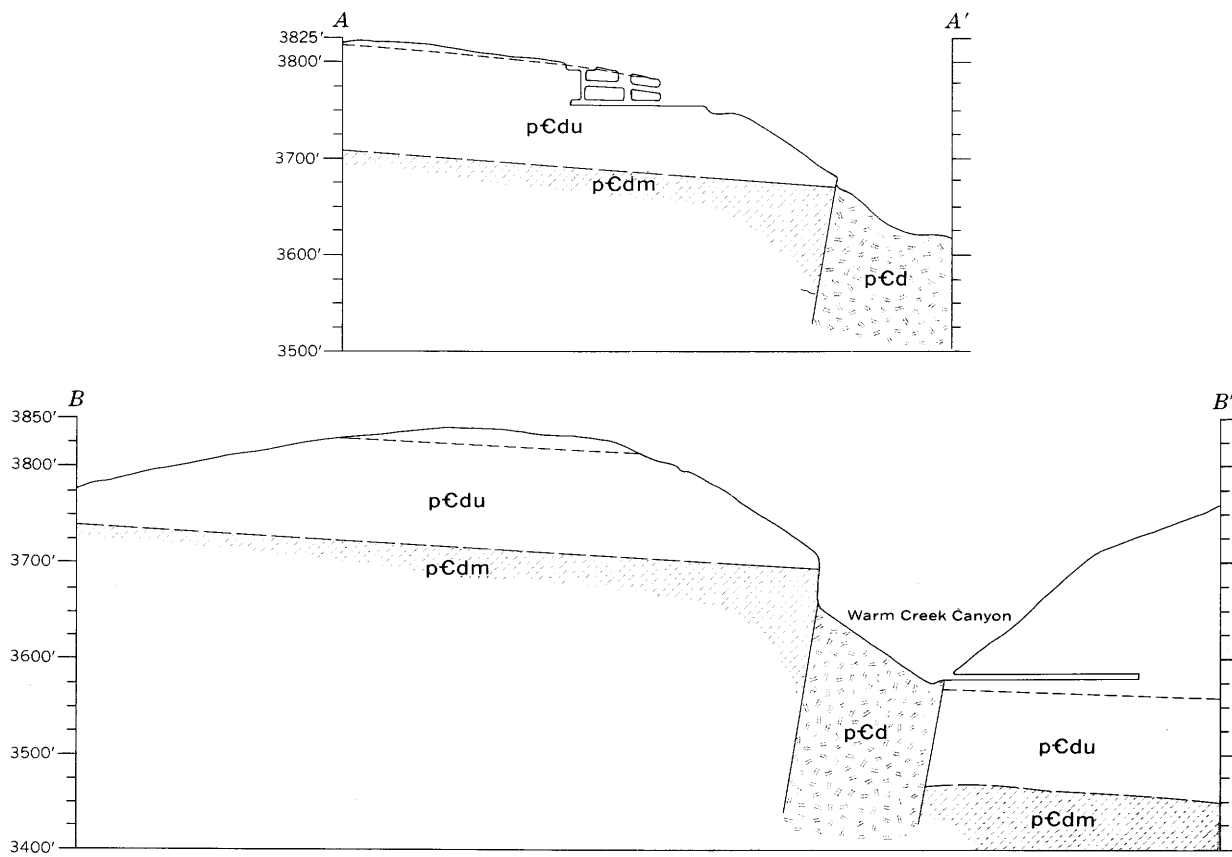
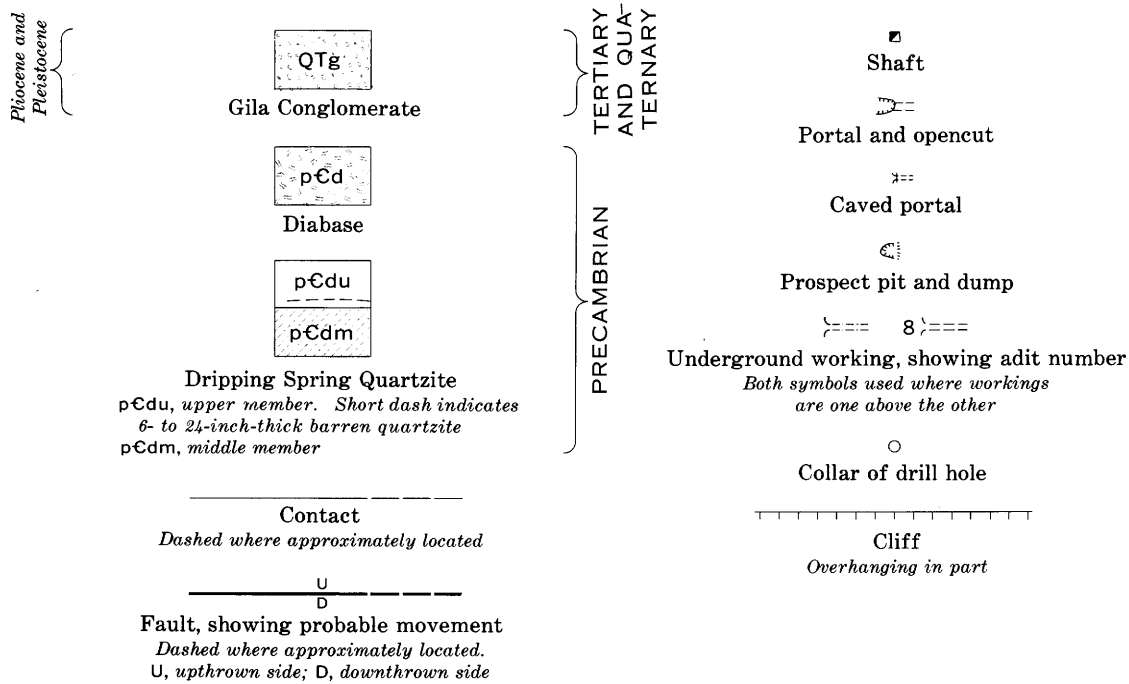


FIGURE 17.—Geologic map and section of the Red Bluff deposits.

Faults that can be classified as of Late Cretaceous(?) to early Tertiary age in Gila County are largely normal faults related to igneous intrusions of the Laramide revolution. Major thrust faults and broad folds typical of Laramide structural features in southern Arizona are less prominent in Gila County.

Thrust faults associated with the Laramide revolution commonly trend northwestward in Gila County, but the normal faults do not show a strong common trend. In the mining districts of the county, the suggestion of a northeastward alinement of Laramide faults, intrusive rocks, and veins has been noted by Butler and Wilson (1938).

No faults that can be classified as related to the Laramide revolution were found in the immediate vicinity of the uranium deposits in the Dripping Spring of Gila County.

Middle and late Tertiary faults are abundant in the southern part of Gila County, where they are largely responsible for the "regional brecciation" noted by Ransome (1903). Faults of this age group affect the middle Tertiary volcanic rocks but do not affect Gila Conglomerate of Pliocene and Pleistocene age. The widespread occurrence of these rocks facilitates the dating of the faults.

Most of the middle and late Tertiary faults are high-angle normal faults that do not show a broad regional alinement. A very prominent effect of orogeny during middle and late Tertiary time, however, was the formation of northwestward-trending ranges such as the Dripping Spring, Mescal, and Hayes Mountains. These ranges are tilted blocks probably bordered by high-angle normal faults or fault zones that have been buried by the extensive gravel deposits in the intermontane basins.

The uranium deposits in the Mescal Mountains are in strata that were tilted to the southwest during the formation of Basin and Range physiography; the uranium deposits north of the Salt River valley, however, are in strata very little affected by Tertiary faults. The major Tertiary faults nearest the Sierra Ancha uranium deposits are in a zone just southwest of the Red Bluff deposit (fig. 16). Faults in this zone are northwest-trending, high-angle normal faults whose southwest sides are downdropped. Displacement along the zone is at least 400-500 feet. Southwest of the faults are extensive deposits of Gila Conglomerate. Middle and late Tertiary faults are rare northeast of the fault zone at Red Bluff.

Quaternary faults have displaced and tilted Gila Conglomerate in many localities, principally south and west of the Sierra Ancha, but most commonly the faults are minor features that may indicate a period of readjustment. These faults have no apparent regional pattern.

Quaternary faults do not seem to have noticeably affected the rocks in the areas of uranium deposits. The late Tertiary faults near Red Bluff, however, show evidence locally of renewed movement in Quaternary time; brecciated Gila Conglomerate is present in the fault zone where it is exposed in Warm Creek canyon just south of the Red Bluff deposits (fig. 17).

### JOINTS

Joints are abundant in the rocks of Gila County, but only those in the Apache Group strata and in the diabase were examined in this study. Joints in the upper member of the Dripping Spring Quartzite, particularly in the gray unit in the areas of uranium deposits, received the most study; joints that cut diabase received less attention, and those that cut other rocks of the Apache Group were given only cursory examination. Most of the data are on joints in the Sierra Ancha region.

The term "joint" as used in this report refers to a fracture along which little or no movement has occurred and, thus, does not exclude fractures along which movement has slightly displaced the opposing walls. Nearly all the fractures in the Dripping Spring Quartzite that are classified as joints show little evidence of displacement except for opening movement normal to the joint surfaces. A few joints, however, do show evidence of slight movement; several contain breccia, some have faintly slickensided walls, and others displace strata a few inches vertically. Movement is nowhere more than several inches. Most of the movement, particularly opening of the joints, probably is due to readjustments after initial fracturing.

### TYPES

Two types of joints occur in the Sierra Ancha region. The more prevalent type is made up of planar joints similar to shear joints. The other type, more closely related to control of uranium deposits, is made up of irregular joints similar to tension joints. The terms "shear joint" and "tension joint" as used in this report refer to these characteristics and do not necessarily indicate the forces that formed the joints.

### TENSION JOINTS

Most of the tension joints recognized in the Sierra Ancha region are in mine workings, because such joints are rarely recognizable at outcrop. Thus the information on tension joints is heavily weighted with examples from the immediate vicinity of uranium deposits.

The most diagnostic characteristics of tension joints in the Dripping Spring Quartzite are irregularity of dip and, to a much lesser extent, irregularity of strike. Undulations or abrupt changes in dip of tension joints

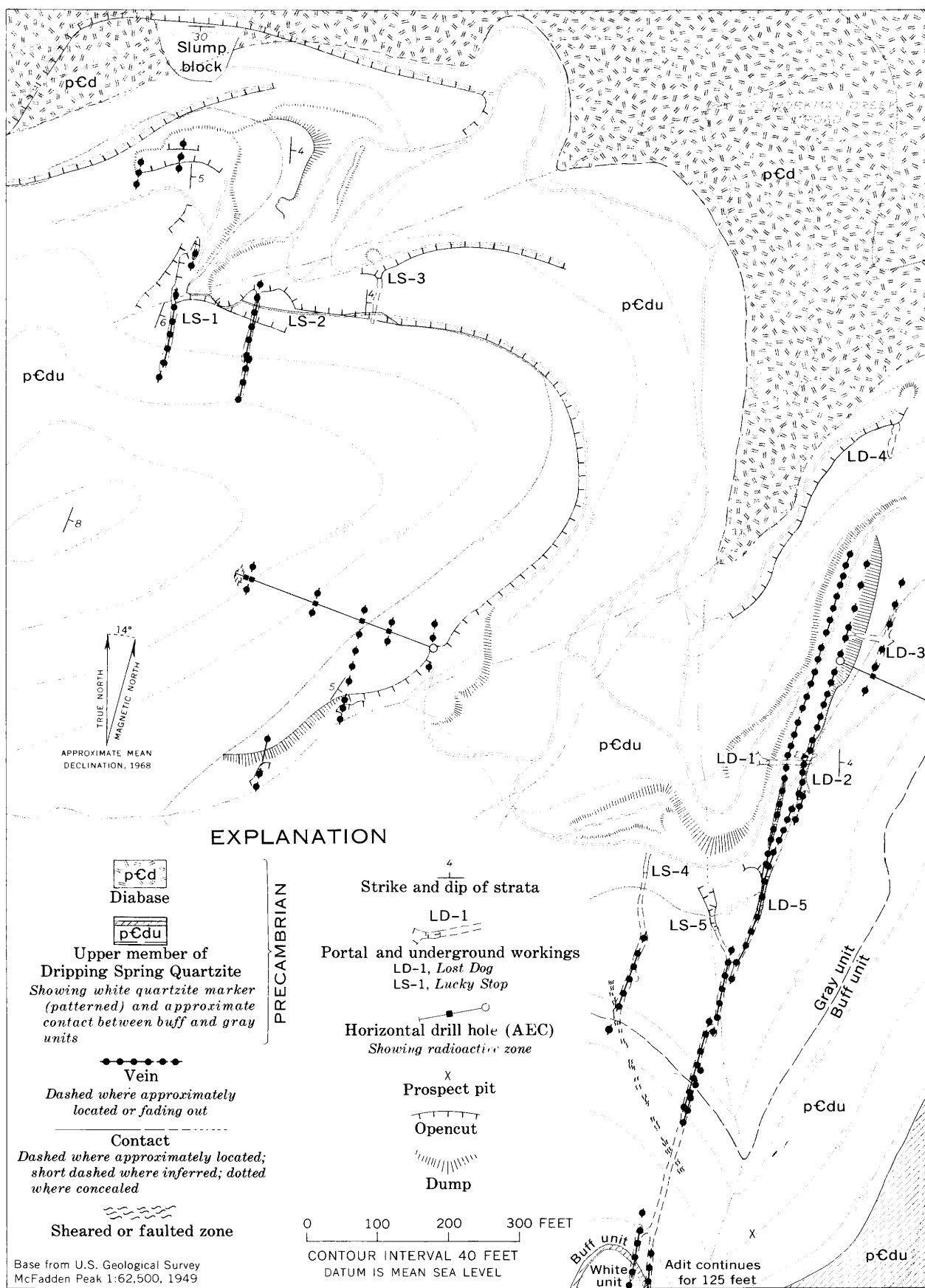


FIGURE 18.—Surficial geology in the vicinity of Lost Dog and Lucky Stop adits.

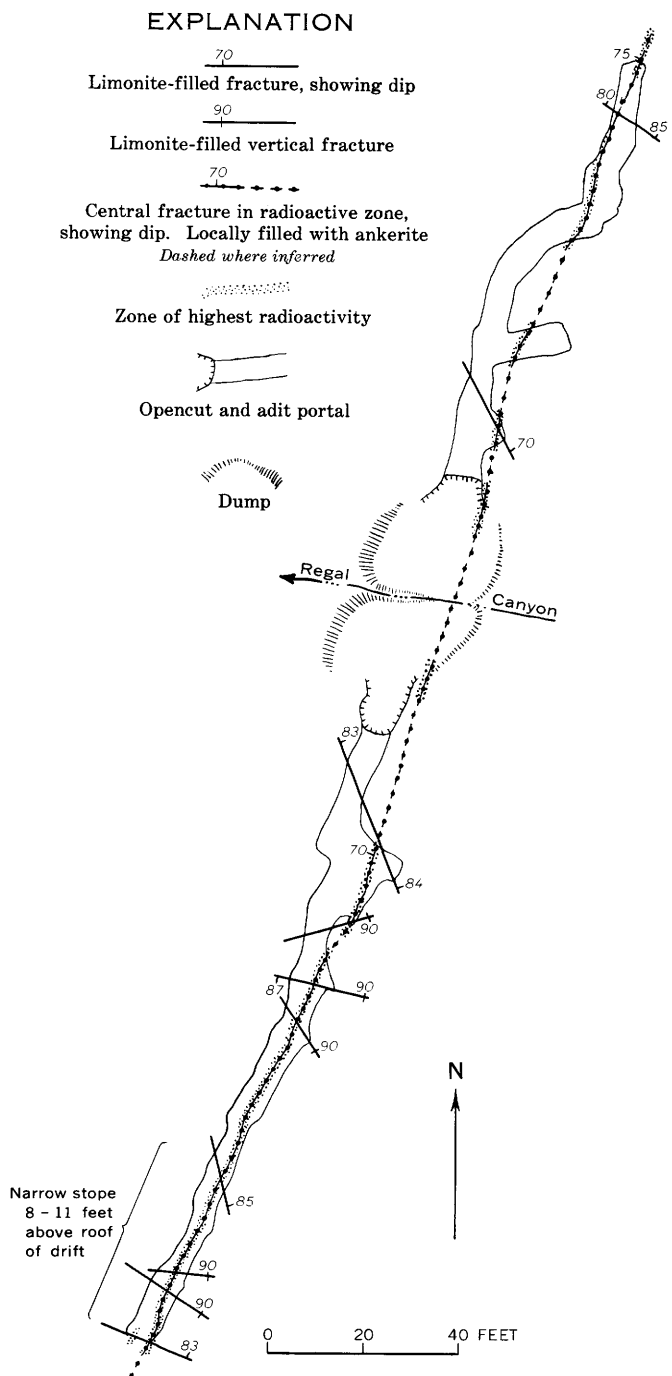


FIGURE 19.—Geologic map of the Tomato Juice adits.

are observable both in hand specimen and on a scale of several feet or tens of feet. In detail, tension joints are irregular even in nearly homogeneous strata; some irregularities of the joint surfaces may be due in part to differential solution of the rock at stratification planes. On a larger scale the joints are also affected by stratification and other inhomogeneities in the rock. Examples of irregular tension joints can be seen in hand specimens of the central, mineral-filled joints from the Tomato

Juice deposit, Rock Canyon deposit, and Hope 2 and 4 adits. On a larger scale the inconstant dip and strike of tension joints is well illustrated by the shapes of stopes and radioactive veins in the Hope adits (pl. 3) and the Alta Vista deposit (Granger and Raup, 1969).

Another characteristic of tension joints in the Dripping Spring Quartzite is their greater strike length and their greater vertical continuity, as compared with shear joints. Several tension joints traceable for several hundred feet are shown by uranium-bearing veins (pl. 3; figs. 18, 19), and vertical continuity of tension joints that is greater than that typical of shear joints is best shown by the vein in the Hope adit 3. A few shear joints are traceable along strike for as much as 100 feet, and possibly, one or more of these is as long as the tension joints but is not as readily traceable.

An en echelon pattern of tension joints, suggested by several uranium-bearing veins, is apparent only because of the presence of the radioactive material. The distribution of tension joints may actually be random, and the en echelon pattern may be a mere reflection of the selectivity of the mineralization. Examples of the possible en echelon pattern as reflected by uranium-bearing veins can be seen in the Lost Dog-Lucky Stop area (figs. 18 and 20), the Hope adit 3 (pl. 3), and the Big Buck deposit (fig. 21) and, on a smaller scale, at the Blue Rock deposit (Granger and Raup, 1969).

#### SHEAR JOINTS

Most joints in the Sierra Ancha region and all prominent joints recognized farther south in Gila County belong to the shear-joint type. These joints generally are nearly perpendicular to the stratification and have planar surfaces; both characteristics result in a fairly constant strike and dip for individual joints even in inhomogeneous rocks. The shear joints rarely are traceable for more than a few tens of feet and are shorter than tension joints in their vertical extent.

Most of the joints recorded as fractures on mine maps are shear joints that cut the uranium deposits and are consequently later than them. Not uncommonly a strong shear joint has nearly the same trend as the uranium-bearing vein, but in several deposits (pl. 3, adit 2; figs. 29, 40), these joints either diverge from the trend of the deposit after following it for several feet or die out. Apparently adjustments that resulted in shear joints were taken up in part by the earlier tension joints.

#### JOINT SYSTEMS

During the field investigation many measurements of joint trends and dips were made on the stronger joints in the upper member of the Dripping Spring Quartzite, largely in the gray unit. More than 750 measurements from joints in the gray unit throughout the Sierra An-

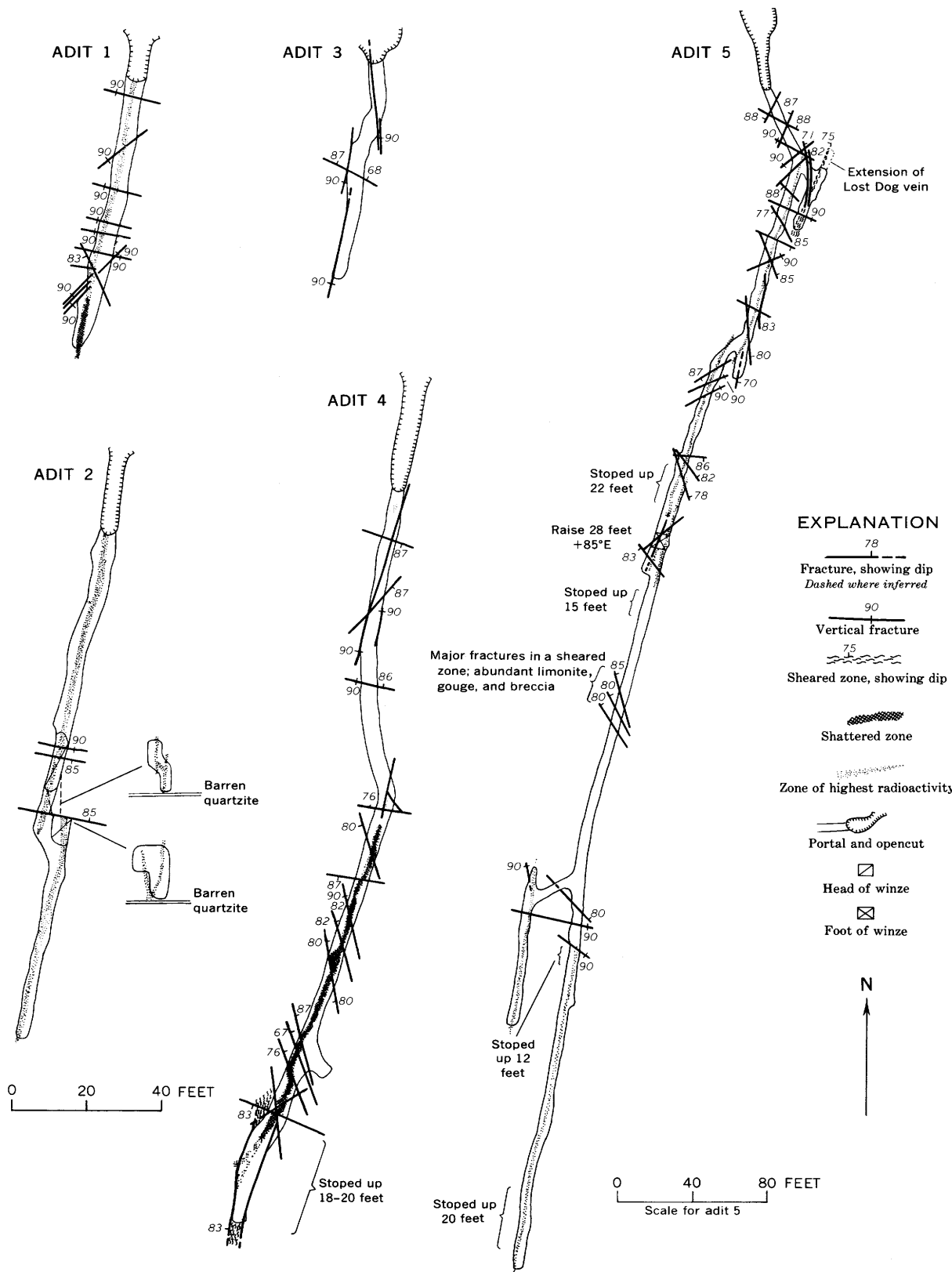


FIGURE 20.—Geologic maps of adits 1-5, Lucky Stop deposits.

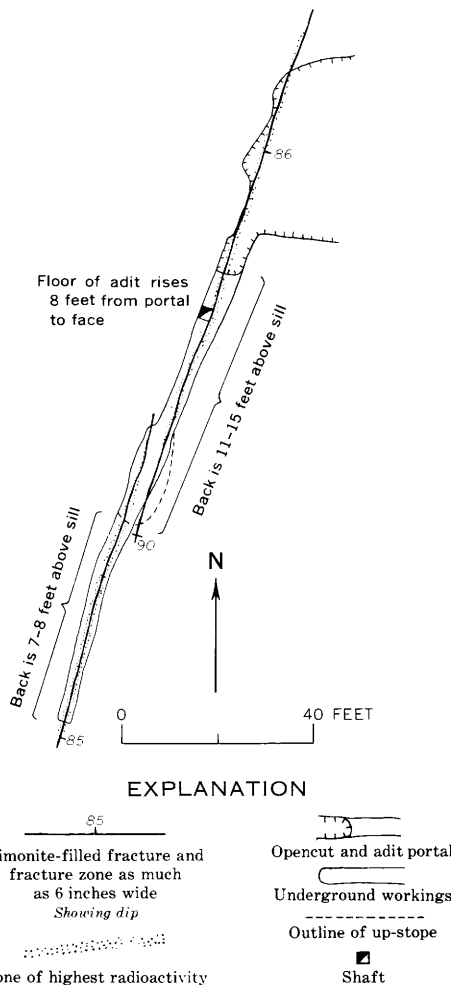


FIGURE 21.—Geologic map of the Big Buck adit.

cha region were plotted on an equal-area projection net and contoured on the basis of abundance (fig. 22).

Figure 22 shows two systems: a major conjugate joint system comprising two sets, and a minor system also comprising two sets. The average trend of the two sets in the major system are N. 17° E. and N. 77° W. These sets are called the north-northeast set and the west-northwest set. The average trends of the two sets of the minor system are N. 45° E. and N. 30° W. These sets are called the northeast and northwest sets.

Both shear joints and tension joints plot as parts of the major system, but shear joints are more abundant. In general, major system shear joints are moderately weak, as they are commonly traceable for less than 100 feet and cut only a few beds. Almost all joints are nearly vertical; dips are rarely less than 70°, and no one direction seems to be preferred. Spacing of the joints is not uniform, but most commonly at least one joint, albeit weak, occurs about every 3 feet laterally; rarely do more than two or three joints occur per foot. Joints in the

north-northeast set apparently are more abundant than are joints in the west-northwest set, but the possibility of sample bias cannot be overlooked because the north-northeast set is parallel to most of the uranium deposits and, thus, was given the closest attention in the field.

Joints of the minor system are all shear joints, as far as is known, but they are weaker in general than those of the major system. Otherwise, except for abundance, they are similar to major system joints in that they are nearly vertical, have short strike lengths, and rarely cut more than a few beds.

Joints in southern Gila County were studied only in the Dripping Spring Quartzite at the Lucky Boy Property (fig. 23) in the Mescal Mountains. These joints, all of which seem to belong to the shear-joint type, trend predominantly north-northwest and northeast. Dips are generally steep, but few joints are vertical. If we assume that these joints predate the tilting of the strata and that the trends of the joints are rotated to their position prior to tilting, the dominant trends become north-northeast and east. The similarity between these corrected trends and the trends of joints in the Sierra Ancha region is striking.

#### MOVEMENT ON JOINTS

Slight movement on some joints in the Dripping Spring is reflected by (1) measurable displacement of strata, (2) slickensides on joint surfaces, (3) gouge and breccia zones parallel to joint trends, and (4) open joints that locally have been filled with later minerals. The first three features indicate movement predominantly parallel to the joints; the last feature indicates movement predominantly perpendicular to the joints. Probably most of the movement on joints was merely a slight jostling motion that pulverized and brecciated the fracture surfaces without displacing opposing walls more than a fraction of an inch. Evidence of movement on most joints is lacking.

Measurable displacement was noted in the Shepp No. 2 mine, where strata are locally offset by faulting along joint trends. Displacement on one of these minor faults has been as much as 1 foot vertically, but plunging slickensides suggest nearly 2 feet of oblique slip. At the Rock Canyon deposit, laminae are offset about a fourth of an inch along an ankerite-filled joint. Similar relations exist on quartz-sulfide-filled joints at the Horse Shoe deposit.

Slickensides are present on joint surfaces of the west-northwest set at Red Bluff as well as those at the Shepp No. 2 mine. Most of the slickensides are horizontal or plunge at low angle.

Narrow zones of gouge and breccia parallel to the prominent joint sets are common. At the Shepp 2 mine (fig. 24), zones several feet wide locally are paral-

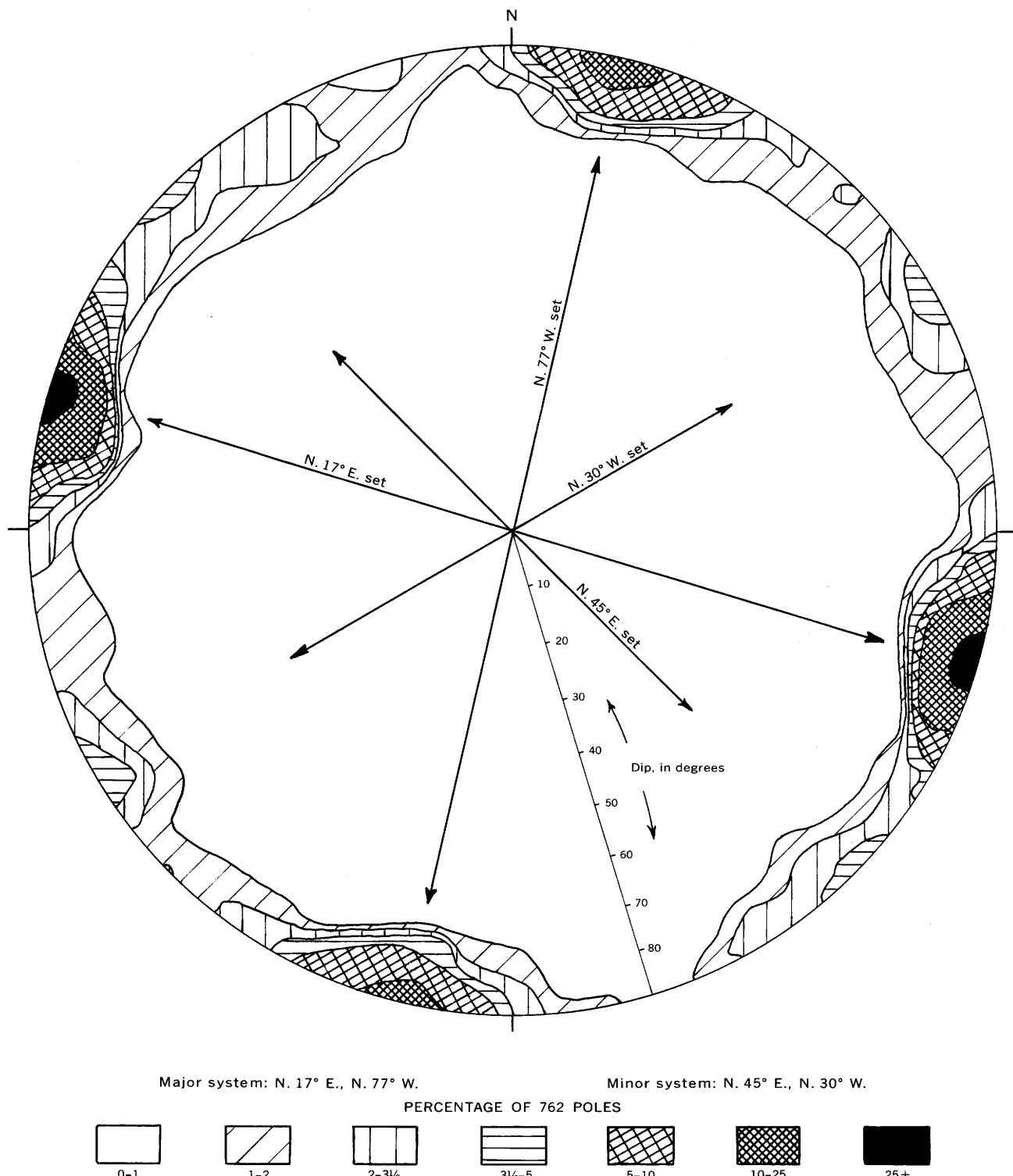


FIGURE 22.—Contour diagram of poles of 762 joints in gray unit, Dripping Spring Quartzite, northern Gila County (upper hemisphere, equal-area projection).

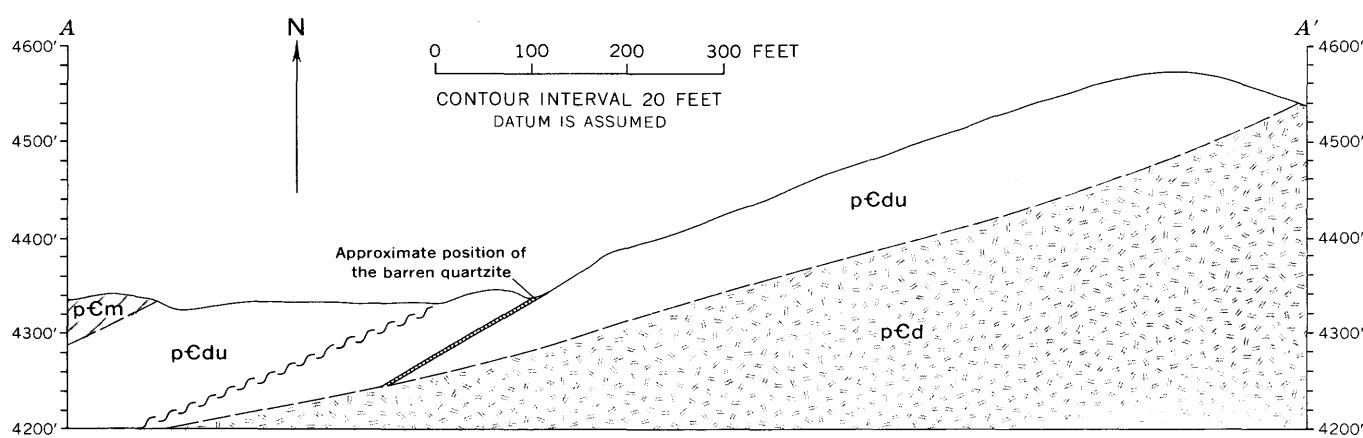
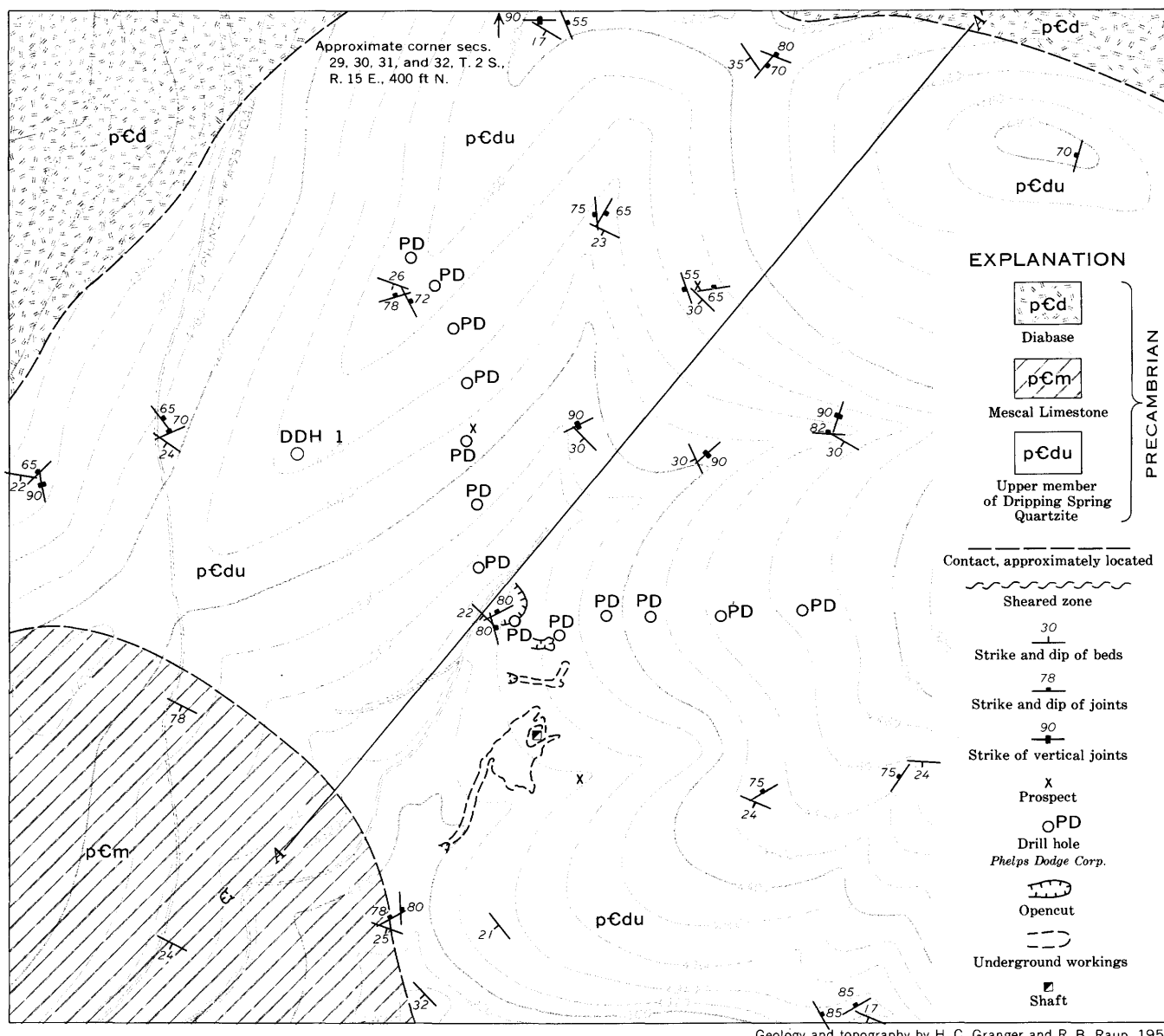


FIGURE 23.—Geologic map and section of the Lucky Boy deposit. Modified from Granger and Raup (1959, pl. 48).

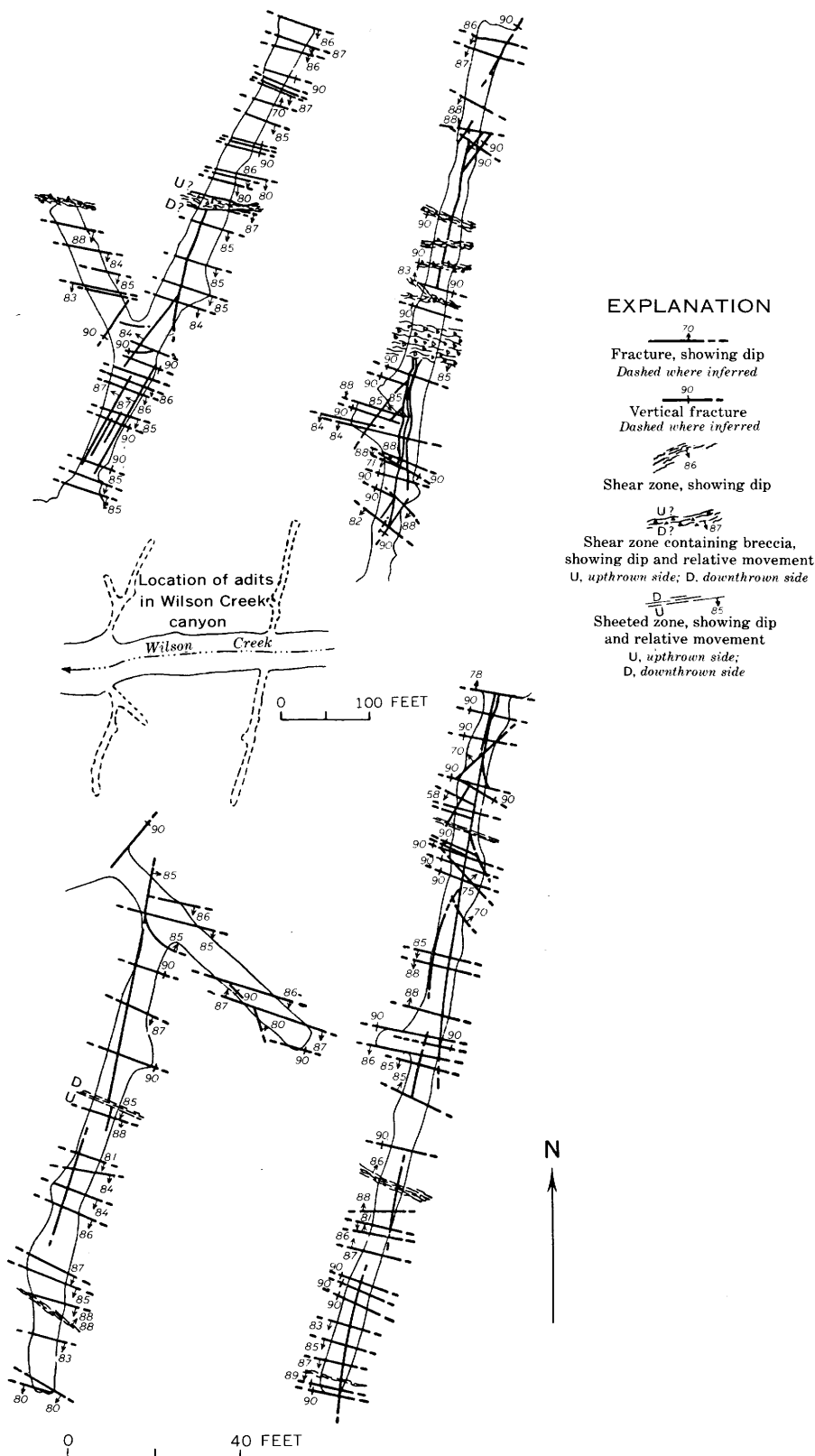


FIGURE 24.—Maps of adits, Shepp 2 deposits. (Granger and Raup, 1959, fig. 69). All workings are in the black facies, Dripping Spring Quartzite.

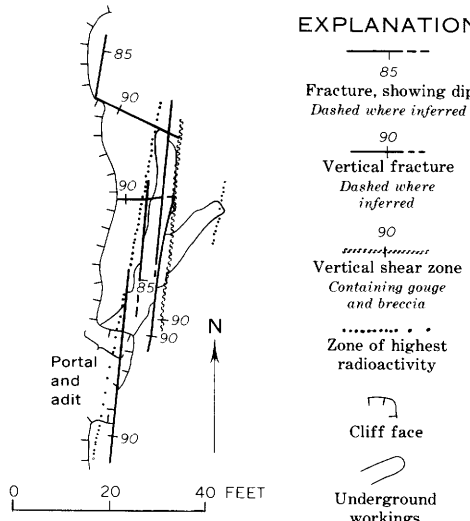


FIGURE 25.—Map of the Andy Gump adit.

lel to the west-northwest set. At the Sue mine, zones of similar trend are locally more than a foot wide but are commonly only a few inches wide. At the Andy Gump and First Chance deposits (figs. 25, 26) gouge and breccia zones are parallel to the north-northeast and northwest sets of joints. Where unoxidized, some of the breccia zones are cemented by calcite.

Minute tensional adjustments perpendicular to the joints slightly opened many joints and permitted some to be filled with quartz, sulfide minerals, or carbonate minerals. Calcite and pyrite, for example, are common in many unweathered joints in the Workman Creek area. Limonitic material in joints at the surface may represent weathered parts of such joints. Calcite-cemented breccia has been noted in the Workman Creek area in the Hope adit 1 (fig. 8). Ankerite fills the tension joints that form the cores of the Rock Canyon and Tomato Juice (fig. 13) deposits. Quartz and fluorite are less common as filling in opened joints.

Joint openings and the fillings in them are most commonly less than 0.1 inch wide. Locally, however, more pronounced movements opened the joints to such an extent that wide fissure veins formed. Several quartz veins near the Blevins Canyon deposit are as much as 10 feet wide. They trend about N.  $80^{\circ}$  W., nearly parallel to the west-northwest joint set. A fluorite vein containing abundant copper minerals near the Quartzite deposit is as much as 6 feet wide. It occupies a fault that trends about N.  $75^{\circ}$  W. and is parallel to prominent joints in the area.

#### HISTORY AND AGE

Two broad periods of joint formation are indicated in the Sierra Ancha region; the periods are separated by the end of the cooling history of the diabase. Prediabase and syndiabase joints are indicated by joint-

controlled diabase dikes (A. F. Shride, written commun., 1958) and by joint-controlled uranium deposits which were mineralized by solutions derived from the cooling diabase. Postdiabase jointing is indicated by the large number of joints that cut both diabase and earlier formed joints.

Prediabase and syndiabase joints are both shear and tension types and are principally in the major system. Forces that formed the northward-trending monoclines probably formed many of the prediabase joints. Forces that attended intrusion and cooling of diabase formed additional joints and very likely enlarged preexisting joints. Some of these forces were tensional, as indicated by normal faults related to the monoclines and by diabase-filled fissures.

The pattern of the prediabase and syndiabase joints, although obscured by postdiabase joints, probably strongly reflects established structural patterns in the lower Precambrian basement rocks. Pseudochannels also may have influenced the prediabase and syndiabase joint pattern, particularly in rocks of the gray and red units of the Dripping Spring Quartzite. The parallelism of pseudochannel and tension joints of the north-northeast set is pronounced in the Sierra Ancha region.

Postdiabase joints, which are far more abundant than the earlier joints, formed largely as shear joints in both major and minor systems in the Sierra Ancha region. Postdiabase tension joints may also have formed, but none were recognized in the field.

Wherever possible the postdiabase joints must have adapted to patterns formed earlier. Thus, in the Sierra Ancha region, postdiabase shear joints commonly are parallel to earlier joints. This is best seen in the mine workings, where many of the later shear joints tend to follow the trends of uranium-bearing veins that were emplaced along earlier tension joints. This influence of earlier formed joint patterns on post diabase joints is shown in the First Chance 1, Jon, Lost Dog 2, and Rainbow mines (figs. 26, 27, 28, and 29). That new patterns were formed, however, is shown by the post-diabase joints that cut the uranium-bearing veins or that branch at low angles from the veins.

The most prominent joints in the Dripping Spring Quartzite apparently formed prior to Quaternary time. In the Red Bluff and Lucky Boy areas, the strongest joints in both flat-lying strata and strata tilted before Quaternary time are nearly perpendicular to the stratification.

#### RADIOACTIVITY AND URANIUM CONTENT OF SELECTED ROCKS

The normal, or background, radioactivity and normal uranium content of several of the rock units of the Apache Group and associated rocks (table 4) have

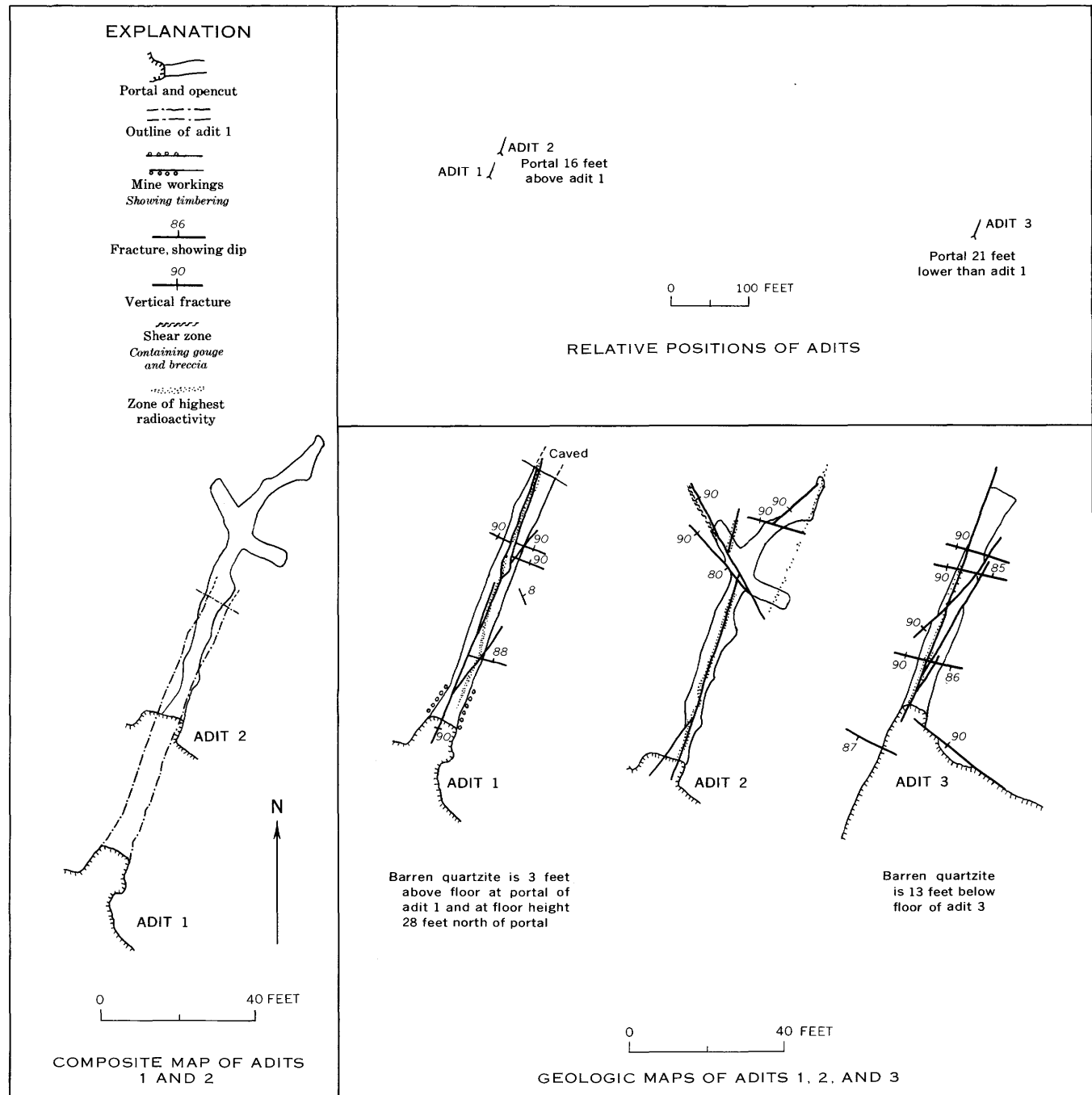
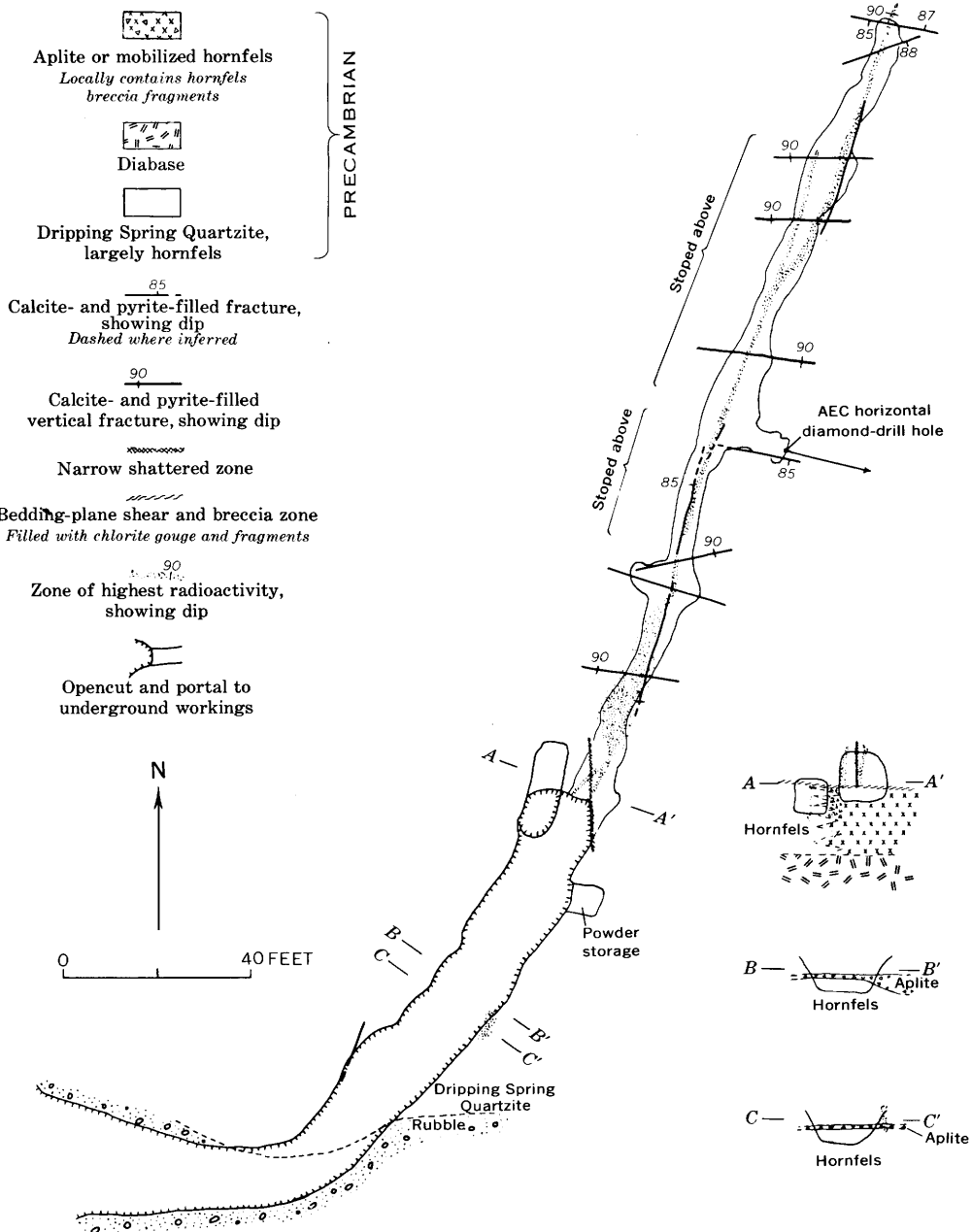


FIGURE 26.—Maps of adits 1-3, First Chance deposits.

## EXPLANATION



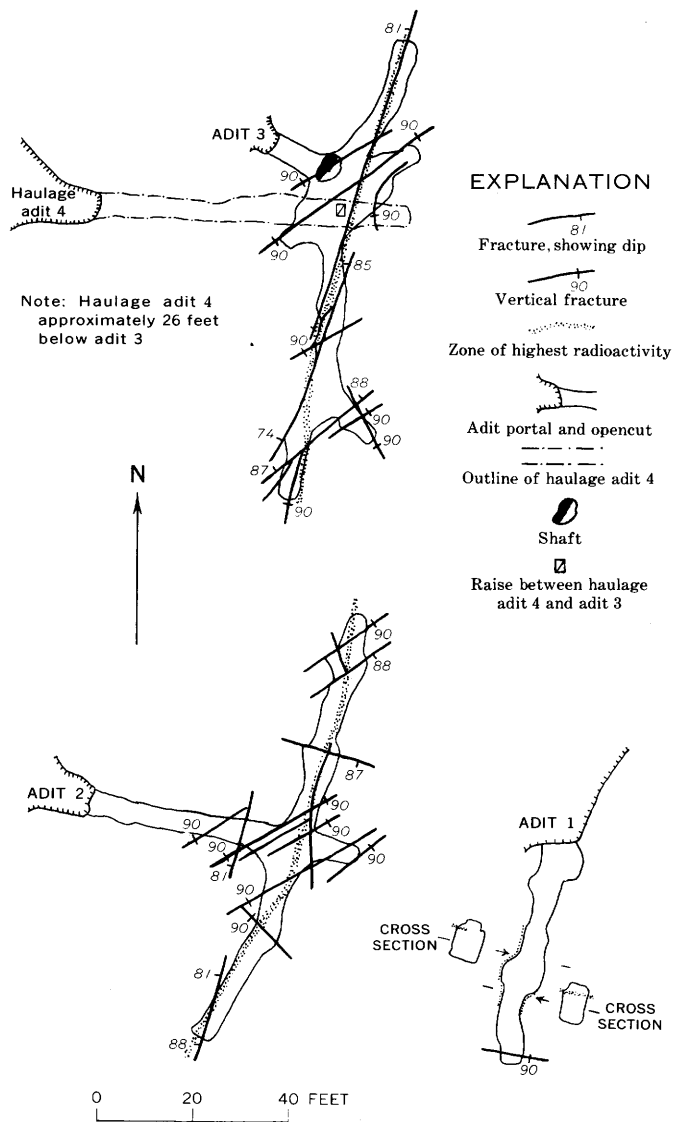


FIGURE 28.—Maps of adits 1-4, Lost Dog deposits.

been investigated during searches for, and studies of, uranium deposits in the Dripping Spring Quartzite. As these studies were largely confined to the Dripping Spring and the related diabase, the data on radioactivity and uranium content of these rocks are more complete than these data for other rocks. These data are illustrated diagrammatically in figure 30.

Several methods were used to determine the radioactivity and uranium content of the rocks herein described. For the most part gamma radioactivity was measured in the field in milliroentgens per hour with a portable scintillation meter held next to the rock outcrop. Average radioactivity of each facies and unit was recorded while stratigraphic sections were being measured during our work on the stratigraphy of the Dripping Spring (Granger and Raup, 1964). Also, while mapping in the Workman Creek and Red Bluff areas

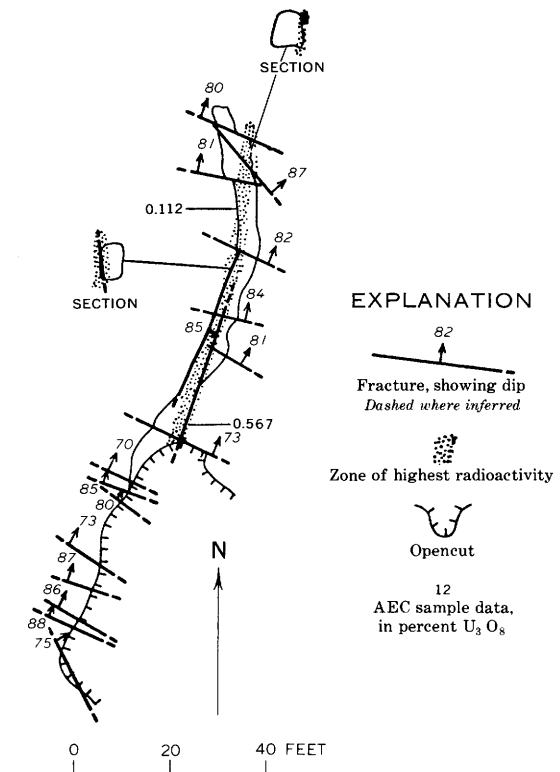


FIGURE 29.—Map and sections of the Rainbow adit (Granger and Raup, 1959, fig. 59).

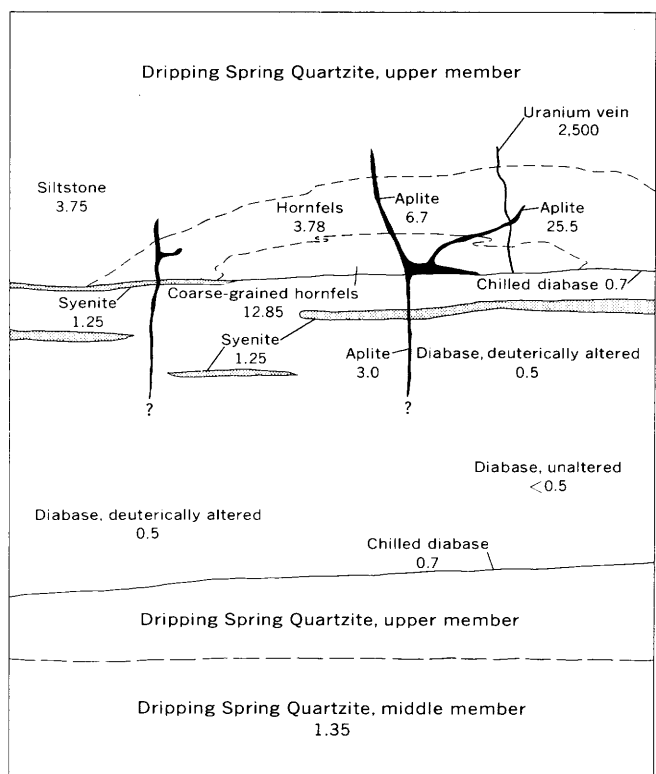


FIGURE 30.—Typical uranium content, in parts per million, of Dripping Spring Quartzite and several related rocks.

TABLE 4.—*Radioactivity and uranium content of the Dripping Spring Quartzite, diabase, and associated rocks*

Rock	Airborne measurements <sup>1</sup> (microamperes)	Ground measure- ments <sup>2</sup> (mr per hr)	Summary of sample data			Adapted from Williams <sup>6</sup> (1957)	
			eU <sup>3</sup> (percent)	U, range <sup>4</sup> (ppm)	U, average <sup>5</sup> (ppm)	U, average <sup>5</sup> (ppm)	U, range (ppm)
Diabase	100	0.01 - 0.015					
Pyrogenic				0.1 - 0.22	0.14 (7)		
Deuterically altered			<.001	.20 - 1.18	.49 (14)	0.554 (5)	0.125 - 0.832
Chilled border			<.001	.44 - .88	.69 (5)	.465 (1)	
Syenite	.015 - .025	.001 - .002		.69 - 1.56	1.25 (4)	3.17 (3)	1.85 - 5.65
Aplitite:							
In diabase	.025 - .03			1.95 - 4.52	3.00 (4)		
In hornfels, away from ore				3.41 - 10.82	6.68 (6)		
In hornfels, near ore				5.74 - 49.72	25.61 (3)	30.7 (1)	
Deuteric veins and bordering rock				.19 - 19.79	1.94 (21)		
Basalt		.01 - .015			.50 (1)		
Mescal Limestone:							
Upper member	375-475	.03 - .05	.007				
Lower and algal members	125-150	.01 - .02					
Dripping Spring Quartzite:							
Upper member	375-475	.035	.006				
Gray unit, unmetamorphosed		.039	.006 - .007	2.2 - 4.8	3.74 (5)	2.97 (1)	
Gray unit, hornfels		.02 - .05	.006	1 - 4	2.67 (3)	4.15 (9)	2.39 - 8.83
Gray unit, coarse-grained hornfels		.02 - .05	.006	6 - 22	11.33 (3)	14.00 (4)	4.67 - 30.7
Middle member	250-350	.022	.002	.92 - 2	1.37 (13)		
Barnes Conglomerate Member		.019		.93 - 1.04	.99 (2)		
Pioneer Formation	200-350	.02 - .04	.006	2.92 - 2.96	2.94 (2)		
Granite	375-500	.03 - .05					

<sup>1</sup> Measurements by Magleby and Mead (1955). Background over water is 75 microamperes.

<sup>2</sup> Measurements by portable scintillation meter at the rock surface. Single values are averages.

<sup>3</sup> Equivalent uranium determined by beta-gamma methods.

<sup>4</sup> Analyses of igneous rocks by J. C. Antweiler and G. J. Neuerburg, sedimentary and metamorphic rocks by E. J. Fennelly.

and doing reconnaissance in Gila County, many measurements were made of the radioactivity of rocks other than the Dripping Spring.

An aerial reconnaissance of the Dripping Spring Quartzite conducted by the U.S. Atomic Energy Commission recorded additional data on radioactivity; Magleby and Mead (1955) reported normal meter readings over several of the more prominent rock types in Gila County. The radiation detection instrument carried in the aircraft measured the effect of gamma radioactivity in microamperes (table 4).

Numerous samples were analyzed for both equivalent uranium (eU) and uranium (U) content to supplement the radioactivity data and to relate the radioactivity to the actual content of uranium in the rocks. Gastil (1953) reported averages of similar analyses of samples of siltstone strata in the Pioneer Formation as well as the upper member of the Dripping Spring.

Williams (1957), using a method involving alpha particle counting, reported the equivalent uranium content of samples from the Dripping Spring and diabase. The analytical method used seems to be remarkably precise for very low level uranium determinations in these rocks, and, probably because of the extremely low thorium content, the results are closely comparable (table 4) to analyses of similar samples determined by precise fluorimetric methods.

Low-level analyses of the uranium content of rocks by routine fluorimetric methods in the Denver laboratories of the U.S. Geological Survey are generally reported to an accuracy of no greater than 0.001 percent. A rock, for example, that actually contains only 2-3

<sup>5</sup> Figures in parentheses indicate number of samples involved in the averages.

<sup>6</sup> Williams' analyses are in terms of equivalent uranium determined by alpha emission. The results are comparable to chemical determinations because of the low thorium-uranium ratio in the rocks.

ppm (parts per million) uranium might be reported as having 0.001 percent uranium (10 ppm U) and conceivably could be reported as 0.002 percent uranium. Many of our samples were analyzed by these methods, but the results are inadequate for this part of the study. Where greater accuracy is required, as in the following pages, the Geological Survey laboratories can routinely report the uranium content to within  $\pm 1$  ppm. The analyses made by J. C. Antweiler were reported to the second decimal in parts per million and are probably accurate to  $\pm 30$  percent of the value reported.

#### PRECAMBRIAN GRANITE

The granite that underlies much of the Apache Group, particularly in the Sierra Ancha, is one of the more radioactive rocks noted in Gila County. The range of most of the field measurements of the radioactivity is shown in table 4. No samples of the granite were analyzed for equivalent uranium and uranium content. Radioactivity in granites is generally caused partly by potassium in feldspars and micas and by uranium and thorium in accessory minerals such as zircon and xenotime, and partly by uranium and thorium distributed along microfissure and crystal interfaces.

#### PIONEER FORMATION

The few measurements of the radioactivity of the Pioneer Formation indicate that much of the Pioneer, particularly the sandy parts, and the middle member of the Dripping Spring generally have similar radioactivity levels. Compared with the upper member of the Dripping Spring, and particularly with the gray unit,

however, the average Pioneer is less radioactive. Gastil (1953) studied the radioactivity of the Pioneer in detail and concluded that siltstone strata in both the Pioneer and the upper-member of the Dripping Spring have similar radioactivity levels; his samples consistently assayed about 0.006 percent equivalent uranium and 0.001 percent uranium. Furthermore, he suggested that the radioactivity of the siltstones is related to both grain size and degree of weathering. Finer grained and fresher rocks were more radioactive.

The uranium content of the Pioneer is low, as is indicated by Gastil's sample data. The difference between the equivalent uranium and uranium content of the rock was not explained by Gastil, but he suggested that the difference is caused in part by the radioactive isotope  $K^{40}$ . Two samples of shaly Pioneer analyzed for us by J. C. Antweiler average 2.94 ppm uranium.

#### DRIPPING SPRING QUARTZITE

##### UNMETAMORPHOSED ROCK

The Barnes Conglomerate Member is the least radioactive part of the Dripping Spring. An average of all the field measurements of radioactivity taken during study of the stratigraphic section (Granger and Raup, 1964) is 0.019 mr per hr (milliroentgen per hour). Two samples of the sandstone matrix of the Barnes taken within a few feet distant from diabase contained 0.93 and 1.04 ppm uranium.

The middle member is only slightly more radioactive than the Barnes. The average of all field measurements of the radioactivity is 0.022 mr per hr. The highly arkosic strata are generally near 0.03 mr per hr, whereas the more quartzose strata are 0.02 mr per hr or less. Several samples of the member taken during the course of measuring the sections contained an average of 1.37 ppm uranium. The arkosic samples contained about 2 ppm uranium in contrast with 1 ppm uranium in the more quartzose samples.

The upper member of the Dripping Spring is unusually radioactive for a clastic sedimentary rock. The average of our measurements is 0.035 mr per hr but some strata are considerably more radioactive. In general the most radioactive rocks in the upper member are composed of silt- and clay-like particles. Gastil's samples (1953) from the upper member coincide with ours in regard to equivalent uranium and uranium content. Most commonly the equivalent uranium content of the rocks is about 0.006–0.007 percent where the rocks are not in proximity to uranium deposits or diabase bodies.

The gray unit is almost without exception the most radioactive part of the upper member. Because of the abnormally high radioactivity and because most of the

better uranium deposits are in the gray unit, the radioactivity of these rocks was studied in greater detail. The average radioactivity of unmineralized parts of the gray unit is 0.039 mr per hr or more than 11 percent higher than the average radioactivity of the entire upper member and nearly twice as high as that of the middle member. However, the normal uranium content of the gray unit, about 3.7 ppm, is not exceptionally high.

Five samples of the gray unit from widely scattered localities in Gila County were selected because of their apparent freshness and great distance from diabase and ore deposits. The uranium content of these samples ranged from 2.2 ppm to 4.8 ppm and averaged 3.74 ppm. The radioactivity of the samples, however, averaged about 0.006 percent equivalent uranium (60 ppm eU). Most of this excess radioactivity is caused by the radioactive isotope  $K^{40}$ . The average potassium content of the above samples is slightly more than 10 percent. Because the amount of beta and gamma radioactivity emitted from 2 percent potassium in a sample is about equal to that from the equilibrium products from 0.001 percent uranium (comparison used in U.S. Geol. Survey Denver Lab., J. N. Rosholt, oral commun., 1958), slightly more than 0.005 percent equivalent uranium (50 ppm eU) in the above samples is caused by potassium content. Many other samples of the gray unit collected nearer to uranium deposits or diabase and containing anomalous but low uranium content seem to have an average equivalent uranium about 0.005 percent in excess of the uranium content. Where the uranium content exceeds a few hundredths of a percent, a lack of equilibrium between uranium and its daughter products commonly masks the effect of radioactivity due to potassium and such samples may be more, or even less, radioactive than can be expected from the uranium and potassium contents alone.

Field measurements of radioactivity do not indicate such an abrupt increase in radioactivity attributable to  $K^{40}$  as do laboratory measurements. This is because the ratio of beta and gamma radiation from  $K^{40}$  is about 8 to 1. Field scintillation meters detect only gamma rays, but the laboratory instruments used detect both beta and gamma radiations. Therefore, the apparent increase of detectable radiation caused by a given increase in potassium content is theoretically about nine times as much in the laboratory as in the field. In actual practice the ratio depends on the extent to which the laboratory instrument filters the beta radiation.

##### METAMORPHOSED ROCK

Most samples of metamorphosed siltstone of the gray unit that we collected were so near a uranium-bearing vein that they could not be relied upon to represent

rocks unaffected by the ore-forming processes. We have, therefore, supplemented our meager sample data with data given by Williams (1957). Williams' sample classification differs somewhat from ours, but from his sample descriptions and our knowledge of the sample localities we were able to classify some of his samples as hornfels and coarse-grained hornfels, as follows:

<i>Rock type</i>	<i>Sample Nos. (Williams, 1957)</i>
Hornfels-----	409, 419, 885, 887, 898, WC3, WC6, WC12
Coarse-grained hornfels--	852, 853, 854, 896

A combination of our data and those of Williams (table 4) indicates that the average normal hornfels contains about the same amount of uranium (3.78 ppm) as the average equivalent siltstone before metamorphism (3.74 ppm). The average coarse-grained hornfels, in contrast, contains more than three times as much uranium (12.85 ppm) as the original siltstone.

This enrichment of the coarse-grained hornfels in uranium may be gradational, corresponding to degree of increase in metamorphism. As the sodium content also increases with the degree of metamorphism, the data imply that metamorphism to the grade of coarse-grained hornfels was accompanied by the introduction of a pervasive sodium- and uranium-bearing fluid from an external source.

#### MESCAL LIMESTONE

The lower and algal members of the Mescal Limestone are the least radioactive sedimentary rocks in the Apache Group (table 4); they are about half as radioactive as the middle member of the Dripping Spring, and about a third as radioactive as the upper member of the Dripping Spring. The radioactivity of the upper member of the Mescal, however, is approximately equal to that of the upper member of the Dripping Spring. Carbonaceous shaly strata in the upper member of the Mescal are especially radioactive. Some silty strata in the upper member of the Mescal are relatively low in uranium content and high in potassium (Neuerburg and Granger, 1960); much of the radioactivity in these rocks is probably due to radioactive K<sup>40</sup> in the abundant potassium feldspar, as is true in the black facies of the upper member of the Dripping Spring.

#### BASALT

The Precambrian basalt that overlies Apache Group strata is less radioactive than any of the sedimentary rocks in the Apache Group. Of the rocks we studied, only "normal" diabase had as little measurable radioactivity. The one sample of basalt that was analyzed for uranium contained 0.50 ppm uranium, which is approximately the same amount as in most of the samples of diabase.

#### DIABASE

The radioactivity and the uranium content of the diabase and related rocks received considerable attention because the diabase was possibly the source of the uranium in the deposits. A detailed discussion of the uranium content of the diabase and related rocks is given by Neuerburg and Granger (1960) and in other parts of this report and is only summarized here. In most samples analyzed by standard fluorimetric methods, the uranium content of "normal" diabase, chilled border, syenite, and aplite is below detectable limits—or somewhat less than 0.001 percent. Similarly, the radioactivity of these rocks is low; nearly all samples analyzed in the laboratory contain less than 0.001 percent equivalent uranium. In the field, detectable radioactivity of "normal" diabase seems slightly lower than that of the differentiates when measured with a scintillation meter. In general, the more salic differentiates are slightly more radioactive.

Low-level uranium analyses of the various facies and differentiates of diabase, however, reveal marked and distinctive differences among them. The lowest uranium contents, all less than 0.5 ppm, are found in pyrogenic diabase—diabase that shows little or no evidence of having been altered by deuterian action. The deuterianally altered diabase generally contains an average of about 0.5 ppm uranium; individual samples may contain much more uranium, but rarely much less. One sample of diabase pegmatite from the Cibique Creek locality contained 0.94 ppm uranium. The average of 0.69 ppm uranium (table 4) for chilled diabase excludes data from several samples taken within 10 inches of the edge of the diabase sill that intruded the middle member of the Dripping Spring at the mouth of Cibique Creek. These samples contained as much as 8.72 ppm uranium and seem to be anomalously enriched relative to similar rocks in the other localities sampled. The chilled contacts are not presumed to be representative of the composition of the original magma, as originally believed (Granger and Raup, 1959), because in most places they have been altered by deuterian action.

The syenites and aplites contain successively larger amounts of uranium than the diabase. In analyzed syenites, the uranium content ranged from 0.69 to 1.56 ppm and averaged 1.25 ppm; in aplites enclosed by diabase, the uranium content ranged from 1.95 to 4.52 ppm and averaged 3.0 ppm. The aplites that have intruded the Dripping Spring seem to have acquired uranium as the feldspars changed from a sodic type to a potassic type. Among the six samples analyzed, the range in uranium content was from 3.41 ppm to 10.82 ppm, and the average was 6.68 ppm.

The uranium content of the narrow black deuterian veinlets was determined with difficulty. The vein mate-

rial proved virtually impossible to separate from the bordering diabase in amounts adequate for analysis. Hence, all the analyses made were of mixtures of vein matter and the enclosing rock. These analyses gave very erratic results; uranium contents ranged from 0.19 ppm to 19.79 ppm. Samples of the bleached or dark aureole in the diabase enclosing the veinlets generally have a uranium content similar to or lower than that of the impure vein matter. Some of the veinlets may, therefore, contain considerably more uranium than the data indicate. Presumably much of the uranium entrapped in the deuteritic veins is contained in zircon, and possibly parts of veinlets with a low uranium content also have a low zircon content.

In summarizing the data on uranium content of the various rocks, two facts seem to be significant: (1) the uranium content of the host rocks for uranium deposits, in general, increases with degree of metamorphism, and (2) the uranium content of various facies of the diabase system increases with degree of differentiation and deuteritic alteration. These observations, coupled with the fact that all the richer uranium deposits are near large diabase bodies, provide strong evidence for a genetic relation between diabase and uranium deposits.

#### URANIUM DEPOSITS

##### MINING HISTORY

The initial discovery of uranium ore in the Dripping Spring Quartzite was made by Carl Larsen on his Red Bluff property in January 1950. The presence of uranium in the rock was confirmed by the U.S. Bureau of Mines, and the discovery was publicized but aroused little interest. By February 1953, Melvin Stockman and O. H. Shepp had discovered other deposits in the Dripping Spring in the Wilson Creek area nearly 20 miles north of Red Bluff.

According to the Arizona Republic, Phoenix, Ariz., for Oct. 3, 1954, Larsen sold his claims for a large sum of money in February 1954. Shortly thereafter the U.S. Atomic Energy Commission announced that it would conduct an aerial radioactivity survey of several areas, starting with the southern Sierra Ancha area, and would make the results available to the public. These two factors, more than any others, were responsible for encouraging the uranium rush throughout Gila County during the rest of 1954 and 1955.

During parts of this rush period as many as 900 claims per month were staked and registered in Gila County, largely for uranium. Many exposures of the Dripping Spring were found to be anomalously radioactive. Development was slow because of the spotty nature of many deposits and the inaccessibility of much of the area.

Ore originally produced from the Red Bluff mine was shipped to the buying depot at Bluewater, N. Mex. The cost of such shipments and the reports that a buying depot would soon be constructed near Globe, caused most of the miners to stockpile their ore during 1954 and 1955. In July 1955, an ore-buying depot managed by the American Smelting and Refining Co. was opened at Cutter about 8 miles east of Globe.

Federal assistance to the miners was provided by an Atomic Energy Commission suboffice established in Globe in early 1955, by a road-building program into particularly inaccessible areas known to contain deposits, by exploratory diamond drilling, and by Defense Minerals Exploration Administration loans.

On January 15, 1957, the U.S. Atomic Energy Commission announced that the Cutter depot would be closed on June 30, 1957, because the ore production and the ore reserves in the area did not indicate any reasonable prospects for an economic milling operation. Production immediately increased, because the mine owners attempted to mine as much ore as possible before the depot closed. Approximately 40 percent of all the ore produced from the Dripping Spring was mined between January and July 1957.

The increased production prompted the U.S. Atomic Energy Commission to determine whether new developments or new information might have improved the outlook for an ore supply. They concluded, however, that:

1. The ore reserves apparently were not large enough to support an economic milling program.
2. Known deposits were too small and of too low grade to be mined economically without the initial production bonus available under Atomic Energy Commission buying schedules.
3. The ore was expensive to mill, and the milling costs would make ore concentration uneconomic.
4. Continued operation of the buying station would result in additional losses to the Government without reasonable prospects of any economic uranium production.

The buying depot was closed on June 30, 1957, and mining of uranium ore from the Dripping Spring ceased except at the Hope 3 mine. The extent of continued production from the Hope was not known as of 1960.

##### PRODUCTION

Production of uranium ore from the Dripping Spring Quartzite has been disappointing in view of the intensive efforts to find and develop the deposits. Shipments have been made from relatively few of the deposits, and some of these were of such low grade (less than 0.10 percent  $U_3O_8$ ) that no payment was made; mining

costs for much of the production exceeded the payments for the ore.

Shipments were made by 16 mines; one of these mines shipped no rock that contained more than 0.10 percent  $U_3O_8$ , and the ore shipped by another mine may not have been produced at that mine. Only five mines—Red Bluff, Hope, Lucky Boy, Suckerite, and Lucky Stop—had produced more than 2,000 tons of ore by June 1957. By that time, total production from the Dripping Spring was 21,274.42 tons of dry rock. Of this amount, 1,192.44 tons contained less than 0.10 percent  $U_3O_8$ , 12,922.8 tons contained from 0.10 to 0.20 percent  $U_3O_8$ , and 7,159.18 tons contained more than 0.20 percent  $U_3O_8$ . These figures were derived largely from quarterly summaries in which only the average tenor for 3-month periods was reported. A detailed summary of individual shipments might result in somewhat different tonnages for each classification.

The total  $U_3O_8$  contained in the rocks delivered to both the Bluewater and Cutter buying depots by June 3, 1957, was approximately 42.1 tons. Of this amount, about 0.9 ton was in rock that contained less than 0.10 percent  $U_3O_8$ , 21.5 tons was in ore that contained 0.10–0.20 percent  $U_3O_8$ , and 19.7 tons was in ore that contained more than 0.20 percent  $U_3O_8$ .

#### TENOR OF ORE

The tenor of uranium deposits in the Dripping Spring is generally low in terms of economic mining. Carload lots of ore are considered to be rich if they approach or exceed 0.25 percent  $U_3O_8$ .

Specimens from the central parts of vein deposits commonly contain from 0.2 to several percent  $U_3O_8$ , but the tenor decreases abruptly away from the vein cores. (See figs. 32–36). In most mines the drift width is at least 4.5 feet, and the outer foot adjacent to the walls is in rock that contains less than 0.1 percent  $U_3O_8$ . To mine economically, therefore, the tenor of the core of the vein must be high.

The problem of recognizing the limits of ore veins whose walls are gradational and whose uranium content can be detected only by assay makes selective mining difficult. The difficulty is further increased by excessive rock breakage during blasting, which results in dilution of the ore by submarginal rock.

Shipments from the various mines have ranged in grade from 0.02 to 0.45 percent  $U_3O_8$ . The average grade of total rock shipped to buying depots is about 0.198 percent  $U_3O_8$ . Excluding the subore shipments whose average grade was less than 0.10 percent  $U_3O_8$ , the average grade was slightly more than 0.205 percent  $U_3O_8$ .

#### GENERAL CHARACTER OF DEPOSITS

Most uranium deposits in the Dripping Spring, particularly the larger ones, have a veinlike shape. The remainder are blanket type, parallel to the stratification, or are of irregular shape and insignificant size.

#### VEIN DEPOSITS

Uranium-bearing veins in the Dripping Spring are unlike most veins in that they do not occupy well-defined fissures and are not clearly distinguishable, megascopically, by mineral content and structure from the enclosing rocks (Stokes and Varnes, 1955). In several of the mines (fig. 31) there is no way of visually distinguishing the veins from adjoining rocks; shapes and positions are determined almost entirely by means of radiation-detection instruments.

In general the veins are steeply dipping tabular bodies of disseminated uranium-bearing minerals. The uranium content decreases outward from the central part of the vein so that the vein zone grades into the enclosing rocks. The central part of some veins is marked by a core of breccia or a narrow fissure filling; in others,



FIGURE 31.—Working face in the Hope 3 mine. The geologists' hammers define the edges of the most radioactive part of a nearly vertical vein zone. Note the lack of any prominent central fracture and the presence of well-preserved bedding in the weakly metamorphosed rocks.

no core is visible. Strata, joints, and a few aplite dikes seem to cross the veins without change.

The veins range widely in size, but they are small by most mining standards. The part of the veins that contains more than 0.1 percent  $U_3O_8$  (figs. 31-36) is rarely more than 3 feet wide and is commonly less than 1 foot.

In the richer veins at depth, such as the Hope 3, uraninite locally occupies narrow lenticular stringers in the central parts of the vein zone. These stringers are rarely more than 0.1 inch thick and are ordinarily 1 foot or less in the other dimensions. They generally occupy fractures in the vein zone, but some are parallel or subparallel to the stratification and occupy bedding fractures or partly replace the host rock. Such visible evidence of primary uranium mineralization is rare, and most fractures in the vein zone contain no visible uranium minerals. Near the surface, however, oxidation of uraninite and finely disseminated sulfides in the vein zone results in a more friable rock containing secondary minerals that clearly define any fractures in the zone.

Quartz is sparse in the uranium-bearing veins. Except for a small amount of secondary quartz found in a fracture in one of the uranium veins at Red Bluff, very little vein quartz is visible at any of the uranium deposits. Carbonate minerals occur in narrow veinlets at several of the deposits, but for the most part they were formed later than the primary uranium-bearing minerals. The only alteration and gangue minerals recognized in association with uraninite at the deposits are chlorite-nontronite and phlogopite, wholly unlike the gangue and alteration minerals at most vein deposits in the Western United States.

The veins have different characteristics, depending somewhat on the host rock and the intensity of mineralization. The Hope 3 vein, in hornfels and slightly recrystallized siltstone, is nearly indistinguishable from the host rock in most places. Joints subparallel to the vein cross the vein zone at a low angle. The central part of the vein is locally defined by a greater concentration of fractures, and, where the mineralization was most intense, the core of the vein zone contains many short narrow stringers filled with uraninite. The appearance of the vein zone is somewhat similar to a narrow shear zone in which numerous stringers define a zone less than 1 foot wide. In some places only one stringer of uraninite is visible; elsewhere all the uraninite is disseminated in the wallrock and no central core is apparent.

In the Hope 1 and Workman 1 deposits a brecciated zone thoroughly cemented by mobilized hornfels coincides with the uranium veins. The mobilized hornfels contains sulfide minerals but is a poor host to the ura-

nium, and only rarely does a veinlet of uraninite penetrate this rock. Most of the uraninite is in the normal hornfels as narrow veinlets and lenses or as disseminated grains. Breccia fragments are particularly good hosts and commonly contain irregular lenses of uraninite subparallel to the relict stratification. Blebs of uraninite are commonly scattered sporadically throughout the vein zone in the hornfels, but for the most part the vein is not well defined by the presence of visible concentrations of uranium or sulfide minerals.

Where siltstone is the host rock no uraninite veinlets are present; all the uranium is disseminated in the wall-rock. Near the surface in most of these deposits, the central part of the vein is defined by one or more limonite-stained fractures, but experience has shown that farther underground these fractures commonly diverge from the vein. Limonite-filled fractures of the same trend as the veins but barren of uranium are common in the Dripping Spring, and we suspect that they are later than the primary uranium minerals but that they followed the same trend as the uranium veins in many places. Very likely they locally follow the original fractures along which the uranium veins were emplaced.

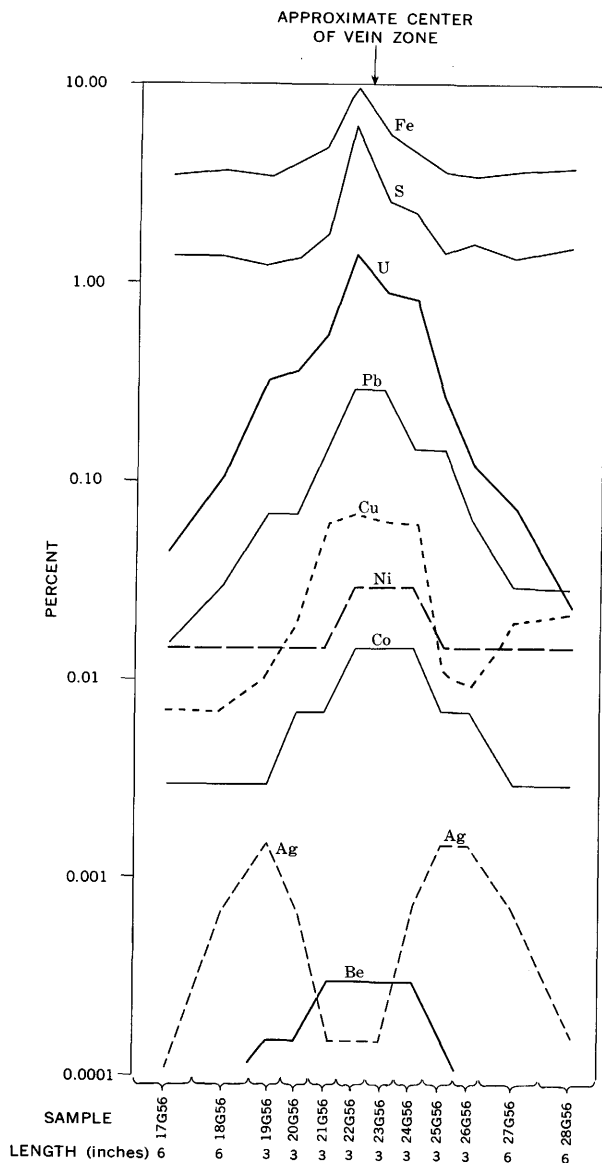
At two deposits, the Tomato Juice and Rock Canyon, the cores of the veins are marked by one or more narrow ankerite-filled fractures. All the uranium minerals are disseminated in the adjacent wallrock, however, and no uranium is associated directly with the ankerite.

The vertical extent of the veins ranges from a few feet to several tens of feet. Uranium content in this dimension is also gradational, so that the vein is commonly traceable vertically beyond the limits of ore-grade material. Parts of veins that contain more than 0.1 percent  $U_3O_8$  have vertical dimensions of as much as 80 feet in some mines. More commonly, vertical dimensions range from 10 to 30 feet.

Ore bodies that bottom on the barren quartzite or on diabase commonly have a convex top and a nearly flat bottom in longitudinal section. The shapes of the longitudinal sections of ore bodies that do not bottom on a distinct horizon are not so well known.

The ore bodies range in length from a few feet to several hundred feet. Most deposits that have a recognizable veinlike shape are at least 50 feet long; the longest continuous ore body (Hope 3) is more than 300 feet long. The longer deposits generally also are larger in the other dimensions.

Most of the veins are planar, but some either split or have an en echelon relation to an adjoining vein. Splits are present at Workman Creek in the Hope 1 and 3, Jon, and Lucky Stop 5 workings (pl. 3; figs. 20, 27). An en echelon relation is indicated in the Lucky Stop 2 adit



### Analytical data and notes for figure 32

Chemical analyses: Total Fe analyzed by volumetric method by E. C. Mallory; organic C, by difference between total C by combustion method and mineral C by gas evolution method by I. C. Frost; total S, by gravimetric method by E. C. Mallory and D. L. Skinner; U, partly by volumetric method and partly by fluorimetric method by H. H. Lipp and J. P. Schuhm. Semiquantitative spectrographic analyses: Tr., trace; 0, looked for but not detected; M, major constituent, greater than 10 percent. Figures reported to the nearest number in the series 7, 3, 1.5, 0.7, 0.3, 0.15. Looked for but not detected: As, Au, B, Bi, Cd, Eu, Gd, Ge, Hf, Hg, Ho, In, Ir, Li, Lu, Os, P, Pd, Pr, Pt, Re, Rh, Ru, Sb, Sm, Sn, Ta, Tb, Te, Th, Tl, Tm, W, Zn. R. G. Havens, analyst.

Field No.	17G56	18G56	19G56	20G56	21G56	22G56	22G56	24G56	25G56	26G56	27G56	28G56
Lab. No.	250361	250352	250353	250354	250355	250356	250357	250358	250359	250360	250361	250362
Specific Gravity	2.50	2.53	2.60	2.63	2.63	2.71	2.68	2.56	2.59	2.56	2.56	2.55

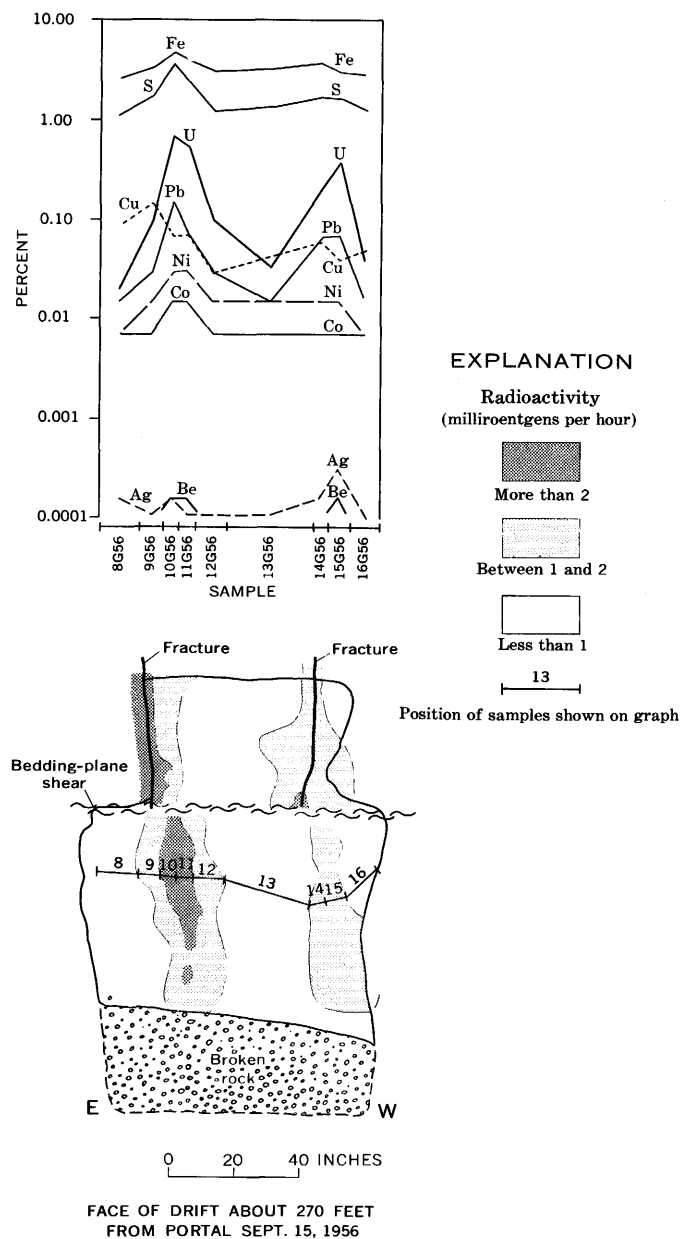
### Chemical analyses (percent)

Fe	3.51	3.75	3.41	3.98	4.96	9.74	5.91	4.66	3.70	3.49	3.76	3.86
C (organic)	.06	.07	.07	.06	.04	.06	.05	.08	.06	.08	.05	.12
C (mineral)	.03	.02	.08	.06	.04	.13	.03	.07	.07	.04	.01	.01
S	1.43	1.42	1.30	1.41	1.83	6.48	2.83	2.28	1.48	1.60	1.44	1.59
U	.043	.12	.31	.57	.35	1.43	.92	.88	.29	.13	.074	.023

### Semiquantitative spectrographic analyses (percent)

Si	M	M	M	M	M	M	M	M	M	M	M	M
Al	M	M	M	M	M	M	M	M	M	M	M	M
Mg	0.7	0.7	0.7	0.7	1.5	1.5	0.7	0.7	0.7	0.7	0.3	0.3
Ca	.7	.7	1.5	1.5	.7	.7	.7	1.5	1.5	1.5	1.5	1.5
Na	.3	.3	.3	.7	1.5	.7	.3	.3	.3	.3	.3	.3
K	M	M	M	M	M	M	M	M	M	M	M	M
Ti	.7	.7	.7	.7	.7	.7	.7	.7	.7	.7	.7	.7
Mn	.03	.03	.03	.03	.07	.07	.07	.03	.03	.03	.03	.03
Ag	.0007	.0015	.0007	.00015	.00015	.00015	.0007	.0015	.0015	.0007	.00015	.00015
Ba	.15	.15	.15	.15	.3	.3	.3	.15	.15	.15	.15	.15
Be	0	0	.00015	.00015	.0003	.0003	.0003	.0003	.00015	0	0	0
Ce	0	0	.015	.015	.015	.015	.015	.015	.015	.015	0	0
Co	.003	.003	.003	.007	.007	.015	.015	.007	.007	.003	.003	.003
Cr	.015	.015	.015	.007	.007	.007	.015	.015	.015	.007	.007	.015
Cu	.0070	.0070	.0105	.019	.061	.069	.065	.0635	.0115	.0095	.0190	.0220
Dy	0	0	.Tr.	.Tr.	.003	.003	.003	.003	.003	0	0	0
Er	0	0	.003	.003	.003	.003	.003	.003	.003	.Tr.	0	0
Ga	.0015	.0015	.0015	.0015	.0015	.0015	.0015	.0015	.0015	.0015	.0015	.0015
La	.Tr.	.003	.007	.003	.003	.007	.007	.007	.007	.003	.003	.003
Mo	.03	.15	.15	.07	.015	.015	.03	.15	.15	.15	.03	.03
Nb	.0015	.0015	.0015	.0015	.0015	.0015	.0015	.0015	.0015	.0015	.0015	.0015
Nd	Tr.	.015	.015	.015	.015	.03	.03	.03	.015	.015	.007	.007
Ni	.015	.015	.015	.015	.015	.03	.03	.03	.015	.015	.015	.015
Pb	.015	.03	.07	.07	.15	.3	.3	.15	.15	.07	.03	.03
Sc	.0015	.0015	.0015	.0015	.003	.003	.003	.003	.0015	.0015	.0015	.0015
Sr	.003	.007	.007	.007	.015	.015	.007	.007	.003	.003	.003	.003
V	.015	.015	.015	.015	.015	.015	.015	.015	.015	.015	.015	.015
Y	.007	.007	.015	.015	.03	.03	.03	.03	.015	.015	.007	.007
Yb	.007	.007	.0015	.0015	.0015	.0015	.0015	.0015	.0015	.0015	.0007	.0007
Zr	.03	.03	.03	.03	.03	.07	.07	.07	.03	.03	.03	.03

FIGURE 32.—Concentration of selected elements in the vein zone of Hope 3 mine. Samples cut across vein in pillar at section F-F', pl. 3. See accompanying table.



### Analytical data and notes for figure 33

Chemical analyses: Total Fe determined by volumetric method; E. C. Mallory, analyst. Cu, partly by colorimetric method and partly by electrolytic method; D. L. Skinner and E. C. Mallory, analysts. Total S, by gravimetric method; W. D. Goss, analyst. U, partly by volumetric method and partly by fluorimetric method; H. H. Lipp and E. J. Fennelly, analysts.

Semiquantitative spectrographic analyses: Reported to the nearest number in the series 7, 3, 1.5, 0.7, 0.3, 0.15. Tr., trace; 0 looked for but not detected; M, major constituent, greater than 10 percent. Looked for but not detected: As, Au, B, Bi, Cd, Eu, Gd, Ge, Hf, Hg, Ho, In, Ir, Li, Lu, Os, P, Pb, Pr, Pt, Re, Rh, Ru, Sb, Sm, Sn, Ta, Tb, Te, Th, Tl, Tm, W, Zn. R. G. Havens, analyst.

Field No.	8G56	9G56	10G56	11G56	12G56	13G56	14G56	15G56	16G56
Laboratory No.	250342	250343	250344	250345	250346	250347	250348	250349	250350

#### Chemical analyses (percent)

Fe.....	2.64	3.20	4.93	3.92	3.05	3.16	3.82	3.00	2.93
Cu.....	.09	.15	.07	.07	.03	.043	.06	.04	.05
S.....	1.19	1.78	3.63	2.22	1.21	1.36	1.74	1.72	1.29
U.....	.020	.10	.68	.53	.10	.032	.19	.39	.033

#### Semiquantitative spectrographic analyses (percent)

Si.....	M	M	M	M	M	M	M	M	M
Al.....	M	M	M	M	M	M	M	M	M
Mg.....	3.	1.5	.7	.3	.7	1.5	.7	.7	1.5
Ca.....	3.	.7	.3	.3	1.5	1.5	.3	.7	.7
Na.....	1.5	.7	.7	.7	1.5	1.5	.7	.7	1.5
K.....	M	M	M	M	M	M	M	M	M
Ti.....	.7	.7	.7	.7	.7	.7	.7	.7	.7
Mn.....	.03	.03	.03	.015	.03	.03	.015	.015	.015
Ag.....	.00015	Tr.	.00015	Tr.	Tr.	Tr.	.00015	.0003	Tr.
Ba.....	.07	.15	.15	.15	.15	.15	.15	.3	.7
Be.....	0	0	.00015	.00015	0	0	0	.00015	0
Ce.....	Tr.	.015	.015	.015	Tr.	.015	.015	.015	.015
Co.....	.007	.007	.015	.015	.007	.007	.007	.007	.007
Cr.....	.007	.007	.007	.007	.007	.007	.015	.015	.007
Dy.....	0	0	.003	.003	0	0	Tr.	Tr.	0
Er.....	0	0	.003	.003	0	0	.003	.003	0
Ga.....	.003	.003	.003	.0015	.003	.0015	.003	.003	.003
La.....	.003	.003	.007	.007	.007	.007	.015	.007	.007
Mo.....	.015	.007	.007	.007	.007	.015	.015	.03	.015
Nb.....	.0015	.0015	.0015	.0015	.0015	.0015	.0015	.0015	.0015
Nd.....	.007	.015	.015	.015	.015	.015	.015	.015	.007
Ni.....	.007	.015	.03	.03	.015	.015	.015	.015	.007
Pb.....	.015	.03	.15	.07	.03	.015	.07	.07	.015
Sc.....	.003	.003	.003	.003	.0015	.0015	.0015	.003	.003
Sr.....	.003	.007	.007	.015	.007	.003	.007	.015	.007
V.....	.015	.015	.015	.015	.015	.015	.015	.015	.015
Y.....	.007	.015	.03	.03	.007	.007	.03	.03	.007
Yb.....	.0007	.0015	.0015	.0015	.0015	.0007	.0015	.0015	.0007
Zr.....	.03	.03	.07	.07	.03	.03	.03	.03	.03

FIGURE 33.—Concentration of selected elements in the vein zones of adit 5 of the Lucky Stop deposits. See accompanying table.

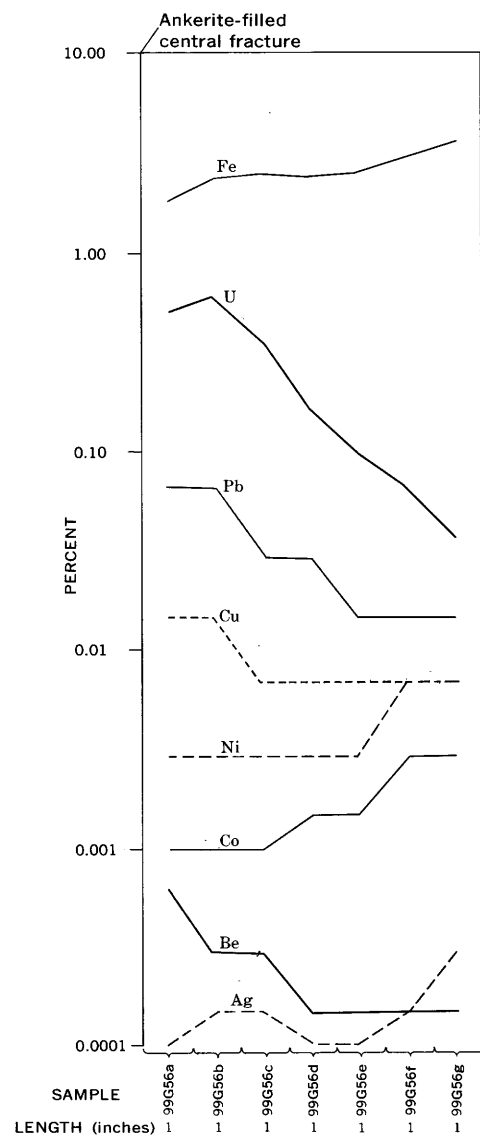


FIGURE 34.—Concentration of selected elements in the vein zone of the Tomato Juice mine. Samples cut from hand specimens. See table at top of facing page.

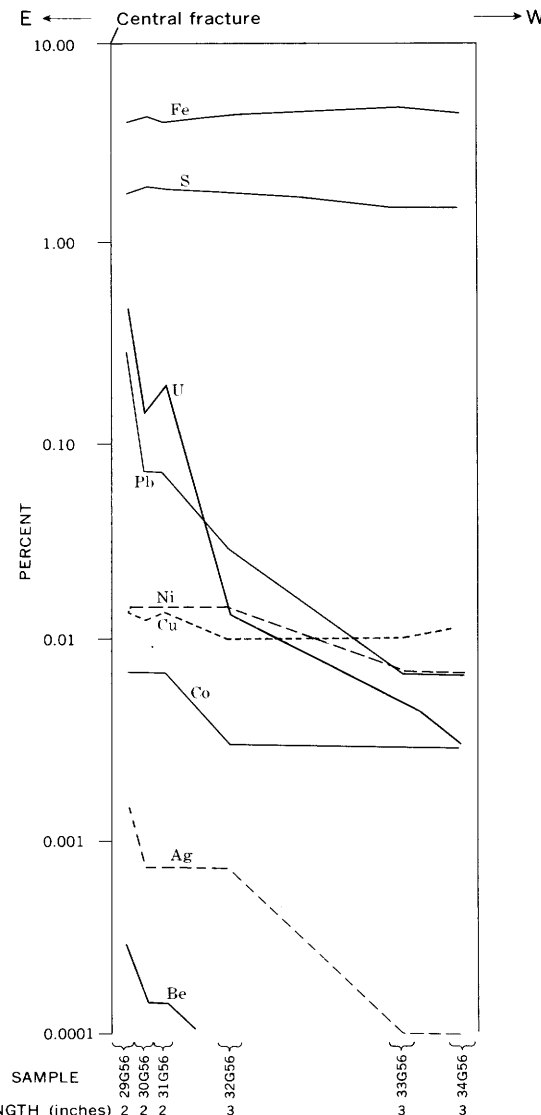


FIGURE 35.—Concentration of selected elements in the west side of the vein zone at portal of the Rainbow adit. See table at top of facing page.

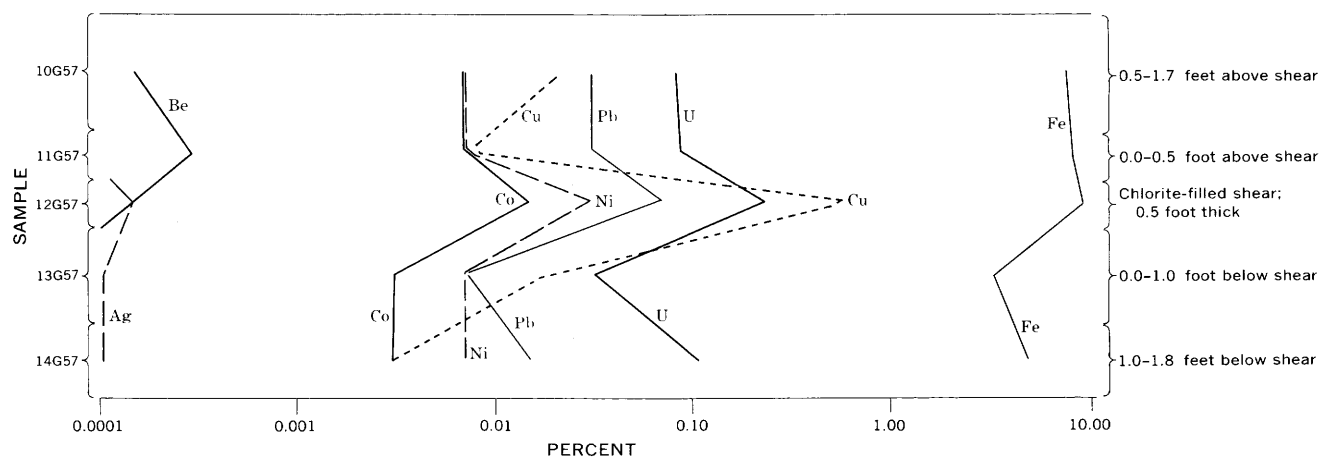


FIGURE 36.—Concentration of selected elements in the vein zone of the second sublevel of the Lucky Boy mine. See table at bottom of facing page.

## Analytical data and notes for figure 34

Chemical analyses: Total Fe, determined by volumetric method; E. C. Mallory, analyst. U, partly by volumetric method and partly by fluorimetric method; James Wahlberg and E. J. Fennelly, analysts.

Semiquantitative spectrographic analyses: Reported to the nearest number in the series 7, 3, 1.5, 0.7, 0.3, 0.15. Tr., trace; 0, looked for but not detected; M, major constituent, greater than 10 percent. Looked for but not detected: As, Au, B, Bi, Cd, Ge, Hf, Hg, In, Ir, Li, Lu, Os, P, Pt, Re, Rh, Ru, Sb, Ta, Tb, Te, Th, Ti, Tm, W. Nancy M. Conklin, analyst.

Field No.	99G56a	99G56b	99G56c	99G56d	99G56e	99G56f	99G56g
Laboratory No.	251832	251833	251834	251835	251836	251837	251838

Chemical analyses (percent)							
Fe	1.83	2.44	2.56	2.42	2.53	3.09	3.66
U	.50	.60	.37	.17	.10	.068	.038

Semiquantitative spectrographic analyses (percent)							
Si	M	M	M	M	M	M	M
Al	M	M	M	M	M	M	M
Mg	1.5	.7	.7	.3	.3	.3	.3
Ca	3.	3.	3.	1.5	1.5	.7	.7
Na	.3	.3	.3	.3	.3	.3	.3
K	M	M	M	M	M	M	M
Tl	.3	.3	.3	.3	.3	.3	.3
Mn	.07	.15	.07	.07	.15	.07	.07
Ag	Tr.	.00015	.00015	Tr.	Tr.	.00015	.0003
Ba	.03	.03	.03	.03	.03	.03	.03
Be	.0007	.0003	.0003	.00015	.00015	.00015	.00015
Ce	.15	.07	.015	.015	.015	.015	.015
Co	.002	.002	.002	.0015	.0015	.003	.003
Cr	.007	.007	.015	.007	.015	.015	.015
Cu	.015	.015	.007	.007	.007	.007	.007
Dy	.015	.015	.007	0	0	0	0
Er	.01	.01	0	0	0	0	0
Eu	Tr.	0	0	0	0	0	0
Ga	.0015	.0015	.0015	.0015	.0015	.0015	.0015
Gd	.03	.015	.007	.007	0	0	0
Ho	Tr.	Tr.	0	0	0	0	0
La	.15	.03	.007	.015	.007	.007	.007
Mo	.015	.07	.03	.03	.015	.007	.007
Nb	0	.0015	0	0	.0015	0	.0015
Nd	.15	.07	.015	.015	.015	.017	.017
Ni	.003	.003	.003	.003	.003	.007	.007
Pb	.07	.07	.03	.03	.015	.015	.015
Pr	.07	Tr.	0	0	0	0	0
Sc	.015	.007	.003	.0015	.003	.003	.003
Sn	.007	.007	.003	.0015	.0015	.0007	.0007
Sr	.007	.003	.003	.003	.003	.003	.003
Sm	.03	.015	.015	Tr.	0	0	0
V	.015	.03	.015	.015	.015	.015	.015
Y	.07	.03	.015	.007	.007	.007	.007
Yb	.007	.003	.0015	.0007	.0007	.0007	.0007
Zn	0	.03	0	0	0	0	0
Zr	.015	.015	.015	.015	.015	.007	.03

## Analytical data and notes for figure 35

Chemical analyses: Total Fe, determined by volumetric method; E. C. Mallory, analyst. Cu, partly by colorimetric method and partly by electrolytic method; D. L. Skinner and E. C. Mallory, analysts. Total S, by gravimetric method; W. D. Goss, analyst. U, partly by volumetric method and partly by fluorimetric method; H. H. Lipp and J. P. Schuch, analysts.

Semiquantitative spectrographic analyses: Reported to the nearest number in the series 7, 3, 1.5, 0.7, 0.3, 0.15. Tr., trace; 0, looked for but not detected; M, major constituent, greater than 10 percent. Looked for but not detected: As, Au, B, Bi, Cd, Eu, Ge, Hf, Hg, Ho, In, Ir, Li, Lu, Os, P, Pt, Pr, Re, Rh, Ru, Sb, Sm, Sn, Ta, Tb, Te, Th, Tl, Tm, W. Nancy M. Conklin, analyst.

Field No.	29G56	30G56	31G56	32G56	33G56	34G56
Laboratory No.	250363	250364	250365	250366	250367	250368

Chemical analyses (percent)							
Fe	4.04	4.21	4.07	4.21	4.77	4.46	
Cu	.014	.013	.014	.0105	.010	.012	
S	1.77	1.95	1.86	1.79	1.57	1.56	
U	.48	.14	.20	.014	.005	.003	
Semiquantitative spectrographic analyses (percent)							
Si	M	M	M	M	M	M	M
Al	M	M	M	M	M	M	M
Mg	1.5	1.5	1.5	1.5	1.5	1.5	.7
Ca	.15	.15	.3	.7	.7	3.	1.5
Na	.3	.3	.3	.3	.3	.3	.3
K	M	M	M	M	M	M	M
Tl	.7	.7	.7	.7	.7	.3	.3
Mn	.015	.015	.015	.015	.015	.03	.03
Ag	.0015	.0007	.0007	.0007	.0007	Tr.	Tr.
Ba	.15	.15	.15	.15	.15	.07	.07
Be	.0003	.00015	.00015	.00015	0	0	0
Co	.03	0	.015	.015	0	Tr.	Tr.
Cr	.007	.007	.007	.007	.007	.007	.007
Dy	.003	.003	.003	.003	.003	0	0
Er	.003	.003	.003	.003	.003	.0015	.0015
Eu	.015	.015	.015	.015	.015	.003	.003
Ga	.003	.003	.003	.003	.003	.0015	.0015
La	.015	.015	.015	.015	.015	.003	.003
Mo	.07	.03	.07	.07	.07	.015	.015
Nb	.0015	.0015	.0015	.0015	.0015	.0015	.0015
Nd	.03	.015	.015	.015	.015	.007	.007
Ni	.015	.015	.015	.015	.015	.015	.007
Pb	.3	.07	.07	.07	.07	.007	.007
Sc	.003	.0015	.0015	.0015	.0015	.0015	.003
Sr	.007	.015	.015	.015	.015	.007	.007
V	.015	.015	.015	.015	.015	.015	.015
Y	.03	.015	.015	.015	.015	.007	.007
Yb	.003	.0015	.0015	.0015	.0007	.0007	.0007
Zn	.03	.015	.015	.015	.015	.015	.015
Zr	.07	.03	.03	.03	.03	.03	.03

## Analytical data and notes for figure 36

Chemical analyses: Total Fe determined by volumetric method; D. L. Skinner, analyst. Cu, partly by colorimetric method and partly by electrolytic method; D. L. Skinner, analyst. U, by fluorimetric method; E. J. Fennelly, analyst.

Semiquantitative spectrographic analyses: Reported to the nearest number in the series 7, 3, 1.5, 0.7, 0.3, 0.15. Tr., trace; 0, looked for but not detected; M, major constituent greater than 10 percent. Looked for but not detected: As, Au, Bi, Cd, Eu, Gd, Ge, Hf, Hg, Ho, In, Ir, Lu, Os, P, Pt, Re, Rh, Ru, Sb, Sm, Sn, Ta, Tb, Te, Th, Tl, Tm, W, Zn, R. G. Havens, analyst.

Field No.	10G57	11G57	12G57	13G57	14G57	Field No.	10G57	11G57	12G57	13G57	14G57
Laboratory No.	256113	256114	256115	256116	256117	Laboratory No.	256113	256114	256115	256116	256117

Chemical analyses (percent)											
Fe	7.00	7.54	8.39	3.04	4.47	U	.075	.083	.23	.03	.10
Cu	.020	.007	.54	.016	.003						
Semiquantitative spectrographic analyses (percent)											
Si	M	M	M	M	M	Er	0	0	.003	0	0
Al	M	M	7.	M	M	Ga	.0015	.0015	.0015	.00007	.0015
Mg	3.	3.	7.	3.	3.	La	.003	0	.003	.003	.003
Ca	3.	7.	7.	3.	3.	Li	0	0	.03	0	0
Na	.7	.3	.15	.7	.7	Mo	.007	.007	.001	.015	.015
K	M	7.	3.	M	M	Nb	0	0	0	.0015	.0015
Ti	.3	.3	.3	.07	.07	Nd	0	0	.015	.007	.007
Mn	.15	.15	.15	.07	.07	Ni	.007	.007	.03	.007	.007
Ag	0	0	.00015	Tr.	Tr.	Pb	.03	.03	.07	.007	.015
B	0	0	.007	0	0	Sc	.007	.007	.007	.003	.003
Ba	.15	.15	.007	.15	.15	Sr	.03	.03	.0015	.03	.07
Be	.00015	.0003	.00015	0	0	V	.07	.07	.3	0	.15
Ce	0	0	.015	0	0	Y	.007	.007	.03	.007	.007
Co	.007	.007	.015	.003	.003	Yb	.0007	.0007	.003	.0007	.0015
Cr	.007	.007	.003	.007	.007	Zr	.03	.03	.015	.03	.03
Dy	0	0	.007	0	0						

(fig. 20) and Big Buck adit (fig. 21), but elsewhere there is little evidence of true en echelon veins, and the Lucky Stop 2 may represent either a poorly developed split or two veins fortuitously close together.

At Red Bluff there is some indication that a stoped-out ore body along the 3 adit (fig. 17) formed at the intersection of a moderately strong and a very weak vein. This type of relation was not recognized elsewhere.

Two deposits, the Suckerite (fig. 37) and the Lucky Boy (figs. 23, 38), are parallel to the stratification but are controlled by bedding-plane shear zones in dipping strata. The strike of the Suckerite deposit is also parallel to that of most of the other uranium deposits in the Workman Creek area. We classify these two deposits with the vein deposits because of their obvious structural control, even though they are parallel to the stratification.

#### BLANKET DEPOSITS

Blanket deposits in this report, are those deposits in the Dripping Spring that are tabular and concordant with the stratification and are not clearly controlled by bedding-plane shear zones. This type of deposit is not abundant, particularly among the larger and richer deposits; it is most common immediately above either the barren quartzite or the base of the upper member.

Generally these deposits are only a few inches thick. Where thicker, they are of very low grade and commonly represent redistributed secondary minerals. No ore has been shipped from any of the blanket deposits.

Little is known about the dimensions of blanket deposits in the planes of stratification. Ordinarily one dimension is considerably longer than the other and reflects some structural or stratigraphic control (fig. 39). The width is probably only a few feet or tens of feet in most deposits. The length may be several hundred feet.

Some deposits have features related to both vein and blanket deposits. The Black Brush deposit (fig. 40) is most strongly mineralized in a thin stratigraphic interval above the barren quartzite on both sides of a nearly vertical veinlike body. In cross section, therefore, the deposit is cross shaped. Many vein deposits are abruptly wider at certain strata that apparently favored the lateral dissemination of minerals. A thin bed at the Red Bluff deposit is mineralized continuously between and beyond the veins in adits 1 and 2. In cross section this deposit looks something like the letter H.

#### IRREGULAR DEPOSITS

Small irregular areas of anomalously high radioactivity are not uncommon on weathered surfaces of the Dripping Spring. Some of these areas represent the exposed parts of blanket or vein deposits, but in several

the radioactivity extends only a few inches or feet below the surface. Typically these deposits are in strongly oxidized rock and are very low grade and small in size.

### DISTRIBUTION OF DEPOSITS

#### STRATIGRAPHIC POSITION

Uranium deposits in the Dripping Spring Quartzite are in the lower part of the upper member; no deposits are known in the middle member. The largest and richest deposits are in a narrow stratigraphic range within the gray unit, but all rock in the upper member below the buff unit is favorable.

The most favorable host rocks for uranium deposits are the basal 40 feet of the black facies immediately above the barren quartzite. The remainder of the black facies contains fewer and generally smaller deposits.

The second most favorable stratigraphic interval is in the gray facies about 20–30 feet below the barren quartzite. Rarely, other parts of the gray facies contain deposits almost to the base of the barren quartzite. No deposits are known in the barren quartzite, but the results of drilling at Red Bluff (pl. 4) show that some deposits extend both above and below, but are interrupted by the barren quartzite.

The remaining deposits are all low-grade blanket deposits just above the contact between the upper and middle members.

#### AREAL DISTRIBUTION

Uranium deposits in the Dripping Spring Quartzite are confined to a small part of the broad areal extent of the formation. All deposits now known to contain more than a few hundred pounds of ore are in Gila County. Although a few deposits are known outside Gila County, none of these has been of economic grade.

Most of the deposits in Gila County are within an area defined by Tonto Creek on the west, U.S. Highway 60 on the east, the Salt River on the south, and the county line or Mogollon Rim on the north. This is the area referred to in this report as the Sierra Ancha region. Most of the Sierra Ancha region is within the McFadden Peak, Blue House Mountain, and Roosevelt NE 15-minute quadrangles. Within the Sierra Ancha region nearly all deposits found to date have been exposed along valley and canyon walls. Physiographic features, therefore, have resulted in apparent alignment of deposits. Examples may be seen at Workman Creek and along Cherry Creek and Deep Creek.

Deposits are sporadically distributed outside the Sierra Ancha region, and no consistent geometric pattern has been noted. Of the deposits that lie outside the region, several are within a few miles south of the Salt River in the Blue House Mountain quadrangle. Others are known in the Mescal Mountains, and at least one of

these has produced ore. The remaining deposits are few and have generally shown little promise of becoming ore producers.

#### RELATIONS TO MAJOR STRUCTURAL FEATURES

Some major structural features seem to have a relation to the distribution of deposits. Prediabase faults, expressed either as diabase dikes or as sharply discordant contacts in diabase sheets, seem to have a strong control over the position of deposits in many places. In the Roosevelt NE 15-minute quadrangle, for example, the Cataract, Great Gain, May, Blevins Canyon, and Fairview deposits are alined along the west side of a major discordance in a large diabase body. Although the structure was not thoroughly investigated, apparently a diabase sheet that intruded the Pioneer(?) Formation east of the deposits abruptly rose stratigraphically on a north-trending fault and intruded the Mescal Limestone above the deposits (the Mescal has been largely removed by erosion).

The Red Bluff veins are adjacent to a diabase-filled fault, and to the best of our knowledge, fade out away from the fault. The Sue, Donna Lee, and other nearby deposits not described herein are alined near a fault that controls the course of Deep Creek canyon for nearly 1 mile. The area was mapped (unpub. map) by C. L. Van Alstine, an Atomic Energy Commission representative, who found diabase along the trend of this fault. His interpretation, according to R. J. Schwartz (oral commun., 1957), was that the fault cut the diabase, although he did not actually see such a relation in the field. Van Alstine's map indicates that diabase sheets in the Pioneer occupy different stratigraphic positions on opposite sides of the fault. It seems likely, therefore, that diabase locally was injected into the fault, which indicates the age of the fault as prediabase.

The spatial relations between deposits and monoclines are striking in some areas. Along the Cherry Creek monocline several deposits are within a few hundred feet of the flexure, and at least one deposit is at the foot of the west flank of the fold. The Workman Creek deposits, particularly the westernmost ones, are fairly close to the Sierra Ancha monocline. The Rock Creek and Tomato Juice deposits are close to the Rock Canyon monocline. Most of the deposits are adjacent to the downthrown side of the monocline.

#### RELATIONS TO DIABASE AND RELATED ROCKS

The most obvious spatial relation of deposits to rocks other than the host rock is the association of the deposits and diabase. Most of the deposits from which ore has been produced are clustered about the Sierra Ancha diabase sheet. Other nearby deposits that have produced

ore or seem to have favorable possibilities for production are within a few tens of feet of diabase.

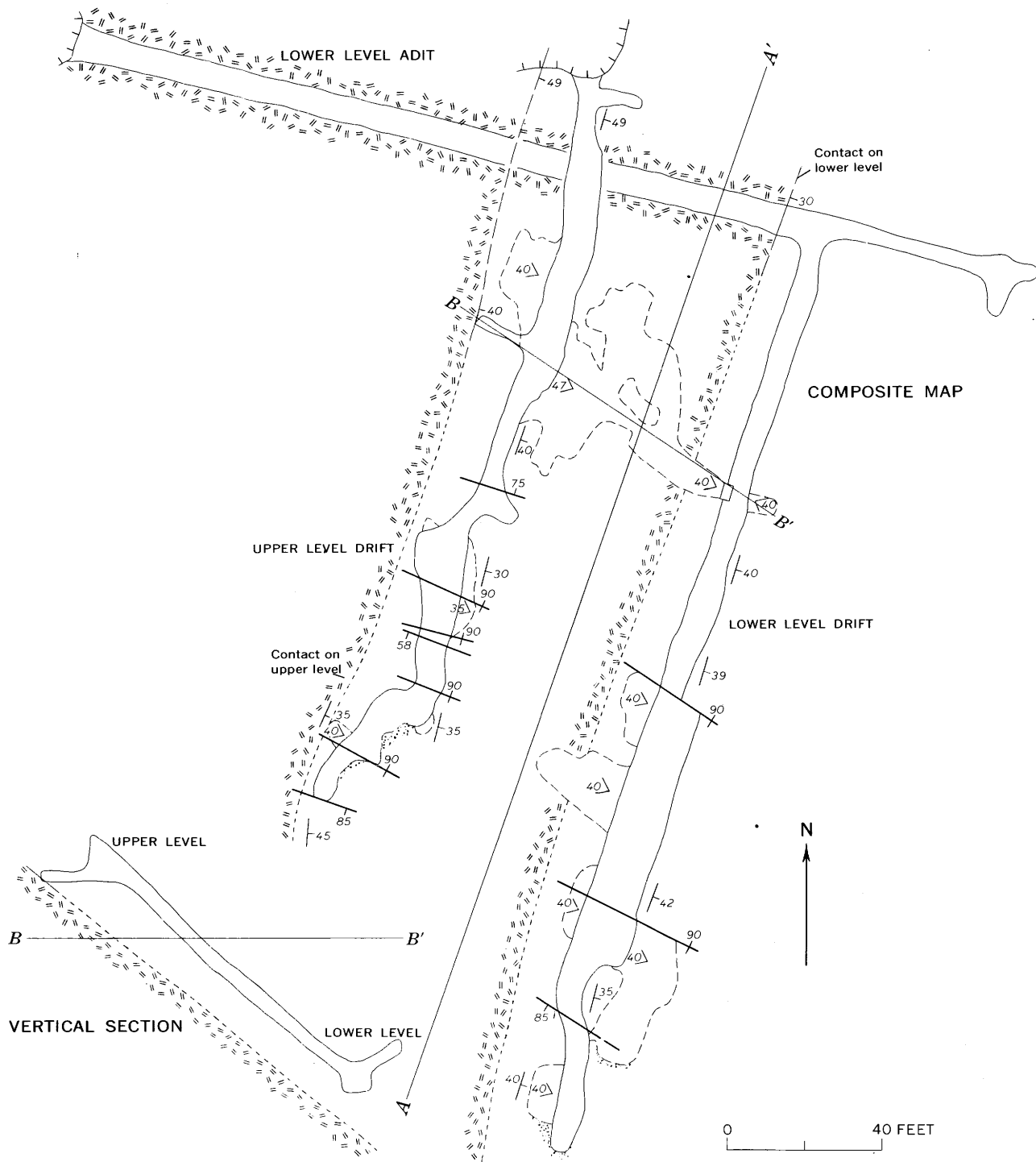
Most of the deposits are near discordant contacts between diabase and the host rock. Deposits near major structural features such as monoclines are generally near discordant diabase bodies whose positions are controlled by the structural elements. For example, the Tomato Juice and Rock Creek deposits are adjacent to the Rock Canyon monocline but are equally close to diabase dikes that probably stem from a thick underlying diabase sill. The deposits along Workman Creek, on the west side of lower Cherry Creek, and at Red Bluff are all adjacent to major discordant contacts between the host rocks and the Sierra Ancha diabase sheet or apophyses from the sheet.

The relation between deposits and differentiated facies from the diabase are more obscure. Only at the Workman Creek, Red Bluff, and lower Cherry Creek areas were diabase, syenite, aplite, and deuteritic veins observed together near uranium deposits.

At Workman Creek, syenite commonly forms a layer between the normal diabase and the Dripping Spring. Other bodies of syenite are abundant in at least the upper 50 feet of the diabase sill. Some of the deposits (Little Joe, Workman 1) are in hornfels immediately above the contact with syenitic rocks. In places such as in the Hope adit 1, however, deposits are adjacent to normal chilled borders of the diabase. Syenite is also common in diabase near the Red Bluff deposit but is less common in diabase near most other uranium deposits. There is no evident consistent spatial or abundance relation between uranium deposits and syenite.

A close spatial relation between aplite and uranium deposits exists only at the Workman Creek and Cherry Creek areas near the Big Six and Sorrel Horse deposits. Aplite occurs as dikes both in the diabase and in the Dripping Spring and as sills immediately above the upper diabase contact in the Workman Creek area. It forms a sill-like body that cements brecciated hornfels just above the diabase at the Sorrel Horse and Big Six deposits.

Only three aplite dikes are known to cross the trends of ore bodies. An aplite dike in the Hope 3 mine (pl. 3) obliquely transects the ore body without causing any noticeable disruption; the dike is unmineralized, and an echelon split in the dike in adit 3 is unrelated to vein genesis. In the Workman 1 adit a small very irregularly shaped aplite body (fig. 13) transects the deposit without disrupting its continuity. This aplite is somewhat altered, however, and nearby sulfides are oxidized in the ore zone. Another aplite dike cuts transversely across the Little Joe 5 deposit in the opencut at the portal to the adit (pl. 1). This aplite seemed to be cut by the



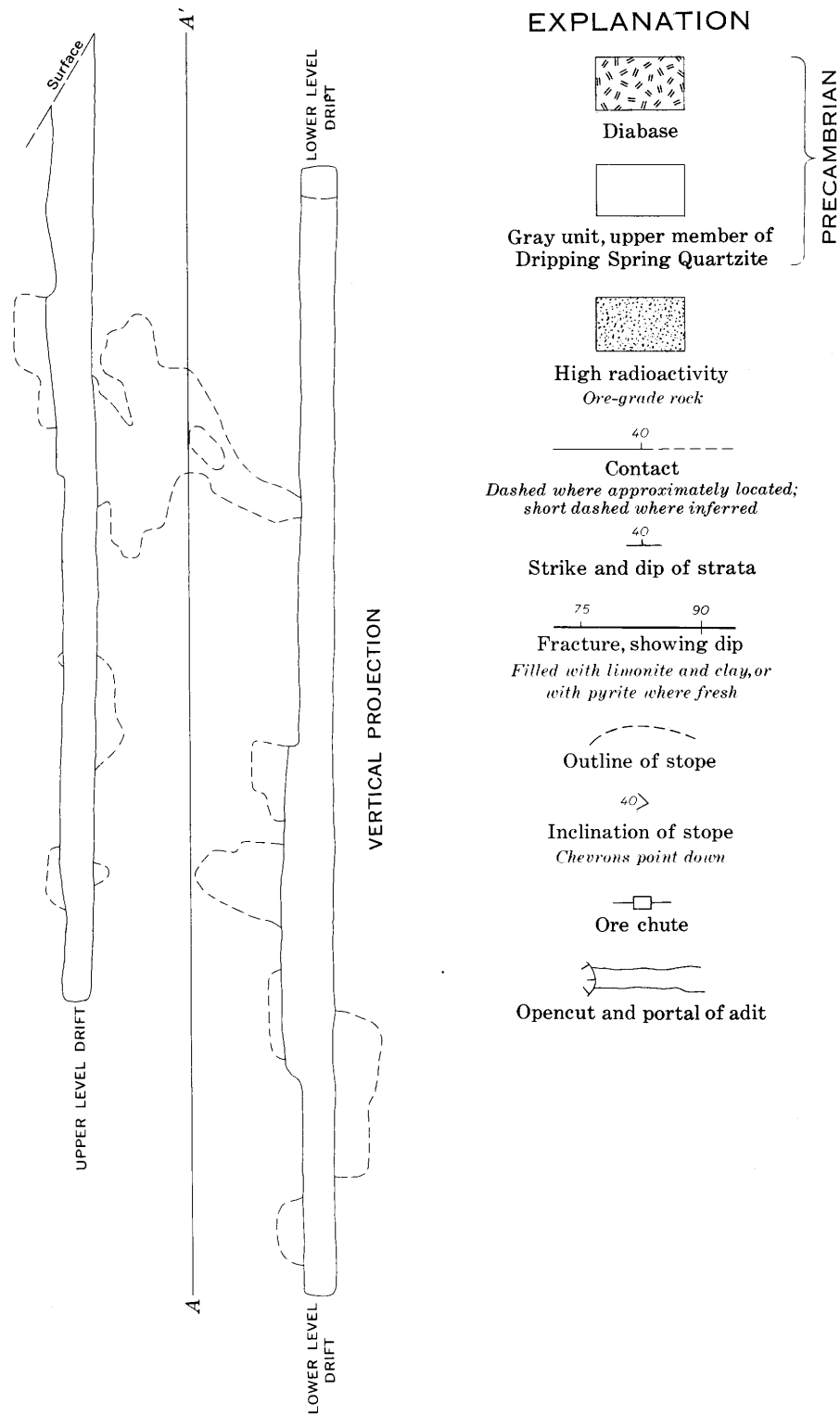


FIGURE 37.—Composite geologic map and sections of the Suckerite mine. Uranium deposit follows obscure bedding-plane shear zone. Drifts and stopes are developed along the shear zone.

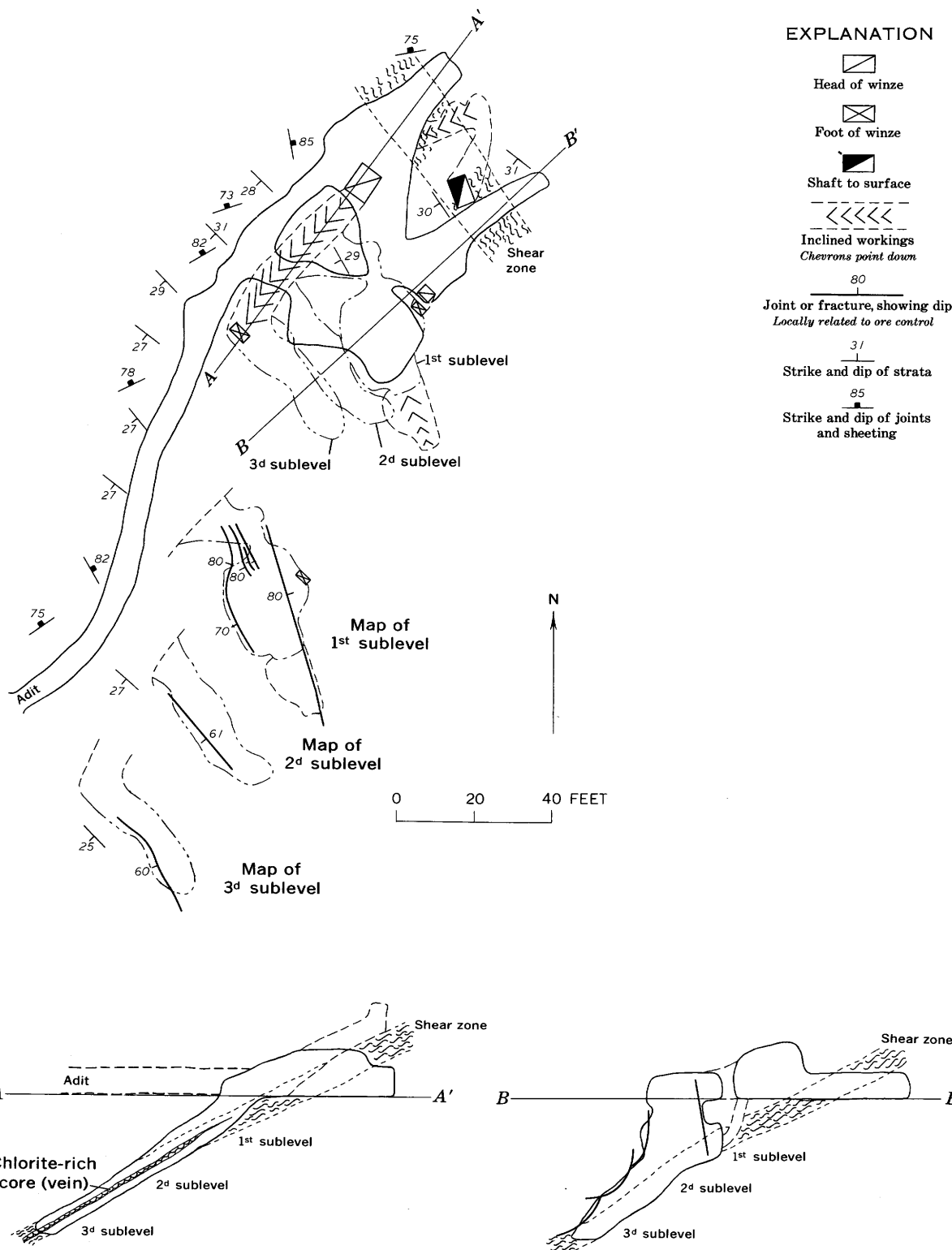


FIGURE 38.—Maps and sections of the Lucky Boy mine.

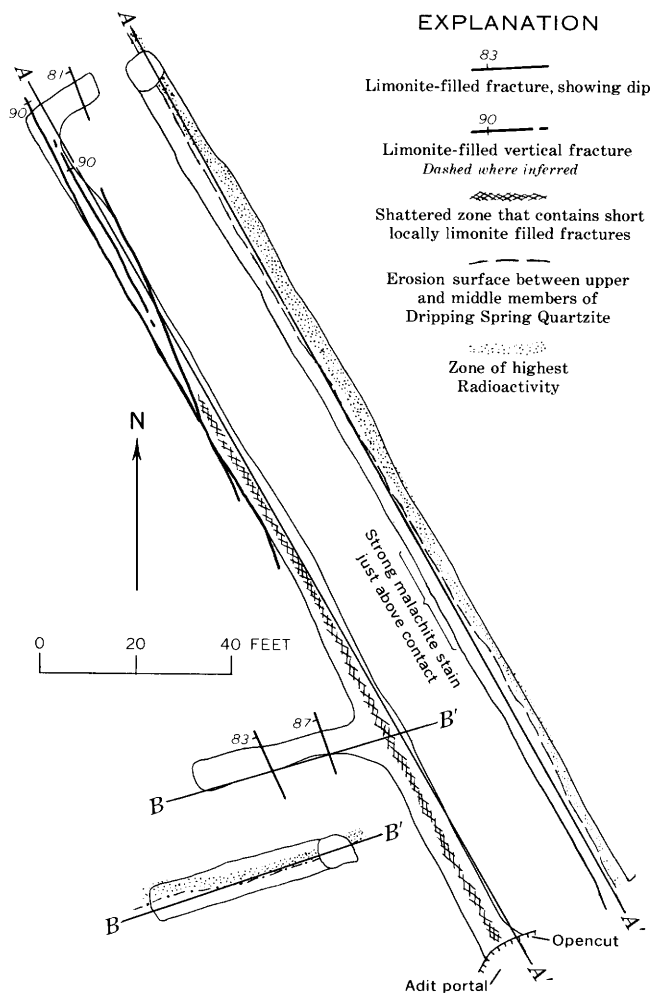


FIGURE 39.—Map and sections of the Cataract adit.

vein and a sample of aplite from the wall of the opencut contained 21.07 ppm uranium.

At Red Bluff a short unmapped leucocratic albitic dike north of the deposits cuts the diabase sill parallel to and just west of the diabase dike in Warm Creek. This leucocratic dike is texturally similar to aplite and is the only aplitelike rock recognized near the deposit.

Near the May deposit, dikelike bodies of an aplitic material are formed along strong joints in the Dripping Spring. No direct relation between these bodies and the uranium deposit was observed.

The relations and abundance of deuteritic veins in diabase near uranium deposits are not well known, partly because the possible significance of deuteritic veins was not suspected until fieldwork for this report was nearly completed, and partly because deuteritic veins are easily obscured by weathering.

The abundance of deuteritic veins in the diabase dike at Red Bluff and their common occurrence in the Workman Creek and Cherry Creek areas are notable. Deu-

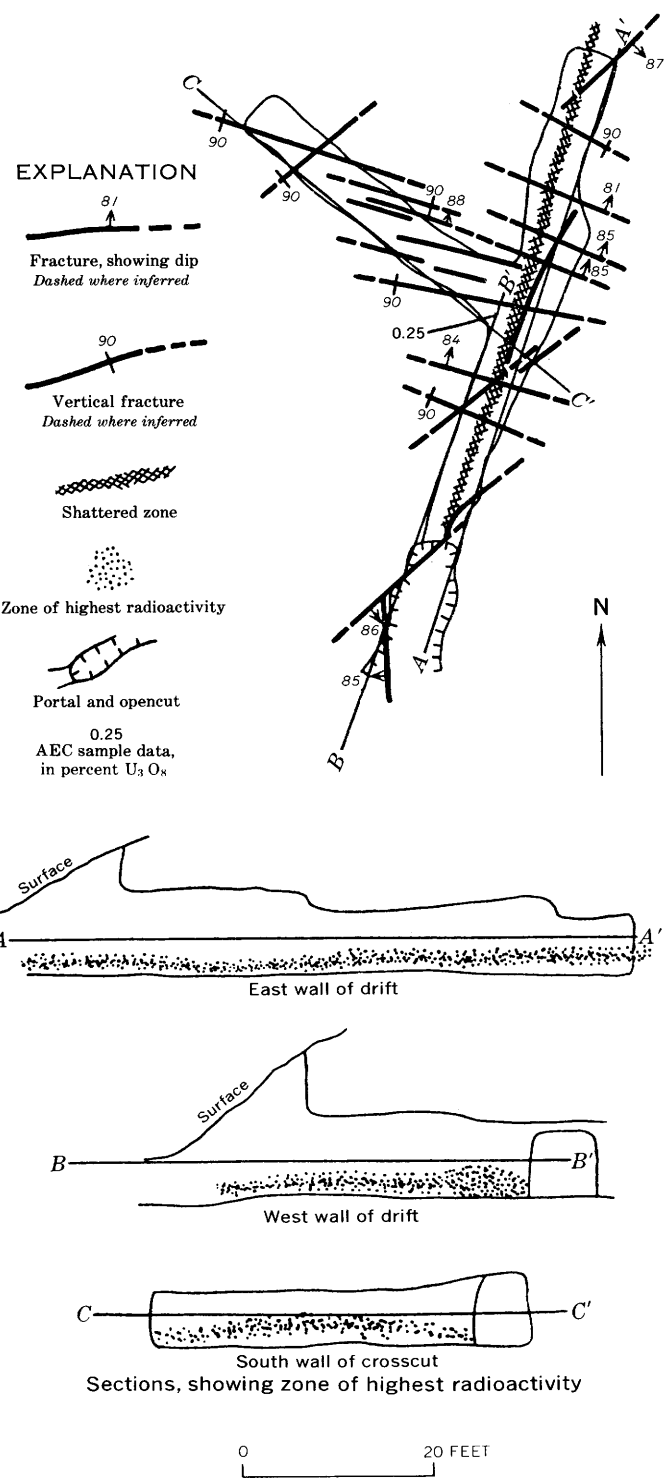


FIGURE 40.—Map and sections of the Black Brush adit (Granger and Raup, 1959, fig. 67). Workings in black facies of Dripping Spring Quartzite.

teric veins are common, however, at many places in the diabase and are not limited to the vicinity of uranium deposits.

#### AGE OF THE URANIUM DEPOSITS

The age of the uraninite in the deposits and of the genetically related diabases has been determined to be about 1,050 million years.

Isotopic age determinations were computed for uraninite from the Red Bluff, Workman, Hope, and Black Brush deposits and for radiogenic lead in galena from the Red Bluff deposit (table 5). Much of the galena in the deposits was found to have an isotopic lead composition comparable to that of much of the galena found on the Colorado Plateau (L. R. Stieff, written commun., 1956) and to that of the galena in the Castle Dome copper (R. S. Cannon, oral commun., 1956); both of these deposits are considered to be post-Cretaceous in age. At first the problem was whether it would be preferable to use the lead in this post-Cretaceous galena as an index lead to correct for common lead in the uraninite samples, or to use a Precambrian lead. Leads of both ages were tried, galena (T-578) from the Coeur d'Alene district of Idaho as an index of Precambrian lead, and galena from the Red Bluff mine (GS-398-55, table 5) as an index of younger lead. The ages determined by using each of these index leads are similar, but the Precambrian lead index was found to yield more concordant  $Pb^{206}$ :  $U^{238}$ ,  $Pb^{207}$ :  $U^{235}$ , and  $Pb^{207}$ :  $Pb^{206}$  ages and for this reason was selected as the more reliable.

A second problem was whether  $Pb^{204}$  (nonradiogenic lead) or  $Pb^{208}$  (end product of thorium decay) would make the more reliable index of common lead in the samples. When analyzed by the mass spectrographic

technique, samples containing large amounts of  $Pb^{206}$  commonly appear to be abnormally high in  $Pb^{204}$ . Because the samples from the Dripping Spring contain negligible, and commonly undetectable, amounts of thorium, it was decided that the  $Pb^{208}$  would serve as a more reliable index of common lead than would the  $Pb^{204}$ . Using either the  $Pb^{204}$  or  $Pb^{208}$  of a younger galena as an index, however, would not change most of the ages enough to make them younger than Precambrian, nor would it make them older than ages assigned to the underlying older Precambrian granites.

The lack of concordance among the lead-lead and lead-uranium ages of the uraninites probably can be attributed partly to differential leaching of the uranium relative to lead and partly to selective loss of certain daughter products. These losses could have been caused by either ground-water or hydrothermal solutions during the relatively recent geologic past. Radiochemical analysis of a uraninite-bearing sample from the Hope adit 3 suggests that both uranium and radium have been leached from the sample. (See p. 78.)

If  $Pa^{231}$  can be assumed to be an index of the original uranium content (Granger, 1963), then some uranium and radium have been lost. The  $Rn^{222}$  is abnormally low, probably chiefly because of loss as a gas during grinding.

All the calculated ages for uraninite (GS-378-55) at the Red Bluff deposit are low relative to the ages of the other uraninites. This may be a result of nonsynchronous lead and uranium leaching. The fact that galena (GS-369-55) composed largely of  $Pb^{206}$  and  $Pb^{207}$  has been found in the deposit attests that radiogenic lead, probably derived from uraninite, has been moved about.

TABLE 5.—Isotope ages of uraninite and galena from deposits in the Dripping Spring Quartzite

Deposit	Field No.	Lab. No. GS-	Weight percent		Atomic ratios <sup>1</sup>			Apparent age, <sup>2</sup> in millions of years		
			U	Pb	$Pb^{204}/Pb^{208}$	$Pb^{208}/Pb^{206}$	$Pb^{207}/Pb^{208}$	$Pb^{206}/U^{238}$	$Pb^{207}/U^{235}$	$Pb^{207}/Pb^{206}$
<b>Uraninite</b>										
Red Bluff.....	Tps. 84-54	378-55	1.49	0.15	0.02901	11.83526	1.22095	587	656	932
Workman 1.....	87G54	379-55	42.9	5.45	.04944	75.44028	6.09824	817	832	1,094
Black Brush.....	33G55	443-55	10.7	1.78	.02885	79.92238	6.38916	1,055	1,070	1,088
Hope 1.....	444-55	1.44	.30	1472	103.0849	7.7667	1,304	1,264	988	
Hope 2.....	113G56	557-57	8.2	1.36	0.	218.6409	16.3096	1,068	1,053	1,026
<b>Galena</b>										
Red Bluff.....	Tps. 83-54	369-54	0.0011	78.50	0.02750	10.92823	1.20790	-----	1,140	
<b>Common lead</b>										
Do.....	398-55	.0003	82.59	.02554	.50294	.40624	(?)	(?)	(?)	(?)
Jon.....	18G55	441-55	.0046	84.9	.02686	.48010	.42291	(?)	(?)	(?)
Hope 1.....	17G55	442-55	.0059	83.1	.02684	.50952	.42466	(?)	(?)	(?)

<sup>1</sup> Sample GS-557-57 analyzed by Maryse Delavaux. The rest were analyzed by W. D. Harman, Assay Laboratory Dept., Carbide and Carbon Chemicals Co., Oak Ridge, Tenn.

<sup>2</sup> Sample GS-369-54 (galena) was corrected for common lead of the composition of GS-398-55. All the uraninite lead was corrected for common lead of the composition of sample T-578, Precambrian galena from the Bunker Hill and Sullivan mine, Coeur d'Alene district, Idaho. The negligible thorium content of the ores permitted the use of  $Pb^{208}$  as an index lead. Calculations by L. R. Stieff.

<sup>3</sup> These lead ratios are similar to those galena samples from many deposits of Tertiary age throughout the Western United States.

Possibly some radiogenic lead was locally leached and redeposited as galena, whereas elsewhere in the deposit uranium was preferentially leached by Tertiary to Recent hydrothermal or ground-water movements. Significantly, a line through the five uraninite samples plotted on a graph (fig. 41) relating the  $N^{207} : N^{235}$ : $N^{206} : N^{238}$  values crosses the "concordia" curve (Russell and Ahrens, 1957) at about 1,050 m.y. This date is very near the average (1,061 m.y.) of all  $Pb^{207} : Pb^{206}$  ages given in table 5. If some sort of selective removal of lead isotopes from uraninite by a distinctive physical process, such as that suggested by Russell and Ahrens (1957), were operative, it might be expected that any galena formed subsequently from this radiogenic lead would be enriched in  $Pb^{207}$ . This enrichment, to the extent suggested, would tend to make the lead-lead age of the galena from Red Bluff somewhat older than the lead-lead age of the source uraninite. Because the calculated age of this galena gives the greatest lead-lead ages among the samples tested, some such selective removal of lead possibly did take place.

An interesting comparison can be made between the ages determined by isotopic ratios and the ages determined by the controversial uraninite unit-cell cube-edge method. Wasserstein (1951) reported "a progressive reduction in the size of the unit cell of uraninite-thoria-nites with time." This, he believed, results from the substitution of radiogenic lead for uranium in the crystal

lattice of uraninite. Subsequent publications (Wasserstein, 1954; 1955a, b, c) dealt with refinements of the method. Although his explanation of the reason for the cube-edge-age relation has been criticized (Hoekstra and Katz, 1955; Hiemstra, 1955), there seems to be some orderly relation among the sizes of the unit cells and the ages of many uraninites.

By Wasserstein's method the cube-edge measurements of uraninites can be properly compared only if the uraninite is entirely in the form  $UO_2$ . Hence, for most uraninites the samples must be heated in  $H_2$  for about 1 hour at 1000°C to eliminate any excess oxygen. A correction is made for thorium if it is present in significant amounts, but this correction was unnecessary for uraninites in the Dripping Spring. (Sample 33G55 from the Black Brush adit had a thorium-uranium ratio of less than 0.007.)

The cube edges of only two samples of uraninite were determined. The cube edge of a uraninite (sample 1G55) from the Hope adit 1 was determined to be 5.458 Å prior to treatment and 5.440 Å after heating at 1000°C for 1 hour in a hydrogen atmosphere. Corresponding measurements for uraninite (sample 33G55) from the Black Brush adit gave 5.464 Å prior to heating and 5.445 Å after heating. Limits of error are less than 0.005 Å for all measurements. These are plotted on a graph (fig. 42) constructed from data reported by Wasserstein (1955b). The unit-cell cube-edge measurements for the treated Hope and Black Brush uraninites correspond to ages of 860 and 710 m.y., respectively.

The ages determined by Wasserstein's method are

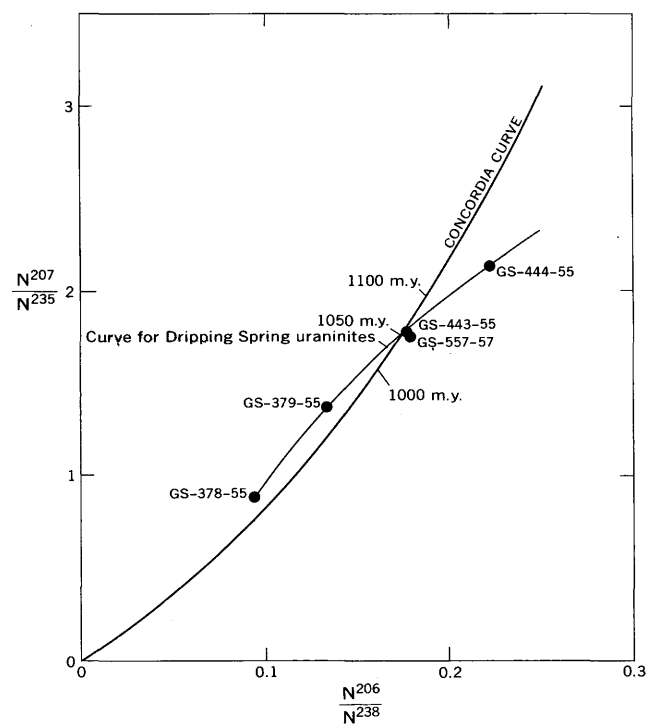


FIGURE 41.—Parent-daughter isotope relationships of uraninites from the Dripping Spring Quartzite.

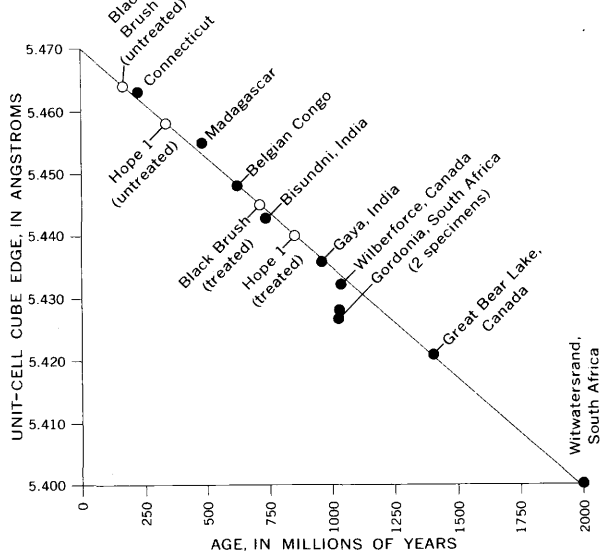


FIGURE 42.—Age of uraninites by unit-cell-edge dimension. Graph constructed from data adapted from Wasserstein (1955b). Black Brush and Hope 1 uraninites determined by H. C. Granger.

young relative to the lead-lead isotope ages. They are similar, however, to some of the lead-uranium ages, and this similarity may lend support to Wasserstein's explanation for the dimension of the unit-cell cube edge decreasing with time.

Wasserstein's method might be improved by heating the uraninite in an ammonia atmosphere rather than hydrogen. According to Katz and Rabinowitch (1951, p. 307), "Above 450°C reduction (by ammonia) to  $\text{UO}_2$  sets in and becomes complete (more complete than with hydrogen as the reductant) at 550°C."

#### RADIOACTIVITY OF THE URANIUM DEPOSITS

A detailed study of the radioactivity of each deposit was made with either a portable gamma-ray detecting scintillation meter or beta-gamma detecting geiger counter. With such instruments the outlines of the deposits can be determined within narrow limits. This method proved to be the only rapid yet reasonably reliable means for guiding mining procedures in deposits where no visible distinction was possible between ore and waste. The recorded radioactivity, however, must be considered with caution because, under certain conditions, it may not be proportional to the uranium content of the rock.

In the deposits in the Dripping Spring, which contain negligible amounts of thorium, radioactivity of the rock can be disproportional to the uranium content for at least three reasons: (1) the uranium may not be in equilibrium with its radioactive daughter products; (2) enough radioactive  $\text{K}^{40}$  may be present to affect the instruments; (3) the uranium-bearing minerals may be concentrated on exposed surfaces.

The ore-bearing rock in unweathered parts of the deposits generally contains about 1.2 times more uranium than would be expected if the uranium were in equilibrium with its daughter products. Figure 43 shows the relation of radioactivity and uranium content for a group of samples collected at several mines that have yielded ore from the Dripping Spring. This relation permits approximate uranium analyses to be made from radioactivity data on unweathered rock in mines, drill holes, or the laboratory.

Ordinarily, uranium that is in excess of equilibrium amounts is considered to have been deposited so recently that it has not yet attained equilibrium. We can be sure, however, that the uranium in the Dripping Spring has had time, since deposition, to attain equilibrium. The discrepancy between radioactivity and uranium therefore presumably is caused by loss of one or more of the daughter products through leaching, diffusion, or some other process. This would restrict the formation of succeeding daughter products and could have a decided effect on the intensity of radioactivity. Below is shown

the results of a chemical, radiometric, and radiochemical analysis of a sample of unweathered ore from the Hope 3 mine (Denver serial No. 245676; field No. 7G56). Uranium (percent) was determined by Henry H. Lipp, equivalent uranium (percent) by Clifford G. Angelo, and radioactive isotopes (percent equivalent) by John N. Rosholt.

U	eU	$\text{Pa}^{231}$	$\text{Th}^{230}$	$\text{Ra}^{226}$	$\text{Rn}^{222}$	$\text{Pb}^{210}$
0.24	0.18	0.28	0.25	0.20	0.15	0.19

Little can be concluded from the one radiochemical analysis available. It appears, however, that  $\text{Pa}^{231}$  and  $\text{Th}^{230}$  are excessive relative to the uranium content and  $\text{Ra}^{226}$ ,  $\text{Rn}^{222}$ , and  $\text{Pb}^{210}$  are deficient. Both uranium and radium were probably, therefore, leached in the recent geologic past. The  $\text{Rn}^{222}$  is probably abnormally low because, being a gas, some of it was lost during sample preparation. The result is that the radioactivity of the ore is less than would be expected from the uranium content because proportionately more radium than uranium has been removed.

The conditions under which the radium and uranium were lost are not known, but probably normal ground waters were the vehicle. Although most of the mines in the Dripping Spring are fairly dry, many of the mine walls are moist, and water has been known to collect in low parts of the mines. Ore shipments from

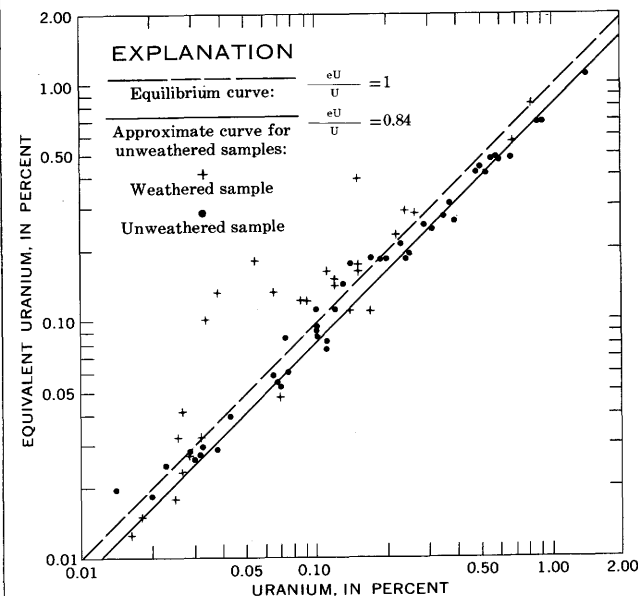


FIGURE 43.—Relation between uranium content and radioactivity of weathered and unweathered samples from 18 deposits in the Dripping Spring Quartzite. All unweathered and most weathered samples were collected and analyzed by the U.S. Geological Survey. Several of the weathered samples were collected and analyzed by the U.S. Atomic Energy Commission.

various mines contained about 1.5–6.0 percent water. This water content is evidence that there is adequate moisture even in unoxidized parts of the ore bodies to provide some transport for soluble elements. As  $\text{UO}_2$  is insoluble under most conditions, until oxidized, waters containing chlorides, for example, could conceivably leach relatively more radium than uranium from the ore. All this leaching could take place under reducing or neutral conditions below the zone of oxidation.

Figure 43 shows that the radioactivity equilibrium of weathered rock is not nearly as constant as that of unweathered rock. Some samples are much more radioactive than would be expected from the uranium content, and others are somewhat less radioactive. These unexpected differences are largely due to the constant redistribution of uranium under weathering conditions. Ordinarily, if sulfide minerals are present, the uranium is highly mobile and radium is nearly static. This is because uranium in the oxidized state ( $\text{U}^{+6}$ ) is very soluble, and radium is nearly insoluble in the presence of the dilute  $\text{H}_2\text{SO}_4$  produced by the oxidation of sulfide minerals (Phair and Levine, 1953). In samples from which uranium has been leached during recent weathering the radioactivity is likely to exceed that expected from the uranium content. Conversely, in places where uranium has recently been deposited the radioactivity will likely be low until equilibrium has been established with the radioactive daughter products.

In some places, however, excess radioactivity may be due to transported radiocolloids. These are generally considered to be daughter products of radioactive decay that are mobile in water solutions because they have attached themselves (by adsorption?) to colloidal particles in the water. For example, ionium, the thorium daughter of  $\text{U}^{238}$  that in turn decays to radium, may be coprecipitated by iron oxides (Phair and Levine, 1953). Evidence that radiocolloids may have been redistributed along with pyrite at some time in the past is given on page 90. Locally, radiocolloids may cause a rock of low uranium content to be highly radioactive.

It has been demonstrated (p. 61) that the  $\text{K}^{40}$  content of the host rock results in radioactivity equivalent to approximately 0.005 percent uranium. Although this radioactivity becomes negligible in rocks that contain more than 0.1 percent uranium, it becomes relatively more significant as the uranium content decreases. For example, the radioactivity of rock in the black facies of the Dripping Spring that contains 0.005 percent uranium in equilibrium with its daughter products is about 0.01 percent equivalent uranium. The radioactivity in excess of that emitted by uranium is emitted by the radioactive  $\text{K}^{40}$  isotope present. Ordinarily, however, this will cause no problems either in the field or in the laboratory.

Despite the rough correlation between uranium content and radioactivity, some factors may accentuate or minimize the radioactivity as detected by portable field instruments. One of these is the mass effect wherein the geometric relation of the radioactive surfaces to the detection instrument can have a decided effect on the measurements. For example, other things being equal, the radioactivity is more intense in the workings of a mine than at an outcrop where the radioactive contribution is only from a flat surface. In like manner, a Geiger counter probe inserted into a drill hole is exposed to considerably more intense radioactivity than if it were merely placed against a specimen of the same rock. Another factor is the distribution of uranium in the rock. If the uranium is distributed as secondary minerals on exposed fracture surfaces, the measured radioactivity may be far greater than would be indicated by the uranium content of the rock as a whole.

Because field radioactivity measurements cannot easily be presented for proper evaluation by the reader, we have shown only the abnormally radioactive area on the mine maps that accompany this report.

## MINERALOGY

### PRIMARY URANIUM-BEARING MINERALS

In unoxidized parts of the deposits, uranium occurs principally in several varieties of uraninite but is also adsorbed on nontronite, chlorite, and, more rarely, graphite. By far the most economically important form is uraninite. Megascopically the uraninite occurs either as fissure and irregular open-space fillings or as blebs and lenses of very fine grained material disseminated in the host rock. The fissure and other open-space fillings are found only in deposits that are near diabase and, with few exceptions, are in hornfels or related metamorphic host rock. Disseminated uraninite is common in all the deposits near diabase, but it also occurs in some of the deposits that are as much as 300 feet distant.

The uraninite that occupies fissures and cavities is black and vitreous and has a conchoidal fracture. Under a hand lens it appears to be nearly pure; associated sulfide minerals are limited largely to the wallrock. Locally, a concentration of sulfide minerals in the highly altered wallrock at the edge of the uraninite filling is obvious.

Disseminated uraninite forms small irregularly shaped bodies and lenticular stringers of somewhat darker color than the surrounding host rock. These zones are typically subparallel to the stratification. In many places, however, the uraninite is so thoroughly disseminated that no visible differences are noticeable between the uranium-bearing and unmineralized rocks.

Uraninite has been recognized in 10 deposits, as indicated in table 6. All these deposits are within 300

feet of diabase, and most are considerably closer, but deposits farther from the diabase possibly contain some very fine grained disseminated uraninite that is difficult to separate and identify.

Microscope studies of polished sections of ore specimens disclose at least three distinct varieties of uraninite, distinguished here as uraninites 1, 2, and 3. Uraninite 1 occurs as streaks and lenses of discrete grains disseminated in the altered host rock or within uraninite 2. Uraninite 2 fills fractures and open spaces but also replaces and is disseminated in the host rocks. Uraninite 3 is largely a sooty variety of pitchblende disseminated in the host rock. Also included with uraninite 3, however, are some varieties of uraninite that apparently are aberrant in these deposits. They include elongate to spheroidal blebs of uraninite, extremely scarce banded botryoidal varieties, and a variety that appears to be an intimate intergrowth of uraninite and cassiterite(?).

## URANINITE 1

Uraninite 1 is the earliest variety in the deposits and is found only in hornfels and related metamorphic rocks. It occurs typically as minute discrete rounded grains enclosed in a matrix either of uraninite 2 or altered host rock (fig. 44C). More rarely it is completely enclosed in molybdenite, pyrrhotite, or one of the decomposition products of pyrrhotite—pyrite or marcasite.

The grain size of uraninite 1 is generally about 10 microns or less. A few of the grains enclosed in pyrrhotite have a maximum diameter of 60 microns (fig. 44D). Most of the uraninite 1 is too fine grained to be seen under medium-power magnification. Many of the following data are from studies of polished ore specimens by use of an oil-immersion objective lens and as much as  $\times$  1,500 magnification.

Much of the uraninite 1 occurs disseminated in altered normal and coarse-grained hornfels. In this environment it is not distributed uniformly but is con-

TABLE 6.—*Minerals found in the uranium vein zones*

[Only identified minerals included; leaders do not necessarily denote absence of mineral. Key to identifications: X, X-ray methods; O, optical methods on thin section, polished section, or fragment; V, visually in field or on hand specimen, generally with aid of hand lens; A, data by R. J. Schwartz, G. Weathers, or others of the U.S. Atomic Energy Commission, but specimens not seen by us.]

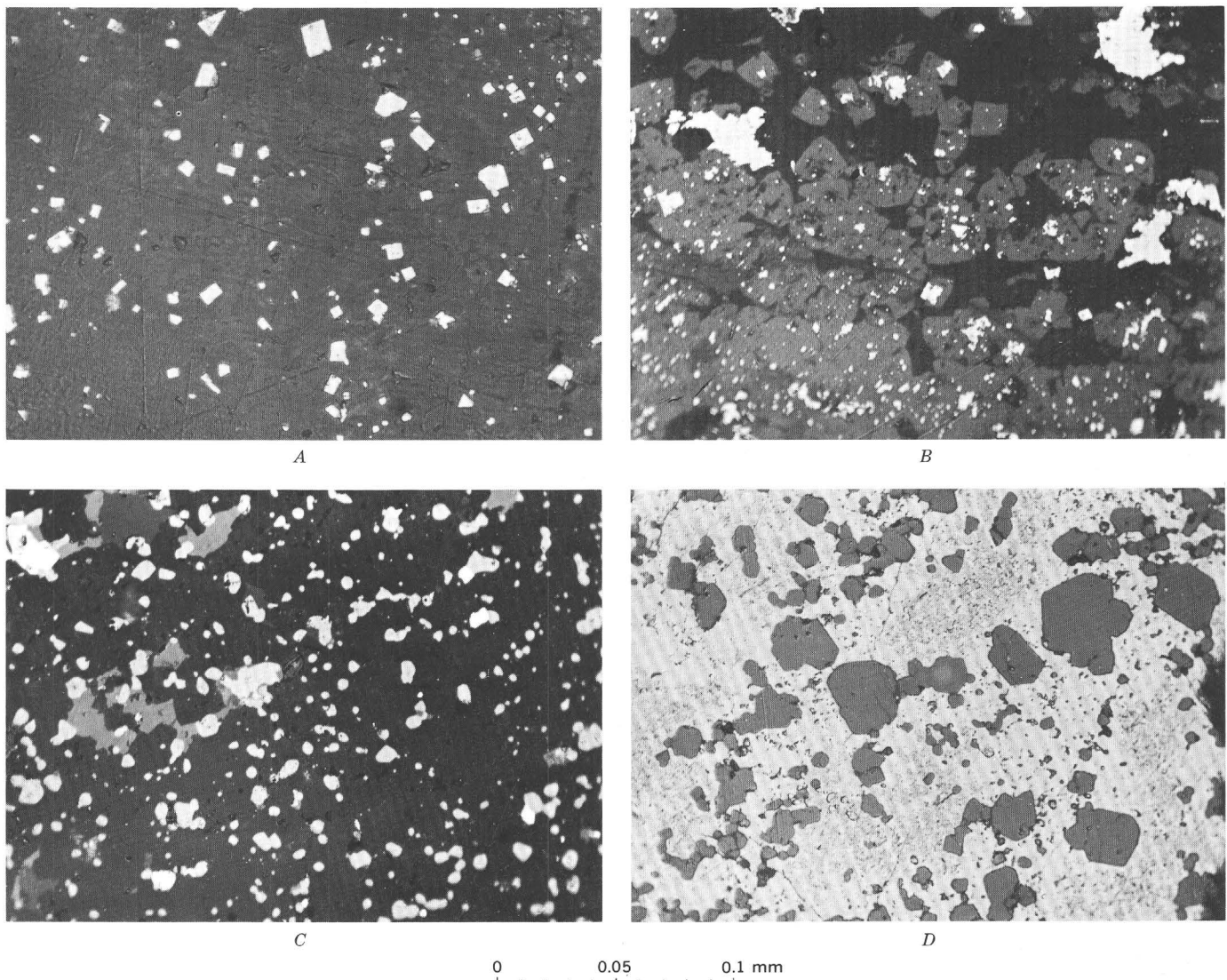


FIGURE 44.—Photomicrographs of uraninite. *A*, Galena cubes enclosed by uraninite 2. Sample 73G55 collected in Hope adit 1. Massive uraninite 2 filling in a fissure veinlet about 2.5 mm across. The mottling in the uraninite is not understood. *B*, Uraninite 2 grains in altered wallrock at the edge of a veinlet. Sample 19G57 collected in the lower level of the Suckerite mine. Subhedral grains of galena are abundant in the uraninite 2. The larger of two white masses at the right edge of the photomicrograph is also galena. The other larger white masses are pyrite, perhaps derived from decomposition of pyrrhotite. The very dark gray to black areas are gangue and altered wallrock. *C*, Typical

concentration of uraninite 1 in a hornfels matrix. Sample 11G66 collected in Hope adit 1. The altered hornfels groundmass is black; quartz is dark gray; uraninite 1 is gray; chalcopyrite and pyrrhotite are white. Note that uraninite 1 grains are generally rounded and have only a faint suggestion of crystal outline. Plane-polarized light. *D*, Particularly large well-developed uraninite 1 in a pyrite matrix. Sample 16G57 collected in Hope adit 3. Uraninite 1 grains have outlines that suggest octahedral crystals. The enclosing pyrite is extremely fine grained and formed by decomposition of pyrrhotite. The gray mottled material in the pyrite was not identified. Plane-polarized light.

centrated as aggregates of disseminated grains in small irregular blebs and lenses subparallel to the stratification. In Little Joe adit 2 some of the uraninite 1 is disseminated along very narrow anastomosing veinlets in thin zones less than 1 inch thick that parallel the relict stratification in coarse-grained hornfels. In Hope 1 adit uraninite 1 is disseminated along discontinuous lenses and irregular blebs in both wallrock and breccia fragments of wall rock enclosed in a matrix of mobilized hornfels. In the Hope 2 and 3 mines much of the uraninite 1 seems to be uniformly distributed in the host rock of the vein zone.

Where the uraninite 1 is enclosed by altered host rock, the tiny grains are ordinarily separated by a space equal to their own diameter. At the edges of the small bodies in which they are concentrated they become more widely spaced and grade into the wallrock. Individual grains have a rounded outline, but a few crystal faces suggest a tendency to idiomorphism. The grains appear gray under a reflecting microscope, and their reflectivity is about equal to that of magnetite.

The grains may occur in the altered host rock nearly unaccompanied by sulfide minerals, but locally pyrrhotite, chalcopyrite, and marcasite are abundant as replacements of the nonopaque minerals that enclose the uraninite 1, and rarely galena is present. In this environment the uraninite grains are not fractured. The sulfide minerals have locally replaced the host rock with little obvious effect on the uraninite, though in some places the margins of uraninite grains appear to be partly replaced and rounded.

In places some of the uraninite 1 is completely or partly enclosed by blebs of sulfide minerals. Where completely enclosed by pyrrhotite, pyrite, marcasite, or molybdenite, the uraninite commonly is subhedral. The forms, although difficult to interpret in polished section, appear to be imperfect dodecahedrons or cubes modified by octahedral faces.

Uraninite 1 is readily distinguished by its greater reflectivity where it occurs enclosed in uraninite 2. Many of the grains of uraninite 1 in this environment are fractured parallel to the veinlet walls and filled with uraninite 2 (fig. 45). Locally galena, pyrrhotite, or one of the other sulfide minerals fills a fracture in uraninite 1.

Uraninite 1 is evidently the earliest ore mineral to have been deposited. An earlier stage of chlorite-type alteration probably occurred, but all the sulfide minerals and other uraninites apparently are later than and cut or enclosed uraninite 1.

#### URANINITE 2

Uraninite 2 forms stringers transverse to stratification and lenses and blebs subparallel to stratification.

It apparently is largely a cavity filling; although gradational into the altered wallrocks, it evidently did not make room for itself exclusively by replacement. Uraninite 2 is a hard brittle vitreous black material that has a conchoidal fracture.

Under the reflecting microscope, uraninite 2 is considerably less reflective than uraninite 1. It is further distinguished by almost invariably containing a myriad of minute galena cubes (fig. 44A). These cubes are generally smaller than the included grains of uraninite 1, which are also abundant in many places. In addition, uraninite 2 locally contains larger galena grains as much as 0.3 mm across that poikiloblastically enclose specks of uraninite 1, uraninite 2, gangue, and other sulfide minerals.

In general, the uraninite 2 seems to be amorphous and completely structureless, but idiomorphic cubic grains (fig. 44B) are common at the margins of veinlets. These are distributed as discrete grains in the altered wallrock and grade by coalescence into the massive apparently amorphous vein filling. The idiomorphic grains are commonly less than 15 microns across but even so may contain several minute cubes of galena. X-ray powder patterns of uraninite 2, though not sharply defined, are adequately clear for identification. The loss of definition is likely due to the  $\text{UO}_3$  content of uraninite 2, as  $\text{UO}_3$  does not give a well-defined X-ray pattern.

Uraninite 2 apparently is earlier than any of the other vein minerals, with the exception of uraninite 1, molybdenite, and pyrrhotite. It fills cracks in uraninite 1,

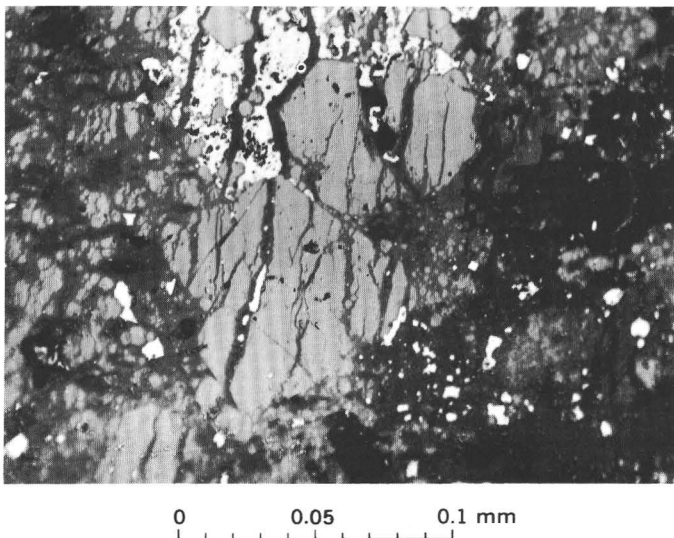


FIGURE 45.—Fractured grains of uraninite 1. Sample 16G57 collected in Hope adit 3. The large fractured white mass at the top is pyrite developed from decomposed pyrrhotite. All the smaller white grains and fracture fillings are galena. Uraninite 2 is dark gray; it occupies fractures and encloses all the galena grains. The black material is gangue. Plane-polarized light.

appears to partly replace molybdenite flakes at the margins and by encroachment along cleavages, and replaces pyrrhotite grains by very irregular marginal encroachment. Pyrite and marcasite that have formed by decomposition of pyrrhotite deceptively appear to be replaced by uraninite 2, but we suspect that they formed as pseudomorphs of pyrrhotite after the deposition of uraninite 2.

#### URANINITE 3

Uraninite 3 is all uraninite or pitchblende not classifiable as uraninite 1 or 2. It is the type of uraninite found in deposits that have a siltstone host rock, it was not recognized in any of the deposits that occur entirely in hornfels and related metamorphic rocks.

Uraninite 3 ordinarily is disseminated as dustlike grains similar to the carbon dust that pervades much of the rock, but it also includes several varieties of pitchblende that form larger grains and blebs. It may form irregular or elongate darker areas in the vein or ore zones, and in some places it forms a black very impure amorphous mass that fills stylolites and very narrow fractures. One specimen from the Tomato Juice deposit contained three small concentrically banded hemispherical botryoidal forms about 15 microns in diameter—the only botryoidal pitchblende seen in any of the specimens of Dripping Spring ore. Other uraninite 3 at the Tomato Juice deposit occurs as rounded and irregularly shaped homogeneous gray blebs less than 50 microns in the longest dimension.

Uraninite at the Rock Canyon deposit forms elongate and irregularly shaped but rounded blebs as much as 200 microns in length. Ordinarily they are less than half this size. This uraninite, in polished section, has a slightly brownish cast and a reflectivity between that of uraninite 1 and uraninite 2. In one polished section the margins of these uraninite grains contain another intergrown mineral. This mineral is more reflective than the uraninite, has a yellow color much paler than that of pyrite, and seems to be strongly anisotropic (fig. 46). The individual grains are about 1 micron or less in length, and determination of the characteristics of the intergrowth is very difficult. The intergrowth may be vermicular or eutectoidlike, or the highly anisotropic grains may be distributed in a decussate arrangement within the uraninite. Apparently the intergrown mineral is inert to all staining agents commonly used on polished sections and is very hard. The specimen from which the polished section was cut contained more tin (about 0.007 percent) than any other sample of the Dripping Spring ore, and possibly this mineral intergrown with uraninite is cassiterite. An X-ray powder film of the mineral showed no pattern whatsoever, per-

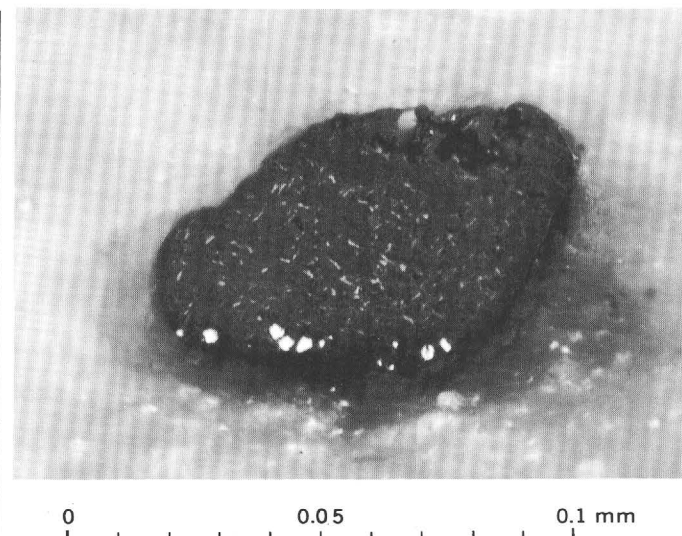


FIGURE 46.—Intergrowth of uraninite and an unknown mineral. Sample 126G56 collected from the Rock Canyon deposit. The uraninite (pitchblende) bleb poikilitically encloses minute grains of an unidentified mineral. The apparent orientation of the included mineral is evident because of its strong anisotropism. White grains near the edge of the bleb are pyrite. The surrounding matrix is feldspar and quartz in weakly metamorphosed siltstone. Partly crossed nicols.

haps because we were unable to pick enough of the material from the polished section.

Uraninite 3 ordinarily is not amenable to study under the reflecting microscope because of its extremely small grain size, low reflectivity, and poor polish. Mineral separates of uraninite 3 have been difficult to make, probably because it is so fine grained that it forms slimes in any separation involving a liquid medium.

Uraninite 3 probably corresponds for the most part to the sooty pitchblende found in many uraninite deposits throughout the world although it does not seem to have a supergene origin. Whether all the material classified as uraninite 3 is of the same age is not known. Its relations to uraninites 1 and 2 are also unknown as it is not associated with them in the same specimens. Much of uraninite 3 very probably represents a phase of either uraninite 1 or 2 that was deposited under lower temperatures and weaker reducing conditions farther from the source of the mineralizing solutions. The variety at the Tomato Juice deposit suspected to be intergrown with cassiterite(?) may, however, have been deposited at high temperatures.

#### URANIFEROUS CHLORITE

In the unoxidized parts of many deposits, especially those several hundred feet from diabase, no primary uranium mineral has been recognized. We believe that much of the uranium in these deposits is adsorbed on

chlorite. Thin sections of some highly radioactive samples from the Red Bluff adit 5 disclosed no opaque minerals and no recognizable secondary uranium minerals. By application of stripping film to one thin section it was found that radioactivity was strongest in the areas of the slide that contained decussate aggregates of a green flaky claylike mineral which showed the following properties: Pleochroism is  $X$ =light yellow green,  $Y$  and  $Z$ =green; refractive indices span 1.61; birefringence is first-order blue; elongation positive. X-ray diffraction patterns of the mineral showed a slight broadening but no significant displacement of the  $2\theta=6.2^\circ$  peak after ethylene glycol treatment—the peak persisted even after heating for half an hour at about  $600^\circ$  C. During heating the material turned from green to orange brown. These results prove the mineral to be an iron-rich chlorite.

By use of the Frantz isodynamic separator we were able to get a fairly good separate of this chlorite. This material was found by J. C. Antweiler to contain 2.39 percent uranium; 2.11 percent was in the oxidized form ( $U^{+6}$ ), and 0.23 percent was unoxidized ( $U^{+4}$ ) (the remainder was lost during analysis). The sample from which this material was selected came from only a few feet below the outcrop, and it was ground to extreme fineness during preparation; either of these factors may have had an effect on the high ratio of  $U^{+6}$  to  $U^{+4}$ . The fact that similar radioactive chlorite has been recognized in unweathered parts of other deposits suggests that the uranium originally adsorbed on the chlorite might be unoxidized.

The composition of the radioactive chlorites apparently varies from deposit to deposit as refraction indices range from about 1.58 to 1.62 and there is a consequent variance in intensity of pleochroism, the intensity being weaker in material of lower birefringence. Some of this material, however, may not be chlorite. Although the X-ray data on the one sample that was thoroughly tested proved it to be chlorite, some of the uraniferous material in other deposits possibly may be nontronite. Certainly the optical properties and occurrence of much of this chloritic aggregate would lead most petrographers to identify it, in thin section, as a nontrottonitic-clay alteration product.

A later nonuraniferous nontronite clay present in many of the deposits has some optical properties very similar to those of the chlorite. In thin section a distinction between the two may be impossible. This nontrottonite is described on page 93.

#### URANIFEROUS CARBON

Direct association between carbon and uranium is rare in most of these deposits, and there is no positive correlation between the uranium and carbon content.

Most carbon separates actually seem to have a lower uranium content than other fractions from the same rock. Maurice Deul and Joseph Houston, of the U.S. Geological Survey (Irving Breger and Maurice Deul, written commun., 1956), separated a sample from the Shepp No. 2 deposit into three fractions by a method described by Deul (1956): organic carbon, mineral, and middlings. The middlings fraction presumably is largely clay minerals. Very little of the uranium is contained in the organic-carbon fraction. About equal amounts of uranium are contained in the mineral and middlings fractions, although the middling fraction contained a much higher percentage of uranium. Results of the analyses are tabulated below. Uranium analyses were made by Emma Campbell; ash analyses, by Alice Caemmerer.

	Weight (grams)	Uranium		Carbon		Ash (percent)
		Percent	Grams	Percent	Grams	
Original sample-----	100.0	0.08	0.080	1.91	1.93	98.0
Organic fraction-----	.75	<.04	Tr.	68.0	.51	22.0
Mineral fraction-----	75.00	.045	.034	1.09	.82	99.0
Middlings-----	23.80	.15	.036	1.80	.43	96.0
Loss-----	0.45	-----	.010	-----	.17	-----

Graphite from the Rainbow deposit apparently contains uranium, possibly in significant amounts. Material separated from ore from the Rainbow adit had a specific gravity somewhat less than that of quartz. Tiny black opaque grains were handpicked from this separate and were identified as graphite by standard X-ray powder methods. Fluorescent flux tests of the graphite indicated that it contained a moderate amount of uranium. Although the method is not strictly quantitative, the intensity of the fluorescence suggested that considerably more than trace amounts of uranium were present. The graphite probably holds the uranium in some way, perhaps by adsorption. The association of uranium with graphite is probably rare and should be considered more as a curiosity rather than as typical of any of the deposits.

The possibility that uranium might be associated with soluble hydrocarbons in some of the deposits was tested and found to be negative. Nine samples from different deposits and having a wide range of uranium content were each ground to pass through a 30-mesh screen and placed in a Soxhlet extractor with a residual solution consisting of several strong organic solvents. If hydrocarbons had been present, the residual solution should have become discolored after a few minutes; colored soluble hydrocarbons were not present in detectable amounts.

The plotting of organic-carbon contents of 28 samples against uranium contents suggests a negative cor-

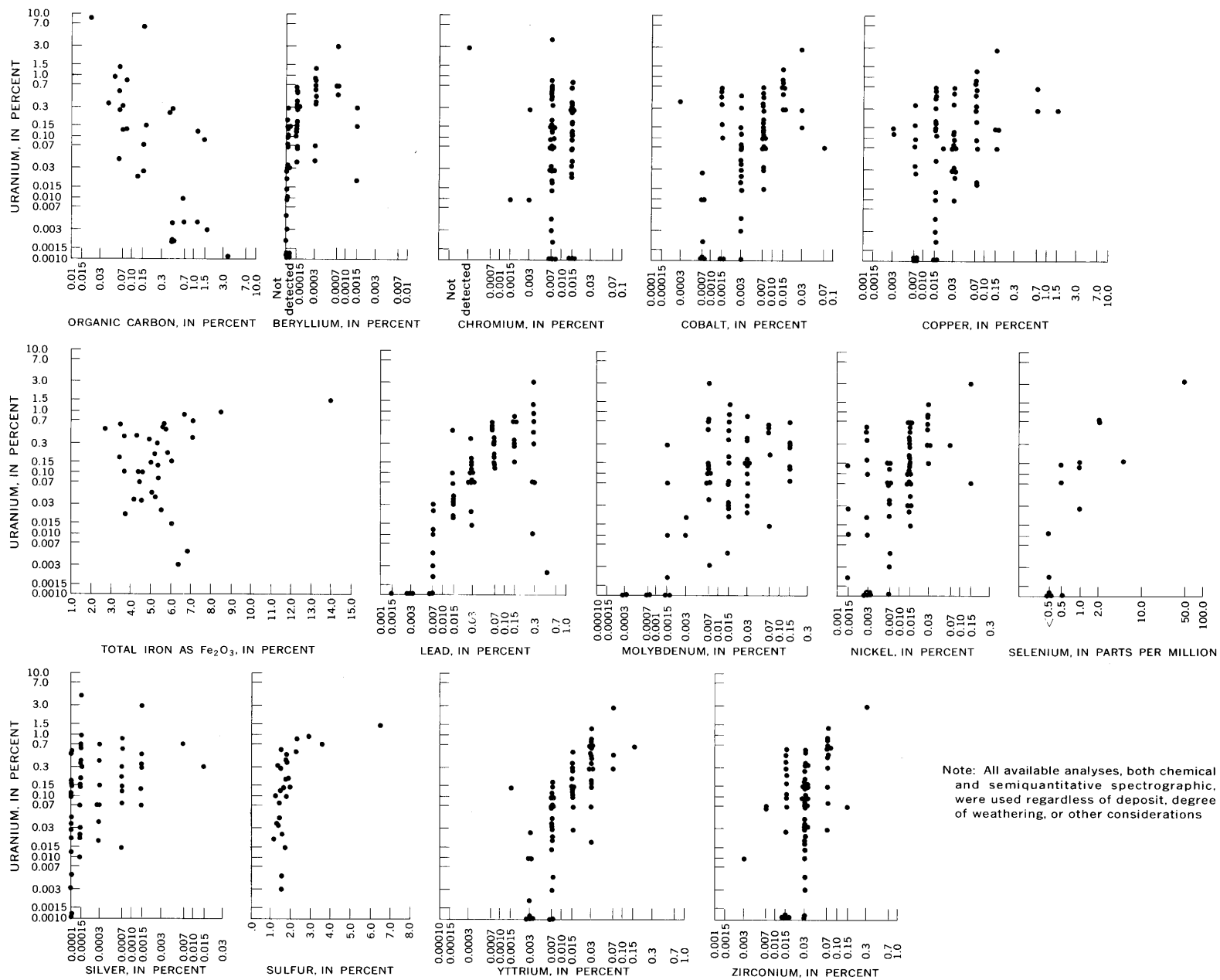


FIGURE 47.—Scatter diagrams showing correlations between uranium and various elements in deposits in the Dripping Spring Quartzite.

relation (fig. 47). This apparent relation may not be real, as half the samples come from the Hope mine and the others come from widely separated localities. All the samples are from the gray unit, however, and further analyses might bear out the indicated relation.

#### COFFINITE

Coffinite, a uranium silicate, was identified by X-ray powder pattern in one sample from the Workman adit 1 (L. R. Stieff, written commun., 1955). It could not be seen in the sample even under high magnification, and it was not detected in subsequent X-ray or optical studies on other samples from the same deposit or from any other deposit.

#### PRIMARY SULFIDE MINERALS

##### MOLYBDENITE

Molybdenite was observed only in the Workman Creek area, and there it occurs near diabase and is most commonly associated with mobilized hornfels. Its occurrence in vugs in mobilized hornfels at the Hope 1 mine is described on p. 37. Minute amounts of molybdenite were also recognized in polished sections of rock that contained sulfide minerals from the Workman adit 1 and the Suckerite mine.

In the Workman adit 1, the molybdenite and other sulfide minerals are disseminated in a host rock of mobilized hornfels. Flakes of molybdenite as much as 1.0 mm across and 0.02 mm thick are enclosed by the gangue or by sulfide minerals. In one polished section (Granger and Raup, 1959, fig. 58), a flake of molybdenite enclosed by pyrrhotite was bordered by a narrow irregular band of chalcopyrite that evidently partly replaced the pyrrhotite along the molybdenite grain boundary.

In the Suckerite deposit, flakes of molybdenite occur with the uraninite and in places completely enclose grains of uraninite 1. These grains of uraninite 1 tend to be idiomorphic and are not fractured, in contrast to many grains outside the molybdenite. The molybdenite is partly replaced by pyrite and by uraninite 2 which seems to have formed along cleavages at the margin of the molybdenite flakes.

The molybdenite apparently fits the paragenetic sequence between the disposition of uraninite 1 and uraninite 2, and it probably formed at about the same time as pyrrhotite. It evidently acted as a malleable shield that buffered the included grains of uraninite 1 against fracturing.

##### PYRRHOTITE

Pyrrhotite commonly is the most abundant sulfide mineral in deposits in hornfels and related metamorphic rocks. It is a common constituent disseminated in

deposits in the Workman Creek area and at the Black Brush, Sorrel Horse, and Citation deposits in the Cherry Creek area. It has been seen in several of the aplite dikes that cut hornfels in the Workman Creek area and is widely disseminated in the hornfels away from uranium deposits.

Most of the pyrrhotite is disseminated. Fissure fillings of pyrrhotite exist only as minute segmented and beadlike stringers a few millimeters long.

In mobilized hornfels and aplite dikes, individual blebs of pyrrhotite are as large as 10 mm across, but generally they are much smaller; in hornfels the disseminated grains are ordinarily less than 1 mm across and are as small as submicroscopic in size. The larger blebs commonly consist of several anhedral grains, but the smaller ones are composed of individual anhedral to subhedral grains.

Most of the pyrrhotite forms anhedral blebs, but in some places tiny perfectly shaped hexagonal plates are enclosed in the host rock. Ordinarily these are found near or in uranium deposits. Their occurrence in vugs was described on page 36; probably most of the well-shaped hexagons were formed in open space rather than by replacement, the way in which anhedral blebs were formed.

A semiquantitative spectrographic analysis, in percent, of pyrrhotite from the Workman 1 adit, sample 55G54, is given below. Analyst was N. M. Conklin. Elements not listed were not detected. Accuracy of data is indicated in figures 32-36 (M, major constituent).

Fe-----	M	Co-----	0.15	Ti-----	0.015
Cu-----	3	Ca-----	.15	Mn-----	.015
Al-----	.7	Zn-----	.07	Ag-----	.0015
Ni-----	.3	Mg-----	.03	Cr-----	.0007

The abundance of pyrrhotite varies from place to place. The greatest concentrations are in the vein zone of deposits that are parallel to mobilized hornfels. This is the only environment where the concentration of pyrrhotite is obvious. Elsewhere, as in deposits in hornfels, the pyrrhotite is commonly so fine grained that it can be seen only under a hand lens. Although it is disseminated in hornfels and aplite dikes in some places, there are also many places where these rocks contain no pyrrhotite whatsoever.

Some of the larger blebs of pyrrhotite are polysynthetically twinned. These twins are not abundant and seem to be limited to areas adjacent to chalcopyrite.

Pyrrhotite completely encloses grains of uraninite 1 in some places. The enclosed uraninite 1 tends to be idiomorphic and is rarely fractured in this environment. Sparse grains of uraninite 1 in which a fracture is filled with pyrrhotite have been noted.

Uraninite 2 apparently replaces the pyrrhotite marginally. At the edges of pyrrhotite masses the uraninite 2 appears to have penetrated short distances into fractures that cut the pyrrhotite.

Galena and chalcopyrite are both later than and replace the pyrrhotite. Chalcopyrite commonly replaces the pyrrhotite marginally but locally has penetrated along fractures. Sparse minute veinlets of galena have been noted in pyrrhotite.

Both pyrite and marcasite are later than pyrrhotite and replace it. In many places these minerals apparently formed by decomposition of the pyrrhotite. (See process described by Edwards (1947, p. 100-101).)

Pyrrhotite apparently was formed at about the same time as molybdenite—after the deposition of uraninite 1 and prior to the deposition of uraninite 2. Whether all the pyrrhotite in the uranium vein zones is the same age as the pyrrhotite disseminated in the hornfels and related rocks is not known. Possibly the pyrrhotite away from the veins is older and is related to the initial recrystallization of a pyrite-bearing siltstone. The pyrrhotite in the vein zones may then represent a later hydrothermal mineral related to the mineralizing processes.

#### CHALCOPYRITE

Chalcopyrite is common in most uranium-bearing vein zones. Ordinarily, however, it is not abundant and is generally disseminated in such small grains that it is not readily observed. It occurs disseminated in and adjacent to uranium vein zones and is distributed as grains and aggregates in fractures within the vein zone. Chalcopyrite is not uncommon in the Dripping Spring Quartzite away from known uranium deposits. In the Globe-Miami, Superior, and Ray areas, much of it is related to nearby porphyry copper deposits.

In hornfels and related rocks the manner of occurrence of chalcopyrite is similar to that of pyrrhotite. Many of the blebs of chalcopyrite may actually represent completely replaced pyrrhotite. Blebs of pyrrhotite partly replaced by chalcopyrite are common. The chalcopyrite both fills fractures in pyrrhotite and replaces the pyrrhotite by marginal encroachment.

In siltstone and locally in hornfels, the chalcopyrite commonly is associated with pyrite, marcasite, sphalerite, and galena, and more rarely with small amounts of quartz in narrow veinlets.

Some of the chalcopyrite from the Workman adit 1 contains a small amount of exsolved cubanite, but this is the only locality at which cubanite was noted.

Specimens from the Snakebit and Sorrel Horse deposits contain sphalerite from which small amounts of chalcopyrite have exsolved as minute elongate blebs and beadlike strings of blebs.

Evidence for the paragenetic position of chalcopyrite is conflicting, and possibly the chalcopyrite was not all deposited during one period of mineralization. All the chalcopyrite observed is later than pyrrhotite. The paragenetic relation between chalcopyrite and uraninite 2 is not known. Although chalcopyrite is disseminated in both the uraninite 2 and the chloritic gangue in which the uraninite is enclosed, no diagnostic relations can be determined to prove which is the earlier. We arbitrarily assume that chalcopyrite in most deposits is later than the uraninite 2.

In the Workman Creek area all pyrite and marcasite is later than the chalcopyrite. Pyrite stringers that cut the chalcopyrite were observed. Outside the Workman Creek area most of the pyrite and marcasite is earlier than the chalcopyrite. At the Tomato Juice deposit disseminated pyrite grains form nuclei rimmed by chalcopyrite as though the chalcopyrite were deposited on top of the pyrite. At the Black Brush deposit grains of chalcopyrite completely enclose some grains of both pyrite and marcasite. At the Horseshoe deposit narrow pyrite stringers locally swell and include small cavities or vugs in which euhedral pyrite forms a drusy coating on the walls. Some of these cavities are entirely filled with chalcopyrite and sphalerite.

The relation between chalcopyrite and sphalerite is also conflicting. Sphalerite is rare in most specimens from the Workman Creek area, but where seen, the chalcopyrite occurs as partial replacements of, or veins in, the sphalerite. Outside the Workman Creek area the chalcopyrite and sphalerite generally have mutual boundaries in the few specimens that show the two minerals in contact.

In one specimen from the Sorrel Horse deposit the caries texture suggests that chalcopyrite locally replaces sphalerite; also, the chalcopyrite appears to extend partly along the boundary between the sphalerite and the enclosing host rock. In another specimen from the same deposit sphalerite partly surrounds masses of chalcopyrite, and stringers of chalcopyrite project into, but rarely cut, the sphalerite. At the Snakebit deposit the caries texture suggests that sphalerite is later than the chalcopyrite. At the Horseshoe deposits blebs of chalcopyrite are generally partly surrounded by a rim of sphalerite, and, more rarely, the sphalerite occupies fractures in the chalcopyrite.

Exsolved chalcopyrite in the sphalerite is abundant at the Sorrel Horse and Snakebit deposits but was not observed at the nearby Horseshoe. There is some suggestion that the exsolved chalcopyrite is more prevalent near masses of chalcopyrite adjacent to sphalerite.

The chalcopyrite apparently is of different age in different deposits. The sphalerite seems to have preceded

chalcopyrite in the Workman Creek area. Elsewhere, the caries texture notwithstanding, much of the chalcopyrite probably preceded the sphalerite. In the process of replacing the chalcopyrite, the sphalerite apparently acquired a considerable copper content locally which later exsolved as chalcopyrite.

Under weathering conditions the chalcopyrite breaks down progressively to chalcocite and covellite, and ultimately to efflorescent hydrous copper sulfate or carbonate minerals.

#### CUBANITE

Cubanite was noted only in specimens from the Workman adit 1, where it occurs in very small amounts as tiny irregularly shaped lenses exsolved from chalcopyrite. The lenses are ordinarily less than 0.05 by 0.02 mm. They seem to be oriented only locally and are generally sporadically disseminated.

#### SPHALERITE

Sphalerite is rare in most of the uranium deposits. Where present, it is nowhere directly associated with uraninite but occupies separate fractures or is disseminated in the wallrock at a distance from the uranium minerals.

Nearly all the sphalerite observed is black and of the type commonly referred to as marmatite or blackjack. Internal reflection from the sphalerite in polished section under crossed nicols is a very dark red brown as a result of high iron content. A specimen of sphalerite from the Jon adit (table 7) contained 12.55 percent FeS in solid solution.

At the Horseshoe deposit many random hairline fractures in and near the radioactive zone are filled exclusively with sphalerite. This sphalerite is dark yellow brown on broken surfaces and is considerably lighter colored than the sphalerite observed elsewhere.

In the Jon adit sphalerite occurs as disseminated grains in the chloritic-hornblendic gouge of a fault parallel to the stratification. It is localized within a few feet of the intersection of this fault and the nearly vertical uranium-bearing vein. Diameter of the grains ranges from microscopic to about 8 mm. The outer few microns of some of the grains are fractured and filled with pyrite-marcasite-calcite veinlets, but the cores are pure sphalerite.

In Hope adit 1, sphalerite is sparse but was noted locally as rounded grains that range in diameter from 0.1 to 0.5 mm and that are disseminated in the wallrock within a few millimeters of a narrow uraninite stringer. Tiny veinlets of marcasite cut the sphalerite, but no other relations between sphalerite and vein minerals were noted.

Sphalerite (variety, marmatite) in a vug from the

Lucky Stop adit is described on page 37. It abuts and partly surrounds euhedral pyrrhotite grains and is cut by fine veinlets of chalcopyrite.

Sphalerite in contact with galena was noted only at the Hope 1 and Snakebit deposits. At the Snakebit deposit a veinlet of galena cuts the sphalerite. At the Hope deposit sphalerite and galena have mutual boundaries that give no indication of age differences.

The paragenetic relations between sphalerite and chalcopyrite are described under the heading "Chalcopyrite."

#### GALENA

Galena is nowhere abundant but is important because of the radiogenic derivation of some of its constituent lead. It was recognized at the deposits shown in Table 6.

The galena that occurs in and near uranium deposits is of three types: (1) anhedral galena that fills fractures and small open spaces; (2) euhedral galena poikilitically enclosed by uraninite 2; and (3) poikiloblastic galena closely associated with uraninite veinlets. Types 2 and 3 generally occur together and may be of similar derivation.

Most of the galena recognizable megascopically is of the type that fills narrow fractures in the host rock. Galena of this type is found in or adjacent to uranium-bearing vein zones but generally is not directly associated with uraninite.

In the Hope adit 1, galena is distributed along marcasite veinlets. In places these stringers seem to be segmented—galena and marcasite alternating as the vein filling. In the Hope adit 3, small galena veinlets only a few microns wide that cut marcasite were noted. This marcasite, however, probably is derived from the decomposition of pyrrhotite, and the galena likely was introduced into the veinlets in the pyrrhotite before or during the time the change took place.

At the Jon deposit, galena occupies veinlets with pyrite, particularly at swells in the normally hair-thin veinlets. The pyrite apparently has locally replaced galena, but because relations are obscure such replacement cannot be proved.

At the Snakebit and Sorrel Horse deposits galena was noted in association with chalcopyrite and sphalerite in fractures and small cavities. Sphalerite is cut by galena veinlets, and galena locally forms a rim between chalcopyrite and the gangue as though the galena had replaced chalcopyrite along the grain boundary. The relations of galena to other vein minerals suggest that it was introduced at about the same time as at least one generation of marcasite and pyrite, but later than the other base-metal sulfide minerals.

At Red Bluff, grains and masses of galena that range from microscopic to about 1 cm on a side have been

observed. These occur in fractures and along planes of stratification. The relation of this galena to other vein minerals was not noted. Some of this galena seems to have a lead isotope composition that is normal for non-radiogenic vein galena, but some has a radiogenic lead content that ranks among the highest of any known in the world. The isotopic composition of several samples of galena (table 5) is discussed under the heading "Age of the Uranium Deposits" (p. 76).

As previously noted on page 82, tiny cubes of galena are almost universally included in uraninite 2. These cubes range from about 10 microns on an edge to sub-microscopic in size. Ordinarily they are disseminated as poikilitic inclusions in masses of uraninite 2. In addition to the tiny cubes are minute irregularly shaped masses of galena that locally fill short fractures only 1-2 microns wide in uraninite 1, pyrrhotite, and uraninite 2. To the best of our knowledge these anhedral masses of galena are paragenetically identical with the euhedral cubes.

Poikiloblastic grains of galena as much as 0.5 mm across are common in and adjacent to veinlets that contain uraninite 2. The galena generally contains an abundance of inclusions of uraninite 1 and 2, pyrrhotite, chalcopyrite, chlorite, and other gangue and wallrock minerals. Although the outline of galena grains is ordinarily very irregular, a tendency for some of them to form skeletal cubic shapes is obvious. This type of galena is concentrated locally in the altered zone within 0.5-1.0 mm of the edge of uraninite veinlets.

By our interpretation the galena cubes disseminated in uraninite 2 probably represent, in large part, radiogenic lead exsolved from the uraninite during the time of deposition of some of the sulfide-bearing minerals. The abundance of these grains thus suggests that considerable radiogenic lead was available at that time, which would indicate that the time of formation of the galena was relatively recent—Tertiary or later. The larger poikiloblastic grains may represent either coalescence of these smaller grains or a later deposition of introduced galena. The fracture fillings are in large part galena composed of normal lead of Tertiary age and deposited after most of the other base-metal sulfides, probably at about the same time as some of the pyrite-marcasite. In some places, however, radiogenic lead may have been leached from uraninite and redeposited nearby as galena by sulfur-bearing solutions. This explanation would account for the predominant radiogenic lead composition that has been found for the galena at the Red Bluff deposit.

#### PYRITE

Pyrite is widespread in the gray unit of the Dripping Spring, and most of it has no relation to uranium de-

posits. Any joint, fracture, or stylolite can contain some pyrite below the zone of weathering. Pyrite does, however, seem to be more abundant in uranium vein zones than elsewhere. Veinlets of short extent and random orientation are present in the vein zone of many deposits and not uncommonly form an anastomosing stockwork in favorable strata laterally for several feet from a uranium vein.

Three general occurrences of pyrite have been noted: fracture fillings and small masses; disseminations; and masses derived from the decomposition of pyrrhotite.

Pyrite-filled fractures, or veinlets, rarely are more than a few millimeters wide, and most are of hairline width. The pyrite may occur with marcasite or, more rarely, with small amounts of galena or chalcopyrite. Gangue and alteration minerals ordinarily are not abundant and may consist of carbonate minerals, nontronitic clay and chlorite, sparse quartz, or fluorite.

The content of the pyrite-filled veinlets varies from place to place. In the Workman Creek area the veinlets generally contain nontronite and calcite. A little dark-purple fluorite is in some of the veinlets in the uranium vein zone of the Hope 3, Tomato Juice, Sorrel Horse, and Big Buck deposits. Small amounts of quartz were noted in veinlets at the Jon mine. The pyrite in most places is later than the alteration minerals and non-carbonate gangue.

At Red Bluff most pyrite-filled veinlets contain no other minerals, but a little chalcopyrite is present locally. Specimens have been found at Red Bluff that contain goethite veinlets cut by pyrite veinlets, indicating a stage of pyrite deposition subsequent to an early stage of weathering.

At the Tomato Juice and Rock Canyon deposits, pyrite preceded the deposition of ankerite in the central fracture. Pyrite borders the ankerite filling and extends into the country rock along stylolites.

At the Horse Shoe deposit masses of pyrite related to vein pyrite and as much as 1 inch across and several inches long are present in sharply warped strata at the crest of a drag fold (fig. 48) adjacent to a low-angle fault. The original pyrite in these masses is slightly fractured and brecciated and is veined and healed by later marcasite.

Although pyrite veinlets are generally not radioactive, a stockwork of pyrite veinlets in a 6-inch-thick stratum between adits 1 and 2 at Red Bluff is highly radioactive. Each veinlet is bordered by a narrow red zone of finely disseminated hematite; the country rock otherwise is bleached. Stripping film applied over a thin section of this rock disclosed that the radioactivity emanates from individual centers distributed sparsely along the margins of the pyrite veinlets. The source

points of the radioactivity were too small to be visible under the microscope. As the radioactivity from these points was so much more intense than could be expected from any known uranium mineral, we concluded that radiocolloids were present. No doubt the solutions from which the pyrite was deposited, or later solutions, acquired the radiocolloids from the leaching of adjacent uranium ore bodies.

Well-formed pyrite crystals are not abundant in the veins. The few that were seen were 1 millimeter or less on an edge and were generally associated with carbonate minerals. Cubic forms are most common, but cubes modified by octahedra are nearly as prevalent. Octahedra are scarce and pyritohedra are absent.

Disseminated pyrite, mostly of microscopic size, is a normal constituent of much of the gray unit. In addition to being distributed throughout the rock, the pyrite is commonly concentrated in the stylolites, where it is associated with carbon, chlorite, and several unidentified alteration minerals. Near veinlets, pyrite may be abundant in stylolites and seems to have been derived from the same source as the pyrite in the veinlets; elsewhere the stylolite pyrite is less abundant and probably was derived from pyrite disseminated in the host rock.

Pyrite has also been derived by the decomposition of pyrrhotite (Edwards, 1947, p. 100, 101). Most of the decomposed pyrrhotite has been converted to a banded

aggregate of marcasite, but in some places pyrite has also been formed. The decomposition of pyrrhotite seems to have been triggered in most places by deposition of fine veinlets of pyrite. These veinlets cut the pyrrhotite and are bordered by either banded marcasite or an extremely fine intergrowth of pyrite and an unidentified mineral.

The evidence suggests that pyrite occupies more than one paragenetic position. No pyrite is known to have preceded uraninite and pyrrhotite in the deposits, although some disseminated pyrite likely has persisted in the gray unit since diagenesis. Pyrite is probably contemporaneous with marcasite in areas of decomposed pyrrhotite, but in some places pyrite is cut by marcasite veinlets. Veinlets of pyrite cut chalcopyrite in some of the deposits, but chalcopyrite is obviously later than pyrite in others; in some deposits disseminated pyrite grains locally form the nuclei for rims of chalcopyrite. The relation of pyrite to galena and sphalerite is not well known, but where chalcopyrite is later than pyrite the galena and sphalerite are also later. Pyrite is generally older than ankerite but younger than most other gangue minerals. It is both nearly contemporaneous with and younger than calcite. In some places the deposition of pyrite continued even after an early stage of weathering, as is shown by the pyrite veinlets that cut goethite at the Red Bluff deposit.

#### MARCASITE

Marcasite has been recognized in and near the vein zone of many of the uranium deposits. It occurs in veinlets closely associated with pyrite and chalcopyrite and in banded masses derived by the decomposition of pyrrhotite.

The marcasite that occurs in veins is commonly associated with pyrite. In many places the narrow parts of the veinlets are largely pyrite; but where the veinlets swell and other sulfides such as chalcopyrite are present, the principal iron sulfide is marcasite, as if pyrite had been converted to marcasite adjacent to base-metal sulfides. At the Horse Shoe deposit, masses of pyrite were slightly brecciated and then were healed by marcasite.

Veinlets of marcasite cut stringers of uraninite 2 at several of the deposits in the Workman Creek area. These are ordinarily lacy and anastomosing and occur in microscopic networks less than 1 mm wide. Chalcopyrite is sparingly present in some of these veinlets but bears no obvious paragenetic relations to the marcasite.

Marcasite derived by the decomposition of pyrrhotite has a characteristic lamellar form; the lamellae range from nearly spherical and concentric to highly irregular. Thin veinlets of pyrite commonly traverse the

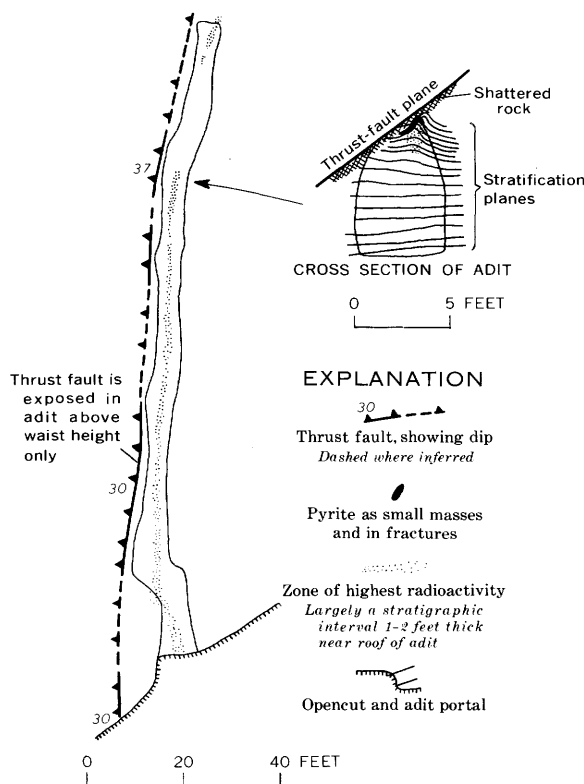


FIGURE 48.—Map and section of the Horse Shoe adit.

banded marcasite, and the forms of the lamellae seem to be controlled in part by the positions of the pyrite veinlets. For example, a common form consists of a pyrite veinlet bordered by bands of marcasite that extend convexly into masses of pyrrhotite (fig. 49).

The marcasite lamellae are interlayered with an unidentified nonopaque extremely fine grained material that has a high index and high birefringence. This material apparently is inert to hydrochloric acid and does not produce a recognizable X-ray pattern. According to Edwards (1947, p. 101), the interlaminar material commonly is a carbonate mineral.

Marcasite and pyrite commonly are very difficult to distinguish in these rocks. Much of the marcasite, particularly the banded variety, is extremely fine grained and appears isotropic. Locally the pyrite has faint anisotropism. Where adjacent to one another in polished section, the marcasite generally is a slightly lighter yellow than the pyrite and reacts more quickly with nitric acid. In a few samples, where distinctions were

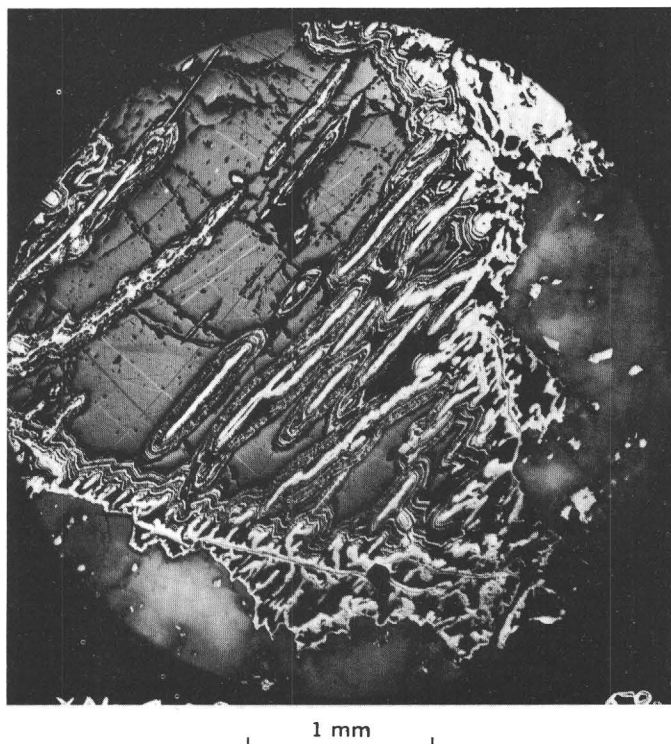


FIGURE 49.—Well-developed concentric pattern in marcasite formed by the decomposition of pyrrhotite. Sample 55G54 from the portal of Workman adit 1. The mottled gray material to the right and bottom of the field is hornfels. Pyrrhotite is uniform gray and is partly decomposed to concentrically banded marcasite. Note how the marcasite seems to have developed outward from minute fractures that are lined with pyrite. The marcasite is so fine grained that individual grains are not distinguishable, and identification by X-ray methods was necessary. Polished section; crossed nicols.

impossible by optical means, the material was determined by X-ray powder patterns.

Marcasite probably occupies more than one position in the paragenetic sequence. The marcasite derived by decomposition of pyrrhotite is later than chalcopyrite and contemporaneous with one stage of pyrite deposition. Marcasite veinlets that cut uraninite 2 are nearly contemporaneous with chalcopyrite. Where veinlets contain pyrite, marcasite, and base-metal sulfide minerals, the introduction of base-metal sulfides seems to have caused an inversion of earlier pyrite to marcasite. In general, marcasite is later than the associated pyrite, but the pyrite may have vastly different ages in different places.

#### PRIMARY GANGUE AND ALTERATION MINERALS

##### FLUORITE

Fluorite was recognized at the Hope 3, Sorrel Horse, Big Buck, and Tomato Juice deposits and at an unnamed nonuraniferous copper-fluorite deposit in the extreme SW cor. sec. 2, T. 6 N., R. 14 E., of the McFadden Peak quadrangle. The copper-fluorite deposit is in the Mescal Limestone in a vein that contains bornite and brecciated white fluorite cemented by secondary copper carbonate minerals. This deposit has no obvious relation to the uranium deposits and, so, is not further considered.

The fluorite, which is sparse in the uranium deposits, is dark purple and occurs as narrow veinlets in the radioactive vein zone. It is locally associated with pyrite, the only sulfide mineral seen in the veinlets. No direct association between the fluorite and uraninite is evident, although the enclosing rock is commonly very radioactive. Presumably the deposition of fluorite followed the uranium mineralization, but no direct evidence corroborates this sequence. The association with pyrite, which is commonly a late mineral, tends to indicate later origin.

##### CALCITE

Calcite is a common constituent of fracture fillings at many of the deposits. It also fills vugs in mobilized hornfels, as described on page 36. Nearly all joints and fractures that are accentuated by limonite stain in outcrops of the gray unit of the Dripping Spring contain calcite associated with sparse pyrite where they extend below the zone of weathering.

At the Jon deposit a conspicuous calcite- and pyrite-filled fracture occupies the central part of the uranium vein zone for about 150 feet. Calcite-filled fractures in the central part of the vein zones at other deposits are ordinarily of shorter extent or diverge from the trend of the vein within a few feet.

Calcite-filled fractures transverse to the uranium vein zones are also common. These range in width from about

1 mm to several tens of centimeters in fissure and breccia zones. Near the south end of the Sue mine workings are several fissures filled with calcite and local kaolinite; a vuggy calcite-cemented breccia zone which contains a little pyrite crosses the trend of the vein about 310 feet from the portal of the Hope adit 1. Calcite-filled bedding-plane points are common in the Hope 3 workings.

Much of the calcite that fills fractures in the Dripping Spring may have been derived by leaching of the nearby overlying Mescal Limestone and redeposition from descending meteoric waters (Sharp, 1956, p. 9).

#### ANKERITE

Ankerite occurs in the central fracture of the uranium vein zone at the Tomato Juice and Rock Canyon deposits and in random fractures in the vein zone at the Sorrel Horse and Horse Shoe deposits.

The ankerite at the Tomato Juice and Rock Canyon deposits forms a fine-grained drusy lining about 0.2 mm wide on each wall of the fracture. Where the fracture exceeds 0.4 mm in width, a mosaic of fine equigranular ankerite fills the intervening space. In hand specimen the ankerite is yellow, and in thin section it is predominantly yellow but has local brown-stained areas. Disseminated ankerite saturates much of the wallrock for a few millimeters on either side of the vein filling, and adjacent stylolites are typically ankerite filled. Pyrite in the veinlets and adjacent wallrock is slightly fractured and is obviously earlier than the ankerite.

The ankerite in the Sorrel Horse and Horse Shoe deposits ranges from white to yellow and occupies very narrow veinlets in the radioactive rock. The relation between this ankerite and either sulfide or uranium minerals was not observed. Siderite rather than ankerite was identified in one veinlet at the Sorrel Horse deposit.

All specimens of ankerite and siderite are easily recognized as carbonate minerals in both hand specimen and thin section; however, all identifications for this report were made by X-ray powder methods.

#### PHLOGOPITE

Phlogopite is not a common mineral in the uranium deposits but was recognized in association with high radioactivity in two places. It was entirely unrelated to radioactivity in another.

At the portal of the Little Joe adit 4, phlogopite occurs with limonite in a highly oxidized vein within the radioactive zone. It also occurs in several subparallel similar veins within a few tens of feet south of the portal. This phlogopite is nearly clear except for iron stain and has a very small (-) 2V; the beta and gamma refractive indices are near 1.57.

Phlogopite is abundant in the ore of the Lucky Boy deposit, where it is the major mineral in the core of the uranium-bearing shear zone (fig. 29) and is disseminated as small aggregates in the adjacent altered rock. This phlogopite is biaxial (-) with a 2V of about 5°; the beta and gamma indices are about 1.595; the color is nearly black in hand specimen but pale smoky olive as seen under a microscope. Associated with and probably derived by alteration of the phlogopite is a chlorite similar in properties to delessite. The identity of both the phlogopite and the chlorite was confirmed by X-ray powder diffractometer analysis.

Phlogopite, associated with quartz and chlorite, was identified in spotted rock (fig. 14) at the Big Six deposits. The mica in most spotted rock, however, seems to be muscovite.

Phlogopite was also identified in a diamond-drill core from a hole drilled on the Last Chance claims a few feet north of the Workman Creek road about 2.5 miles from its intersection with the Globe-Young road. This phlogopite appears to be identical in optical properties with that recognized at the Lucky Boy deposit. It cements brecciated weakly metamorphosed siltstone at the top of the Dripping Spring Quartzite. Most is about 15 feet below the collar of the drill hole, at a horizon in the white unit approximately 5 feet below the base of the Mescal Limestone.

#### CHLORITE

Chlorite is the most abundant alteration mineral associated with uraninite. Typically it is a pleochroic green or brown variety and has indices near 1.60 and abnormally high birefringence. In thin section this material has the appearance of nontronitic clay, but samples subjected to X-ray analysis proved to be chlorite. The alteration mineral herein described as chlorite possibly may include a series of minerals which have similar properties that range from those of chlorite to those of nontronite.

The chlorite occurs as decussate aggregates closely associated with both uraninites 1 and 2 and is locally distributed as disseminated blebs and veinlets in the enclosing host rock. It also occurs with sulfide minerals in some places and as aggregates that contain absorbed (?) uranium in others. (See p. 83.)

The chlorites exhibit a considerable range of optical properties. Pleochroism ranges from  $X$  = pale greenish yellow,  $Y$  = green,  $Z$  = deep green; through  $X$  = pale yellow,  $Y$  = yellow green,  $Z$  = brownish green; to  $X$  = pale yellow brown,  $Y$  = greenish brown,  $Z$  = brown. All have positive elongation. Indices range from about 1.57 to 1.62; birefringence generally is about 0.02 to 0.025. Observed interference figures indicate that the chlorite is biaxial (-) and has a moderate 2V.

This chlorite is almost identical in appearance with the nontronite associated with pyrite at the Jon and other deposits.

#### NONTRONITE

Nontronite is associated with sulfide minerals, particularly pyrite, in the Workman Creek area. It occurs alone in narrow veinlets or coats the walls of veinlets containing pyrite and other sulfide minerals. In hand specimen the nontronite is nearly black and has a distinctly slimy feel when wet.

As seen under the microscope, the nontronite is pleochroic green and has a low second-order birefringence. It is distinguishable from the pleochroic green chlorite described above principally by the mode of occurrence of nontronite and a somewhat lower refractive index that ranges from 1.53 to 1.57.

X-ray diffraction patterns of the chlorite and nontronite are very similar, but distinction can be made if the sample is subjected to saturation with ethylene glycol vapor. This shifts the position of a prominent peak on the X-ray pattern significantly if the mineral is nontronite.

#### UNIDENTIFIED CLAY

Much of the uraninite 1 and some of the uraninite 2 is accompanied by an alteration mineral that imparts a dense brown cloudy appearance to the adjacent altered potassium feldspars. The material is presumably a clay, but the grain size is so small that individual grains are not visible in thin section. Although this variety of alteration is typical of the Little Joe, Hope 1, Rock Canyon, and other deposits, we were unable to isolate and identify the mineral.

#### QUARTZ

Quartz is scarce in the uranium deposits. No quartz, other than quartz in the host rock, is directly associated with unaninite in any of the deposits. A few sparse grains of idiomorphic quartz line the walls of sulfide-bearing veinlets in some places. All the sulfide minerals found in these veinlets apparently are later than and are deposited against euhedral faces of this quartz. Molybdenite and pyrrhotite were not observed in association with vein quartz.

The minor amount of quartz found in some of the sulfide-mineral veinlets possibly represents redistribution of the silica derived by the mineralizing solutions in their feeble attack on the wallrock minerals. The general effect of the alteration seems to be one of desilication and the deposition of silica-poor minerals, such as chlorite, nontronite, and sulfide minerals, in the place of feldspar and quartz.

#### SECONDARY MINERALS

Secondary minerals related to the uranium deposits are largely restricted to bedding planes and narrow randomly trending fractures in and near the uranium vein zones. Some of the minerals, particularly limonite, are disseminated in the host rock, but they are either less abundant or less conspicuous than the minerals in the fractures. The apparent concentration of secondary minerals in the fractures suggests considerable redistribution of material by meteoric waters during weathering. On the whole, however, the material probably did not move far, because the secondary uranium minerals are ordinarily much more strongly concentrated in the original uranium vein zone than they are a few feet distant from it.

#### METATORBERNITE

Metatorbernite ( $\text{Cu}(\text{UO}_2)_2(\text{PO}_4)_2 \cdot 8\text{H}_2\text{O}$ ) is the most prevalent secondary uranium mineral and was identified at nearly all the deposits. Generally it is more abundant in the weathered parts of deposits in siltstone than in deposits for which the host rock is hornfels.

The mineral occurs as coatings and as scattered flakes on the surfaces of fractures and bedding planes and more sparingly as a disseminated mineral in the host rock. Tiny rosettes less than 2 mm across and composed of radiating aggregates of crystals are also common.

The metatorbernite ranges in color from pale to dark green, and individual crystals are minute translucent rectangular to square flakes. It is never more than faintly fluorescent in ultraviolet light.

The metatorbernite is associated with limonite, gypsum, hyalite, and, more rarely, kaolinite, malachite, and barite. A crusty vitreous variety of limonite is generally earlier and underlies the metatorbernite flakes, but brown pulverulent limonite is later and stains the metatorbernite in some deposits. Hyalite, where present, is almost invariably later than the metatorbernite and forms films on it, except at the Lucky Boy deposit, where the reverse seems to be true. The paragenetic relations of the metatorbernite with other secondary minerals are less obvious.

#### BASSETITE

Bassetite ( $\text{Fe}(\text{UO}_2)_2(\text{PO}_4)_2 \cdot 8\text{H}_2\text{O}$ ) is a common secondary uranium mineral. It occurs as nonfluorescent flakes of platy to bladed crystals that, at several deposits, form coatings and rosettes as much as 8 mm across on fracture surfaces. Colors generally range from golden brown to greenish brown but locally include pale green. No obvious difference in the X-ray powder patterns of the variously colored varieties was seen.

Bassetite commonly forms crystals mixed with saléeite. These occur either as apparently homogeneous flakes that show faint fluorescence and give an X-ray pattern for both species or as rectangular flakes in which saléeite forms a narrow rim that is gradational into the bassetite core. At the Sue mine some homogeneous-appearing bassetite-saléeite crystals had narrow rims of metanovacekite (described below).

Bassetite is rarely associated with any secondary minerals other than limonite and the platy uranium minerals. It is evidently later than some of the limonite and may be earlier than the saléeite and metanovacekite that form rims around it.

#### METANOVACEKITE

One specimen from the Sue mine yielded a mineral whose X-ray powder pattern was determined to be that of metanovacekite ( $Mg(UO_2)_2(AsO_4)_2 \cdot 8H_2O$ ). The mineral is pale yellowish green and platy and has a strong green fluorescence. It rarely occurs as individual flakes but forms rims 0.2–0.5 mm wide on mixed bassetite-saléeite crystals. The position of metanovacekite suggests that it is later than and has marginally replaced the bassetite-saléeite crystals; its relation to other minerals, however, was not observed.

#### SALÉEITE

Saléeite ( $Mg(UO_2)_2(PO_4)_2 \cdot 8H_2O$ ) was identified at several of the deposits but is nowhere abundant. It occurs on fracture surfaces as platy rectangular crystals that form coatings, books, and rare small rosettes less than 8 mm across.

Saléeite ranges in color from yellow through pale greenish yellow to pale apple green and in fluorescence from green through pale yellow to nonfluorescent. Megascopically it cannot be distinguished from meta-autunite.

Saléeite is associated with bassetite as mixed crystals and as rims on flakes that have bassetite cores. It is also associated with gypsum and kaolinite and commonly coats limonite.

#### META-AUTUNITE

Meta-autunite ( $Ca(UO_2)_2(PO_4)_2 \cdot nH_2O$ ) was identified only at the Sue, Red Bluff, and Little Joe deposits, where it occurs in much the same manner as the other hydrated uranium phosphate minerals. It is a platy translucent yellow mineral that has a strong greenish-yellow fluorescence. It is most common on the surfaces of bedding planes and apparently is later than limonite.

Meta-autunite was originally identified as uranocircite (Granger and Raup, 1959), but careful measurement of the X-ray powder patterns established its true identity. The possibility of an error in our original iden-

tifications was first pointed out by Alice Weeks (oral commun., 1958); this error was later confirmed by Daphne Ross (written commun., 1958).

Admixed with meta-autunite and other secondary minerals at the Sue mine is a mineral that may be hydrogen autunite. Positive identification could not be established (Daphne Ross, written commun., 1958).

#### SODIUM ANALOG OF ZIPPEITE

The sodium analog of zippeite, hydrated sodium uranyl sulfate (?), was found in only one specimen from the Sue mine. It occurs as a yellow powdery coating on bassetite and saléeite and has a faint greenish-yellow fluorescence. First identified as beta-zippeite, its correct identity was pointed out by Daphne Ross (written commun., 1958).

#### METAZEUNERITE

Metazeunerite ( $Cu(UO_2)_2(AsO_4)_2 \cdot 8H_2O$ ) was found only at the Easy deposit. It forms apple-green, translucent to nearly opaque flakes that coat limonite-covered fractures surfaces. Some specimens fluoresce green; others are nonfluorescent. It is evidently later than limonite but is locally coated with hyalite.

#### URANOPHANE AND BETA-URANOPHANE

Uranophane and beta-uranophane ( $Ca(UO_2)_2(SiO_3)_2(OH)_2 \cdot 5H_2O$ ) are dimorphous and are described together. Specimens of uranophane identified by X-ray methods were found at the Fairview, Little Joe, and Red Bluff deposits; those of beta-uranophane identified by X-ray were found at the Red Bluff, Lucky Stop, and Hope deposits. Much of the material identified as uranophane in the field is probably beta-uranophane.

Both uranophane and beta-uranophane are bright-lemon-yellow minerals that have no fluorescence. The uranophane tends to form small radiating clusters of needles (resembling minute yellow pincushions) attached to the surface of a limonite- or hyalite-coated fracture. Open spaces, therefore, seem to be favorable for the growth of this mineral. The beta-uranophane, on the other hand, generally forms dense yellow crusts and fillings in fractures. Locally, beta-uranophane, bordered by thin layers of limonite, completely fills a narrow fracture. Under magnification, it is generally seen to be made up of a dense matte of fine acicular crystals.

One specimen from the Red Bluff deposit gave an X-ray powder pattern that matches a standard pattern (D-1532) of the U.S. Geological Survey that has been tentatively identified as the pattern of potassium-uranophane. The specimen seems to have the same habit as ordinary uranophane and is megascopically indistinguishable from it.

Both uranophane and beta-uranophane are later than much of the limonite. Uranophane and potassium uranophane are later than hyalite, but no relations between beta-uranophane and hyalite were noted.

#### HYALITE

Fluorescent hyalite (opal) is commonly associated with other secondary minerals at several of the deposits. The fluorescence of hyalite is generally considered to be caused by uranyl ions held in some way by the hyalite structure, and hence the mineral can be termed "uranium bearing."

The hyalite occurs on fracture surfaces as thin botryoidal crusts less than 1 mm thick. Most of it is glassy and colorless, but varieties range from milky white to fluorescent green. The glassy varieties in particular are shattered by syneresis cracks. The fluorescence of hyalite under ultraviolet light ranges from pale yellow green to brilliant green, and is perhaps dependent on the uranium content.

Hyalite was deposited on and is later than most varieties of crusty or vitreous limonite, but it is earlier than some of the pulverulent limonite. Except at the Lucky Boy deposit, it coats and is later than all the platy uranium phosphate and arsenate minerals. Uranophane, however, is deposited over and is later than the hyalite crusts.

#### LIMONITE AND GEOTHITE

Limonite, the general term applied to hydrous iron oxides that have not been positively identified as either goethite or lepidocrocite, is present in the weathered parts of all the uranium deposits, and occurs in a wide variety of forms. It commonly is concentrated in veinlets with other secondary minerals, but it also occurs disseminated throughout rock that is strongly weathered. Its anhydrous equivalent, hematite, is locally present, but ordinarily is not nearly so abundant as limonite.

One of the earliest forms of limonite is a boxwork type that is partly pseudomorphous after the original sulfide minerals in veinlets. This form is, however, fairly rare. A later, but still an early form, is a variety that forms thin vitreous and commonly iridescent films on fracture surfaces. This type ranges from orange brown to nearly black; in some places it has a botryoidal surface. Most other secondary minerals are later than this form of limonite.

The latest type of limonite generally forms brown, orange, or red pulverulent layers or stains on the surfaces of the earlier secondary minerals. Presumably it still is being formed and redistributed in the near-surface parts of deposits.

The most common types of limonite described above do not include all the forms recognized at the various deposits. Several minerals believed to be aberrant forms

were X-rayed, but none of the X-ray patterns matched any known standards. Probably many complex hydrous iron, manganese, and copper oxides that superficially appear to be a form of limonite occur in the deposits.

#### CHRYSOCOLLA

Chrysocolla was recognized only at the Cataract and Alta Vista deposits. At the Cataract deposit it forms pale-blue-green rosettes, as much as 10 mm across, of radiating crystals and occurs as amorphous-appearing to faintly crystalline appearing layers on fracture surfaces. A few apple-green crystals of malachite are disseminated near the centers of some of the rosettes.

Chrysocolla at the Alta Vista is sparingly present in random fractures that are a few feet away from the fracture that marks the center of the radioactive vein zone.

#### HEMIMORPHITE

Hemimorphite ( $\text{H}_2\text{ZnSiO}_5$ ) was identified, by X-ray, only from the Horse Shoe deposit, where it occurs sparingly as a thin white crust on fracture surfaces.

#### MALACHITE AND AZURITE

Malachite and azurite occur at several deposits, but malachite is much the more prevalent. Azurite was not found at some deposits. Both occur as thin sporadic layers and stains on fracture and bedding-plane surfaces. Ordinarily neither is closely associated with strongly radioactive rock or with uranium-bearing minerals, although both are present in the general zone of the radioactive vein.

Both azurite and malachite probably were derived from oxidized copper sulfide minerals, but they must have been transported some distance from the primary copper minerals, because they do not ordinarily pseudomorph or coat the primary minerals.

#### BARITE

Barite was identified by X-ray only from the Sky deposit but was tentatively identified by U.S. Atomic Energy Commission geologists at the Lucky Stop deposit. Perhaps it was overlooked in other places. The barite at the Sky deposit forms thin yellow to colorless flakes associated with metatorbernite on fracture and bedding-plane surfaces. Megascopically it has an appearance nearly identical with that of gypsum in the Lucky Stop deposit.

#### GYPSUM

Gypsum is very common although not abundant in the weathered parts of many deposits. It occurs as scattered thin transparent rectangular plates or as continuous coatings of selenite associated with most of the other secondary minerals on fracture surfaces. It is

definitely later than most limonite, but its paragenetic relation to the other secondary minerals is not known. At the Roxy deposit, it seems to be nearly contemporaneous with metatorbernite.

#### JAROSITE

This mineral may be much more prevalent than is indicated in table 6, as it is easily overlooked in highly limonitic rocks. Jarosite from the Little Joe deposit was identified by X-ray; a specimen from the Shepp 2 deposit was identified in thin section. Elsewhere it was tentatively identified in hand specimens. A closely related mineral, carphosiderite, was identified by X-ray in a specimen from the Black Brush adit and is here included with jarosite.

Most of the jarosite and the carphosiderite form yellow crusts or pulverulent coatings on fracture surfaces and are associated with limonite and locally with gypsum. Thin sections cut across the boundary between weathered and unweathered pyrite-bearing rock locally contain a jarosite-rich zone between the pyrite-bearing and the strongly limonitic rock. Fracture coatings of jarosite commonly are overlain in places by limonite. This evidence suggests that jarosite, which is formed by oxidation of pyrite, precedes the formation of limonite. Probably moderate weathering of pyrite results in jarosite, whereas strong weathering produces limonite.

#### COPIAPITE

Copiapite ( $2\text{Fe}_2\text{O}_3 \cdot 5\text{SO}_3 \cdot 18\text{H}_2\text{O}$ ) was identified only at the First Chance mine, where it occurs as a pale-greenish-yellow to orange powdery to crusty efflorescent mineral on the mine walls. At many other mines, however, a yellow-tinged sulfate mineral that may be copiapite is mixed with white and blue sulfate minerals. This yellowish mineral is much less abundant than the white sulfate minerals.

#### CHALCANTHITE

Chalcantite ( $\text{CuSO}_4 \cdot 5\text{H}_2\text{O}$ ) formed generally thin powdery efflorescent incrustations on the walls of several of the mines within a few months after mining. It is largely restricted to the near-surface walls in moderately to strongly weathered rock. Possibly chalcantite eventually will be recognizable on the walls of all the mines, but by mid-1957 it had been found only in the Donna Lee, First Chance, Little Joe, and Shepp No. 2 mines.

Probably because of variable admixtures of white iron sulfate minerals, the chalcantite appears to range from nearly white to deep translucent blue. The coatings of chalcantite are variously pulverulent, botryoidal, drusy, and fibrous.

#### UNIDENTIFIED WHITE SULFATE MINERALS

White and pale-colored sulfate minerals form efflorescent coatings on the walls of many of the mines and also occur in fractures and on bedding planes in the most highly weathered rocks. They are also common on many outcrops of the gray unit of the Dripping Spring where the outcrops are protected from rain.

At several of the uranium deposits the outcrops of certain strata are covered with a fine network of white sulfate minerals that marks a system of random fractures in the rock.

Most of the predominantly white sulfate minerals have not been identified because their X-ray patterns do not match known standard patterns. Some, however, seem to be closely related to certain sulfate-mineral groups. A yellow to white magnesium-rich sulfate mineral of the melanterite group has been recognized at Red Bluff. White to pink and yellow efflorescences of the pickeringite-halotrichite group were found at the Ancient deposit in the Mescal Limestone in Pueblo Canyon (McFadden Peak quadrangle) and in alcoves of cliff faces in the Dripping Spring near the Rock Canyon deposit. They may also be present in some of the mines in the Dripping Spring.

Presumably the sulfate ion for the formation of these minerals is derived under weathering conditions from the oxidation of sulfide minerals, principally pyrite. The metallic ions—calcium, magnesium, iron, aluminum, and others—are derived both from the sulfide and carbonate minerals and from strongly weathered rock-forming minerals.

#### KAOLINITE

Kaolinite occurs sporadically in fractures at several deposits. It forms dense white pulverulent coatings, fillings, and aggregates on limonite-covered fracture surfaces. It is both earlier than and later than the crusty and vitreous forms of limonite, but it is commonly stained, and its identity may locally be obscured by later pulverulent limonite. Kaolinite generally occurs separately from the uranium minerals, and no paragenetic relations with them were found.

#### PARAGENETIC SEQUENCE OF PRIMARY MINERALS

Evidence from which to establish a paragenetic sequence of primary minerals in the ore deposits is fragmentary at all deposits. Either certain minerals are not present or they are not in contact with one another so that relations may be observed.

Evidence from two or more deposits is commonly conflicting. For example, pyrite apparently precedes chalcopyrite in some deposits and succeeds it in others; the base-metal sulfide minerals have different relations to each other in different deposits. Different sources for the

same minerals also account for some of the discrepancies: pyrite and marcasite both were introduced from an outside source and were derived by decomposition of pyrrhotite; chalcopyrite was both introduced separately and derived by exsolution from sphalerite; galena was in part introduced as normal lead sulfide and in part derived from radiogenic lead in the associated uraninite.

We have attempted to reconstruct the paragenetic sequence from these inadequate data, and the results are shown in figure 50.

#### ORE DEPOSITION

##### EMPLACEMENT CONTROLS

All the deposits known to contain primary uranium minerals are in the gray unit of the upper member of the Dripping Spring Quartzite. Uranium-bearing solutions probably were not restricted to this unit, nor were they denied access to the other rocks, so the unit must have possessed properties that made it susceptible to mineralization. Factors to be considered that could contribute to susceptibility are geologic structure, mineralogy and chemical composition, and permeability. As no quantitative data are available on permeability, that factor cannot be adequately evaluated, but no significant differences between the permeabilities of the gray unit and enclosing rocks were revealed by this study. Also, if simple reduction of pressure or temperature in the ore-bearing solutions were a significant localizing control, deposits should be present in rocks other than the upper member of the Dripping Spring. Structure, mineralogy,

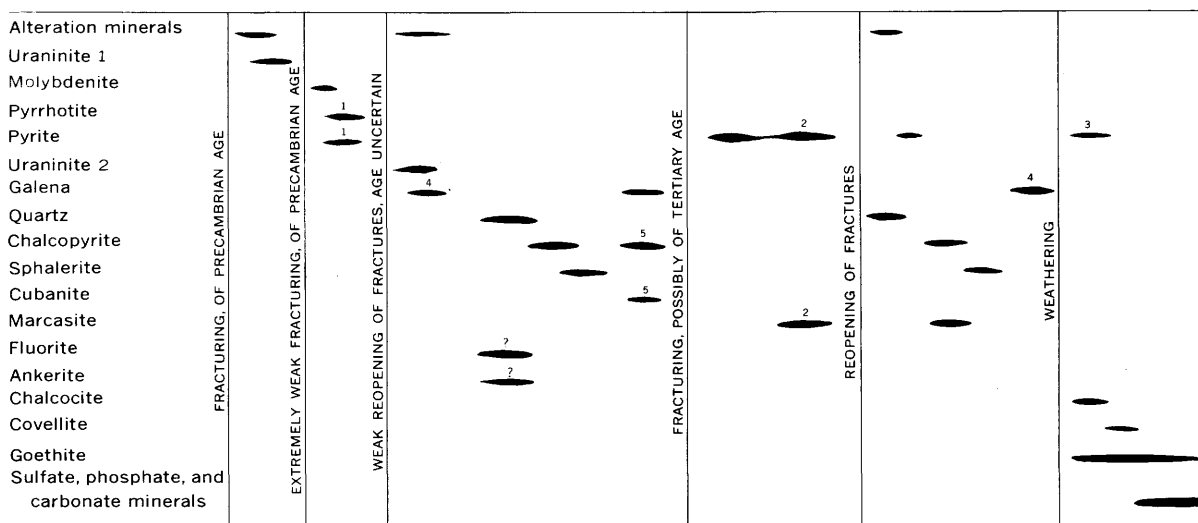
and chemical composition of the gray unit remain as the major possible controlling factors in emplacement.

##### STRUCTURAL CONTROL

As most of the uranium-bearing ore bodies have a tabular shape transverse to the stratification, structural features must have been important in localizing ore. Specific characteristics of these structures are obscured, however, by lack of mineral filling in the original structure and by strong joints formed subsequent to the mineralization. To determine which fracture or fractures guided the flow of the original mineralizing solutions is, therefore, generally difficult and commonly not possible.

In some of the mines the center of the uranium vein zone is defined by an obvious fracture. Where this fracture marks the plane of highest radioactivity in the mine it can be assumed that the uranium was carried by and distributed from solutions which traversed the fracture. In mines in which this central fracture can be identified it has certain characteristics that relate it to the ore body and distinguish it from other joints that are invariably present. These characteristics are described on page 48 under "Tension joints." It should be reemphasized here that the term "tension joint" is not necessarily to be construed as a genetic term.

No tension joints have been recognized in rocks other than the gray unit. This may not be surprising in view of their poor definition, even where mineralized. It may, however, be significant. Possibly the fairly high competence of the gray unit, particularly where metamorphosed, permitted the development of tension joints, whereas the low competence of other rocks did not.



<sup>1</sup> Pyrrhotite formed in hornfels and related host rock, pyrite in remainder

<sup>2</sup> Derived by decomposition of pyrrhotite

<sup>3</sup> Supergene

<sup>4</sup> Radiogenic lead in part

<sup>5</sup> Exsolved

FIGURE 50.—Paragenetic sequence of mineral deposition in uranium deposits in the Dripping Spring Quartzite.

#### MINERALOGY AND CHEMICAL COMPOSITION

Certain properties of a favorable host rock that is carrying mineralizing solutions may ultimately result in saturation or supersaturation of the solutions either by increasing the concentration or by lowering the solubility of the ore minerals in the solutions and thus causing precipitation. Chemical composition of wallrocks commonly has such an effect.

The mineralogy and chemical composition of the gray facies were probably the primary factors in causing the precipitation and localization of uranium and many of the sulfide minerals in the deposits in the Dripping Spring Quartzite. The gray facies differs in mineral and chemical composition from the adjacent rocks in three ways: it has an abnormally high potassium feldspar content, an abnormally high carbon content, and a relatively high sulfide mineral content. Of these, the potassium feldspar content seems least likely to have effected precipitation. Although less abundant than in the gray unit, potassium feldspar is certainly common in the rocks above and below that unit. In addition, the chemistry of potassium feldspar should have no effect on the precipitation of uranium or sulfide minerals. This is particularly true in environments such as this, where the mineralizing solutions have not strongly reacted with or altered the feldspars.

The carbon and sulfide-mineral contents of the gray facies, therefore, are probably the major factors that effected precipitation of vein minerals, but the abundance of carbon and sulfide minerals varies considerably from place to place. Also, evidence shows that the carbon content is low where the uranium content is highest. This seems to be incompatible with any thesis linking uranium precipitation to carbon and sulfide minerals except for the reasons that follow.

The gray unit prior to uranium mineralization likely was similar in most respects to the gray unit as it is today. It was probably a rock containing a small but significant amount of organic carbon or carbon compounds that varied in concentration from place to place. Rocks that contain appreciable amounts of organic carbon generally contain disseminated biogenic iron sulfide because of the conditions under which the rocks were deposited. The gray unit, therefore, may be inferred to have contained both organic carbon (or carbon compounds) and iron sulfide. Elemental carbon is generally considered to be nearly inert, and its effect on the Eh of any solution in rock is not well known; however, many organic carbon compounds are very active chemically, and certainly finely divided iron sulfide can impose an environment that is low in Eh.

Uranium probably exists in the oxidized state,  $U^{+6}$ , in a hydrothermal solution and would have to be re-

duced to precipitate as  $UO_2$ . This reduction could take place at the expense of carbon, hydrocarbons, or sulfide compounds. Hydrogen sulfide is probably the most efficient among these reducing agents, but at elevated temperatures sulfide minerals are also effective. In the deposits in the Dripping Spring, nothing suggests that  $U^{+6}$  was reduced at the expense of sulfide minerals; in fact, the early position of uraninite in the depositional sequence precludes most sulfide minerals as the instrumental reducing agents. Although there is a lack of correlation between uranium and sulfur in the samples that were analyzed (fig. 47), the observed association between uraninite and sulfide minerals suggests that sulfur may have been present in the uranium-bearing solutions. The negative correlation between uranium and organic carbon (fig. 47), however, leads us to believe that at the specific sites of uranium deposition some carbon was used up in an oxidation-reduction reaction. Possibly both carbon compounds and hydrogen sulfide had some control over the precipitation of uraninite.

#### COMPONENTS OF THE ORE-FORMING FLUIDS

Comparisons of chemical and semiquantitative spectrographic analyses of samples taken within and at some distance from uranium-bearing deposits indicate that several elements are concentrated in the uranium veins. From these data alone, reconstruction of the composition of the mineralizing solution or solutions is not possible, but at least qualitative identification of some of the elements transported by the solutions should be possible.

Figures 32-36 shows analyses of sequences of channel samples across uranium-bearing vein zones. The graphs and tables show that the contents of certain elements correlate with the concentration of uranium in the veins. This correlation does not necessarily mean that the solutions that introduced the uranium also introduced the other elements. It does indicate, however, that if there were more than one solution, these solutions tended to follow approximately the same channelways, and that the wallrock conditions conducive to deposition of uranium were also favorable for deposition of the correlative elements.

Generally the contents of nonferrous base metals, silver, beryllium, and the rare earths tend to correlate positively with the content of uranium. Iron and magnesium generally correlate with uranium but are independent to the extent that they show a negative correlation in some places. Magnesium concentrations very likely correlate with the abundance of alteration and gangue minerals, such as chlorite and phlogopite. The graphs of selected elements at the Tomato Juice and Lucky Stop deposits suggest that nickel and cobalt are

more closely related to iron concentration than to uranium concentration. This relation is supported by semi-quantitative spectrographic analysis (p. 86) of a pure pyrrhotite sample from the Workman deposit which contained more nickel and cobalt than did any other sample analyzed. Apparently the nickel and cobalt are contained largely in the iron sulfide minerals.

Copper has an inconstant relation to uranium, although it generally shows a positive correlation. Lead shows the most obvious positive correlation to uranium, owing at least partly to significant amounts of radiogenic lead.

The relations between concentrations of uranium, molybdenum, and chromium are noteworthy. In some deposits they are positive correlations; in others, negative. At no place does chromium show a large increment or depletion over its content in unmineralized rock, and possibly the variations in chromium content largely reflect leaching and redistribution along the vein zone by the mineralizing solutions. The molybdenum, however, shows a strong correlation with uranium when all samples are plotted as a scatter diagram (fig. 47). In general, molybdenum is concentrated in uranium vein zones but is depleted in the central part of the veins, where uranium is concentrated the most.

Tin was detected only in the samples from the Tomato Juice deposit, but there a close correlation existed between it and uranium. Thus, the extremely fine grained anisotropic mineral intergrown with uraninite at this deposit may be cassiterite.

Sodium shows a distinct correlation with uranium in some of the deposits, but it is positive in some and negative in others. Oddly, sodium and barium tend to correlate with each other.

Calcium and manganese are similar to sodium in that they have no consistent correlation with uranium; moreover, there is no consistent correlation among these elements. The calcium content is probably dependent in large part on the amount of calcite in the rock.

Sulfur tends to correlate closely with iron and no doubt reflects in large part the iron sulfide content of the rock and to a lesser extent the base-metal sulfide minerals.

The analyses suggest that more than one mineralizing solution may have passed through some of the uranium vein zones. Possibly the iron, nickel, and cobalt mineralization was not entirely related to nor contemporaneous with the uranium mineralization. In like manner the copper, lead, and zinc may have been supplied in part by different mineralizing solutions. The paragenetic sequence in which some of the uranium, iron, and base-metal minerals are separated by periods of fracturing suggests that this may be true.

The mineralizing processes concentrated the following elements in some of the vein zones (the elements in boldface are those that show positive correlation with uranium in all vein zones in which they were sufficiently abundant to determine by the methods employed): Ag, Ba, **Be**, Ca, **Ce**, Co, Cr, Cu, **Dy**, Er, Fe, Ga, Gd, La, Mg, Mo, Mn, Na, Ni, Nd, Pb, Pr, S, Sc, Sm, Sn, Sr, Y, **Yb**, Zr. The mineralizing solutions probably contained the elements in boldface and at least redistributed the remainder.

#### FACTORS THAT DETERMINED THE MINERALOGY SPATIAL RELATION TO DIABASE

The primary mineralogy of the uranium deposits is dependent in part on the position of the deposit relative to diabase and in part on the size of the diabase body. Uraninite has not been recognized in the uranium deposits that occur more than about 300 feet from diabase; in these deposits chlorite or nontronite seems to be the predominant uranium-bearing mineral. Uraninite 1 and uraninite 2 are probably restricted to a closer spatial relation to diabase than is uraninite 3. Pyrrhotite and molybdenite also are restricted to deposits near diabase.

The controlling influence of the size of the diabase body is indicated by the presence of uraninite, pyrrhotite, or molybdenite near such large bodies as the nearly 1,000-foot-thick Sierra Ancha diabase sheet. Deposits near thin sills or dikes of diabase are not known to contain these minerals.

#### TYPE OF HOST ROCK

The nature of the host rock evidently has some effect on the mineralogy of the uranium deposits. The host rocks range from siltstone through partly recrystallized siltstone, hornfels, and coarse-grained hornfels to mobilized hornfels, depending on the effects of diabase intrusion. This suggests, therefore, that the variation of mineralogy of the deposits is more directly dependent on the diabase than on the host rock.

Where siltstone is the host rock, no pyrrhotite, molybdenite, uraninite 1, or uraninite 2 were recognized. Uraninite 3 was recognized at the Red Bluff, Tomato Juice, and Rock Canyon deposits, where minor recrystallization of the host rock has taken place. All these minerals were found in normal hornfels, however. Coarse-grained hornfels, conversely, is seemingly a poor host for uraninite 2 and uraninite 3. Mobilized hornfels is a very good host for the sulfide minerals, but only rarely does it contain uraninite.

The mineral assemblage of deposits in various host rocks may be a function of both the relation of deposit to diabase and the carbon content of host rocks. In general, the siltstone host rocks contain a significant amount

of carbon—enough to impart a gray color; the coarse-grained hornfels apparently has retained much carbon only locally, and the mobilized hornfels is almost devoid of it.

The secondary minerals also seem to be controlled in part by the nature of the host rock. The platy uranate minerals and opal are generally much more prevalent than the uranophane minerals in the weathered parts of deposits in siltstone host rocks; the reverse is ordinarily true for deposits in hornfels.

#### WEATHERING

Weathering has a pronounced effect on the mineralogy of near-surface parts of uranium deposits. Sulfide minerals and uraninite are destroyed in strongly weathered rock. Chalcopyrite, for example, alters initially to chalcocite and covellite; these in turn alter to chrysocolla or malachite and azurite in some environments and to chalcanthite in others. Uraninite alters to hydrous uranium silicates, phosphates, arsenates, and sulfates, and to hyalite. The iron-bearing sulfide minerals weather to limonite or to efflorescent iron-bearing sulfate minerals.

The gangue minerals, with the exception of the carbonates, remain unaltered the longest under weathering conditions. Quartz, chlorite, and, more rarely, fluorite may be found in parts of the deposits where sulfide minerals and uraninite have been destroyed.

#### TEMPERATURE OF DEPOSITION

For several reasons we believe that the uranium deposits were emplaced at a high temperature. The probability that the uranium was deposited during late stages of diabase cooling suggests that the surrounding rocks were hot at the time of introduction of the mineralizing solutions. The presence in the deposits of well-crystallized molybdenite and pyrrhotite, as well as cubanite exsolved from chalcopyrite and chalcopyrite exsolved from sphalerite, probably indicates a high-temperature origin. Idiomorphic grains of uraninite also attest to a high-temperature origin, as nearly all the well-crystallized uraninite, worldwide, has been found in pegmatites or in hydrothermal deposits with a high-temperature mineral assemblage.

Kullerud (1953) proposed that the iron content of sphalerite can be used as an index of the temperature of deposition. His studies suggested that zinc sulfide forming in the presence of excess available iron will form a zinc sulfide-iron sulfide solid solution in which the proportion of iron varies with temperature. He reasoned that the occurrence of pyrrhotite, and possibly of pyrite associated with sphalerite, can be taken as evidence that the sphalerite formed in an environment of excess iron.

Arnold (1962) suggested that the iron content of pyrrhotite also can be used as a geothermometer, provided the pyrrhotite coexisted with pyrite in equilibrium at the time of formation. It must be assumed that the composition has not changed since that time.

More recently, Barton and Toulmin (1964) showed that the composition of ferroan sphalerite depends on the chemical potential of sulfur in the system but stated, "uncertainties in extrapolation of the phase relations \* \* \* do not yet permit quantitative geothermometry below 580° C." Perhaps, also, use of pyrrhotite as a geothermometer has not yet been adequately investigated to yield quantitative results.

Because of the uncertainties in the use of sphalerite and pyrrhotite in geothermometry, the following data are presented for information only. The temperatures postulated should not necessarily be construed as the temperatures of formation of the deposits in the Dripping Spring.

Sample 115G56 consists of sphalerite from a bedding-plane fault at its intersection with the uranium vein in the Jon adit. The sphalerite occurs as blebs less than 5 mm across embedded in green altered fault gouge composed of feldspar, hornblende, and chlorite. Abundant fine-grained pyrite is disseminated in the gouge, and some of the sphalerite blebs are cut by minute veinlets of pyrite and calcite. Disseminated pyrrhotite is abundant in the enclosing rocks, but none was recognized in the gouge.

Sample 131G56 consists of pyrrhotite and sphalerite from a vug in mobilized hornfels within the uranium vein zone in the Hope adit 1. The sphalerite in the specimen partly fills the spaces between pyrrhotite crystals that locally line the walls of the vug; narrow veinlets of chalcopyrite cut the sphalerite. The central cavity in the vug is partly filled with a fine-grained porous green aggregate of pyroxene and chlorite.

A partial chemical and spectrographic analysis of sample 115G56 is shown in table 7. Kullerud (1953) showed that small amounts of manganese sulfide and cadmium sulfide have a negligible effect on the solubility of iron sulfide in sphalerite. He assumed that copper was in the form of chalcopyrite, and he corrected the iron content accordingly. Toulmin (1960) found, however, that a small amount of copper sulfide is soluble in sphalerite, although it has little effect on iron sulfide solubility. We therefore made no corrections for manganese, cadmium, or copper in sample 115G56 and used only the iron-zinc sulfide relation to find the temperature of formation, about 430°C at 1 atmosphere, according to the method proposed by Kullerud (1953).

The proportion of iron sulfide dissolved in sphalerite can also be found by the following relation (Skinner, 1961):

$$a_o = 5.4093 + 0.000456X + 0.00424Y + 0.00202Z$$

where  $a_o$  is the unit-cell edge, in angstrom units, and  $X$ ,  $Y$ , and  $Z$  are the iron, cadmium, and manganese sulfide contents, respectively, in mol percent. This relationship is an expression of the observation that these sulfides all cause an increase in the unit-cell dimensions of sphalerite (Kullerud, 1953; Skinner, 1961). Toulmin (1960) found that copper sulfide decreases the unit cell of ferroan sphalerites, but we do not know the magnitude of this effect and have ignored it in the following discussion on the assumption that the effect is negligible.

The unit-cell dimensions of sphalerite samples 115G56 and 131G56 were measured by an X-ray diffractometer using nickel-filtered  $\text{Cu}_{\kappa_1}$  radiation. The powdered samples were placed in aluminum holders with HCl-washed quartz from an unknown source as an internal standard. Sphalerite peaks were measured to a tolerance of  $\pm 0.02^\circ 2\theta$  relative to the (101), (211), and (310) quartz peaks. From these measurements a least-squares refinement of cell parameters was programmed by D. E. Appleman for analysis by the U.S. Geological Survey's B220 computer. The results are shown in table 8.

The unit-cell dimensions of sample 115G56 calculated from the compositional relation shown above (Skinner, 1961) are  $a_o = 5.4170$ ; this compares quite favorably with the calculated unit cell,  $a_o = 5.41685$ , derived from the X-ray measurements.

Sample 131G56 was not chemically or spectrographically analyzed, but if its cadmium sulfide and manganese sulfide contents can be assumed to be similar to those of sample 115G56, its unit-cell dimensions indicate that it contains approximately 16.2 mol percent iron sulfide. This corresponds to a temperature of deposition of about  $475^\circ\text{C}$ , according to the method proposed by Kullerud (1953).

Arnold (1962) demonstrated that the  $d$ -spacing of the (102) peak of pyrrhotite is dependent on the iron plus nickel, cobalt, and copper content and that, if the pyrrhotite formed in equilibrium with pyrite, the metal content of the pyrrhotite would be dependent on the temperature of formation. The position of the (102) peak of pyrrhotite associated with sphalerite in sample 131G56 was measured by the same procedure described above, except that silicon (220) was used as an internal standard. The  $d(102)$   $\text{\AA} = 2.0678$  value for the pyrrhotite corresponds to about 47.6 atomic percent iron, nickel, cobalt, and copper combined. Such a large proportion of metals places this pyrrhotite completely out-

side the experimental limits of Arnold's (1962) studies and suggests that the pyrrhotite formed below  $325^\circ\text{C}$ . Because no pyrite was found in the sample, however, the pyrrhotite may not have formed under the equilibrium conditions specified in Arnold's studies, and it could have formed at a much higher temperature. It should be noted, for example, that Arnold was able to prepare pyrite-free pyrrhotite with approximately the same  $d(102)$   $\text{\AA}$  values as those of sample 131G56 at temperatures of  $402^\circ$ ,  $600^\circ$ , and  $800^\circ\text{C}$ .

Probably the only significant conclusion that can be drawn from this study is that all the data suggest temperatures of deposition of several hundred degrees Celsius. We would not want to speculate further in view of the questionable reliability of the methods used.

TABLE 7.—Analyses, in percent, of sphalerite, sample 115G56, Jon adit

[Chemical analyses: total Fe by E. C. Mallory, Zn by W. D. Goss, Cu by D. L. Skinner total S by W. D. Goss. Semiquantitative analyses: J. C. Hamilton]

Chemical analyses		Mg	.007
Fe	7.97	Ca	.07
Zn	54.98	Ag	.00015
Cu	.12	Ba	.0003
S	32.70	Cd	.15
Semiquantitative spectrographic analyses		Co	.015
Si	0.15	Ga	.0015
Al	.007	Sn	.003
		Mn	.15

TABLE 8.—X-ray data and unit-cell edge ( $a_o$ ) of sphalerite

Jon adit Sample 115G56 $a_o = 5.4168552^1$			Lucky Stop adit 2 Sample 131G56 $a_o = 5.4177896^1$		
$d(\text{\AA})$ observed	$d(\text{\AA})$ calculated <sup>1</sup>	Intensity	$d(\text{\AA})$ observed	$d(\text{\AA})$ calculated <sup>1</sup>	Intensity
3.128073	3.127423	100	3.125926	3.127962	100
2.709607	2.708428	12	2.704831	2.708895	9
1.913631	1.915148	60	1.914011	1.915478	72
1.613577	1.633243	44	1.632375	1.633525	32
1.562756	1.563711	2	1.563720	1.563981	2
1.353709	1.354214	6	1.353197	1.354447	4
1.242644	1.242712	12	1.242507	1.242926	11
1.211577	1.211246	1	1.211064	1.211455	2
1.105626	1.105711	10	1.105427	1.105902	11
1.042143	1.042474	6	1.042143	1.042654	7
.957637	.957574	4	.957328	.957739	4
.915677	.915616	8	.915472	.915774	7
.856436	.856480	6	.856254	.856628	4
.825994	.820063	4	.825771	.826205	3
.781893	.781856	3	.782217	.781991	2

<sup>1</sup> Determined by D. E. Appleman.

#### ORIGIN OF THE DEPOSITS

We propose that the uranium in deposits in the Dripping Spring Quartzite was provided by the diabase magma and was concentrated during the crystallization of the diabase (Nuerburg and Granger, 1960) and then emplaced in carbon-rich siltstone of the gray unit late in the cooling history of the diabase. Other hypotheses were considered but were rejected as unsupportable.

Some data seemingly indicate an age of ore deposition other than contemporaneous with the emplacement of diabase. For example, uranium-bearing veins at the Hope 1, Workman 1, and Red Bluff properties end abruptly at contacts with diabase dikes and sills, as though the diabase had cut them. The basalt of the Apache Group is the only known prediabase igneous rock that can be related to a deep-seated source for the uranium, but we can find no relation between the basalt and the uranium deposits. Furthermore, no relation exists between the deposits and the structural elements that could have been channelways for solutions from some unknown source.

Age determinations on the uraninite prove that it was deposited long before the major metalogenic epochs of late Mesozoic and Cenozoic age in southern Arizona. Some base-metal sulfide minerals in the uranium deposits, in the Dripping Spring particularly those associated with minor amounts of vein quartz, possibly are related to these later periods of metalization, but most of them probably were deposited with uranium during the general period of diabase intrusion. Silification, sericitization, and argillic alteration of the wall-rocks are pervasive characteristics of the later periods of metalization in southern Arizona, and these features are notably absent from the deposits in the Dripping Spring.

Also rejected, but not so readily, is the hypothesis that the uranium was syngenetic in the sedimentary rocks and was redistributed at the time of diabase intrusion. The black facies of the Dripping Spring contains about 2-5 ppm uranium, which, if concentrated, would be adequate to form many ore bodies of the size known to occur. If only 1 ppm were removed from a block of black facies 100 feet by 1,000 feet by 1,000 feet and concentrated along a fracture, it could yield an ore body that would contain approximately 4,250 tons of ore with an average grade of 0.2 percent  $U_3O_8$ .

If solutions were funneled into dilatant zones by some process of lateral secretion, they would likely form fracture fillings instead of being distributed largely in the wallrock as though forced outward from the fractures by considerable pressure. Such readily mobilized gangue minerals as quartz also might be expected, but they rarely occur, in association with uraninite. No evidence was found to suggest that rocks near the ore bodies were depleted in uranium, as might be expected if syngenetic uranium had been mobilized and concentrated. In fact, coarse-grained hornfels host rock in the Workman Creek area seems to be generally richer in uranium than its unmetamorphosed equivalent.

Williams (1957) proposed that the diabase magma partly assimilated large blocks of Dripping Spring and, in so doing, efficiently removed syngenetic uranium from

the sedimentary rock and added it to the hyperfusible constituents of the magma. Escaping gases and hyperfusibles could then have deposited uranium in the fractures where it is now found. As pointed out on page 40, however, simple hybridization between diabase magma and siltstone would not result in a rock of syenite composition unless a selective exchange of constituents took place. We consider the syenite facies as either a deuterically altered diabase or an alkalic differentiate from the diabase magma.

The preponderance of evidence seems to indicate nearly contemporaneous uranium deposition and diabase cooling: the uranium deposits and diabase are spatially related; the uraninite and some associated minerals are of probable high-temperature origin; age determinations of the uraninite are compatible with the Precambrian age of the diabase; and the diabase magma seems to have lost uranium during its cooling and recrystallization history (Neuerburg and Granger, 1960). Thus, we prefer a hypothesis of epigenetic uranium contemporaneous with diabase and believe that a logical sequence of events can be postulated to trace the uranium from the diabase magma to deposition in primary ore minerals.

#### BEHAVIOR OF URANIUM DURING THE INTRUSION AND DIFFERENTIATION OF DIABASE

The diabase magma was intruded into the Dripping Spring at a high temperature as a mobile mafic fluid that probably contained less than 1 ppm uranium. As the magma came in contact with wallrock it was quickly chilled, and the chilled area formed a thin layer of very fine grained rock in which most of the constituents of the magma were frozen in their original proportions. Such elements as uranium, which are usually expelled from the early crystallizing rock minerals, were abruptly locked into the lattices of these minerals because of their rapid formation. Within this envelope of chilled rock the magma began to crystallize and differentiate. The early formed minerals within the envelope did not include uranium in their crystal lattices as they crystallized, which caused a progressive concentration of uranium in the residual liquid. Throughout this period the diabase bodies were continually losing their heat to the enclosing rocks. Locally, where the conditions were favorable, hornfels and related metamorphic rocks were formed. Eventually the diabase magma had crystallized to a mass having considerable competency but containing vast amounts of intergranular fluids consisting of alkalic and mafic constituents in excess of the amounts required for the diabase. Readjustments, perhaps due to shrinkage, at this time produced dilatant zones into which some of these late-stage fluids were drawn. Here they either crystallized

or reacted with the diabase to produce syenite. This rock, having formed from a liquid in which uranium had become relatively concentrated, retained a larger percentage of uranium when it had crystallized than did the diabase.

The formation of the syenite, however, did not completely exhaust the residual liquors of differentiation. These liquors were now both strongly alkalic and iron rich. Perhaps two immiscible or separate solutions were present. One may have been mafic and hydrous, the other alkalic and more nearly anhydrous. In any event, further readjustments resulted in dilatant zones into which the sodic and potassic silica-rich components were drawn. These formed the aplite dikes that are largely restricted to the diabase but that locally extend into the enclosing sedimentary rocks.

Ultimately very little residual liquor remained, and this was extremely iron rich. Ions of uranium, zirconium, and perhaps other elements whose radii would not readily fit into the crystal lattices of other minerals were relatively concentrated in this residual solution. Presumably the residual liquor had originally been well distributed along intergranular boundaries and minute cavities, but the dilatant processes that released the alkalic components probably also tended to concentrate the iron-rich solutions in certain areas. Minor readjustments in the diabase at this time, perhaps related to regional jointing, tended to form dilatant zones, and the iron-rich liquors were drawn into and along narrow channelways that also locally penetrated the enclosing sedimentary rocks. Where trapped in the diabase, the solutions crystallized to hornblende-rich deuteritic veins that contained radioactive zircon. Under some conditions these solutions reacted with the enclosing rocks to form magnetite deposits, and the other constituents escaped. Possibly some of these late-stage solutions were richer in magnesia than in iron and contributed to the development of asbestos deposits. But of more immediate interest in this report is the probability that some of the solutions escaped into the Dripping Spring Quartzite and reacted to form the uranium deposits.

#### TRANSPORTATION AND LOCALIZATION OF URANIUM

The paths of the uranium-bearing solutions between diabase and individual uranium deposits are difficult to trace. The solutions did not have to travel far to reach areas of present deposits adjacent to the diabase, but to reach areas of deposits such as the Sue, Donna Lee, Rainbow, and many others they had to travel as much as several hundred feet from the diabase; yet they did not leave any obvious evidence of their paths.

The close spatial relation between the barren quartzite and many of the uranium deposits may be significant. Within the stratigraphic interval favorable for uranium

deposits the barren quartzite contains the only strata continuous enough and porous enough to allow appreciable lateral movement of fluids. As such, the barren quartzite may have been a channelway for some of the uranium-bearing solutions from their sources to sites of deposition.

Once the solutions had reached the fractures along which the deposits occur, the uranium and other metallic elements precipitated because of a combination of factors. The solutions probably were highly undersaturated under the conditions of pH, Eh, pressure, and temperature that existed within the juvenile fluids expelled from the diabase. As soon as the solutions entered the Dripping Spring, these conditions must have begun to change. However, it is doubtful that the immediate changes were adequate in most places to cause precipitation. Distribution of uraninite and the metal sulfides in the wallrock rather than in the central fracture suggests that solutions flowing through the central fracture rarely reached saturation. Presumably the hydrostatic pressures were high. If so, the solutions would have been forced into the minute fracture systems and along grain boundaries in the wallrock. Here, perhaps, the solvent (water(?)) was able to diffuse outward more readily than the metallic ions. Thus, the metallic ions probably concentrated in the wallrock immediately adjacent to the central fracture by a process of ultrafiltration corresponding to that proposed by Mackay (1946). In this wallrock environment the solutions encountered conditions of lowered temperature and pressure and, perhaps, lowered Eh caused by the preexisting carbon and iron sulfide content. When the solutions became saturated under these environmental conditions, precipitation occurred.

To satisfy the requirements of this postulated process, the host rock must (1) be nearly impervious yet allow both access and slow diffusion of solutions under pressure, (2) have chemical conditions conducive to low Eh, and (3) provide a conduit of some kind to permit ready transfer of solutions between their sources and their sites of deposition. The gray unit of the Dripping Spring Quartzite is the only such rock that is widely distributed in the Apache Group. It is significant that the only other rock that approaches fulfillment of these conditions, a local unit of carbon-rich shale in the upper member of the Mescal Limestone, contains a small low-grade uranium-copper deposit on the Ancient claims in Pueblo Canyon (McFadden Peak 15-minute quadrangle). A large discordant diabase body, associated with the Cherry Creek monocline, cut across the Mescal within, at most, a few thousand feet east (A. F. Shrider, oral commun., 1962) of the deposit prior to incision of the Cherry Creek canyon. No attempt was made to fur-

ther relate this deposit to deposits in the Dripping Spring.

#### SUGGESTIONS FOR PROSPECTING

##### STRATIGRAPHIC CONSIDERATIONS

The results of the present study suggest that there is little if any chance of finding an economic uranium deposit in any part of the Apache Group other than the gray unit of the Dripping Spring Quartzite. Of course a uranium deposit of entirely different genesis may possibly be found elsewhere in the Apache Group, and it is true that small subeconomic deposits have been found in the Mescal Limestone.

Serious prospecting, however, should be limited largely to the gray unit, particularly near the horizon of the barren quartzite. In general, the most favorable host rock seems to be medium gray and very fine grained or silty. Strongly weathered and bleached rocks should not be ignored, however; the ore bodies on the west side of Warm Creek canyon at Red Bluff are in highly bleached rock.

##### STRUCTURAL CONSIDERATIONS

Fractures along which uranium veins are localized had the most direct structural control over the emplacement of the deposits. These structures are generally obscure at the surface, however, and are complicated by many later joints and fractures that have trends both parallel to and diverse from the trends of the veins. Generally, detection of the radioactivity of veins at the surface is much simpler than the recognition of the structures along which the veins were emplaced.

An effort should be made to recognize structures, such as prediabase faults and monoclines, that exerted control over the emplacement of diabase. Areas near such structures evidently were favorable for the formation of uranium deposits.

The gray unit should be investigated intensively adjacent to any diabase dikes or other discordant contacts between diabase and favorable host rock. As these discordances commonly are obscure or concealed, a thorough prospect of all exposures of the gray unit within 300 feet of any diabase body seems advisable.

##### PROSPECTING MEDIA

Prospecting can be done from aircraft or automobile, on foot, or on horseback. Each has its advantages and disadvantages.

Prospecting from aircraft is most efficient if the geologic setting is known or can be interpreted from the air. Nearly all prospecting for uranium deposits from the air is done with the aid of a scintillation meter or a specially constructed Geiger counter that detects only gamma radiation. Where the geologic setting is known, scanning of large areas of outcrop for abnormal radio-

activity is possible. Where the topography is favorable, the aircraft can fly very close to the surface; but in many places, such as in narrow canyons, it cannot fly sufficiently close for any abnormal radioactivity to be detected. For example, flights over the Shepp No. 2 deposits in Wilson Creek canyon failed to detect any abnormal radioactivity except by unusual maneuvering of the plane (Magleby and Mead, p. 13). Prospecting by aircraft is the fastest method of reconnaissance prospecting and may materially aid in delineating favorable areas, but it cannot entirely replace traverses on foot.

Prospecting from an automobile is much more limited than prospecting from an airplane, because adequate exposures of favorable rocks do not ordinarily occur on terrain that can be traversed by automobile.

Prospecting on foot or horseback is much slower but can be more thorough than prospecting from a vehicle. The prospector can restrict his activities to the favorable rock units and search for anomalous radioactivity in places inaccessible by other methods of approach. Available instruments consist of portable scintillation meters that detect gamma radiation, and portable Geiger counters that detect both beta and gamma radiations.

Perhaps the most efficient method of prospecting large areas is the one utilized by the U.S. Atomic Energy Commission and several private companies. This consists of the detection of areas of anomalous radioactivity from the air and a followup by thorough ground checking of these areas.

##### PROSPECTING FOR CONCEALED DEPOSITS

A wholly adequate method of prospecting for concealed deposits is not known. Every economic deposit that has been found to date was exposed at the surface or was an extension of a deposit found at the surface. Some of the mining companies have unsuccessfully attempted drilling programs in areas that they judged to be favorable.

Geophysical methods might aid in the discovery of a hidden ore body, but they have not been tried, and we believe that most of the known methods likely would be unsuccessful.

##### SUGGESTIONS FOR DEVELOPMENT

Development of known deposits is done by drilling or by drifting. Drilling from the surface has proved to be of value only on the few deposits, such as the Lucky Boy, in which the ore body dips at a moderate to low angle. It could have proved to be of value at more steeply dipping deposits that had considerable vertical extent, such as the Hope 3, but was not tried. In general, though, drilling from the surface is not the

most economical means of development, because the limited extent of the deposits allows only small drilling targets, and the average grade of most of these deposits is so low that under present economic conditions a profit could not be realized after the expense of determining the extent of the deposit from the surface had been met.

The more economical method of development of a deposit exposed at the surface is generally that of drifting along the vein. An additional advantage of drifting is that widely spaced wall drilling may disclose parallel ore bodies. Wall drilling may be particularly effective at the termination of an ore body. Drilling diagonally ahead of the end of the drift may also disclose an en echelon or parallel vein.

#### SUGGESTIONS FOR MINING PROCEDURE

A thorough understanding of the shape and the geologic relations of any ore body is a valuable aid in planning the mining procedures to be employed in exploitation of a deposit. Some of the procedures employed in mining several of the deposits in the Dripping Spring did not result in the most economic extraction of the ore.

Major factors to be considered in mining the deposits in the Dripping Spring are the tendency of the ore bodies to have a rather flat bottom, the narrowness of the vein zones, and the breakage characteristics of the host rock when blasted. Driving a narrow level along the bottom of the ore and then working an even narrower upward stope seems to result in the most economic removal of the ore. Care must be taken to avoid excessive dilution as a result of wallrock breakage, as the wallrock tends to shatter and separate along joints subparallel to the vein zone.

#### REFERENCES CITED

- Allen, M. A., and Butler, G. M., 1921, Asbestos: Arizona Bur. Mines Bull. 113, 31 p.
- Arnold, R. G., 1962, Equilibrium relations between pyrrhotite and pyrite from 325° to 743° C: Econ. Geology, v. 57, no. 1, p. 72-90.
- Barton, P. B., Jr., and Toulmin, Priestley, 3d, 1964, Sphalerite phase equilibria in the system Fe-Zn-S between 580°C and 850°C [abs.] in, Abstracts for 1963: Geol. Soc. America Spec. Paper 76, p. 8-9.
- Bateman, A. M., 1923, An Arizona asbestos deposit, *with discussion* by G. F. Loughlin, E. S. Bastin, H. M. Chance, J. E. Spurr, and A. C. Spencer: Econ. Geology, v. 18, no 7, p. 663-683.
- Bishop, O. M., 1935, Geology and ore deposits of the Richmond Basin area, Gila County, Arizona: Arizona Univ. Master's thesis.
- Butler, B. S., and Wilson, E. D., 1938, Some Arizona ore deposits; pt. 1, General features: Arizona Bur. Mines Bull. 145, Geol. ser. 12, p. 9-25.
- Butler, G. M., 1929, Geological occurrence of Arizona asbestos: Pan-Am. Geologist, v. 52, no. 1, p. 19-26.
- Carpenter, R. H., 1947, The geology and ore deposits of the Vekol Mountains, Pinal County, Arizona: Stanford Univ. Ph.D. dissert.
- Cook, F. S., 1938, The geology of the Seven Dash Ranch area, Cochise County, Arizona: Arizona Univ. Master's thesis.
- Cooper, J. R., 1950, Johnson Camp area, Cochise County, Arizona, chap. 3 in pt. 1 of Arizona zinc and lead deposits: Arizona Bur. Mines Bull. 156, Geol. ser. 18, p. 30-39.
- Darton, N. H., 1925, A résumé of Arizona geology: Arizona Bur. Mines Bull. 119, Geol. ser. 3, 298 p.
- Deer, W. A., and Wager, L. R., 1939, Olivines from the Skaergaard intrusion, Kangerdlugssuak, east Greenland: Am. Mineralogist, v. 24, no. 1, p. 18-25.
- Deul, Maurice, 1956, Colloidal method for concentration of carbonaceous matter from rocks: Am. Assoc. Petroleum Geologists Bull., v. 40, no. 5, p. 909-917.
- Edwards, A. B., 1947, Textures of the ore minerals and their significance: Australasian Inst. Mining and Metallurgy, 185 p.
- Galbraith, F. W., 3d, 1935, Geology of the Silver King area, Superior, Arizona: Arizona Univ. Ph. D. thesis. [Copy on deposit in U.S. Geol. Survey Library, Washington, D.C.]
- Gastil, R. G., 1953, The geology of the eastern half of the Diamond Butte quadrangle, Gila County, Arizona: California Univ. Ph. D. dissert.
- Gilbert, G. K., 1875, Report on the geology of portions of Nevada, Utah, California, and Arizona: U.S. Geog. Geol. Surveys West of 100th Meridian (Wheeler), v. 3, pt. 1 p. 503-567.
- Goodspeed, G. E., 1948, Replacement and rheomorphic dikes [Cornucopia, Oreg.] [abs.]: Geol. Soc. America Bull., v. 59, no. 12, pt. 2, p. 1371.
- Goodspeed, G. E., and Fuller, R. E., 1944, Replacement aplite breccia [Cornucopia, Oreg.]: Jour. Geology, v. 52, no. 4, p. 264-274.
- Granger, H. C., 1963, Radium migration and its effect on the apparent age of uranium deposits at Ambrosia Lake, New Mexico, in Short papers in geology and hydrology: U.S. Geol. Survey Prof. Paper 475-B, p. B60-B63.
- Granger, H. C., and Raup, R. B., Jr., 1959, Uranium deposits in the Dripping Spring quartzite, Gila County, Arizona: U.S. Geol. Survey Bull. 1046-P, p. 415-486.
- 1964, Stratigraphy of the Dripping Spring Quartzite, southeastern Arizone: U.S. Geol. Survey Bull. 1168, 119 p.
- 1969, Detailed descriptions of uranium deposits in the Dripping Spring Quartzite, Gila County, Arizona: U.S. Geol. Survey open-file report.
- Harker, Alfred, 1952, Metamorphism; a study of the transformations of rock-masses: 3d ed., London, Methuen & Co., 362 p., 185 diagrams.
- Harshman, E. N., 1940, Geology of the Belmont-Queen Creek area, Superior, Arizona: Arizona Univ. Ph. D. dissert.
- Hiemstra, S. A., 1955, Age of uraninites from dimensions of their unit cells [a discussion]: Nature, v. 176, no. 4478, p. 405.
- Hoekstra, H. R., and Katz, J. J., 1955, Age of uraninites from crystallographic data [a discussion]: Nature, v. 175, no. 4457, p. 605.
- Huddle, J. W., and Dobrovolny, Ernest, 1952, Devonian and Mississippian rocks of central Arizona: U.S. Geol. Survey Prof. Paper 233-D, p. 67-112.
- Kaiser, E. P., 1951, Uraniferous quartzite, Red Bluff prospect, Gila County, Arizona: U.S. Geol. Survey Circ. 137, 10 p.
- Katz, J. J., and Rabinowitch, Eugene, 1951, The chemistry of uranium. Pt. 1—The element, its binary and related com-

- pounds: Natl. Nuclear Energy Ser., Manhattan Proj. tech. section, div. 8, v. 5: New York, McGraw-Hill Book Co., 609 p.
- Krieger, M. H., 1961, Troy Quartzite (younger Precambrian) and Bolsa and Abrigo formations (Cambrian), northern Galiuro Mountains, southeastern Arizona, in Short papers in the geologic and hydrologic sciences: U.S. Geol. Survey Prof. Paper 424-C, p. C160-C164.
- Kullerud, Gunnar, 1953, The FeS-ZnS system; a geological thermometer: Norsk Geol. Tidsskr., v. 32, nos. 2-4, p. 61-147.
- Mackay, R. A., 1946, The control of impounding structures on ore deposition: Econ. Geology, v. 41, no. 1, p. 13-46.
- Magleby, D. N., and Mead, W. E., 1955, Airborne reconnaissance project, Dripping Spring quartzite, Arizona: U.S. Atomic Energy Comm. RME-2023, 23 p., issued by U.S. Atomic Energy Comm. Tech. Inf. Service, Oak Ridge, Tenn.
- Mead, W. E., and Wells, R. L., 1953, Preliminary reconnaissance of the Dripping Spring quartzite formation in Gila and Pinal Counties, Arizona: U.S. Atomic Energy Comm. RME-4307, 11 p., issued by U.S. Atomic Energy Comm. Tech. Inf. Service, Oak Ridge, Tenn.
- Mead, W. J., 1925, The geologic role of dilatancy: Jour. Geology, v. 33, no. 7, p. 685-698.
- Neuerburg, G. J., and Granger, H. C., 1960, A geochemical test of diabase as an ore source for the uranium deposits of the Dripping Spring district, Arizona: Neues Jahrb. Mineralogie Abh., v. 94, pt. 2, p. 759-797.
- Nockolds, S. R., 1954, Average chemical compositions of some igneous rocks: Geol. Soc. America Bull., v. 65, no. 10, p. 1007-1032.
- Peterson, N. P., Gilbert, C. M., and Quick, G. L., 1951, Geology and ore deposits of the Castle Dome area, Gila County, Arizona: U.S. Geol. Survey Bull. 971, 134 p.
- Phair, George, and Levine, Harry, 1953, Notes on the differential leaching of uranium, radium, and lead from pitchblende in  $H_2SO_4$  solutions: Econ. Geology, v. 48, no. 5, p. 358-369.
- Ransome, F. L., 1903, Geology of the Globe copper district, Arizona: U.S. Geol. Survey Prof. Paper 12, 168 p.
- 1917, Some Paleozoic sections in Arizona and their correlation: U.S. Geol. Survey Prof. Paper 98-K, p. 133-166.
- 1919, The copper deposits of Ray and Miami, Arizona: U.S. Geol. Survey Prof. Paper 115, 192 p.
- Reagan, A. B., 1903, Geology of the Fort Apache region in Arizona: Am. Geologist, v. 32, p. 265-308.
- Russell, R. D., and Ahrens, L. H., 1957, Additional regularities among discordant lead-uranium ages: Geochim. et Cosmochim. Acta, v. 11, no. 4, p. 213-218.
- Sampson, Edward, 1924, Arizona asbestos deposits: Econ. Geology, v. 19, no. 4, p. 386-388.
- Sharp, B. J., 1956, Preliminary report on a uranium occurrence and regional geology in the Cherry Creek area, Gila County, Arizona: U.S. Atomic Energy Comm. RME-2036 (revised), 16 p., issued by U.S. Atomic Energy Comm. Tech. Inf. Service, Oak Ridge, Tenn.
- Short, M. N., and Ettlinger, I. A., 1926, Ore deposition and enrichment at the Magma mine, Superior, Arizona: Am. Inst. Mining Metall. Engineers Trans., v. 74, p. 174-222.
- Short, M. N., Galbraith, F. W., Harshman, E. N., Kuhn, T. H., and Wilson, E. D., 1943, Geology and ore deposits of the Superior mining area, Arizona: Arizona Bur. Mines Bull. 151, Geol. ser. 16, 159 p.
- Shride, A. F., 1952, Localization of Arizona chrysotile asbestos deposits [abs.]: Geol. Soc. America Bull., v. 63, no. 12, pt. 2, p. 1344.
- Silver, L. T., 1960, Age determinations on Precambrian diabase differentiates in the Sierra Ancha, Gila County, Arizona [abs.]: Geol. Soc. America Bull., v. 71, no. 12, pt. 2, p. 1973-1974.
- Skinner, B. J., 1961, Unit-cell edges of natural and synthetic sphalerites: Am. Mineralogist, v. 46, nos. 11 and 12, p. 1399-1411.
- Stokes, W. L., and Varnes, D. J., 1955, Glossary of selected geographic terms, with special reference to their use in engineering: Colorado Sci. Soc. Proc., v. 16, 165 p.
- Toulmin, Priestley, 3d, 1960, Effect of Cu on sphalerite phase equilibria—A preliminary report [abs.]: Geol. Soc. America Bull., v. 71, no. 12, pt. 2, p. 1993.
- Turner, F. J., and Verhoogen, John, 1951, Igneous and metamorphic petrology: 1st ed., New York, McGraw-Hill Book Co., 602 p.
- Walker, Frederick, 1940, Differentiation of the Palisade diabase, New Jersey: Geol. Soc. America Bull., v. 51, no. 7, p. 1059-1105.
- Wardwell, H. R., 1941, Geology of the Potts Canyon mining area near Superior, Arizona: Arizona Univ. Master's thesis.
- Wasserstein, Benno, 1951, Cube-edges of uraninites as a criterion of age?: Nature, v. 168, no. 4270, p. 380.
- 1954, Ages of uraninites by a new method: Nature, v. 174, no. 4439, p. 1004-1005.
- 1955a, Age of uraninites from crystallographic data: Nature, v. 175, no. 4457, p. 605-606.
- 1955b, Ages of pitchblends by X-ray diffraction: Nature, v. 176, no. 4473, p. 159-160.
- 1955c, Age of uraninites from dimensions of their unit cells: Nature, v. 176, no. 4478, p. 405-406.
- Wells, R. L., and Rambosek, A. J., 1954, Uranium occurrences in Wilson Creek area, Gila County, Arizona: U.S. Atomic Energy Comm. RME-2005 (revised), 17 p., issued by U.S. Atomic Energy Comm. Tech. Inf. Service, Oak Ridge, Tenn.
- Williams, F. J., 1957, Structural control of uranium deposits, Sierra Ancha region, Gila County, Arizona: U.S. Atomic Energy Comm. RME-3152, 121 p., prepared by Columbia University for and issued by U.S. Atomic Energy Comm. Tech. Inf. Service, Oak Ridge, Tenn.
- Wilson, E. D., 1928, Asbestos deposits of Arizona, with an introduction Asbestos minerals, by G. M. Butler: Arizona Bur. Mines Bull. 126, 97 p.
- 1939, Pre-Cambrian Mazatzal revolution in central Arizona: Geol. Soc. America Bull., v. 50, no. 7, p. 1113-1163.
- Wright, R. J., 1950, Reconnaissance of certain uranium deposits in Arizona: U.S. Atomic Energy Comm. RMO-679, 21 p., issued by U.S. Atomic Energy Comm. Tech. Inf. Service, Oak Ridge, Tenn.

## INDEX

[Italic page numbers indicate major references]

A	Page	Chemical analyses—Continued	Page	Page		
Accessibility of report area	4	Rainbow adit	69	Gangue minerals, ore deposits	65, 91	
Acknowledgments	4	sphalerite	101	Geologic history, report area	4	
Age-determination methods, diabase	24	Tomato Juice deposit	69	Geothermometry	100	
uraninite	76	Cherry Creek monocline	43	Geothite	95	
Albite, aplite facies	18	Chlorite	92	Gila Conglomerate	5	
coarse-grained hornfels	33, 34	uraniferous	89	Gouge zones	52	
normal hornfels	30	Chrysocolla	95	Granite, radioactivity	60	
syenite facies	17	Chrysotile	40	Gray unit, upper member, analyses	31	
American Smelting and Refining Co.	63	Clay minerals	93, 96	upper member, facies	7	
Ankerite	92	Coffinite	86	Gypsum	95	
Apache Group	5	Contact metamorphism, upper member	25		H	
diabase	10	Copiapite	96	Harshman, E. N., quoted	25, 40	
structure	42	Cubanite	88	Hemimorphite	95	
Aplite	35, 37	Cutter depot	63	Hope deposits, mobilized hornfels	35	
radioactivity	60			ore veins	65	
uranium content	60, 62	D		uraninite	82	
wallrock reactions	40	Deuteric alteration, diabase	15, 23	Hope 3 mine, analyses	66	
Aplite facies	18	Deuteric veins	21, 75	radiochemical analysis	78	
chemical analyses	12	classification	22	Hornblende, diabase	14	
mineralogy	18, 20	properties	14	Hornfels, coarse-grained	32, 34, 62	
paragenetic relations	20	radioactivity	60	lit-par-lit	32, 34	
properties	14	uranium content	23, 60, 62	mobilized	34	
textural varieties	19	Diabase	10	origin	37	
Asbestos	40	age	24	vugs	36	
Augite, diabase	12	aplite facies	18	normal	26, 30, 34	
syenite facies	17	chemical analyses	12	specific gravity	26	
Azurite	95	definition	11	uraninite	65	
	B	deuteric veins	21	uranium content	62	
Barite	95	faults	45	varieties	26, 27	
Barnes Conglomerate Member	5, 7	ophitic	11	wallrock reactions	41	
radioactivity	60	pegmatite	15	Horse Shoe deposit, pyrite	89	
uranium content	60	Pioneer Formation	39	Hyalite	95	
Barren quartzite	70	properties	14	Hypersthene, diabase	12	
relation to ore deposition	103	radioactivity	60		I	
Basalt, radioactivity	60, 62	relation to ore deposits	71, 99	Ilmenite, aplite facies	20	
uranium content	60	specific gravity	26	Isotopic ratios, age determinations, diabase	23	
Basalt flows	5	syenite facies	17	age determinations, uraninite	76	
Bassettite	93	textural varieties	11		J, K	
Beta-uranophane	94	uranium content	23, 60, 62	Jarosite	96	
Big Buck deposit, tension joints	50	wallrock reactions	40	Joints, age	56	
Big Six deposit, spotted rocks	39	Diabase differentiates	15, 23	definition	48	
Biotite, aplite facies	20	chemical analyses	12	movement	52	
coarse-grained hornfels	33	specific gravity	26	shear	50	
diabase	14	Diabase dikes	5	systems	50	
normal hornfels	28	Dikes, aplite facies	18	tension	48	
Blanket ore deposits	70	Dripping Spring Quartzite	5		Kaolinite	96
Blue Rock deposit, tension joints	50	members. See Barnes Conglomerate Mem-		Katz, J., and Rabinowitch, Eugene, quoted	78	
Bluewater deposit	63	ber, Middle member, and Upper			L	
Breccia zones	52	member.		Laramide revolution, faulting	48	
Buff unit, upper member	8	radioactivity	60, 61	Lead isotope ratios, age determination	76	
	C	specific gravity	26	Limonite	95	
Calcite	91	stratigraphic section	6	Little Joe deposit, coarse-grained hornfels	32	
Canyon Creek monocline	43	uranium content	60, 61	mobilized hornfels	35	
Carbon, uraniferous	84	F		Location of deposits	2	
Chalcanthite	96	Faults	43	Location of report area	2	
Chalcopyrite	87	age	48	Lost Dog deposit, tension joints	50	
Chemical analyses, diabase	12	relation to ore deposits	71	Lucky Boy mine, analyses	69	
diabase differentiates	12	Fluorite	91	Lucky Stop deposits, analyses	67	
gray unit, upper member	31	Fucoidlike markings	9	tension joints	50	
Hope 3 mine	66	G				
Lucky Boy mine	69	Galbraith, F. W., quoted	25, 40			
Lucky Stop deposits	67	Galena	88			
		age	76			

## INDEX

M, N	Page	Pioneer Formation—Continued	Page	Page	
Malachite.....	95	radioactivity.....	60	Styolites.....	9
Marcasite.....	90	uranium content.....	61	Sulfate minerals.....	96
Mazatzal Revolution.....	5	Plagioclase, diabase.....	11	Sulfide minerals, association with uranium.....	82
Meskal Limestone.....	5	Precambrian granite, radioactivity.....	60	normal hornfels.....	29
coarse-grained hornfels.....	32	Precambrian rocks, stratigraphy.....	4	ore deposits.....	86
metamorphism.....	26, 40	Preconsolidation deformation features.....	9	Syenite, radioactivity.....	60
radioactivity.....	60, 62	Prehnite, diabase.....	11	relation to ore deposits.....	71
spotted rocks.....	40	Prospecting suggestions.....	104	uranium content.....	60, 62
uranium content.....	60	Pseudochannels.....	9	Syenite facies.....	17
Mesozoic rocks.....	5	Pyrite.....	89	chemical analyses.....	12
Meta-autunite.....	94	Pyrogenic alteration, diabase differentiates.....	23	origin.....	102
Metanovacakeite.....	94	Pyroxene, aplite facies.....	20	properties.....	14
Metageunerite.....	94	hornfels.....	29, 34	T	
Metatorbernite.....	93	Pyrrhotite.....	88, 101	Tertiary faulting.....	48
Microcline, aplite facies.....	20	coarse-grained hornfels.....	34	Tertiary rocks.....	5
Middle member.....	7	geothermometry.....	100	Tomato Juice deposit, analyses.....	69
radioactivity.....	60	spectrographic analyses.....	86	tension joints.....	50
uranium content.....	60	Quartz.....	93	uraninite.....	83
Mining procedures.....	105	aplite facies.....	20	Troy Quartzite.....	5, 24, 25
Molybdenite.....	86	coarse-grained hornfels.....	33	U	
Monoclines.....	42	normal hornfels.....	28	Unit-cell cube-edge method of age determina-	
relation to faults.....	43, 45	Quaternary faulting.....	48	tion, uraninite.....	77
relation to ore deposits.....	71	Quaternary rocks.....	5	U.S. Atomic Energy Commission.....	63
Mule Hoof monocline.....	43	R		Upper member, Buff unit.....	8
Muscovite, spotted rocks.....	39	Radioactivity, diabase.....	60	contact metamorphism.....	25
Nontronite.....	93	gray unit, analyses.....	31	facies.....	7
spotted rocks.....	39	Dripping Spring Quartzite.....	60, 61	ore deposits.....	70
O		methods of determining.....	56	radioactivity.....	60
Olivine, diabase.....	13	ore deposits.....	78	sedimentary structures.....	9
Ophitic diabase.....	11	relation to uranium content.....	78	spotted rocks.....	38
Optical properties, augite.....	12, 17	selected rocks.....	56, 60	stratigraphic divisions.....	7
chlorite.....	92	zircon.....	22	uranium content.....	60, 61
uraniferous.....	84	Radiochemical analysis, Hope 3 mine.....	78	white unit.....	8
hornblende.....	14, 21	Radiocolloids.....	79	Uraniferous carbon.....	84
nontronite.....	93	Rainbow adit, analyses.....	69	Uraniferous chlorite.....	85
olivine.....	13	Ransome, F. L., quoted.....	25	Uraninite, age.....	76
phlogopite.....	92	Red Bluff deposits, pyrite.....	89	Hope deposits.....	82
pyroxene.....	29, 34	uraniiferous chlorite.....	84	hornfels.....	65
sphene.....	33	Red unit, upper member.....	7	relation to galena.....	89
Ore deposition, factors affecting.....	97	References cited.....	105	Rock Canyon deposit.....	83
Ore deposits.....	63	Ripple marks.....	9	Tomato Juice deposit.....	83
age.....	76	Rock Canyon deposit, uraninite.....	83	varieties.....	80
alteration minerals.....	65, 91	Rock Canyon monocline.....	43	vein deposits.....	65
development.....	104	S		Uranium-bearing minerals.....	79
emplacement factors.....	97	Saléeite.....	94	Uranium content, diabase.....	23, 60, 62
gangue minerals.....	65, 91	Scanlan Conglomerate Member.....	5	Dripping Spring Quartzite.....	60, 61
minerals.....	80	Secondary minerals, ore deposits.....	93	Pioneer Formation.....	61
mining history.....	63	Sedimentary structures, middle member.....	7	relation to contents of other elements.....	98
origin.....	101	upper member.....	9	relation to radioactivity.....	78
radioactivity.....	78	Sericite, diabase.....	11	selected rocks.....	56, 60
relation to diabase.....	71, 102	Serpentine, Mescal Limestone.....	40	Shepp No. 2 deposit.....	84
relation to structural features.....	48, 71	Shepp No. 2 deposit, gouge and breccia zones.....	52	Uranium deposits. See Ore deposits.....	
secondary minerals.....	93	uranium and carbon content.....	84	Uranium isotope ratios, age determination.....	76
stratigraphic and areal distribution.....	70	Shride, A. F., quoted.....	40	Uranophane.....	94
sulfide minerals.....	86	Shrinkage cracks.....	9	V, W	
uraninite.....	79	Sierra Ancha diabase sheet.....	10, 42	Vein deposits.....	64
Ore-forming fluids.....	98	Sierra Ancha monocline.....	42	minerals.....	80
Ore production.....	63	Spectrographic analyses, gray unit, upper		Vugs, mobilized hornfels.....	56
Ore tenor.....	64	member.....	31	W	
Orthoclase, spotted rocks.....	39	Hope 3 mine.....	66	Wasserstein, Benno, quoted.....	77
P		Lucky Boy mine.....	69	White unit, upper member.....	8
Paleozoic rocks.....	5	Lucky Stop deposits.....	67	Wilson, E. D., quoted.....	40
Paragenetic relations, aplite facies.....	20	pyrrhotite.....	86	Workman Creek area, hornfels.....	26, 32, 34
chalcopyrite.....	87	Rainbow adit.....	69	Workman deposit, spectrographic analysis,	
primary minerals.....	96	sphalerite.....	101	pyrrhotite.....	86
Pegmatite diabase.....	15	Tomato Juice mine.....	69	X, Y, Z	
Petrography, aplite facies.....	18	Sphalerite.....	88	Xenoliths, aplite facies.....	18
coarse-grained hornfels.....	32	analyses.....	101	Dripping Spring Quartzite.....	42
diabase.....	11, 15	crystallographic data.....	101	Yavapai Schist.....	4
normal hornfels.....	26	geothermometry.....	100	Zippeite, sodium analog.....	94
syenite facies.....	17	relation to chalcopyrite.....	87	Zircon, deuterio veins.....	22
Phlogopite.....	92	Sphene, aplite facies.....	20		
Pigeonite, diabase.....	13	coarse-grained hornfels.....	33		
Pinal Schist.....	4	normal hornfels.....	28		
Pioneer Formation.....	5				
diabase.....	39				



